Doctoral thesis

Convergent Approach of Carbocations and Organolithiums Using Integrated Flow System

（カルボカチオンと有機リチウム種の収束的フロー反応）

Hiroki Soutome
（早乙女広樹）

Graduate School of Chemical Sciences and Engineering
Hokkaido University

2025

Contents

Chapter 1
General Introduction

1. Reaction Integration in Flow Microreactors

In organic synthesis, the two primary approaches are batch and flow synthesis, with the former being the focus of much academic and industrial research. However, flow synthesis[1], which involves passing the reaction solution through a narrow reaction tube, exhibits distinct characteristics compared to the batch method (Table 1).

Table 1: Comparison of batch and flow methods

	batch	flow
Requirement for scale-up	scaling-up experiments	production ∝ time
Number of studies	large	small
Controllability of reaction	standard as batch	highly controllable

In terms of the manufacturing aspects of flow synthesis, it is easy to downsize the equipment[2], allowing for large-scale production in a table-sized reactor. Additionally, since product yield increases proportionally with reaction time[1,2], there is a strong correlation between laboratory studies and practical production. Moreover, as the reaction is controlled by mechanical systems such as pumps, it offers high reproducibility and can be easily integrated with analytical equipment[3], making it a highly advantageous approach for manufacturing. While the batch method is typically used in chemical research, the flow method presents distinct advantages of its own.

Focusing on reactions in flow synthesis, many reactions that are difficult to achieve using batch synthesis can be readily performed[4]. Flow microreactors[5], which feature microscale reactors, offer several advantages: the mixing of the reaction solution is completed in a short time due to the small mixing distance; the reaction temperature can be precisely controlled because of the reactor's small size; and the reaction time can be adjusted arbitrarily by selecting the flow rate of the reaction solution and the reactor volume (Figure 1). Leveraging these features, by mixing the next reaction solution after a chosen reaction time, it becomes possible to instantaneously generate short-lived active species in flow systems and perform subsequent reactions before decomposition occurs[6].

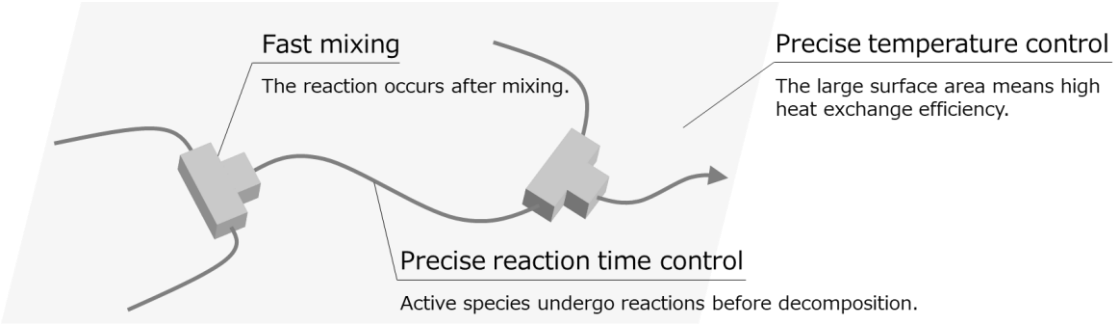

Figure 1: Characteristics of flow synthesis in terms of reaction controllability

A prominent example of such a reaction system is the use of carbanions generated through halogen-lithium exchange reactions[7], which have been extensively studied. By supplying electrophiles shortly after the rapid generation of reactive species, the desired nucleophilic reactions can proceed without the decomposition of unstable functional groups, such as esters and ketones. In this manner, leveraging the advantages of the flow method has enabled reactions involving active species that are too unstable to be employed in batch synthesis.

In flow synthesis, two integration methods are well-known: the linear integration method[8], where the reaction proceeds sequentially by introducing reactants in succession, and the convergent integration method[9], where reaction intermediates generated separately in flow systems are reacted with each other (Figure 2(a)). By integrating chemical reactions, the time, manpower, and environmental costs associated with synthesis are reduced, as pre- and post-reaction processes, including purification operations, are no longer necessary. In the example shown in Figure 2(b), a pharmaceutical structure is constructed in a single flow by integrating six reactions with 1,3,5-tribromobenzene[10]. One reason for the high yield of this reaction is attributed to the precise controllability of the reactions in flow synthesis. Therefore, the flow method can be considered a suitable mode for reaction integration. Additionally, using the convergent reaction integration system shown in Figure 2(c), it is possible to react the active species of both the chlorosilane derivative generated in R2 and the oligostyrene living anion generated in R3 within micromixer M4[11]. These reaction integration methods can efficiently assemble complex frameworks. The integration of these high-speed reactions also holds potential for on-site synthesis, where necessary compounds are synthesized and when and where required[12].

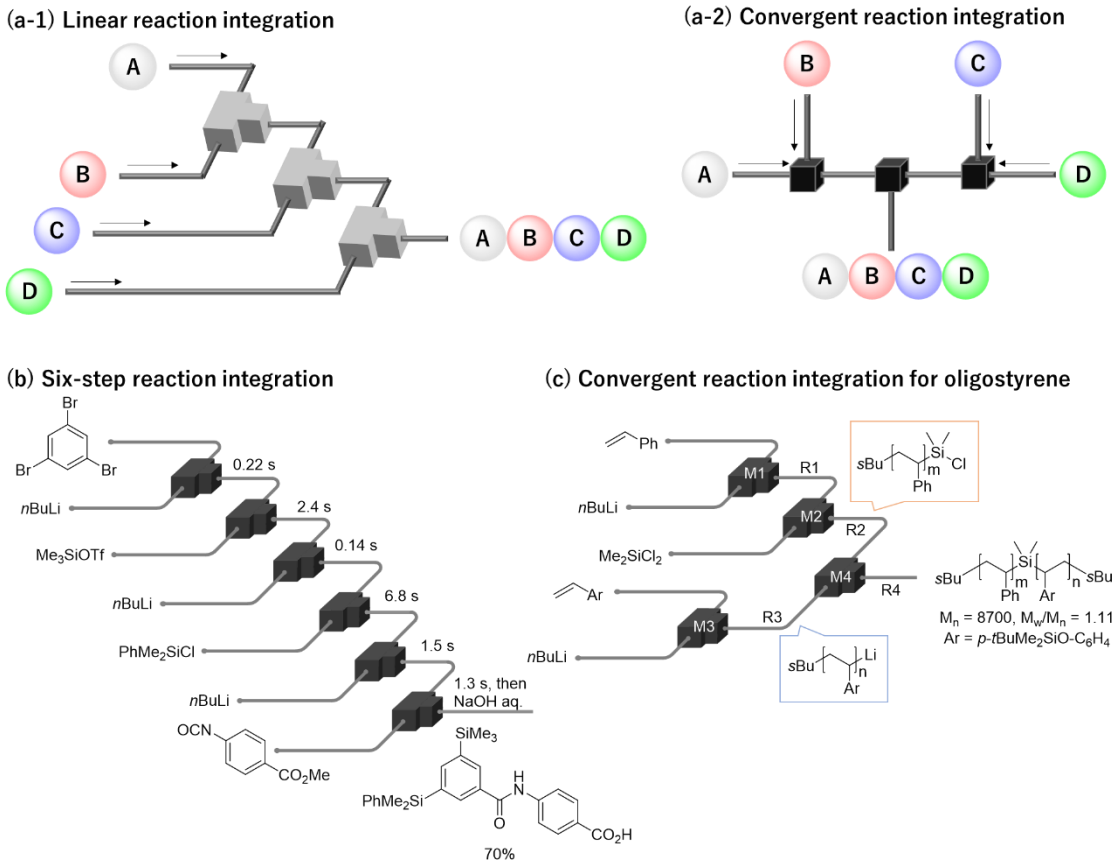

Figure 2: (a) scheme of reaction integration, (b) six-step reaction integration, (c) convergent reaction integration for oligostyrene

2. Flash Generation of Carbocations

Although carbocations are generally recognized as unstable chemical species, they play a crucial role in organic synthetic chemistry due to their broad range of applications[13]. In typical organic reactions, carbocations are generated by activating cation precursors with acids in a reversible process, and then trapping them with coexisting nucleophiles. However, in flow synthesis reaction integration, if a nucleophile for subsequent reactions is introduced before the precursor has fully converted to the carbocation, the reagent may react with the anion-activating agent. Therefore, for successful reaction integration involving carbocations, the irreversible generation of active species is essential.

Several methods for generating irreversible carbocations have been developed using electrochemical reactions (Figure 3). One such method, known as the cation pool method[14] enabling the generation and accumulation of carbocations through electrochemical reactions at low temperatures, after which a nucleophile can be added to initiate the following reaction. This technique allows the use of oxidation-sensitive nucleophiles. It was further demonstrated that carbocations accumulated by the cation pool method could be employed as substrates in

microflow reactions[15]. However, since electrolysis is used in both of these techniques, the required electrolysis time typically exceeds several hours before the active species are fully generated. Therefore, the carbocations employed in this reaction format must have a lifetime that exceeds the electrolysis activation time. To address this issue, our research group developed a method for generating carbocations in just a few seconds using high-speed electrolysis in a flow system with a custom-built large-current electrolysis apparatus[16]. Such methods for the rapid and irreversible generation of carbocations are extremely limited, and it is anticipated that the development of novel activation techniques will further enhance the availability of flow synthesis.

The method of using a superacid to irreversibly generate carbocations[17] was developed by Olah and others in the past. However, there are very few reports on the synthesis of complex compounds involving the irreversible generation of carbocations by Brønsted acids or Lewis acids, even when utilizing flow methods[18].

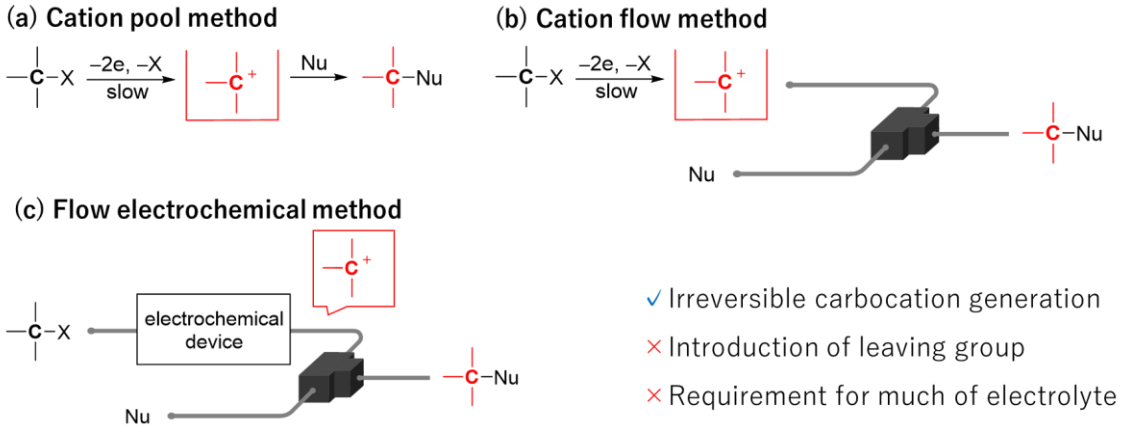

Figure 3: Methods for generating carbocations using electrochemical reactions

3. Overview of this Doctoral Thesis

As discussed in the previous sections, flow synthesis is a highly advantageous method for the efficient synthesis of complex compounds, as it reduces production costs through reaction integration and enables precise reaction control. While much of the research on microflow synthesis to date has focused on reactions utilizing carbanions as reactive species, the development of new methods for handling carbocations, which are notoriously difficult to manage, would significantly contribute to advancing this field.

Although generating carbocations quickly and irreversibly is challenging, it may be achievable using microflow synthesis with superacids. If carbocations can be efficiently generated, the impact on organic synthetic chemistry would be profound. For instance, by combining cation generation with convergent reaction integration in flow systems, it becomes

possible to design reactions that directly involve the interaction of carbocations and carbanions, which has been difficult to achieve in traditional methods. To the best of our knowledge, due to the limited generation methods and the very short lifetimes of these active species, no reports exist of such reactions. Consequently, there is no established understanding of whether direct interactions between cations and anions would result in C–C bond formation or acid-base neutralization reactions.

In this context, the objective of this doctoral thesis is to establish efficient systems for reaction integration using flow synthesis. In Chapter 2, the borylation reaction via the lithiation of aromatic bromine compounds was optimized, and the Suzuki-Miyaura cross-coupling reaction was integrated into this process. Typically, this coupling reaction requires several hours; however, by improving mixing efficiency and selecting appropriate additives, the reaction was significantly accelerated. This sequence of reactions enabled the production of a pharmaceutical precursor within a few minutes, starting from two aromatic bromine derivatives.

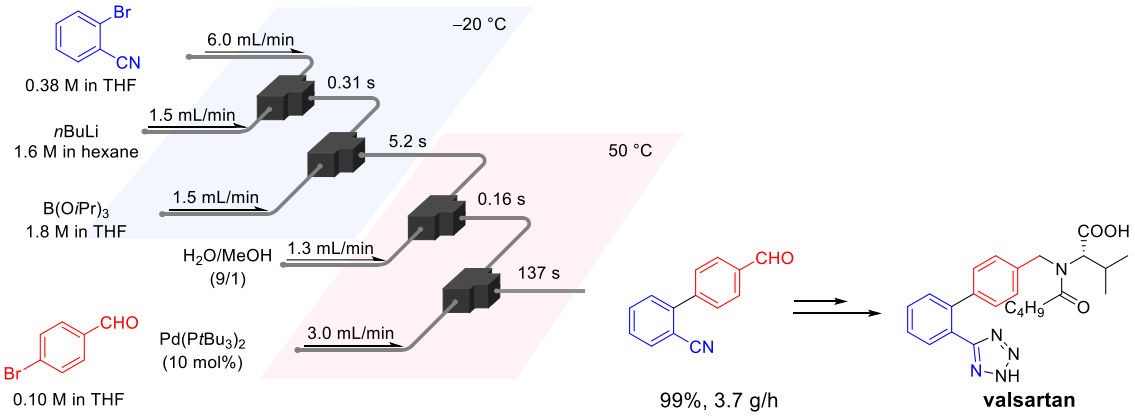

Figure 4: Linear integration of lithiation and accelerated coupling reactions (Chapter 2)

In Chapter 3, the author investigated the integration of aqueous layer separation as a pretreatment for reactions. Since pyridine hydrochlorides are typically insoluble in organic solvents, a desalting process using a basic aqueous solution is required to carry out organic reactions. After desalting, although the aqueous layer must be separated and the organic layer dried, the unstable desalted compound may decompose during this process. To address this, the author developed an one-flow reaction system that enables the linear integration of desalting, water separation, and water-sensitive reactions without isolating the desalted compounds. This one-flow reaction system yields higher amounts of the target product compared to batch desalting, and by integrating coupling reactions, it allows for the synthesis of pharmaceutical key precursors in a single step.

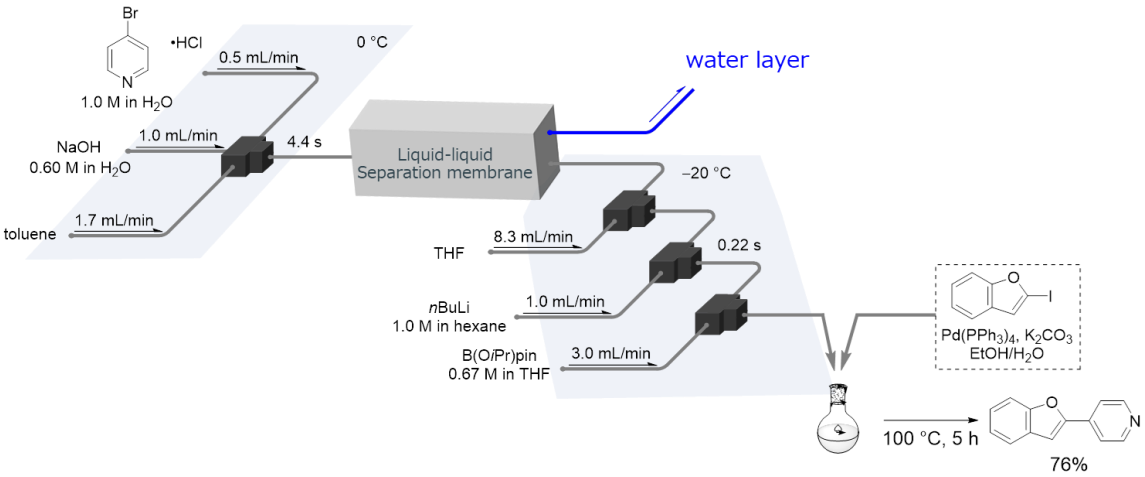

Figure 5: One-flow reaction through linear integration of desalination, water separation and water-sensitive reactions (Chapter 3)

In Chapter 4, the author demonstrated a rapid activation method for irreversibly generating carbocations using superacids in a flow system, followed by their direct reaction with carbanions in a convergent manner. The mixing efficiency of olefin derivatives and superacids was found to be critical for carbocation generation, and the microflow synthesis method proved to be highly effective in this process. Surprisingly, it was revealed that when carbocations and carbanions directly react, C–C bond formation occurs. This reaction can be applied to various cation and anion structures. Using this method, the author successfully achieved the efficient synthesis of asymmetric alkynes, which had previously been difficult to access.

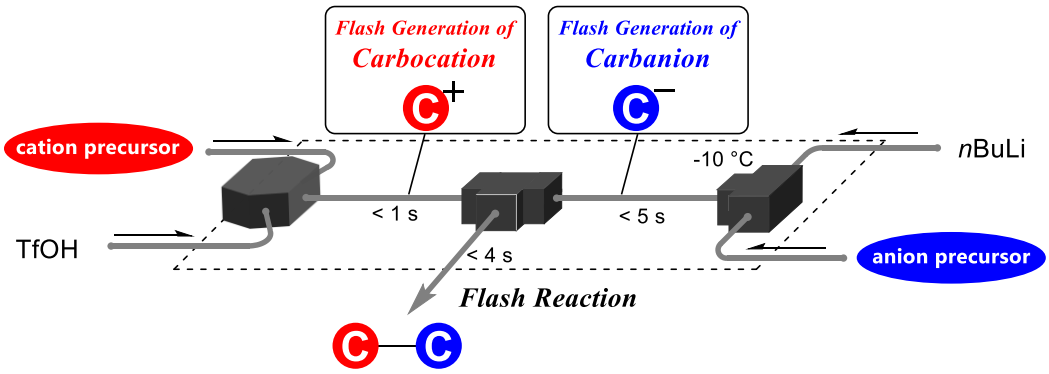

Figure 6: Direct C-C bond formation reaction between carbocation and carbanion by convergent reaction integration (Chapter 4)

References

1. (a) Capaldo, L.; Wen, Z.; Noël, T. *Chem. Sci.* **2023**, *14*, 4230. (b) Plutschack, M. B.; Pieber, B.; Gilmore, K.; Seeberger, P. H. *Chem. Rev.* **2017**, *117*, 11796. (c) Hartman, R. L.; McMullen, J. P.; Jensen, K. F. *Angew. Chem. Int. Ed.* **2011**, *50*, 7502. (d) Hessel, V.; Mukherjee, S.; Mitra, S.; Goswami, S.; Tran, N. N.; Ferlin,F.; Vaccaro,L.; Galogahi, F. M.; Nguyen, N.-T.; Escribà-Gelonch, M. *Green Chem.* **2024**, *26*, 9503.
2. R. L. Hartman, K. F. Jensen, *Lab on a Chip* **2009**, *9*, 2495.
3. (a) Monbaliu, J.-C. M.; Legros, J. *Lab Chip*, **2023**, *23*, 1349. (b) Rodriguez-Zubiri, M.; Felpin, F.-X. *Org. Process Res. Dev.* **2022**, *26*, 1766.
4. (a) Laporte, A. A. H.; Masson,T. M.; Zondag, S. D. A.; Noël, T. *Angew. Chem. Int. Ed.,* **2024**, *136*, e202316108. (b) Britton, J.; Raston, C. L. *Chem. Soc. Rev.*, **2017**, *46*, 1250. (c) Kobayashi, S. *Chem. Asian J.* **2016**, *11*, 425.(d) Gutmann, B.; Cantillo, D.; Kappe, C. O. *Angew. Chem. Int. Ed.* **2015**, *54,* 6688. (e) Tonhauser, C.; Natalello, A.; Löwe, H; Frey, H. *Macromolecules* **2012**, *45*, 9551.
5. (a) Petersen, T. P.; Becker, M. R.; Knochel, P. *Angew. Chem. Int. Ed.* **2014**, *53*, 7933. (b) Yoshida, J.; Takahashi, Y.; Nagaki, A. *Chem. Commun.* **2013**, *49*, 9896. (c) Nagaki, A.; Ashikari, Y.; Takumi, M.; Tamaki, T. *Chem. Lett.* **2021**, *50*, 485. (d) Shamoto, O.; Komuro, K.; Sugisawa, N.; Chen, T-H. Nakamura, H.; Fuse, S. *Angew. Chem. Int. Ed.* **2023**, *62*, e202300647.
6. (a) Usutani, H.; Nihei, T.; Papageorgiou C. D.; Cork, D. G. *Org. Process Res. Dev.* **2017**, *21*, 663. (b) Lee, H.-J.; Joo, J.-U.; Yim, S.-J.; Kim, D.-P.; Kim,H. *Nat. Commun, **2023**, 14*, 1231. (c) Colella, M.; Tota, A.; Takahashi, Y.; Higuma, R.; Ishikawa, S.; Degennaro, L.; Luisi, R.; Nagaki, A. *Angew. Chem. Int. Ed.* **2020**, *59*, 10924. (d) Fuse, S.; Mifune, Y.; Takahashi, T. *Angew. Chem. Int. Ed.* **2014**, *53*, 851.
7. (a) Nagaki, A.; Ashikari, Y.; Takumi, M.; Tamaki, T. *Chem. Lett.* **2021**, *50*, 485. (b) Yoshida, J.; Takahashi, Y.; Nagaki, A. *Chem. Commun.* **2013**, 49, 9896.
8. (a) Ashikari, Y.; Kawaguchi, T.; Mandai, K.; Aizawa, Y.; Nagaki, A. *J. Am. Chem. Soc.* **2020**, *142*, 17039. (b) Ichinari, D.; Ashikari, Y.; Mandai, K.; Aizawa, Y.; Yoshida, J.; Nagaki, A. *Angew. Chem. Int. Ed.* **2020**, *59*, 1567. (c) Nagaki, A.; Yamashita, H.; Hirose, K.; Tsuchihashi, Y.; Takumi, M.; Yoshida, J. *Chem. Eur. J.* **2019**, *25*, 13719.
9. Nagaki, A.; Yoshida, J. *J. Am. Chem. Soc.*, **2014**, *136*, 12245.
10. Takahashi, Y.; Ashikari, Y.; Takumi, M.; Shimizu, Y.; Jiang, Y.; Higuma, R.; Ishikawa, S.; Sakaue, H.; Shite, I.; Maekawa, K.; Aizawa, Y.; Yamashita, H.; Yonekura, Y.; Colella, M.; Luisi, R.; Takegawa, T.; Fujita, C.; Nagaki, A., *Eur. J. Org. Chem.* **2020**, 618. (b) Nagaki, A.; Imai, K.; Kim, H.; Yoshida, J. *RSC Adv.*, **2011**, *1*, 758.
11. Nagaki, A.; Tomida, Y.; Yoshida, J. *Macromolecules,* **2008***, 41*, 6322.
12. Schwieter, K. E.; Schwieter, J. N. *J. Am. Chem. Soc.* **2016**, *138*, 14160.

13. Olah, G. A.; Prakash, G. K. S. Carbocation Chemistry (Joen Wiley & Sons, Inc., 2004).
14. (a) Yoshida, J.; Shimizu, A.; Hayashi, R. *Chem. Rev.,* **2018***, 118,* 4702. (b) Suga, S.; Nishida, T.; Yamada, D.; Nagaki, A.; Yoshida, J. *J. Am. Chem. Soc.* **2004**, *126*, 14338. Yoshida, J.; Suga, S. *Chem. Eur. J.* **2002**, *8*, 2650.
15. (a) Nagaki, A.; Takumi, M.; Tani, Y.; Yoshida, J. *Tetrahedron,* **2015**, *71*, 5973. (b) Ashikari, Y.; Nagaki, A.; Yoshida, J. *Chem. Eur. J.* **2019**, *25*, 15239.
16. Takumi, M.; Sakaue, H.; Nagaki, A. *Angew. Chem. Int. Ed.* **2022***, 134*, e202116177.
17. Olah, G. A.; Prakash, G. K. S.; Molnar, A.; Sommer, J. Superacid Chemistry (Wiley, 2009).
18. Lebedel, L.; Yamashita, H.; Shimizu, Y.; Bhuma, N.; Abada, Z.; Ardá, A.; Désiré, J.; Michelet, B.; Mingot, A.; Abou-Hassan, A.; Takumi, M.; Jiménez-Barbero, J.; Nagaki, A.; Blériot, Y.; Thibaudeau, S. *Angew. Chem., Int. Ed.* **2021**, *60*, 2036.

Chapter 2
Highly productive flow synthesis for lithiation, borylation, and/or Suzuki coupling reaction

Abstract

The efficient synthesis of aromatic boronic acids was achieved by the increasing concentration, flow rate, and mixer diameter to pre-vent clogging. One hour synthesis actually produced 180 g of boronic acid. The real-time analysis of the reaction solution was investigated using in-line analyzers suitable for high flow rates. Additives were also studied to accelerate the Suzuki coupling reaction of boronic acids. Integrated one-flow reactions combining boronic acid synthesis and Suzuki coupling produced pharmaceutical pre-cursors in 97–143seconds.

Introduction

Organic synthesis has traditionally been performed in a batch system; however, in recent years, flow-type organic synthesis has attracted attention for its reaction selectivity, scalability, safety, and space efficiency.[1,2] Flow synthetic reactions increase production by extending the reaction time.[3]

For large-scale production, it is important to increase the production per unit time. To increase productivity, the concentration and flow rate should be increased: however, the following problems are expected when aiming for a continuous flow reaction. When the flow rate is increased, the reactor must be longer to complete the reaction, resulting in higher pressure. When the chemical reaction is slow, the reactor must be longer or the flow rate must be lower to complete the reaction, making it unsuitable for the design of highly productive flow reaction systems. However, a fast reaction requires short reactors even under high flow rate conditions, making it easier to design synthetic systems that can tolerate highly productive flow conditions (Fig. 1a). An example of a fast reaction is the halogen-lithium exchange reaction, which can be completed within seconds for the subsequent reaction with electrophiles. We have previously reported selective halogen-lithium exchange reactions using flow microreactors.[4] In addition, by connecting the flow reactors and integrating multiple chemical reactions, it is possible to synthesize high-value compounds, such as pharmaceuticals, in a single flow reaction.[5]

As the concentration increases to enhance productivity, operational problems such as side reactions and clogging are more likely to occur. If clogging events are anticipated under high concentration conditions, it is important to analyze the reaction mixture using in-line analytical techniques (Fig. 1b).[6]

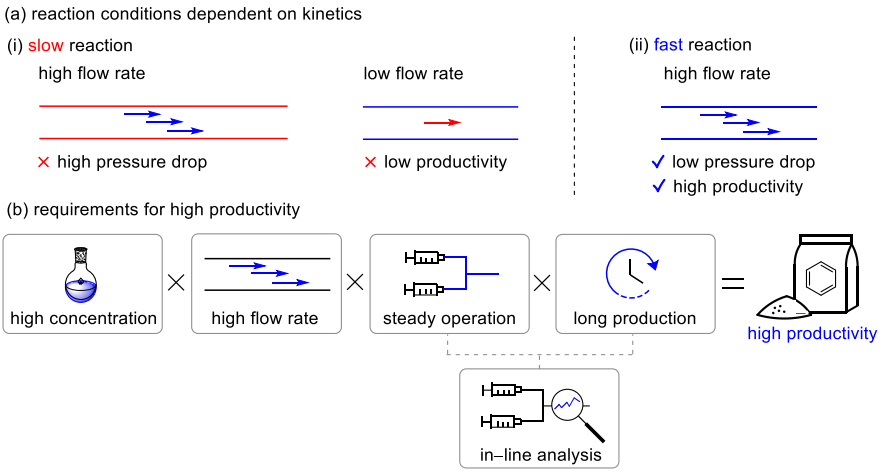

Figure 1. Requirements for high productivity synthesis.

Herein, I report a study on the efficient conditions for the production of key pharmaceutical precursors using flow-type reactions; a one-hour-continuous operation successfully yielded 197 g of a boronic acid. By selecting in-line analytical equipment that can be used even under high flow rate conditions, it was confirmed that in-line NIR and IR would not exhibit spectral changes in the range of 1–45 mL/min. Finally, I investigated the conditions for fast Suzuki coupling reactions of boronic acids, integrated these reactions, successfully constructed one-flow reactions that can be completed within a few minutes, and synthesized pharmaceutical precursors in high yields.

Results and discussion

Aromatic boronic acids are used in the synthesis of pharmaceuticals and other value-added compounds.[7] I studied the lithiation and subsequent borylation of aryl bromides to determine the highly productive conditions by increasing the concentration and flow rate. Especially, I chose 4-bromobenzonitrile (**1a**), because of its applicability to pharmaceuticals, as the substrate. I tested lithiation of **1a** with *n*BuLi followed by reaction with B(O*i*Pr)$_3$ in batch reactors with varying the temperature and the concentration. Under the low temperature (−78 °C) with diluted (0.1 mol/L) condition, desired product **2a** was obtained in moderate yield. Whereas the higher temperature and/or the condensed condition resulted in low yields (Fig. 2a), presumably owing to side reactions in which organolithium species react with the cyano groups.[8] We have reported that such lithiation reactions with the fragile functional groups can be performed with high selectivity using flow microreactors.[9] In fact, when this reaction was performed in flow microreactors, **2a** was obtained in 88% yield even under the intense condition of high concentration at 0 ºC. Furthermore, I successfully synthesized boronic acids of various pharmaceutical precursors (**2b**–**2d**) at high concentrations in 90–94% yields (Fig. 2b).

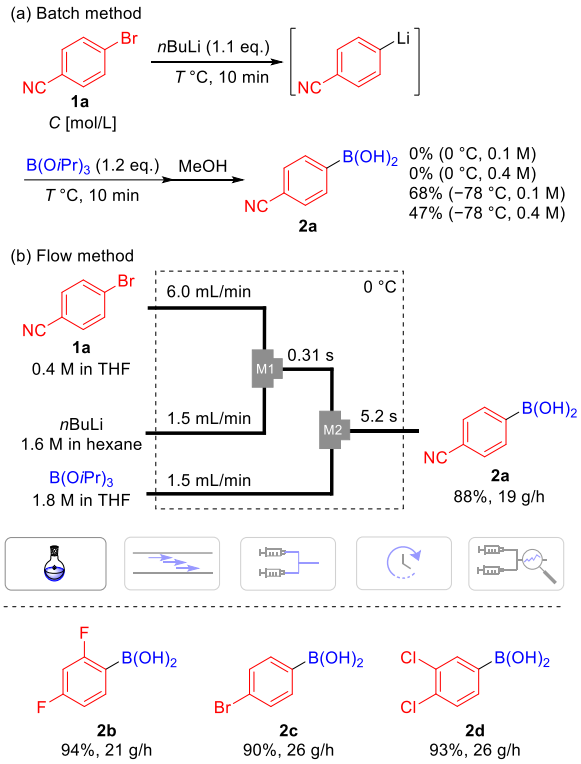

Figure 2. Synthesis of boronic acids through lithiation (a) in batch reactor or (b) in flow microreactor. Yields were determined by LC.

Subsequently, I focused on the flow rate (Fig. 3). Increasing the flow rate did not diminish the reaction yield, leading to a proportional increase in productivity. Additionally, a lower temperature (−20 °C) slightly increased the yield to 93%, which was achieved with a total reaction time of only 0.83 seconds, and the productivity reached 197 g/h. This indicates that a lower temperature can suppress side reactions, and improve the yield. However, the lower temperature increases the risk of clogging due to a decrease in the solubility of the compounds. In fact, when the reaction was carried out −40 °C, the reactor was clogged.

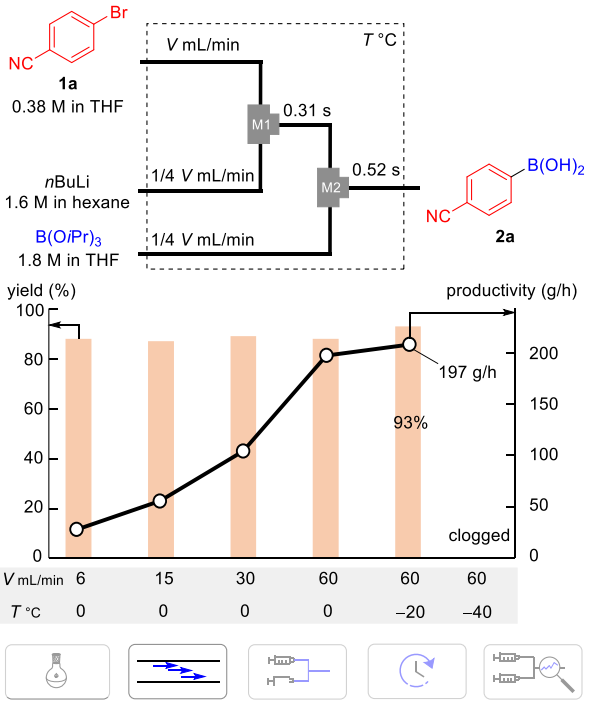

Figure 3. Flow synthesis of boronic acid **2a** with varying the flow rate and the temperature. Yields were determined by LC.

Since the clogging may ruin the continuous operation, we evaluated the conditions under which the product yield could be maintained even when the inner diameter of the micromixer was increased. The yield decreased when the inner diameter of the mixer was changed from 0.5 mm to 1.3 mm, but the yield improved when the temperature was lowered. Lowering the temperature to −40 °C resulted in a tendency to clog, hence the mixer inner diameter of 1.3 mm and temperature of −20 °C were determined as the optimum conditions that would provide good yields and reduce clogging events (Fig. 4a). Continuous operation under the optimized condition showed no yield changes for 60 minutes, producing 187 g of **2a** (Fig. 4b).

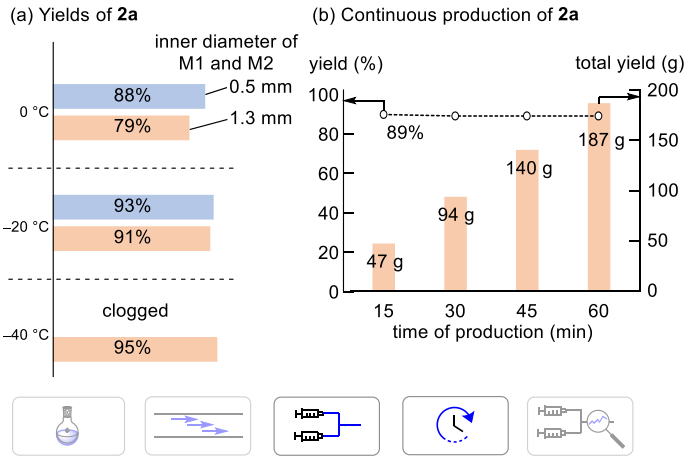

Figure 4. Study of (a) steady operation and (b) continuous flow synthesis of **2a**. Yields were determined by LC.

Since the highly productive flow synthesis of boronic acids was established, I then moved to in-line analyses. As a starting material, 1-bromo-2,4-difluorobenzene (**1b**), which is prone to occur clogging events owing to the possible side reactions of benzyne generation,[10] was selected. To determine the practical and highly productive synthetic conditions, I examined the high flow rate conditions. Unfortunately, the too high flow rate condition resulted in moderate yield, presumably because higher flow rate conditions diminished the heat removal from the reaction and caused the side reactions of benzyne generation. However, with a relatively high flow rate, where flow rate of **1b** was 30 mL/min, desired boronic acid **2b** was obtained in a high yield (Fig. 5a).

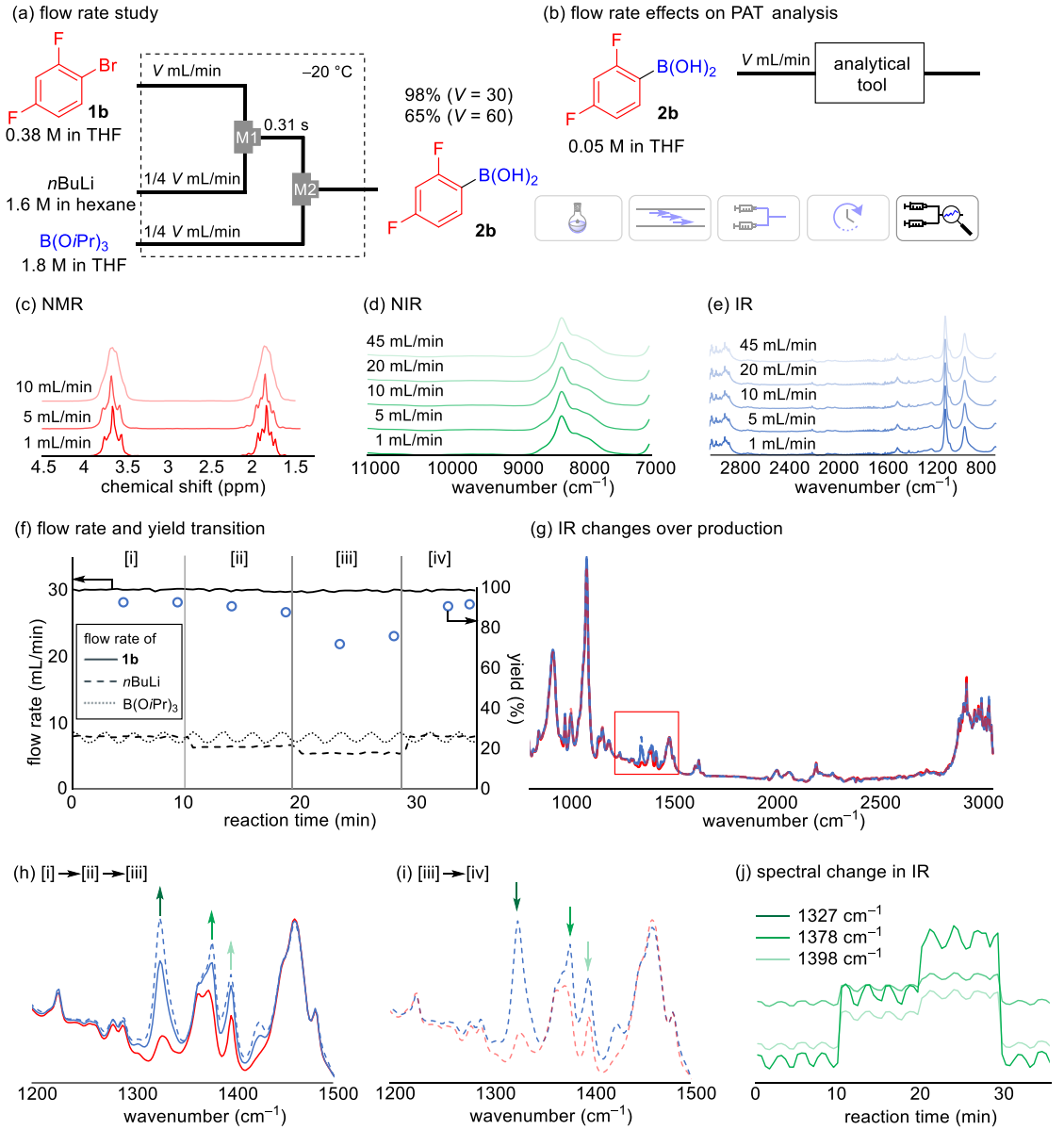

Figure 5. In-line analysis of continuous production. (a) Schematic of flow synthesis. (b) Schematic for in-line monitoring test. (c) in-line ^{1}H NMR with varying flow rate, (d) in-line NIR with varying flow rate (e) in-line FTIR with varying flow rate. (f) Changes of **2b** yields and flow rate in continuous operation with changing the flow rate of *n*BuLi. (g)–(j) Changes of in-line FTIR spectra.

To detect errors in the reaction mixture during operation, I constructed continuous flow systems connected to real-time analyzers. To select the suitable analytical tool, I performed in-line analysis of **2b** with varying the flow rate (Fig. 5b). The spectra obtained from in-line ^{1}H NMR (Magritek, Spinsolve 60) were strongly influenced by the flow rate, and the high flow rate made the peaks vague (Fig. 5c). This is because the relaxation time for the ^{1}H NMR measurements is not enough faster than the residence time of the solution in the probe.[11] Whereas, NIR (BeatSensing, BS-F1700, Fig. 5d) and FTIR (Mettler Toledo, ReactIR 15, Fig. 5e) showed no changes within the range of the flow rate from 1.0 to 45 mL/min. Thus, I deduced that the flow in-line analysis of NIR and IR was possible even at the high flow rate of 45 mL/min. Since NIR showed simpler spectra, and FTIR is more likely to exhibit the characteristics of each compound, we selected FTIR as the suitable in-line measurement.

In demonstration of the in-line error detection, I primarily focused on validating clogging, a critical incident in the flow reaction. In this reaction, clogging may occur owing to insoluble LiOH generated from *n*BuLi with water, leading to a decrease in the amount of *n*BuLi. Assuming such situations, I sequentially conducted the reaction under the optimal condition and the conditions with lower flow rate of *n*BuLi, simulating a clogging situation. I initially conducted the reaction of **1b** with *n*BuLi under the optimized condition for 10 minutes, which afforded **2b** in 95% yield (Fig. 5f-[i]). Subsequently, I reduced the flow rate of *n*BuLi to 80% of the optimal one, and after 10 minutes, I further reduced the flow rate to two-thirds of the optimal one (Fig. 5f-[ii] and [iii]). After the 30-minutes reaction, I restored the flow rate to the optimal one (Fig. 5f-[iv]). In the condition [ii] and [iii], the yields decreased, but the original condition ([iv]) restored the yield to 95%.

I then focused on the internal properties of the reaction. In-line FTIR, especially wavenumbers of 1300–1400 cm^{-1}, showed a remarkable difference in reaction solution (Fig. 5g). The intensity of the peaks in this area increased when the flow rate of *n*BuLi was decreased (Fig. 5h). Whereas, when the flow rate was returned to the original one ([iii] to [iv]), the intensity was decreased (Fig. 5i), and finally, the spectrum was the same as the initial one (Fig. 5j). These results showcase the feasibility of in-line validation of the clogging of the flow reaction.

As demonstrated above, I have investigated the effects on the flow rate, the concentration, and the inner diameter of the mixer on the boronic acid synthesis reaction. I demonstrated continuous boronic acid operation for 60 minutes, and explored analytical methods using in-line analyzers under high flow-rate conditions. This study showcases a highly productive approach to the flow synthesis of boronic acids.

In flow synthesis, complex compounds can be synthesized in a single flow system through reaction integration,[1c] and this method can be used to obtain compounds with drug-like structures. Actually, by integrating the lithiation, borylation, and Suzuki coupling reactions,[12,13] I have demonstrated one-flow synthesis of pharmaceutical precursors.[14] When integrating multi-step reactions, it is preferable to use fast reactions in terms of the pressure drop. However, Suzuki coupling reactions are relatively slow, and the key to constructing a one-flow reaction system is how short it takes to complete the whole reaction. Thus, to achieve the one-flow reaction system, I initially investigated the acceleration of the flow coupling reaction. I chose the coupling reaction of lithium 2-cyanophenylboronate (**3e**), which is the crude product of the lithiation and borylation of 2-bromobenzonitrile (**1e**), with 4-bromobenzaldehyde (**4a**), because their coupling product **5ea** is a precursor of sartan drugs.[15]

I studied the additives of the reaction (Table 1) because we have already reported that Suzuki coupling using arylboronates could be accelerated by addition of water.[12b] The reactions of **3e** with **4a** showed the similar tendency; the reaction was significantly accelerated when water was added (entries 1–3). When the reaction time was elonged to 411 seconds, **4a** was almost fully consumed and the **5ea** was obtained in 90% yield (entry 4). Further evaluation of the mixing efficiency showed the acceleration of the reaction (entry 5). Interestingly, when the additive was mixed at room temperature, the yield was slightly diminished (entry 6), indicating the additive led to hydrolysis of **3e** to generate reactive intermediate. Finally, by adjusting the amount of water, **5ea** was obtained in 94% yield with a reaction time of 137 s (entry 7).

Table 1. Optimization of Suzuki coupling reaction of borate compound 3e.[a]

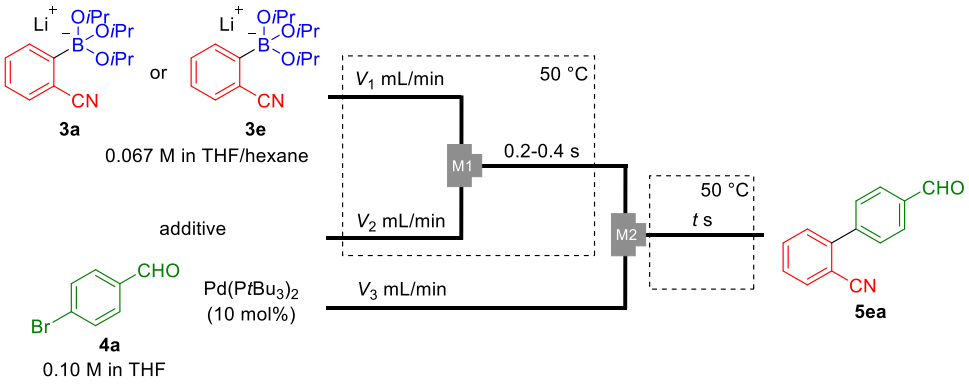

entry	additive	flow rate (mL/min) V_1	V_2	V_3	t (s)	recovery of **4a** (%)[c]	yield (%)[c]
1[a]	None	3.0	1.0	1.0	137	86	2
2[a]	MeOH	3.0	1.0	1.0	137	42	18
3[a]	H_2O	3.0	1.0	1.0	137	54	36
4[a]	H_2O	3.0	1.0	1.0	411	1	90
5[b]	H_2O	3.0	1.5	1.5	137	54	36[d]
6[b]	H_2O	8.0	2.7	2.7	137	34	69[d]
7[b]	H_2O	8.0	2.7	2.7	137	15	88
8[b]	H_2O	9.0	1.3	3.0	137	5	94

[a]The substrate was **3a.** [b]The substrate was **3e**. [c]Yields and recoveries were determined by GC. [d]The temperature of the first bath was room temperature.

The one-flow lithiation-borylation-coupling was performed using the integrated flow reactor shown in Figure 6. As optimized in Table 1, the Suzuki coupling was carried out for 137 seconds, enabling that valsartan precursor **5ea** could be obtained from the arylbromides in 99% yield within 143 seconds (Fig. 6a). This strategy was also applicable for synthesizing the precursor of diflunisal, a nonsteroidal anti-inflammatory drug.[16] The one-flow reaction of **1b** with methyl 2-methoxy-5-bromobenzoate (**4b**) was successfully carried out with 91% yield and a total reaction time of 97 seconds (Fig. 6b).

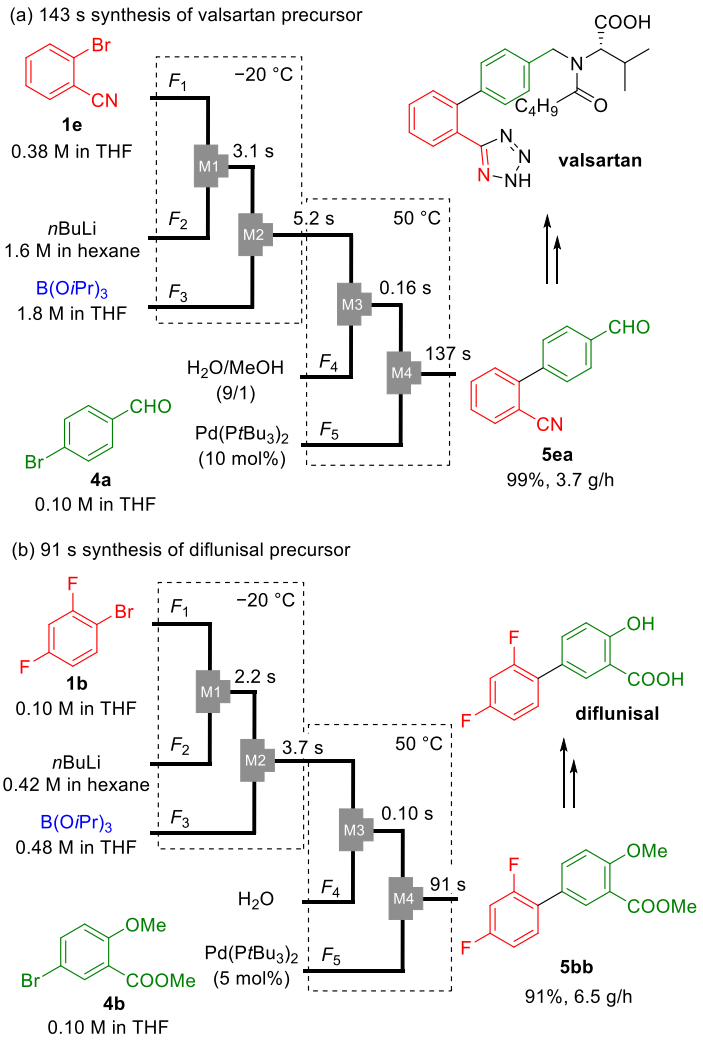

Figure 6. One-flow synthesis for drug precursors. (a) Synthesis of valsartan precursor. Flow rates: **1e**: 6.0 mL/min, *n*BuLi: 1.5 mL/min, B(O*i*Pr)$_3$: 1.5 mL/min, additive: 1.3 mL/min, **4a** and catalyst: 3.0 mL/min (b) Synthesis of diflunisal precursor. Flow rates: **1b**: 8.5 mL/min, *n*BuLi: 2.1 mL/min, B(O*i*Pr)$_3$: 2.1 mL/min, additive: 3.0 mL/min, **4a** and catalyst: 4.3 mL/min.

Conclusion

In summary, I developed the efficient flow synthesis conditions for aromatic boronic acid compounds. We found the conditions for both high productivity and steady operation by examining the flow rate, concentration, and the mixer diameter using a fast chemical reaction. In fact, 180 g of boronic acid was synthesized by continuous operation for 1 hour. In addition, an in-line analyzer applicable to the high flow rate conditions was selected and evaluated for the real-time analysis of the system during the operation. Additives were investigated to accelerate Suzuki coupling reaction using borate compounds generated by the flow reaction. These were combined to synthesize key precursors for pharmaceuticals in a one-flow reaction.

References

1. (a) Cambié, D.; Bottecchia, C.; Straathof, N. J. W.; Hessel, V.; Noël, T. *Chem. Rev.* **2016**, *116*, 10276–10341. (b) Plutschack, M. B.; Pieber, B.; Gilmore, K.; Seeberger, P. H. *Chem. Rev.* **2017**, *117*, 11796–11893. (c) Nagaki, A.; Ashikari, Y.; Takumi, M.; Tamaki, T. *Chem. Lett.* **2021**, *50*, 485–492.
2. (a) Petersen, T. P.; Becker, M. R.; Knochel, P. *Angew. Chem. Int. Ed.* **2014**, *53*, 7933–7937. (b) Fukuyama, T.; Fujita, Y.; Rashid, M. A.; Ryu, T. *Org. Lett.* **2016**, *18*, 5444–5446. (c) Ashikari, Y.; Kawaguchi, T.; Mandai, K.; Aizawa, Y.; Nagaki, A. *J. Am. Chem. Soc.* **2020**, *142*, 17039–17047. (d) Elsherbini, M.; Huynh, F.; Dunbabin, A. Allemann, R. K.; Wirth, T. *Chem. Eur. J.* **2020**, *26*, 11423–11425. (e) Ahn, G.-N.; Sharma, B. M.; Lahore, S.; Yim, S.-J.; Vidyacharan, S.; Kim, D.-P. *Commun. Chem.* **2021**, *4*, 53. (f) Saito, Y.; Nishizawa, K.; Laroche, B.; Ishitani, H.; Kobayashi, S. *Angew. Chem. Int. Ed.* **2022**, *61*, e202115643. (g) Steiner, A.; Krieger, J.; Jones, R.; Böse, D.; Wang, Y.; Eggenweiler, H.-M.; Williams, J. D.; Kappe, C. O. *ChemCatChem* **2022**, *14*, e202201184. (h) Jiang, Y.; Yorimitsu, H. *JACS Au* **2022**, *2*, 2514–2521. (i) Okamoto, K.; Higuma, R.; Muta, K.; Fukumoto, K.; Tsuchihashi, Y.; Ashikari, Y.; Nagaki, A. *Chem. Eur. J.* **2023**, *29*, e202301738. (j) Usutani, H.; Yamamoto, K.; Hashimoto, K. *ACS Omega* **2023**, *8*, 10373–10382. (k) Shamoto, O.; Komuro, K.; Sugisawa, N.; Chen, T-H. Nakamura, H.; Fuse, S. Angew. Chem. Int. Ed. 2023, 62, e202300647.
3. (a) Usutani, H.; Nihei, T.; Papageorgiou C. D.; Cork, D. G. *Org. Process Res. Dev.* **2017**, *21*, 669–673. (b) Nakahara, Y.; Furusawa, M.; Endo, Y.; Shimazaki, T.; Takahashi, Y.; Jiang, Y.; Nagaki, A. *Chem. Eng. Technol.* **2019**, *42*, 2154–2163.
4. (a) Nagaki, A.; Kim, H., Yoshida, J. *Angew. Chem. Int. Ed.* **2008**, *47*, 7833–7836. (b) Nagaki, A.; Kim, H.; Yoshida, J. *Angew. Chem. Int. Ed.* **2009**, *48*, 8063–8065. (c) Kim, H.; Nagaki, A.; Yoshida, J. *Nat. Commun.* **2011**, *2*, 264. (d) Colella, M.; Tota, A.; Takahashi, Y.; Higuma, R.; Ishikawa, S.; Degennaro, L.; Luisi, R.; Nagaki, A. *Angew. Chem. Int. Ed.* **2020**, *59*, 10924–10928.
5. (a) Nagaki, A.; Imai, K.; Kim, H.; Yoshida, J. *RSC Adv.* **2011**, *1*, 758–760. (b) Nagaki, A.; Imai, K.; Ishiuchi, S.; Yoshida, J. *Angew. Chem., Int. Ed.* **2015**, *54*, 1914–1918. (c) Nagaki, A.; Takahashi, Y.; Yoshida, J. *Angew. Chem., Int. Ed.* **2016**, *55*, 5327–5331. (d) Ichinari, D.; Ashikari, Y.; Mandai, K.; Aizawa, Y.; Yoshida, J.; Nagaki, A. *Angew. Chem. Int. Ed.* **2020**, *59*, 1567–1571.
6. Rodriguez-Zubiri, M.; Felpin, F.-X. *Org. Process Res. Dev.* **2022**, *26*, 1766–1793.
7. Hall, D. G. *Boronic Acids: Preparation and Applications in Organic Synthesis, Medicine and Materials*; Wiley-VCH, **2011**.
8. Parham, W. E.; Lawrence D. Jones, L. D. *J. Org. Chem.* **1976**, *41*, 1187–1191.
9. Nagaki, A.; Kim, H.; Usutani, H.; Matsuo, C.; Yoshida, J. *Org. Biomol. Chem.* **2010**, *8*, 1212–1217.
10. (a) Usutani, H.; Tomida, T.; Nagaki, A.; Okamoto, H.; Nokami, T.; Yoshida, J. *J. Am. Chem. Soc.* **2007**, *129*, 3046–3047. (b) Nagaki, A.; Ichinari, D.; Yoshida, J. *J. Am. Chem. Soc.* **2014**, *136*, 12245–12248.
11. The relaxation time of ^{1}H NMR is basically more than seconds, whereas the residence time in the channel of Spinsolve 60 is only 3 seconds at a flow rate of 10 mL/min (the volume of the flow tube: 0.523 mL).
12. (a) Shu, S.; Pellegatti, L.; Oberli, M. A.; Buchwald, S. L. *Angew. Chem. Int. Ed.* **2011**, *50*¸10665–0669. (b) Nagaki, A.; Moriwaki, Y.; Yoshida, J. *Chem. Commun.* **2012**, *48*, 11211–11213.
13. In addition to Suzuki coupling, one-flow lithiation-metallation-cross coupling reactions have been reported. For see; (a) Becker, M. R.; Ganiek, M. A.; Knochel, P. *Chem. Sci.* **2015**, *6*, 6649–6656. (b) Roesner, S.; Buchwald, S. L. *Angew. Chem. Int. Ed.* **2016**, *55*, 10463–10467. (c) Ashikari, Y.; Guan, K.; Nagaki, A. *Front. Chem. Eng.* **2022**, *4*, 964767.
14. (a) Takahashi, Y.; Ashikari, Y.; Takumi, M.; Shimizu, Y.; Jiang, Y.; Higuma, R.; Ishikawa, S.; Sakaue, H.; Shite, I.; Maekawa, K.; Aizawa, Y.; Yamashita, H.; Yonekura, Y.; Colella, M.; Luisi, R.; Takegawa, T.; Fujita, C.; Nagaki, A. *Eur. J. Org. Chem.* **2020**, 618–622. (b) Ashikari, Y.; Maekawa, K.; Takumi, M.; Tomiyasu, N.; Fujita, C.; Matsuyama, K.; Miyamoto, R.; Bai, H.; Nagaki, A. *Catal. Today* **2022**, *388–389*, 231–236.

15. (a) Bühlmayer, P.; Furet, P.; Criscione, L.; de Gasparo, M.; Whitebread, S.; Schmidlin, T.; Lattmann, R.; Wood, J. *Bioorg. Med. Chem. Lett.* **1994**, *4*, 29–34. (b) Goossen, L.J.; Melzer, B.J. *J. Org. Chem.* **2007**, *72*, 7473–7476. (c) Nagaki, A.; Hirose, K.; Tonomura, O.; Taga, T.; Taniguchi, S.; Hasebe, S.; Ishizuka, N.; Yoshida, J. *Org. Process Res. Dev.* **2016**, *20*, 687–691. (d) Tonomura, O.; Taniguchi, S.; Nishi, K.; Nagaki, A.; Yoshida, J.; Hirose, K.; Ishizuka, N.; Hasebe, S. *Catalysts* **2019**, *9*, 308.
16. Hannah, J.; Ruyle, W. V.; Jones, H.; Matzuk, A. R.; Kelly, K. W.; Witzel, B. E.; Holtz, W. J.; Houser, R. A.; Shen, T. Y.; Sarett, L. H. *J. Med. Chem.* **1978**, *21*, 1093–1100.

Supporting Information

1. General Information

Abbreviations. Butyl (Bu), degrees Celsius (°C), deuteritated chloroform ($CDCl_3$), centimeter(s) (cm), equivalent (eq.), ethyl acetate (EtOAc), Fourier transform infrared spectroscopy (FTIR), gram(s) (g), gas chromatography (GC), hour(s) (h), high performance liquid chromatography (HPLC), length of tubes (L), liter(s) (L), mol L^{-1} of molar concentration (M), milligram(s) (mg), minute(s) (min), milliliter(s) (mL), millimole(s) (mmol), mole(s) (mol), normal (*n*), near - infrared spectroscopy (NIR), nuclear magnetic resonance (NMR), poly(tetrafluoroethylene) or Teflon (PTFE), second(s) (s or sec), tetrahydrofuran (THF), thin layer chromatography (TLC), residence time of microtube reactor R_n (t^{Rn}), inner diameter of tubes and mixers (φ), micrometer(s) (μm).

General. NMR spectra were recorded on JEOL JNM-ECZ400S (^{1}H 400 MHz, ^{13}C 100 MHz). Chemical shifts are recorded using a solvent peak; 7.26 ppm for ^{1}H, 77.36 ppm for ^{13}C. NMR yields were calculated by NMR analyses with internal standards such as 1,1,2,2-tetrachloroethane. HPLC was performed on Shimadzu LC-10 with YMC TA12S05-2546WT (4.6 × 250 mm, acetone/water = 9/1, v/v, flow rate = 1.0 mL/min, 30 °C, UV = 220 nm) using commercial compounds. GC analysis was performed on a SHIMADZU GC-2014 gas chromatograph equipped with a flame ionization detector using a fused silica capillary column (column, CBP1; 0.22 mm x 25 m). Temperature of GC oven was 50 °C at first, and after 5min the temperature was increased 10 °C per min. GC yields were calculated by GC analyses with internal standards such as *n*-undecane using calibration lines derived from commercial or isolated compounds. Merck pre-coated silica gel F254 plates (thickness 0.25 mm) were used for TLC analyses. All batch reactions were carried out in a flame-dried glassware under argon atmosphere.

Flow Synthesis and Analysis. Stainless steel (SUS304) T-shaped micromixers with inner diameter of 500 was manufactured by Sanko Seiki Co., Inc. T-shaped mixer with inner diameter of 1300 μm was purchased from GL Science. Stainless steel (SUS316) microtube reactors with 1000 and 2200 μm inner diameter and PTFE tube with inner diameter of 1000 μm were purchased from GL Sciences. The syringe pumps (Harvard Model PHD ULTRA) equipped with gastight syringes (purchased from SGE) were used for introduction of the solutions into the micromixer systems via stainless steel fittings (GL Sciences, 1/16 OUW). Flow microreactor system is composed with stainless steel pre-cooling units (**P1**, **P2**, etc.), stainless steel microtube reactors (**R1**, **R2**, etc.), T-shaped micromixers (**M1**, **M2**, etc.), and, if necessary, PTFE tube with inner diameter of 1000 μm. Unless otherwise noted, the inner

diameter of the stainless and PTFE tubes is 1000 μm, and the length of the pre-cooling units is 100 cm. Unless otherwise noted, the inner diameter of micromixers is 500 μm. Spinsolve 60 (Magritek) was used for in-line ^{1}H NMR measurement; scan number: 4, acquisition time: 6.4 seconds, repetition time: 7 seconds, pulse angle: 90° . BS-F1700 (BeatSensing Co., Ltd.) was used for in-line NIR measurement. ReactIR 15 (Mettler Toledo) was used for in-line FTIR analysis; scan number: 76, scan interval: 30 seconds. The solution of *n*-butyllithium was prepared by dilution of the commercial solution with dehydrated *n*-hexane.

Materials. Dehydrated THF and *n*-hexane were purchased from FUJIFILM Wako Pure Chemical Corporation and Kanto Chemical Co., Inc., and were used without further purification. A solution of *n*-butyllithium (in *n*-hexane, 1.6 M) was purchased from Kanto Chemical Co., Inc. and stored at −20 °C. 4-Bromobenzonitrile, 1,4-dibromobenzene, 1-bromo-2,4-difluorobenzene, 1-bromo-3,4-dichlorobenzene, 4-bromobenzaldehyde, triisopropyl borate, methanol, water, and Pd(P*t*Bu$_3$)$_2$ were purchased from commercial suppliers, and were used without further purification.

2. Synthetic procedures

2.1 Halogen-lithium exchange reaction followed by reaction with B(O*i*Pr)$_3$ in batch reactors

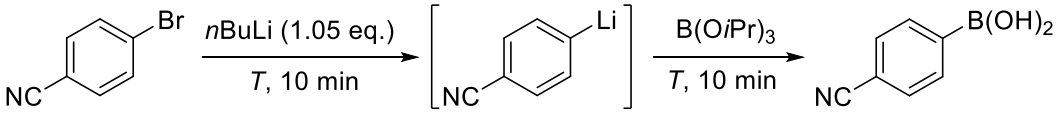

1a, *C* mol/L **2a**

To a solution of **1a** (*C* M in THF, 3.0 mL) was added *n*BuLi (1.51 M (1.05 eq.)) dropwise in a cooling bath (*T* °C). The mixture was stirred 10 min at the same temperature. To the reaction mixture was added B(O*i*Pr)$_3$ (1.2 eq.). After stirring at the same temperature for 10 min, the reaction was quenched with MeOH (4.0 mL). The yield of **2a** was analyzed by LC and was summarized in Table S1. The spectral data of **2a** were identical to those of reported in the literature.[1]

Table S1. Synthesis of **2a** in batch reactor

C (mol/L)	*T* (°C)	yield (%)
0.10	0	0
0.10	−78	68
0.40	0	0
0.40	−78	47

2.2 Halogen-lithium exchange reaction followed by reaction with $B(OiPr)_3$ in flow microreactors

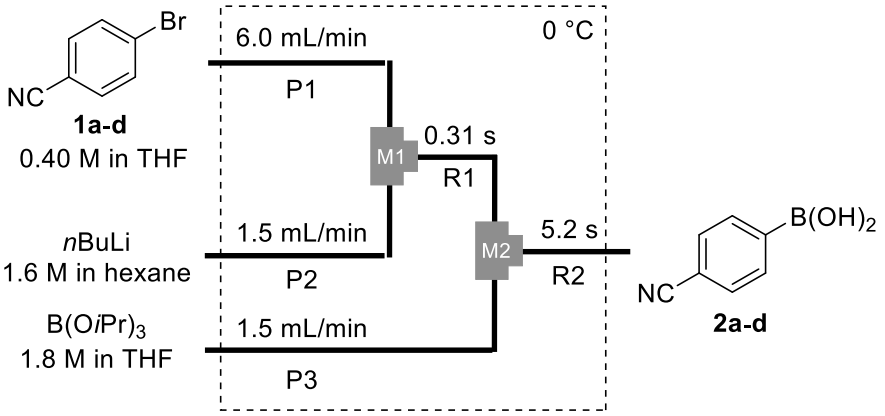

A flow microreactor system consisting of a T-shaped micromixer (**M1** and **M2**, φ = 500 μm), two microtube reactors (**R1** and **R2**), and three pre-cooling units (**P1**–**P3**) was used. The flow microreactor system was dipped in a cooling bath (0 °C). A solution of arylbromides (**1a**–**1d**, 0.38 M in THF, flow rate: 6.0 mL/min) and a solution of *n*BuLi (1.6 M in hexane, flow rate: 1.5 mL/min) were introduced into **M1** using syringe pumps. The mixed solution was passed through **R1** (5 cm, 0.31 s), and was mixed with a solution of $B(OiPr)_3$ (1.8 M in THF, flow rate: 1.5 mL/min) in **M2.** The resulting solution was passed through **R2** (100 cm, 5.2 s). After a steady state was reached, an aliquot of the reacting solution was collected and was treated with MeOH. The yields were determined by LC.

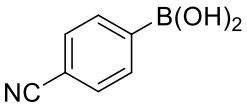

2a

4-Cyanophenylboronic acid (2a)
Obtained from 4-bromobenzonitrile (**1a**) in 88% yield. The spectral data were identical to those of reported in the literature.[1]

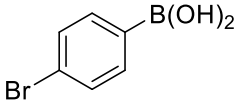

2b

4-Bromophenylboronic acid (2b)
Obtained from 1,4-dibromobenzene (**1b**) in 90% yield. The spectral data were identical to those of reported in the literature.[2]

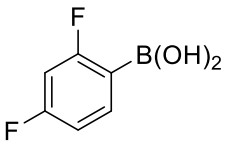

2c

2,4-Difluorophenylboronic acid (2c)
Obtained from 1-bromo-2,4-difluorobenzene (**1c**) in 94% yield. ^{1}H NMR (400 MHz, $CDCl_3$) δ 6.78-6.85 (m, 1H), 6.87-6.94 (m, 1H), 7.47-7.55 (m, 1H); ^{13}C NMR (100 MHz, DMSO-d_6) δ 103.4 (dd, *J* = 14.4Hz, 12.5 Hz), 110.0 (dd, *J* = 10.1 Hz, 1.5 Hz), 137.1 (d *J* = 5.3 Hz), 162.6 (d, *J* =6.2 Hz), 165.0 (dd, *J* = 6.2 Hz, 3.9 Hz), 167.4 (d, *J* = 6.2 Hz); HRMS (APCI) calcd for $C_6H_4O_2BF_2$ $[M-H]^+$: 157.0278, found: 157.0279.

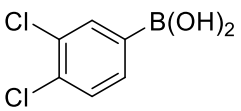

2d

3,4-Dichlorophenylboronic acid (2d)
Obtained from 1-bromo-3,4-dichlorobenzene (**1d**) in 93% yield. The spectral data were identical to those of reported in the literature.[3]

2.3 Investigation of flow rate and temperature for the synthesis of 2a

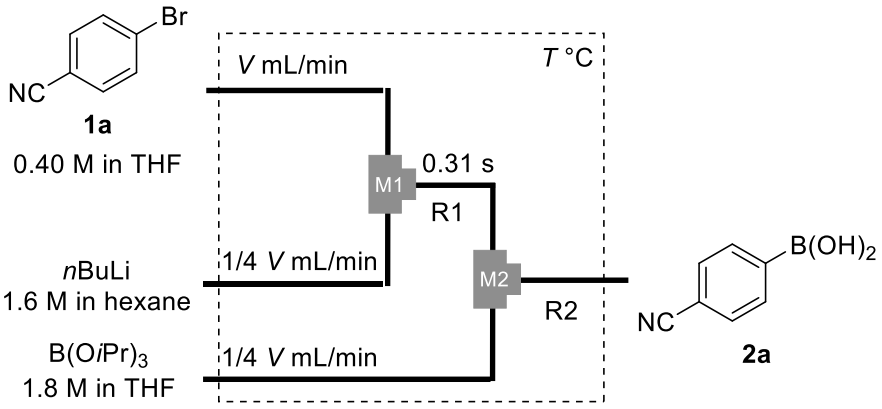

A flow microreactor system consisting of a T-shaped micromixer (**M1** and **M2**, inner diameter: φ_m μm), two microtube reactors (**R1** and **R2**), and three pre-cooling units (**P1**–**P3**, inner diameter: φ_p μm) was used. The flow microreactor system was dipped in a cooling bath (T °C). A solution of **1a** (0.40 M in THF, flow rate: V mL/min) and a solution of *n*BuLi (1.6 M in hexane, flow rate: 1/4 V mL/min) were introduced into **M1** using syringe pumps. The mixed solution was passed through **R1** (L cm, 0.31 s), and was mixed with a solution of B(O*i*Pr)$_3$ (1.82 M in THF, flow rate: 1/4 V mL/min) in **M2.** The resulting solution was passed through **R2** (100 cm). After a steady state was reached, an aliquot of the reacting solution was collected and was treated with MeOH. The yields were determined by LC and were summarized in Table S2.

Table S2. Flow synthesis of **2a** with varying flow rate, temperature, and inner diameters.

V (mL/min)	L (cm)	T (°C)	φ_m (μm)	φ_p (mm)	yield (%)	productivity (g/h)
6	5.0	0	500	1.0	88	19
15	12.5	0	500	1.0	87	46
30	25	0	500	1.0	89	94
60	50	0	500	1.0	88	186
60	50	−20	500	1.0	93	197
60	50	−40	500	1.0		clogged
60	50	0	1300	2.2	79	167
60	50	−20	1300	2.2	91	193
60	50	−40	1300	2.2	95	201

2.4 Continuous flow synthesis of 2a for 60 min

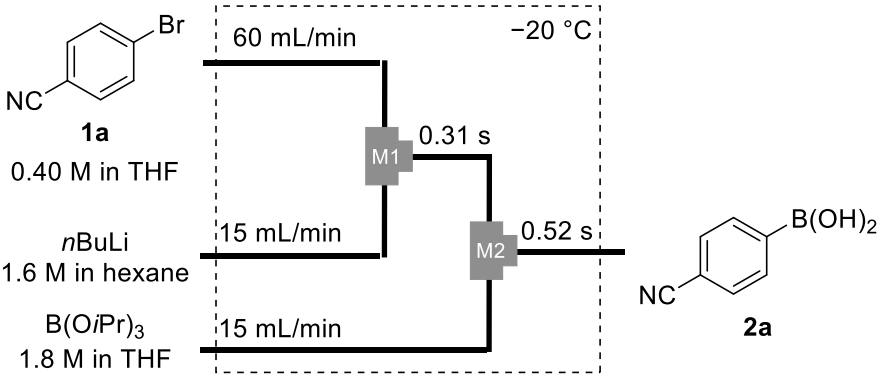

A flow microreactor system consisting of a T-shaped micromixer (**M1** and **M2**, φ = 1300 μm), two microtube reactors (**R1** and **R2**), and three pre-cooling units (**P1**–**P3**, φ = 2.2 mm) was used. The flow microreactor system was dipped in a cooling bath (−20 °C). A solution of **1a** (0.38 M in THF, flow rate: 60 mL/min) and a solution of *n*BuLi (1.6 M in hexane, flow rate: 15 mL/min) were introduced into **M1** using syringe pumps. The mixed solution was passed through **R1** (5 cm, 0.31 s), and was mixed with a solution of B(O*i*Pr)$_3$ (1.8 M in THF, flow rate: 15 mL/min) in **M2.** The resulting solution was passed through **R2** (100 cm, 0.52 s). After a steady state was reached, aliquots of the reacting solution was collected for every 15 minutes, and were treated with MeOH. The yields were determined by LC and were summarized in Table S3.

Table S3. Continuous synthesis of **2a**.

operating time (min)	yield (%)	total yield (g)
15	89	47
30	88	94
40	88	140
45	88	187

2.5 Investigation of flow rate for the synthesis of 2b

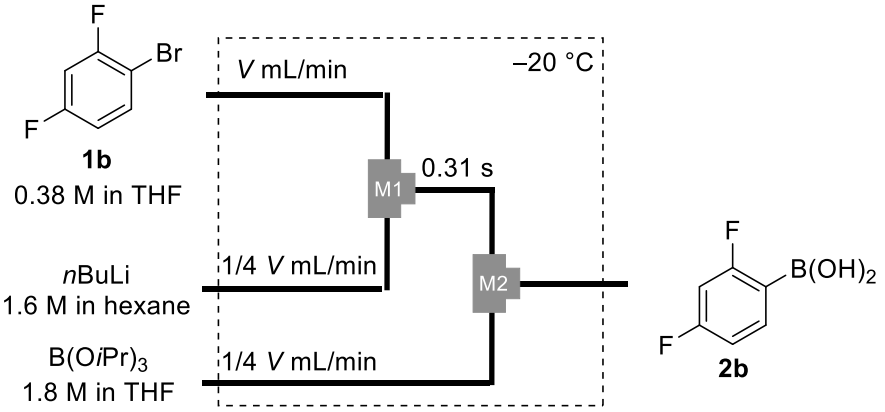

A flow microreactor system consisting of a T-shaped micromixer (**M1** and **M2**, φ = 500 μm), two microtube reactors (**R1** and **R2**), and three pre-cooling units (**P1**–**P3**) was used. The flow microreactor system was dipped in a cooling bath (−20 °C). A solution of **1b** (0.38 M in THF, flow rate: *V* mL/min) and a solution of *n*BuLi (1.6 M in hexane, flow rate: 1/4 *V* mL/min) were introduced into **M1** using syringe pumps. The mixed solution was passed through **R1** (5 cm, 0.31 s), and was mixed with a solution of B(O*i*Pr)$_3$ (1.82 M in THF, flow rate: 1/4 *V* mL/min) in **M2.** The resulting solution was passed through **R2** (100 cm). After a steady state was reached, an aliquot of the reacting solution was collected and was treated with MeOH. The yields of **2b** were determined by LC; 98% (*V* = 30), and 65% (*V* = 60).

2.6 Investigation of the flow rate dependency of in-line analytical tools

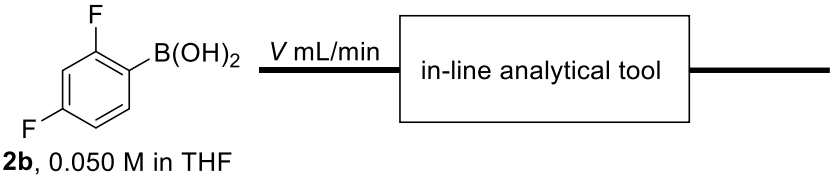

2b, 0.050 M in THF

A solution of **2c** (0.05 M in THF, flow rate: *V* mL/min) was introduced into in-line analytical tools (^{1}H NMR, NIR, and FTIR). The spectrum data collected by NMR (Figure S1), NIR (Figure S2), and FTIR (Figure S3) varying the flow rate (*V*) are shown below.

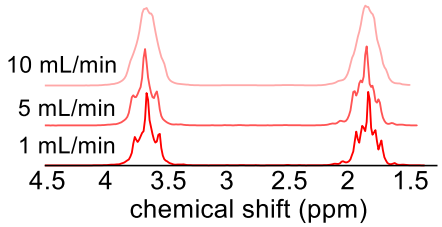

Figure S1. In-line ^{1}H NMR measurement of **2b** with varying flow rate.

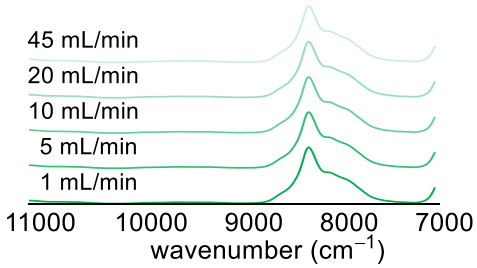

Figure S2. In-line NIR measurement of **2b** with varying flow rate.

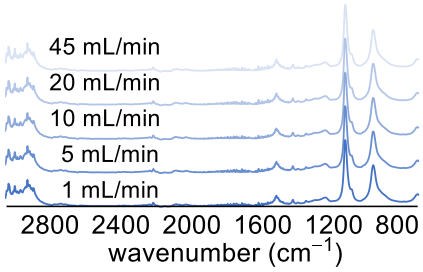

Figure S3. In-line FTIR measurement of **2b** with varying flow rate.

2.7 Continuous flow synthesis of 2b using reactIR with changing the flow rate of *n*BuLi

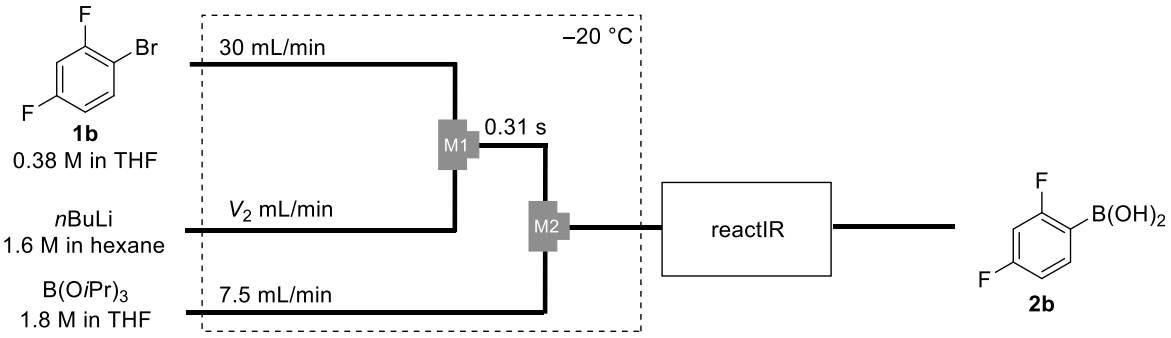

A flow microreactor system consisting of a T-shaped micromixer (**M1** and **M2**, φ = 500 μm), two microtube reactors (**R1** and **R2**), and three pre-cooling units (**P1**–**P3**) was used. The flow microreactor system was dipped in a cooling bath (−20 °C). A solution of **1b** (0.38 M in THF, flow rate: 30 mL/min) and a solution of *n*BuLi (1.6 M in hexane, flow rate: V_2 = 7.5 mL/min) were introduced into **M1** using syringe pumps. The mixed solution was passed through **R1** (5 cm, 0.31 s), and was mixed with a solution of B(O*i*Pr)$_3$ (1.8 M in THF, flow rate: 7.5 mL/min) in **M2.** The resulting solution was passed through **R2** (L^{R2}= 100 cm), and was passed through reactIR. After a steady state was reached, the reaction was continued in 10 min. Then, the flow rate of a solution of *n*BuLi was changed (V_2 = 6.0 mL/min). After 10 min, the flow rate of a solution of *n*BuLi was changed (V_2 = 5.0 mL/min). After 10 min, the flow rate of a solution of *n*BuLi was changed (V_2 = 7.5 mL/min). Over the continuous flow reaction, an aliquot of the reacting solution was collected every 5 min and was treated with MeOH. The yields were determined by LC and were summarized in Table S4. The IR char and its change are shown in Figure S4. The time course of the flow rate was measured with digital flow sensor (Keyence, FD-SS02A).

Table S4. Flow synthesis of **2b** with varying flow rate of *n*BuLi

flow rate of *n*BuLi (mL/min)	reaction time (min)	yield of **2b** (%)
7.5	5	95
	10	95
6.0	15	93
	20	90
5.0	25	74
	30	78
7.5	35	93
	40	94

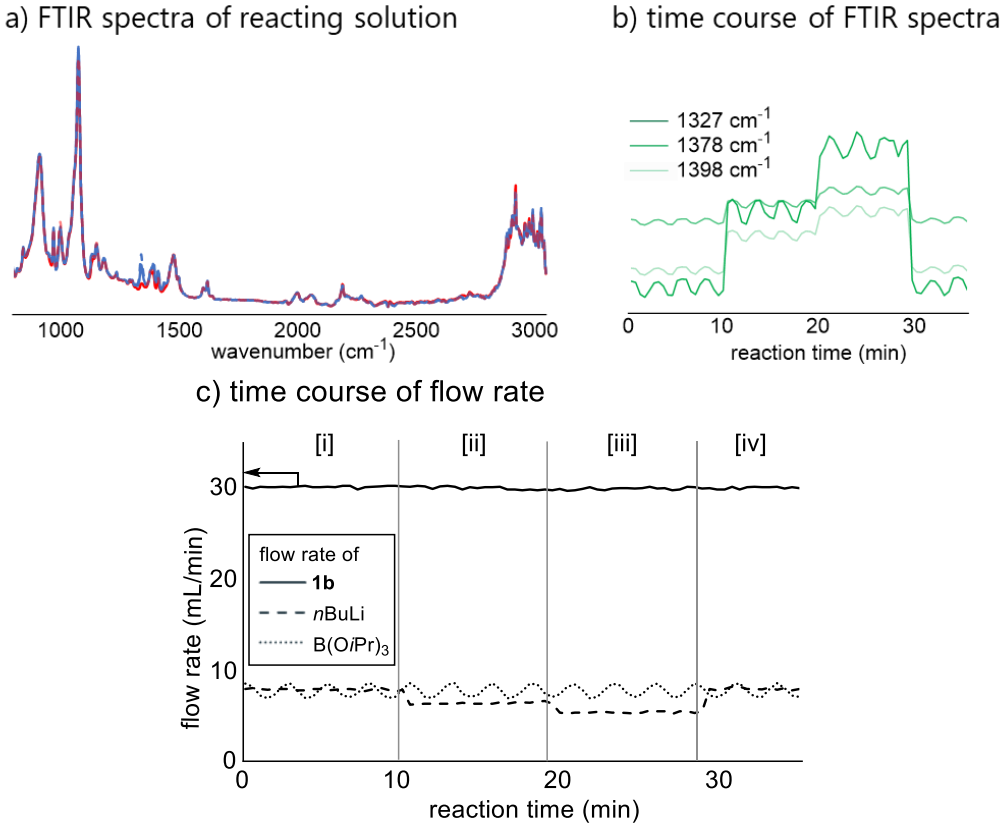

Figure S4. (a) FTIR spectra. (b) time course of FTIR spectra. (c) time course of flow rate

2.8 Additive study of Suzuki coupling reaction for reaction acceleration

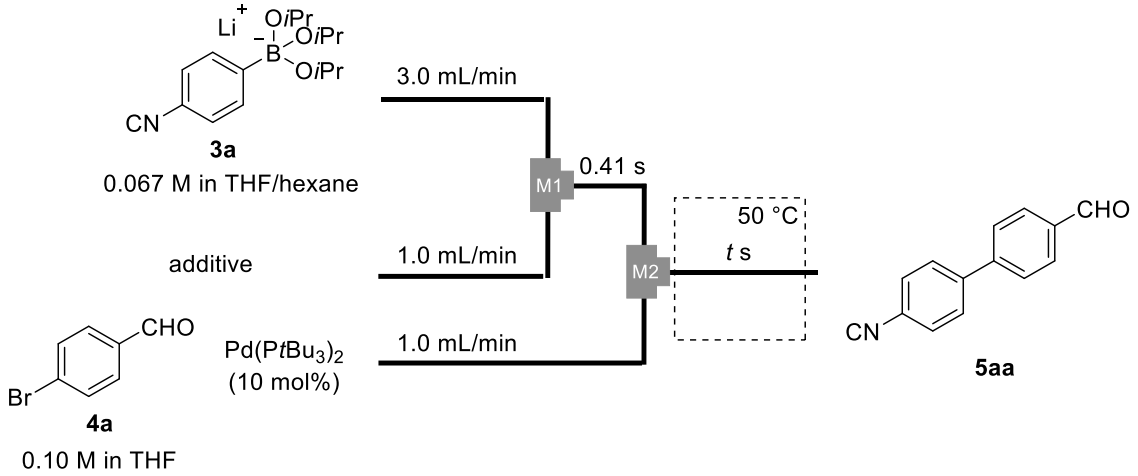

A flow microreactor system consisting of a T-shaped micromixer (**M1** and **M2**, φ = 500 μm), two microtube reactors (**R1** and **R2**), and three pre-cooling units (**P1**–**P3**) was used. The part of the flow microreactor system composed with **R2** was heated at 50 °C. A solution of **3a** (0.067 M in THF/hexane, flow rate: 3.0 mL/min, synthesized according to the procedure 2.2 ($C_{\mathbf{1a}}$ = 0.10 M)) and additive (1.0 mL/min) were introduced into **M1** using syringe pumps. The mixed solution was passed through **R1** (3.5 cm, 0.41 s), and was mixed with a solution of 4-bromobenzaldehyde (**4a**, 0.10 M) and Pd(P*t*Bu$_3$)$_2$ (10 mol% in THF, flow rate: 1.0 mL/min) in **M2.** The resulting solution was passed through **R2** (φ = 2.2 mm, L^{R2} cm, t^{R2} s). After a steady state was reached, an aliquot of the reacting solution was collected and was treated with a solution of NH_4Cl. The yields were determined by GC and were summarized in Table S5. The spectral data were identical to those of reported in the literature.[4]

Table S5. Additive effect for the reaction of **3a** with **4a**.

additive	L^{R2} (cm)	t^{R2} (s)	yield of **5aa** (%)	recovery of **4a** (%)
none	300	137	2	86
MeOH	300	137	18	42
water	300	137	36	54
water	800	411	90	1

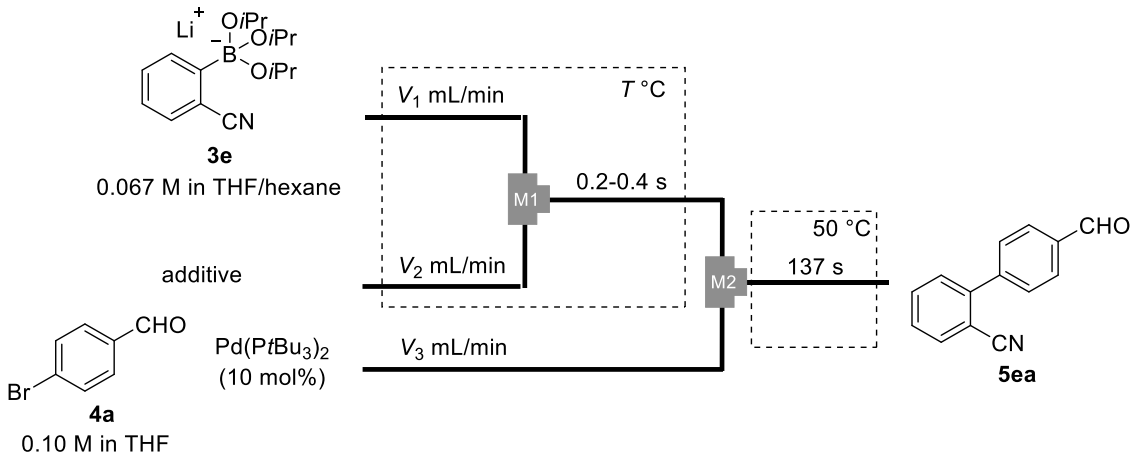

A flow microreactor system consisting of a T-shaped micromixer (**M1** and **M2**, φ = 500 μm), two microtube reactors (**R1** and **R2**), and three pre-cooling units (**P1**–**P3**) was used. The part of the flow microreactor system composed with **P1, P2, M1,** and **R1** was at *T* °C and the part of the flow microreactor system composed with **R2** was heated at 50 °C. A solution of **3e** (0.067 M in THF/hexane, flow rate: 3.0 mL/min, synthesized according to the method 2.2 ($C_{\mathbf{1e}}$ = 0.10 M)) and additive (1.0 mL/min) were introduced into **M1** using syringe pumps. The mixed solution was passed through **R1** (3.5 cm), and was mixed with a solution of **4a** (0.10 M) and Pd(P*t*Bu$_3$)$_2$ (10 mol% in THF, flow rate: 1.0 mL/min) in **M2.** The resulting solution was passed through **R2** (φ = 2.2 mm, L^{R2} cm, 137 s). After a steady state was reached, an aliquot of the reacting solution was collected and was treated with a solution of NH_4Cl. The yields were determined by GC and were summarized in Table S6. The spectral data were identical to those of reported in the literature.[5]

Table S6. Additive effect for the reaction of **3e** with **4a**

flow rate (mL/min)						
V_1	V_2	V_3	T (°C)	L^{R2} (cm)	yield (%)	recovery of **4a** (%)
3.0	1.5	1.5	r.t.	300	36	54
8.0	2.67	2.67	r.t.	800	69	34
8.0	2.67	2.67	50	800	88	15
9.0	1.33	3.0	50	800	94	5

2.9 One-flow synthesis of drug precursors

One-flow synthesis of precursor of sartans (General Procedure)

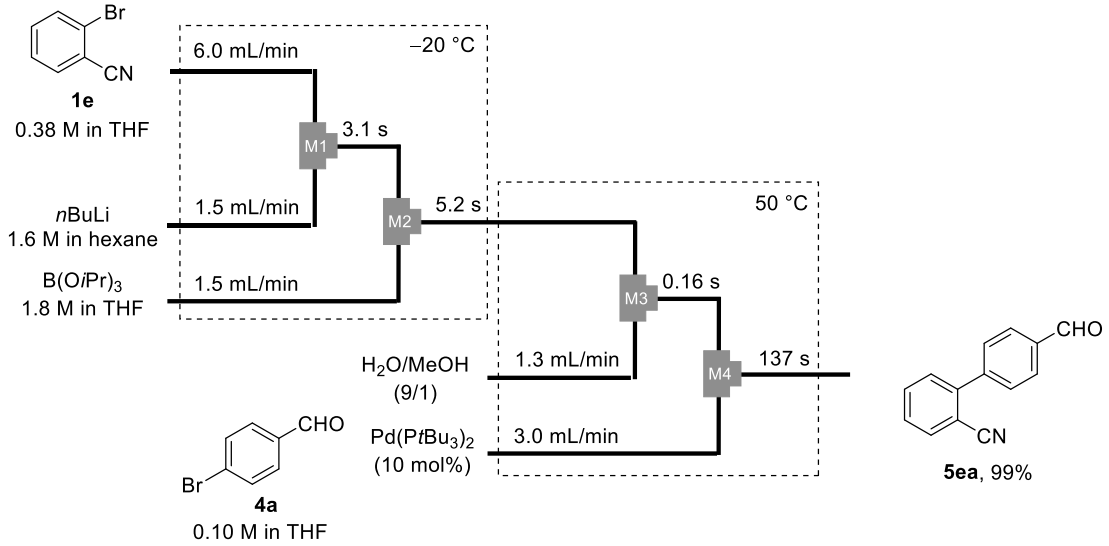

A flow microreactor system consisting of four T-shaped micromixers (**M1, M2, M3,** and **M4**, $\varphi_{M1, M2}$ = 500 μm, $\varphi_{M3, M4}$ = 1000 μm), four microtube reactors (**R1, R2, R3,** and **R4**), and three pre-cooling units (**P1**–**P5**, L_{P5} = 12.5 cm) was used. The part of the flow microreactor system composed with **P1, P2, P3, M1, M2, R1,** and **R2** was at −20 °C and the part of the flow microreactor system composed with **P4, P5, M3, M4, R2, R3,** and **R4** was heated at 50 °C. A solution of **1e** (0.38 M in THF, flow rate: 6.0 mL/min) and *n*BuLi (1.6 M in hexane, 1.5 mL/min) were introduced into **M1** using syringe pumps. The mixed solution was passed through **R1** (50 cm, 3.1 s), and was mixed with a solution of triisopropyl borate (1.8 M in THF, flow rate: 1.5 mL/min) in **M2.** The resulting solution was passed through **R2** (100 cm, 5.2 s) and was mixed with a solution of H_2O/MeOH (v/v = 9/1, flow rate: 1.3 mL/min) in **M3**. The resulting solution was passed through **R3** (3.5 cm, 0.16 s) and was mixed with a solution of **4** (0.10 M) and Pd(P*t*Bu$_3$)$_2$ (10 mol% in THF, flow rate: 3.0 mL/min) in **M4**. The resulting solution was passed through **R4** (φ = 2.2 mm, 800 cm, 137 s). After a steady state was reached, an aliquot of the reacting solution was collected and was treated with a solution of NH_4Cl, affording 2-cyano-4'-formylbiphenyl (**5ea**) in 99% yield determined by ^{1}H NMR.

One-flow synthesis of diflunisal precursor

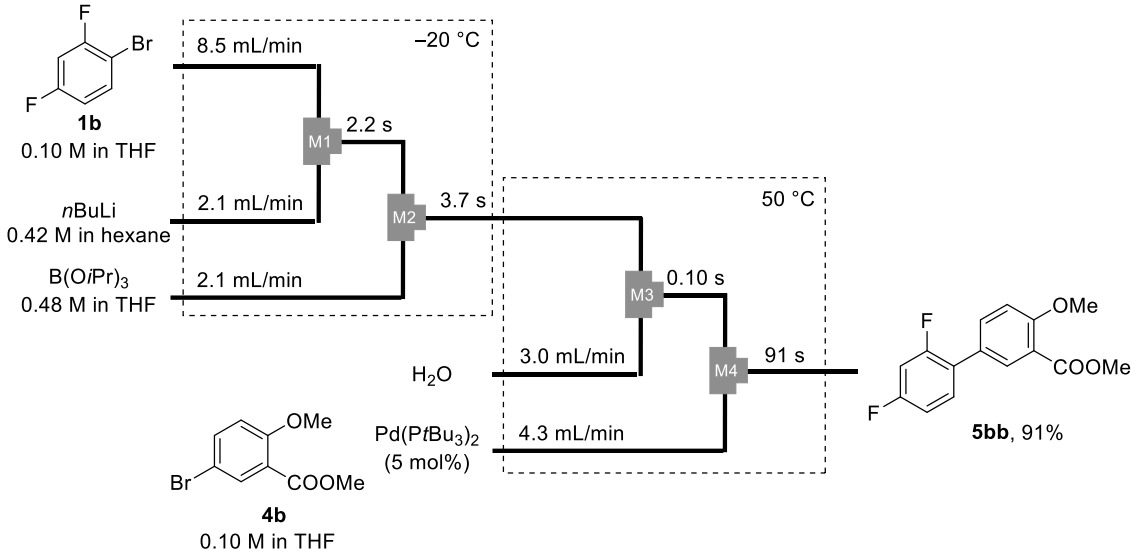

A flow microreactor system consisting of four T-shaped micromixers (**M1, M2, M3,** and **M4**, $\varphi_{M1, M2}$ = 500 μm, $\varphi_{M3, M4}$ = 1000 μm), four microtube reactors (**R1, R2, R3,** and **R4**), and three pre-cooling units (**P1**–**P5**, L_{P5} = 12.5 cm) was used. The part of the flow microreactor system composed with **P1, P2, P3, M1, M2, R1,** and **R2** was at −20 °C and the part of the flow microreactor system composed with **P4, P5, M3, M4, R2, R3,** and **R4** was heated at 50 °C. A solution of **1b** (0.10 M in THF, flow rate: 8.5 mL/min) and *n*BuLi (0.42 M in hexane, 2.1 mL/min) were introduced into **M1** using syringe pumps. The mixed solution was passed through **R1** (50 cm, 2.2 s), and was mixed with a solution of triisopropyl borate (0.48 M in THF, flow rate: 2.1 mL/min) in **M2.** The resulting solution was passed through **R2** (100 cm, 3.7 s) and was mixed with a solution of H_2O (flow rate: 3.0 mL/min) in **M3**. The resulting solution was passed through **R3** (3.5 cm, 0.10 s) and was mixed with a solution of methyl 2-methoxy-5-bromobenzoate (**5**, 0.10 M) and Pd(P*t*Bu$_3$)$_2$ (5 mol% in THF, flow rate: 4.3 mL/min) in **M4**. The resulting solution was passed through **R4** (φ = 2.2 mm, 800 cm, 91 s). After a steady state was reached, an aliquot of the reacting solution was collected and was treated with a solution of NH_4Cl to afford methyl 2-methoxy-5-(2,4-difluorophenyl)benzoate (**5bb**) in 91% yield determined by ^{1}H NMR. The spectral data were identical to those of reported in the literature.[6]

2.10 References

1. W. Erb, A. Hellal, M. Albini, J. Rouden, J. Blanchet, *Chem. Eur. J.* **20**, 6608–6612 (2014).
2. A. Hafner, M. Meisenbach, J. Sedelmeier, *Org. Lett.* **18**, 3630–3633 (2016).
3. L. D. Marciasini, J. Richard, B. Cacciuttolo, G. Sartori, M. Birepinte, L. Chabaud, S. Pinet, M. Pucheault, *Tetrahedron*. **75**, 164–171 (2019).
4. L. J. Goossen, B. Melzer, *J. Org. Chem.* **72**, 7473–7476 (2007).
5. J. I. Urgel, D. Ecija, W. Auwärter, D. Stassen, D. Bonifazi, J. V. Barth, *Angew. Chem. Int. Ed Engl.* **54**, 6163–6167 (2015).
6. W.-B. Chen, C.-H. Xing, J. Dong, Q.-S. Hu, *Adv. Synth. Catal.* **358**, 2072–2076 (2016).

Chapter 3
One-flow operation via 4-bromopyridine enables flash synthesis of AChE inhibitor

Abstract

4-Bromopyridine is a building block that can be converted into valuable compounds, but due to its low stability, it is commercially available in the form of hydrochloride salt. Therefore, the hydrochloride salt is usually desalted with a basic aqueous solution and dried before organic reaction. In this study, to simplify the preparation and reaction procedure of 4-bromopyridine, multiple operations, desalting with a base, separation of the aqueous layer, and subsequent halogen-lithium exchange reaction, were integrated into a single flow reaction. The reaction sequence was completed within 20 seconds and the yields were higher than the conventional methods. I believe this is because the subsequent reaction can be performed immediately after the generation of 4-bromopyridine, which is unstable under ambient conditions.

Introduction

Efficiency and sustainability are significant issues in modern organic chemistry,[1] and there is a constant need to rapidly obtain profitable compounds at a low cost. In terms of reaction efficiency, concepts such as atom,[2] step,[3] and pot economies[4] have been proposed. As noted in step and pot economy, reducing the number of synthetic reaction steps is essential for minimizing time, labor, waste, and expense while improving the overall yield of reactions.

However, to improve the efficiency of the organic reactions, it is important to reduce the number of operations involved.[5] In practice, it may be time-consuming to prepare the starting materials prior to synthesis. For example, some commercial compounds require specific processing operations such as dissolving and removing unnecessary inorganic salts in an aqueous layer as a pretreatment, extracting compounds to be used in a subsequent reaction into an organic solvent, separate water phase, and drying to replace the reaction solvent. These operations consume a significant amount of time compared to the actual reaction duration. If such experimental operations can be reduced, various costs can be reduced, and the efficiency of synthetic reactions can be enhanced.

In addition, simplifying the preparation of starting materials is beneficial when dealing with unstable compounds. Pyridine derivatives include unstable compounds, such as those with carbonyl chloride, carboxyamidine, acetic acid, and bromine groups at the 4-position, which

are commercially available in the form of stable hydrochloride salts. In particular, 4-bromopyridine can be transformed into useful compounds in various fields, such as pharmaceuticals[6] and materials,[7] and more efficient synthetic methods are required. When performing reactions where water must be avoided, such as halogen-lithium exchange reactions, commercial hydrochloride salts usually require multiple operations,[8] including desalting with a basic aqueous solution, water separation, drying the organic layer, and solvent replacement (Fig. 1(a)), which may lead to the decomposition of 4-bromopyridine.[9] If these operations can be simplified to shorter processes, this method could be used as a more practical organic synthesis method.

For example, the synthesis of pharmaceuticals with complex structures such as acetylcholinesterase (AChE) inhibitors, which are used in the treatment of Alzheimer's disease, requires multi-step reactions.[10]

Several studies have developed flash chemistry using flow microreactors that have been generated and reacted with highly reactive lithium intermediates.[11] Pyridyllithiums produced by the halogen-lithium exchange reactions of halopyridines are unstable and have been efficiently generated by flash reactions using flow microreactors.[12] Because 4-bromopyridine is commercially available in the form of the hydrochloride salt and its stability decreases after desalting, the yields may decrease in some operations. Therefore, I hypothesized that if 4-bromopyridine could be prepared in a simplified manner, it would be possible to generate 4-puridyllithium with high efficiency. Herein, I report a sequence of flow equipment that can be used for the treatment of 4-bromopyridine hydrochloride as a model compound, from the preparation of the starting material to the halogen-lithium exchange reactions. More specifically, 4-bromopyridine was prepared by desalting with a basic aqueous solution and extraction into organic solvents, and the organic layers were separated by a flow separation membrane, followed by a flash halogen-lithium exchange reaction in 0.22 s (Fig. 1(b)). The obtained organolithium compounds can be derivatized into various compounds by reaction with electrophiles, and Suzuki-Miyaura cross-coupling can be applied to borate compounds, resulting in the efficient synthesis of AChE inhibitor precursors.

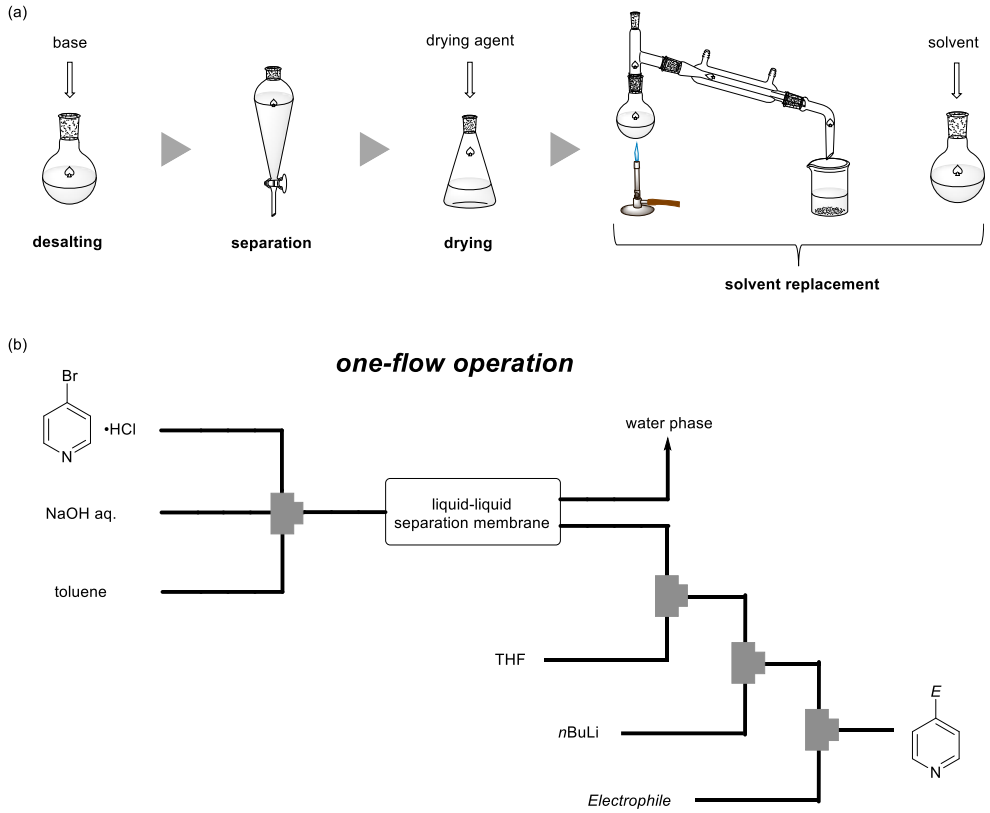

Figure 1. Pretreatment operations of hydrochloride compounds in (a) conventional batch methods, or (b) one-flow methods

Results and discussion

The organic solvent used for the extraction of 4-bromopyridine was selected to reduce the time required for the removal of water from the organic solvent during conventional treatment.[8] I measured (1) the water content of a solution containing a mixture of water and an organic solvent when the solution was separated in a batch operation, and (2) the water content when the solution was dried over $MgSO_4$ after separation. When toluene was used as the extraction solvent, the water content remained low even when the drying process was skipped (Table 1).

Table 1. Water content of organic solvents before or after mixing and separation of organic and aqueous phases

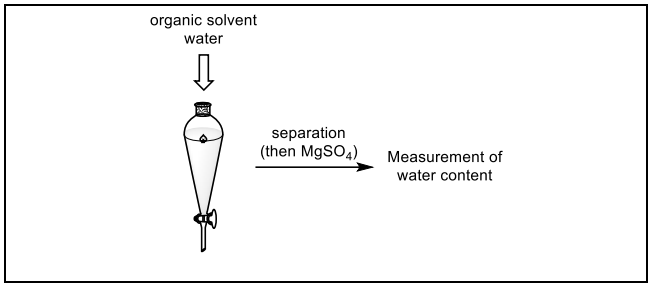

Solvent	Water concent (ppm)[a]		
	Before operations	After operation	
		(1) Without drying[b]	(2) Drying over $MgSO_4$[c]
THF	451	Not separate	
Et_2O	456	8110	2186
iPr_2O	75	3955	1167
toluene	129	281	177

[a]Water content was determined by Karl Fischer moisture titrator. [b]Organic solvent and water (1/1=v/v) were mixed and separated in a separatory funnel. [c]After separation, the organic layer was dried over $MgSO_4$.

To investigate whether it is possible to skip the drying step and proceed to water-sensitive reactions, halogen-lithium exchange reactions of desalted 4-bromopyridine (**2**) with *n*BuLi, followed by reactions with iodomethane, were performed (Fig. 2). Because the halogen-lithium exchange reactions are expected to be slow in nonpolar solvents such as *n*-hexane,[12] THF was added prior to the reaction with *n*BuLi. Subsequent reactions were performed with iodomethane as the electrophile; however, the batch method afforded the desired product **3** in low yield at all temperatures (Fig. 2(b) and (c)).

4-Pyridyllithium is considered unstable,[9,13] which may explain why the batch system resulted in low yields due to the decomposition of the 4-pyridyllithium. Therefore, I determined the conditions required to obtain the target product in high yield by conducting flash reactions using a flow microreactor, which allows unstable compounds to react immediately after generation.

Evaluation of the stability of 4-pyridyllithium by controlling the reaction time and temperature using flow microreactors[14] revealed that reactions exceeding 0.22 s, the reaction time that gives a maximum yield of 70%, resulted in lower yields due to degradation of the 4-pyridyllithium (Fig. 2 (c) and (d)). These results indicate that the halogen-lithium exchange reaction can be performed in good yield even if the drying step duration is reduced to 8.4 seconds in flow separator. In this reaction, various substituents were introduced to the 4-position of pyridine by choosing the electrophile (Fig. 3). The addition reactions with aryl- and alkyl-aldehydes, ketones, organotins, and organoborons afforded the products **3**–**10** in

moderate-to-good yields. Furthermore, if flow separation membranes can be used to separate the water and organic layers after desalting in this reaction, it will be possible to connect the starting material preparation and subsequent reaction into a single flow system.

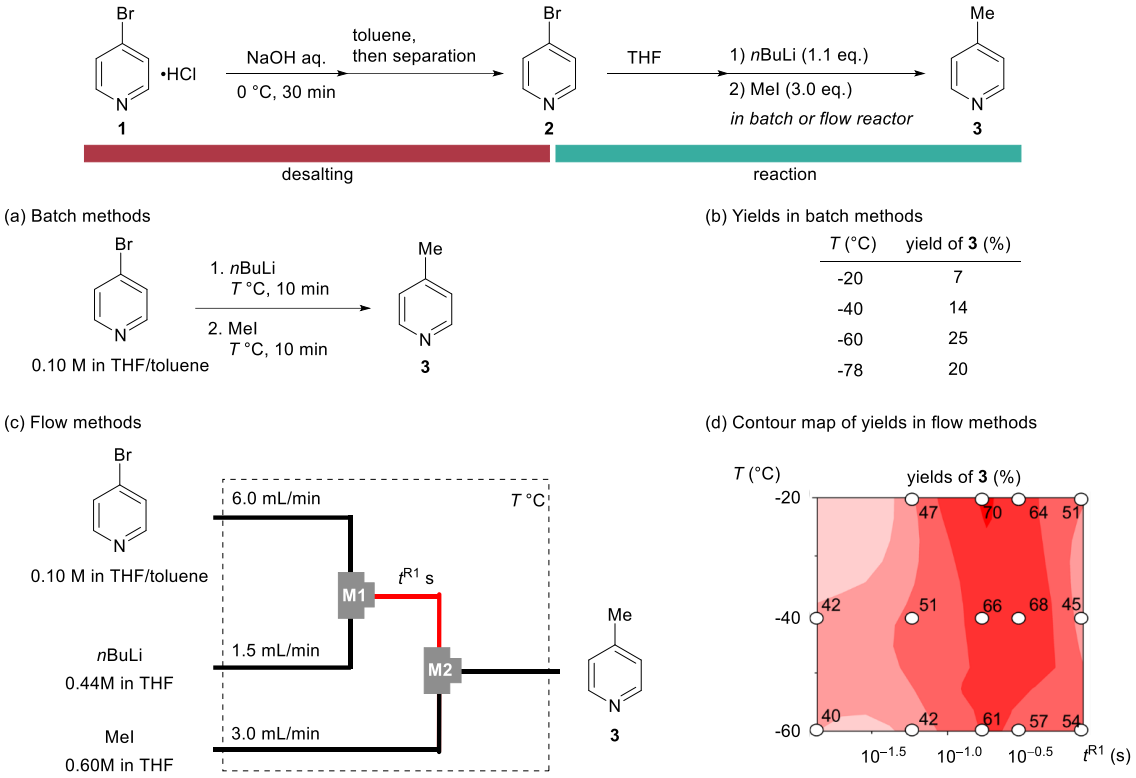

Figure 2. Reactions of desalted 4-bromopyridine chloride followed by the reaction with *n*BuLi (1.1 eq.) and iodomethane (3.0 eq.) in batch and flow. (a) Reactions in batch, (b) yields of 3 in batch methods, (c) reactions in flow microreactors, (d) the contour map of yields of 3; spot: yield, vertical axis: temperature *T*, horizontal axis: residence time t^{R1}. The yield of the condition with 0.014 s and −20 °C could not be determined because the flow reactor was clogged. The yield of the condition with 0.22 s and 0 °C was 38%. Yields were determined by GC.

To confirm that the drying process could also be skipped when using flow separation membranes, I measured the water content of the organic layer after flow separation using the flow liquid/liquid separator, SEP-10 flow separation membrane.[15] The results showed that, as in batch separation, the use of toluene as the extraction solvent resulted in a moisture content of less than 400 ppm, even when the drying process was reduced (see supporting information, Fig. S3).

Desalting, separation, lithiation, and electrophile reactions were then connected to a sequence of flow-through devices to synthesize 4-borylpyridine **10** from hydrochloride salt **1**

in a one-flow reaction. This reaction was completed 20 s after starting the flow reaction, yielding 78% of **10** (Fig. 4(a)). This yield was slightly higher than that obtained by batch separation method (Fig. 3). This can be a potential benefit of the one-flow reaction that allows the moderately unstable 4-bromopyridine to be used in the reaction immediately after its generation.

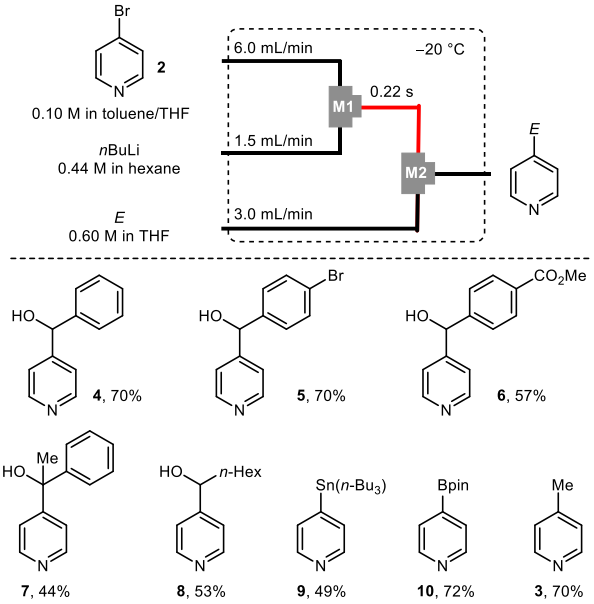

Figure 3. Reactions of **2** with electrophiles (3.0 eq.) in flow microreactors. "Bpin" means pinacol boranyl group.

Finally, to demonstrate the synthetic utility of this one-flow operation system, I utilized cross-coupling reaction into sequential batch reaction. After generation of **10**, the resulting solution was directly mixed with a solution of 2-iodobenzofuran, catalyst, and base.[16] The cross-coupling reaction proceeded well, and the desired product **11**, which can be converted into AChE inhibitors in one step,[17] was obtained with a 76% yield (Fig. 4(b)). Since conventional methods need several operations for obtaining **11**, this one-flow process served as a shorter synthetic route. This showcases that desalination, separation, flow reaction and batch reaction can be seamlessly connected to afford the drug precursor.

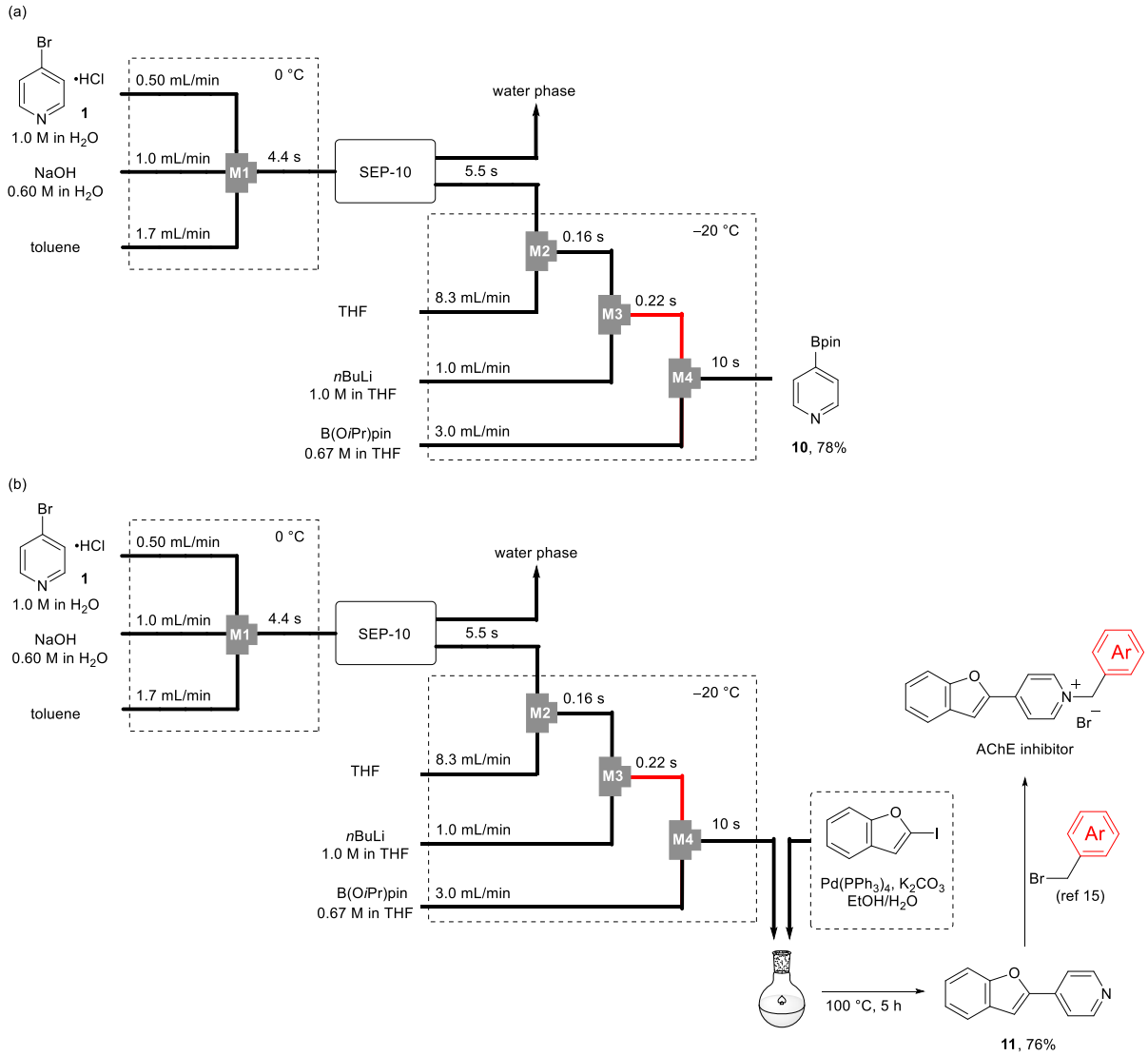

Figure 4. One-flow operation for desalination, separation, and reaction. (a) One-flow operation for the synthesis of borylpyridine **10** (b) One-flow synthesis of **10**, following the Suzuki-Miyaura cross-coupling reaction for AChE inhibitor precursor **11**.

Conclusion

In summary, an integrated flow system allows efficient pretreatment and reaction of 4-bromopyridine within 20 seconds. The pretreatment step included the desalting of 4-bromopyridine hydrochloride with a basic aqueous solution and the liquid-liquid separation using a flow separation membrane, followed by halogen-lithium exchange with *n*BuLi and reaction with B(O*i*Pr)pin. Since the reaction was performed immediately after the formation of the unstable desalted compound, the target product was obtained in a higher yield than in the conventional methods. The boryl compound obtained in this one-flow reaction was used for the Suzuki-Miyaura cross-coupling reaction, yielding the AChE inhibitor precursor. Since the time-consuming process, desalination and liquid/liquid separation, can be seamlessly operated, this one-flow process served as a new tactic for designing organic synthesis, which enhances efficiency and sustainability of organic synthetic systems.

References

1. Sheldon, R. A. *Chem. Soc. Rev.* **2012**, *41*, 1437.
2. (a) Trost, B. M. *Science*, **1991**, *254*, 1471. (b) Trost, B. M. *Angew. Chem. Int. Ed.* **1995**, *34*, 259. (c) Newhouse, T.; Baran, P. S.; Hoffmann, R. W. *Chem. Soc. Rev.* **2009**, *38*, 3010.
3. (a) Wender, P. A.; Verma, V. A.; Paxton, T. J.; Pillow, T. H. *Acc. Chem. Res.* **2008**, *41*, 40. (b) Wender, P. A. *Tetrahedron* **2013**, *69*, 7529.
4. (a) Hayashi, Y. *Chem. Sci.* **2016**, *7*, 866. (b) Hayashi, Y. *Acc. Chem. Res.* **2021**, *54*, 1385.
5. Li, C.-J.; Trost, B. M. *Proc. Natl. Acad. Sci. U. S. A.* **2008**, *105*, 13197.
6. (a) Matsumoto, Y; Tsuzuki, R.; Matsuhisa, A.; Takayama, K.; Yoden, T.; Uchida, W.; Asano, M.; Fujita, S.; Yanagisawa, I.; Fujikura, T. *Chem. Pharm. Bull*. **1996**, *44*, 103. (b) Choi-Sledeski, Y. M.; McGarry, D. G.; Green, D. M.; Mason, H. J.; Becker, M. R.; Davis, R. S.; Ewing, W. R.; Dankulich, W. P.; Manetta, V. E.; Morris, R. L.; Spada, A. P.; Cheney, D. L.; Brown, K. D.; Colussi, D. J.; Chu, V.; Heran, C. L.; Morgan, S. R.; Bentley, R. G.; Leadley, R. J.; Maignan, S.; Guilloteau, J. P.; Dunwiddie, C. T.; Pauls, H. W. *J. Med. Chem.* **1999**, *42*, 3572. (c) Russo, O.; Alami, M.; Brion, J.-D.; Sicsic, S.; Berque-Bestel, I. *Tetrahedron Lett.* **2004**, *45*, 7069.
7. (a) Savanor, P. M.; Jathi, K.; Bhat, S. K.; Tantry, R. N. *Res. J. Chem. Sci.* **2013**, *3*, 38. (b) Dutta, B.; Dey, A.; Sinha, C.; Ray, P. P.; Mir, M. H. *Dalton Trans. J. Inorg. Chem.* **2019**, *48*, 11259 (c) Heitz, W.; Rehder, A.; Nießner, N. *Makromol. Chem.* **1991**, *12*, 637.
8. (a) Mayer, N.; Schweiger, M.; Fuchs, E.; Migglautsch, A. K.; Doler, C.; Grabner, G. F.; Romauch, M.; Melcher, M.-C.; Zechner, R.; Zimmermann, R.; Breinbauer, R.; *Bioorg. Med. Chem.* **2020**, *28,* 115610. (b) Kadri, M.; Hou, J.; Dorcet, V.; Roisnel, T.; Bechki, L.; Miloudi, A.; Bruneau, C.; Gramage-Doria, R. *Chem. Eur. J.* **2017**, *23*, 5033. (c) Li, J.-Y.; Lee, C.; Chen, C.-Y.; Lee, W.-L.; Ma, R.; Wu, C.-G.; *Inorg. Chem.* **2015**, *54*, 10483.
9. (a) Berlin, A. A.; Razvodovskii, E. F.; *J. Polym. Sci. C Polym. Symp.* **2007**, *16*, 369. (b) Wibaut, J. P.; Broekman, F. W. *RECUEIL* **1959**, *78*, 593.
10. (a) Anand, P.; Singh, B.; Singh, N.; *Bioorg. Med. Chem.* **2012**, *20*, 1175. (b) Eckroat, T. J.; Manross, D. L.; Cowan, S. C.; *Int. J. Mol. Sci.* **2020**, *21*, 5965.
11. (a) Nagaki, A.; Ashikari, Y.; Takumi, M.; Tamaki, T. *Chem. Lett.* **2021**, *50*, 485. (b) Gutmann, B.; Cantillo, D.; Kappe, C. O. *Angew. Chem. Int. Ed.* **2015**, *54,* 6688. (c) Capaldo, L.; Wen, Z.; Noël, T. *Chem. Sci.* **2023**, *14*, 4230. (d) Hartman, R. L.; McMullen, J. P.; Jensen, K. F. *Angew. Chem. Int. Ed.* **2011**, *50*, 7502. (e) Tonhauser, C.; Natalello, A.; Löwe, H; Frey, H. *Macromolecules* **2012**, *45*, 9551.
12. Bailey, W. F.; Luderer, M. R.; Jordan, K. P. *J. Org. Chem.* **2006**, *71*, 2825.
13. (a) Nagaki, A.; Yamada, S.; Doi, M.; Tomida, Y.; Takabayashi, N. Yoshida, *J. Green Chem.* **2011**, *13*, 1110. (b) Nagaki, A.; Yamada, D.; Yamada, S.; Doi, M.; Ichinari, D.; Tomida, Y.; Takabayashi, N.; Yoshida, J. *Aust. J. Chem.* **2013**, *66*, 199. (c) Wakabayashi, S.; Takumi, M.; Kamio, S.; Wakioka, M.; Ohki, Y.; Nagaki, A. *Chem. Eur. J.* **2023**, *29*, e202202882.
14. (a) Harenberg, J. H.; Weidmann, N.; Knochel. P. *Synlett* **2020**, *31*, 1880. (b) Hessel, V.; Kralisch, D.; Kockmann, N.; Noël, T.; Wang, Q. *ChemSusChem* **2013**, *6*, 746. (c) Fuse, S.; Otake, Y.; Nakamura, H. *Chem. Asian J.* **2018**, *13*, 3818. (d) Ramanjaneyulu, B. T.; Vishwakarma, N. K.; Vidyacharan, S.; Adiyala, P. R.; Kim, D.-P. *Bull. Korean Chem. Soc.* **2018**, *39*, 757.
15. (a) Sagmeister, P.; Lebl, R.; Castillo, I.; Rehrl, J.; Kruisz, J.; Sipek, M.; Horn, M.; Sacher, S.; Cantillo, D.; Williams, J. D.; Kappe, C. O. *Angew. Chem. Int. Ed.* **2021**, *60*, 8139. (b) Jaman, Z.; Sobreira, T. J. P.; Mufti, A.; Ferreira, C. R.; Cooks, R. G.; Thompson, D. H. *Org. Process Res. Dev.* **2019**, *23*, 334.
16. The direct use of arylborates generated in flow microreactors for cross-coupling reactions has been reported: (a) Nagaki, A.; Moriwaki, Y.; Yoshida, *J. Chem. Commun.* **2012**, *48*, 11211. (b) Ashikari, Y.; Kawaguchi, T.; Mandai, K.; Aizawa, Y.; Nagaki, A. *J. Am. Chem. Soc.* **2020**, *142*, 17039.
17. Baharloo, F.; Moslemin, M. H.; Nadri, H.; Asadipour, A.; Mahdavi, M.; Emami, S.; Firoozpour, L. R.; Mohebat, L.; Shafiee, A.; Foroumadi, A. *Eur. J. Med. Chem.* **2015**, *93*, 196.

18. Tong, Z.; Garry, O. L.; Smith, P. J.; Jiang, Y.; Mansfield, S. J.; Anderson, E. A. *Org. Lett.* **2021**, *23*, 4888.
19. Jiang, Q.; Fang, L.-Q.; Li, Y.-H.; Wang, J.; Li, J.-H. *ChemistrySelect.* **2023**, doi:10.1002/slct.202300780.
20. (a) Zhou, H.-J.; Huang, J.-M. *J. Org. Chem.* **2022**, *87*, 5328. (b) Sterckx, H.; Sambiagio, C.; Médran-Navarrete, V.; Maes, B. U. W. *Adv. Synth. Catal.* **2017**, *359*, 3226.
21. DeBerardinis, A. M.; Turlington, M.; Ko, J.; Sole, L.; Pu, L. *J. Org. Chem.* **2010**, *75*, 2836.
22. (a) Zhang, X.; Yang, C.; Gao, H.; Wang, L.; Guo, L.; Xia, W. *Org. Lett.* **2021,** *23*, 3472. (c) Wang, G.; Cao, J.; Gao, L.; Chen, W.; Huang, W.; Cheng, X.; Li, S. *J. Am. Chem. Soc.* **2017**, *139*, 3904.
23. (a) Fargeas, V.; Favresse, F.; Mathieu, D.; Beaudet, I.; Charrue, P.; Lebret, B.; Piteau, M.; Quintard, J.-P. *Eur. J. Org. Chem.* **2003**, *2003*,
24. 1711. (b) Nicolaou, K. C.; Hepworth, D.; King, N. P.; Finlay, M. R.; Scarpelli, R.; Pereira, M. M.; Bollbuck, B.; Bigot, A.; Werschkun, B.; Winssinger, N. *Chemistry*. **2000**, *6*, 2783. Yang, L.; Semba, K.; Nakao, Y. *Angew. Chem. Int. Ed.* **2017**, *56*, 4853. (b) Cook, M. J.; Fernandes, I. WO 2002096913 A1, Dec 5, 2002.
25. Lansakara, A. I.; Farrell, D. P.; Pigge, F. C. *Org. Biomol. Chem.* **2014**, *12*, 1090. (b) Wu, G.; Yin, W.; Shen, H. C.; Huang, Y. *Green Chem.* **2012**, *14*, 580.

Supporting Information

3. General Information

Abbreviations. Acetylcholinesterase (AChE), pinacol boranyl group (Bpin), butyl (Bu), degrees Celsius (°C), calculated (calcd), deuteritated chloroform ($CDCl_3$), centimeter(s) (cm), doublet (d), equivalent (equiv or eq.), electrospray ionization (ESI), ethyl (Et), ethyl acetate (EtOAc), gram(s) (g), gas chromatography (GC), hour(s) (h), high resolution mass-spectrometry (HRMS), hertz (Hz), hexyl (Hex) coupling constant (*J*), length of tubes (L), liter(s) (L), mol L^{-1} of molar concentration (M), methyl (Me), milligram(s) (mg), megahertz (MHz), minute(s) (min), milliliter(s) (mL), millimole(s) (mmol), mole(s) (mol), normal (*n*), nuclear magnetic resonance (NMR), parts per million (ppm), polytetrafluoro-ethylene or Teflon (PTFE), second(s) (s or sec), singlet (s), tetrahydrofuran (THF), residence time of microtube reactor R_n (t^{Rn}), temperature (T), inner diameter of tubes and mixers (φ), micrometer(s) (μm).

General. NMR spectra were recorded on JEOL JNM-ECZ400S (^{1}H 400 MHz, ^{13}C 100 MHz). Chemical shifts are recorded using a solvent peak; 7.26 ppm for ^{1}H, 77.36 ppm for ^{13}C. NMR yields were calculated by NMR analyses with internal standards such as 1,1,2,2-tetrachloroethane. GC analysis was performed on a SHIMADZU GC-2014 gas chromatograph equipped with a flame ionization detector using a fused silica capillary column (column, CBP1; 0.22 mm x 25 m). Temperature of GC oven was 50 °C at first, and after 5min the temperature was increased 10 °C per min. GC yields were calculated by GC analyses with internal standards such as *n*-undecane using calibration lines derived from commercial or isolated compounds. Mass spectra were obtained on Thermo Scientific Exactive Plus. Merck pre-coated silica gel F254 plates (thickness 0.25 mm) were used for TLC analyses. Water content was measured by coulometric KF titrator C10S (Mettler Toledo). All batch reactions were carried out in a flame-dried glassware under argon atmosphere.

Flow Synthesis. Stainless steel (SUS304) T-shaped micromixers with inner diameter of 250 and 500 μm were manufactured by Sanko Seiki Co., Inc. Stainless steel (SUS316) microtube reactors with 1000 μm inner diameter and PTFE tube with inner diameter of 1000 μm were purchased from GL Sciences. The syringe pumps (Harvard Model PHD ULTRA) equipped with gastight syringes (purchased from SGE) were used for introduction of the solutions into the micromixer systems via stainless steel fittings (GL Sciences, 1/16 OUW). Flow microreactor system is composed with stainless steel pre-cooling units (**P1**, **P2**, etc.), stainless steel microtube reactors (**R1**, **R2**, etc.), T-shaped micromixers (**M1**, **M2**, etc.), and, if necessary, PTFE tube with inner diameter of 1000 μm. Unless otherwise noted, the inner diameter of the stainless and PTFE tubes is 1000 μm, and the length of the pre-cooling units

is 100 cm. Unless otherwise noted, the inner diameter of micromixers is 250 μm. SEP-10 (Zaiput Flow Technologies) was used for liquid-liquid separation. The solution of *n*-butyllithium was prepared by dilution of the commercial solution with dehydrated *n*-hexane.

Materials. Dehydrated THF, toluene, diethyl ether, diisopropyl ether, ethanol, and *n*-hexane were purchased from FUJIFILM Wako Pure Chemical Corporation and Kanto Chemical Co., Inc., and were used without further purification. A solution of *n*-butyllithium (in *n*-hexane, 1.6 M) was purchased from Kanto Chemical Co., Inc. and stored at −20 °C. 4-Bromopyridine hydrochloride, sodium hydroxide, iodomethane, benzaldehyde, 4-bromobenzaldehyde, methyl 4-formylbenzoate, acetophenone, 1-hexanal, tributyltin chloride, 2-isopropoxy-4,4,5,5-tetramethyl-1,3,2-dioxaborolane, isopropoxyboronic acid pinacol ester, and tetrakis(triphenylphosphine)palladium (0) were purchased from commercial suppliers, and were used without further purification. 2-Iodobenzozfuran was prepared according to the literature.[1]

4. Synthetic procedures

2.1 Water separation, drying, and measurement of water content in batch reactors

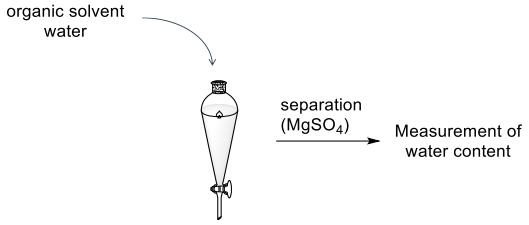

Without drying

Organic solvent and water (1/1=v/v) were mixed and separated in a separatory funnel. The water content of organic layer was determined by the Karl Fischer titration.

Drying over $MgSO_4$

Organic solvent and water (1/1=v/v) were mixed and separated in a separatory funnel. The organic layer was dried over $MgSO_4$. The water content of organic layer was determined by the Karl Fischer titration.

4.2 Desalting to prepare a THF/toluene solution of 4-bromopyridine in batch reactors

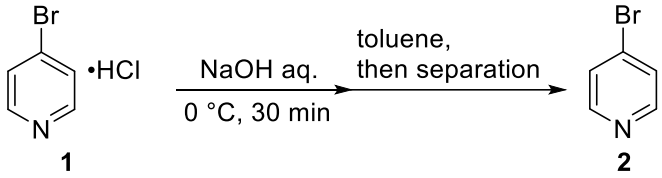

To an aqueous solution of NaOH (5 M, 8.6 mL) and toluene (9.1 mL) was added **1** (7.02 g) at 0 °C, and the solution was stirred for 30 minutes at the same temperature. The resulting mixture was separated and extracted with toluene (9.1 mL). The organic layer was dried over $MgSO_4$, filtered. To the organic layer was added THF to give a 0.1 M solution of **2**.

4.3 Halogen-lithium exchange reaction followed by reaction with electrophiles in batch reactors

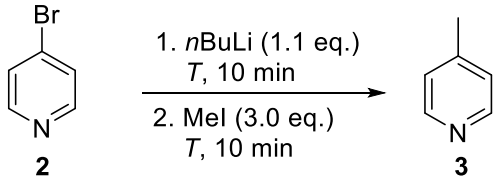

To a solution of **2** (0.1 M in THF/toluene, 3.0 mL) was added *n*BuLi (0.75 mL, 1.56 M) dropwise in a cooling bath (T °C). The mixture was stirred 10 min at the same temperature. To the reaction mixture was added MeI (1.14 g) in THF (1.5 mL). After stirring at the same temperature for 10 min, the reaction was quenched with brine. The yield of **3** was analyzed by GC, and was summarized in Table S1.

Table S1 Yields of **3** with varying temperature (T) in batch methods

T (°C)	yield of **3** (%)
−20	7
−40	14
−60	25
−78	20

4.4 Halogen-lithium exchange reaction followed by reaction with iodomethane with varying temperature (T) and residence time (t^{R2}) in flow microreactors

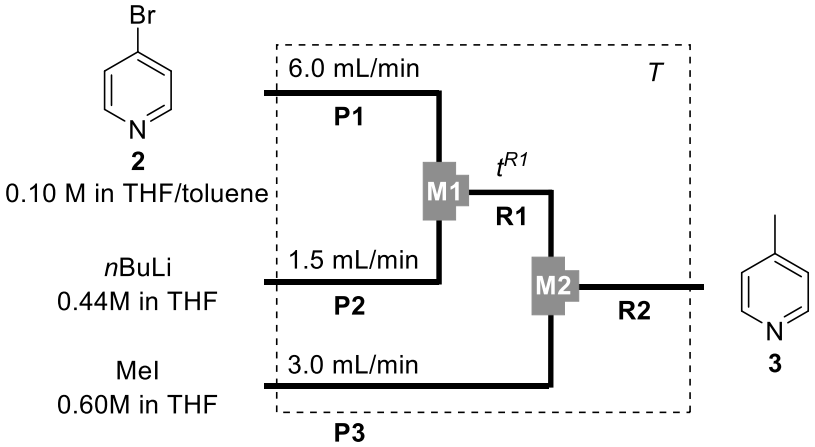

A flow microreactor system consisting of a T-shaped micromixer (**M1** and **M2**, φ = 250 μm), two microtube reactors (**R1** and **R2**), and three pre-cooling units (**P1**–**P3**) was used. The flow microreactor system was dipped in a cooling bath (T °C). A solution of **2** (0.10 M in THF/toluene (prepared in section 2.3), flow rate: 6.0 mL/min) and a solution of *n*BuLi (0.44 M in hexane, flow rate: 1.5 mL/min) were introduced into **M1** using syringe pumps. The mixed solution was passed through **R1** (φ^{R1} μm, L^{R1} cm, t^{R1} s), and was mixed with a solution of MeI (0.60 M in THF, flow rate: 3.0 mL/min) in **M2.** The resulting solution was passed through **R2** (L^{R2}= 1000 cm, t^{R2} = 9.0 s). After a steady state was reached, an aliquot of the reacting solution was collected and was treated with a saturated NH_4Cl aqueous solution. The yield of **3** was analyzed by GC, and was summarized in Table S2.

Table S2 Yields of **3** with varying temperature (T) and residence time in **R1** (t^{R1}) in flow mictoreactors[a]

T (°C)	φ^{R1} (μm)	L^{R1} (cm)	t^{R1} (s)	yield of **3** (%)
−20	250	3.5	0.014	Clogged
	500	3.5	0.055	47
	1000	3.5	0.22	70
	1000	5	0.31	64
	1000	12.5	0.78	51
−40	250	3.5	0.014	42
	500	3.5	0.055	51
	1000	3.5	0.22	66
	1000	5	0.31	68
	1000	12.5	0.78	45
−60	250	3.5	0.014	47
	500	3.5	0.055	42
	1000	3.5	0.22	61
	1000	5	0.31	57
	1000	12.5	0.78	54

[a]Yields were determined by GC using an internal standard. Retention time: 7.8 min

4.5 Halogen-lithium exchange reaction followed by reaction with electrophiles in flow microreactors

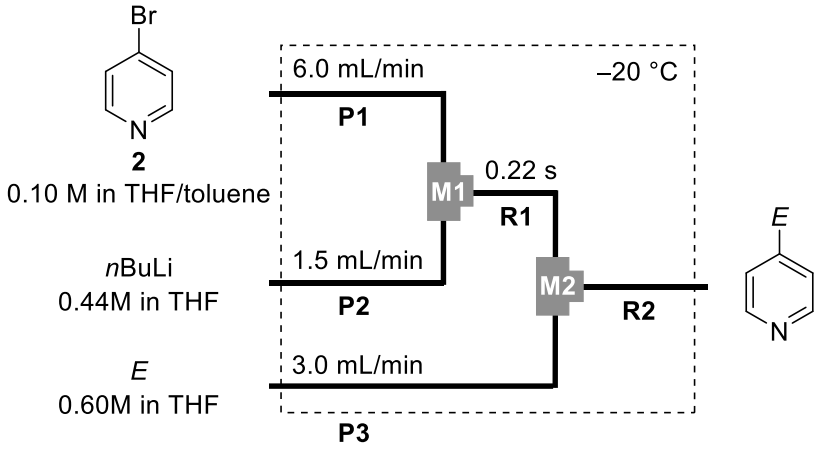

A flow microreactor system consisting of two T-shaped micromixers (**M1** and **M2**, φ = 500 μm), two microtube reactors (**R1** and **R2**), and three pre-cooling units (**P1**–**P3**) was used. The flow microreactor system was dipped in a cooling bath (T = −20 °C). A solution of **2** (0.10 M in THF/toluene (prepared in section 2.3), flow rate: 6.0 mL/min) and a solution of *n*BuLi (0.44 M in hexane, flow rate: 1.5 mL/min) were introduced into **M1** using syringe pumps. The mixed solution was passed through **R1** (φ 1000 μm, 3.5 cm, 0.22 s), and was mixed with a solution of electrophile (0.60 M in THF, flow rate: 3.0 mL/min) in **M2.** The resulting solution was passed through **R2** (L^{R2}= 1000 cm, t^{R2} = 9.0 s). After a steady state was reached, an aliquot of the reacting solution was collected and was treated with a saturated NH_4Cl aqueous solution. The yields were analyzed by NMR or GC.

3

4-Methylpyridine (3)
Obtained with iodomethane in 70% yield determined by GC (retention time 7.8 min). The spectral data were identical to those of reported in the literature.[2]

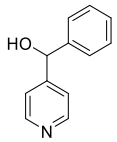

4

Phenyl(pyridin-4-yl)methanol (4).
Obtained with benzaldehyde in 70% yield determined by NMR. After extraction, the crude product was purified by chromatography (hexane/EtOAc = 80/20 → 0/100) to afford **4**. The spectral data were identical to those of reported in the literature.[3]

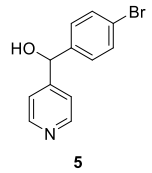

5

4-Bromophenyl(pyridine-4-yl)methanol (5).
Obtained with 4-bromobenzaldehyde in 70% yield determined by NMR. After extraction, the crude product was purified by chromatography (hexane/EtOAc = 80/20 → 0/100) to afford **5**. ^{1}H NMR (400 MHz, $CDCl_3$) δ 2.59 (s, 1H), 5.77 (s, 1 H), 7.23 (dd, J = 8.4 Hz, 2.0 Hz, 2 H), 7.29 (dd, J = 5.6 Hz, 2.0 Hz, 2 H), 7.49 (dd, J = 8.4 Hz, 2.0 Hz, 2 H), 8.55 (dd, J = 6.4 Hz, 2.0 Hz, 2 H); ^{13}C NMR (100 MHz, $CDCl_3$) δ 74.4, 121.3, 122.3, 128.6, 132.1, 141.8, 149.8, 152.3; HRMS (ESI) calcd for $C_{12}H_{11}BrNO$ $[M+H]^+$: 264.0017, found: 264.0019.

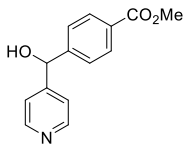

6

Methyl 4-(hydroxy(pyridine-4-yl)methyl)benzoate (6)
Obtained with methyl 4-formylbenzoate in 57% yield determined by NMR. After extraction, the crude product was purified by chromatography (hexane/EtOAc = 80/20 → 0/100) to afford **6**. The spectral data were identical to those of reported in the literature.[4]

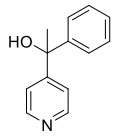

7

1-Phenyl-1-(pyridin-4-yl)ethan-1-ol (7)
Obtained with acetophenone in 44% yield determined by NMR. After extraction, the crude product was purified by chromatography (hexane/EtOAc = 80/20 → 0/100) to afford **7**. The spectral data were identical to those of reported in the literature.[5]

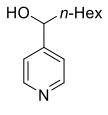

8

1-(Pyridin-4-yl)heptan-1-ol (8)
Obtained with *n*-heptanal in 53% yield determined by NMR. After extraction, the crude product was purified by chromatography (hexane/EtOAc = 80/20 → 0/100) to afford **8**. The spectral data were identical to those of reported in the literature.[3]

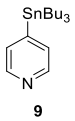

9

4-(Tri-*n*-butylstannyl)pyridine (9)
Obtained with tri-*n*-butylstannyl chloride in 49% yield determined by GC (retention time 23.7 min). After extraction, the crude product was purified by chromatography (hexane/EtOAc = 95/5 → 84/16) to afford **9**. The spectral data were identical to those of reported in the literature.[6]

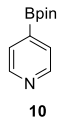

10

4-(4,4,5,5-Tetramethyl-1,3,2-dioxaboran-2-yl)pyridine (10)
Obtained with isopropoxyboronic acid pinacol ester in 72% yield determined by GC (retention time 16.1 min). The spectral data were identical to those of reported in the literature.[7]

2.6 Water separation and measurement of water content using SEP-10 liquid-liquid membrane flow system

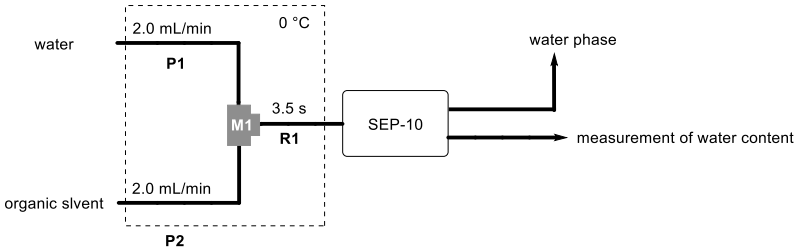

A flow microreactor system consisting of a T-shaped micromixer (**M1**, φ = 500 μm), a microtube reactor (**R1**), two pre-cooling units (**P1**, **P2**), and SEP-10 flow liquid-liquid separator (with a hydrophobic PTFE membrane OB-900) was used. The flow microreactor system was dipped in a cooling bath (T = 0 °C). Water (flow rate: 2.0 mL/min) and organic solvent (flow rate: 2.0 mL/min) were introduced into **M1** using syringe pumps. The mixed solution was passed through **R1** (φ 1000 μm, 30 cm, 3.5 sec), and was separated by SEP-10. The results are summarized in Table S3.

Table S3 Water contents of organic solvent before/after water separation using SEP-10 liquid-liquid separation flow system

solvent	water content (ppm)	
	Before mixing	After separation
THF	451	Not separated
Et_2O	467	11800
iPr_2O	49.0	5280
toluene	178	362

2.7 One-flow operation through preparation of 4-bromopyridine to halogen-lithium exchange reaction following a reaction with isopropylboronic acid pinacol ester

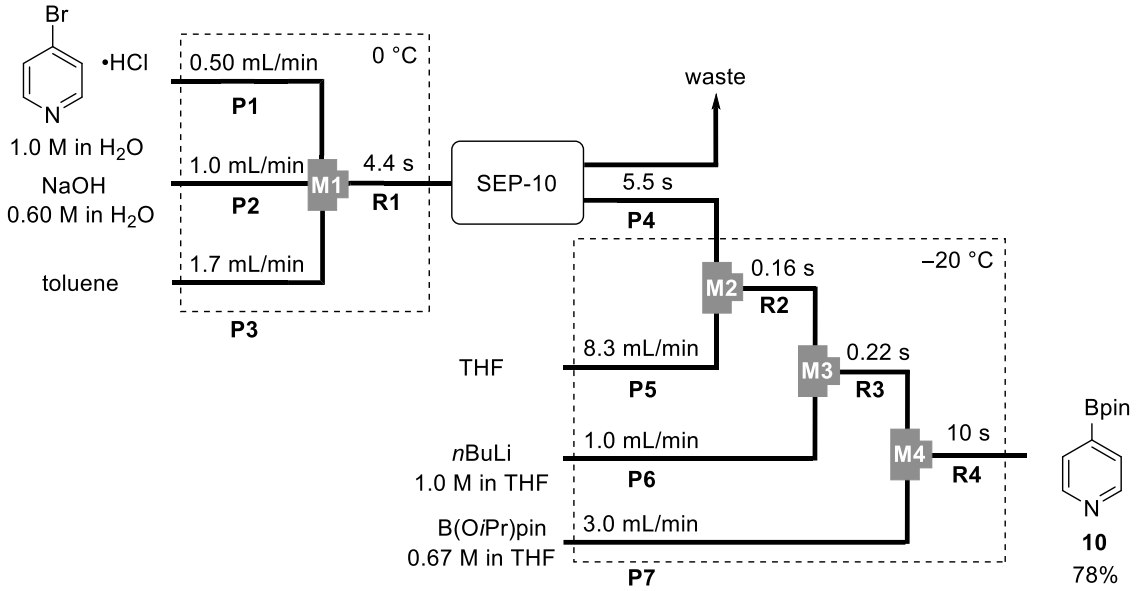

A flow microreactor system consisting of a three-way micromixer (**M1**, φ = 500 μm), three T-shaped micromixers (**M2**–**M4**), four microtube reactors (**R1**–**R4**), seven pre-cooling units (**P1**–**P7**), SEP-10 flow liquid-liquid separator (with a hydrophobic PTFE membrane OB-900) was used. The flow microreactor system before SEP-10 was dipped in a cooling bath (T = 0 °C) and the flow microreactor system after SEP-10 was dipped in a cooling bath (T = −20 °C). An aqueous solution of **1** (1.0 M, flow rate: 0.50 mL/min), an aqueous solution of NaOH (0.60 M, flow rate: 1.0 mL/min), and toluene (flow rate: 1.7 mL/min) were introduced into **M1** using syringe pumps. The mixed solution was passed through **R1** (30 cm, 4.4 s), and the organic and water layer were separated with SEP-10. The organic layer was passed through **P4** and mixed with THF (flow rate: 8.3 mL/min) in **M2**. The mixed solution was passed through **R2** (20 cm, 5.5 s), and mixed with a solution of *n*BuLi (1.0 M in hexane, flow rate: 1.0 mL/min) in **M3**. The mixed solution was passed through **R3** (3.5 cm, 0.22 s), and mixed with a solution of isopropoxyboronic acid pinacol ester (0.67 M in hexane, flow rate: 3.0 mL/min) in **M4**. After a steady state was reached, an aliquot of the reacting solution was collected and was treated with a saturated NH_4Cl aqueous solution. The organic layer was analyzed by GC to determine the yield of **10** (78%).

2.8 One-flow operation through preparation of 4-bromopyridine to Suzuki-Miyaura cross-coupling reaction to reach the precursors of AChE inhibitor

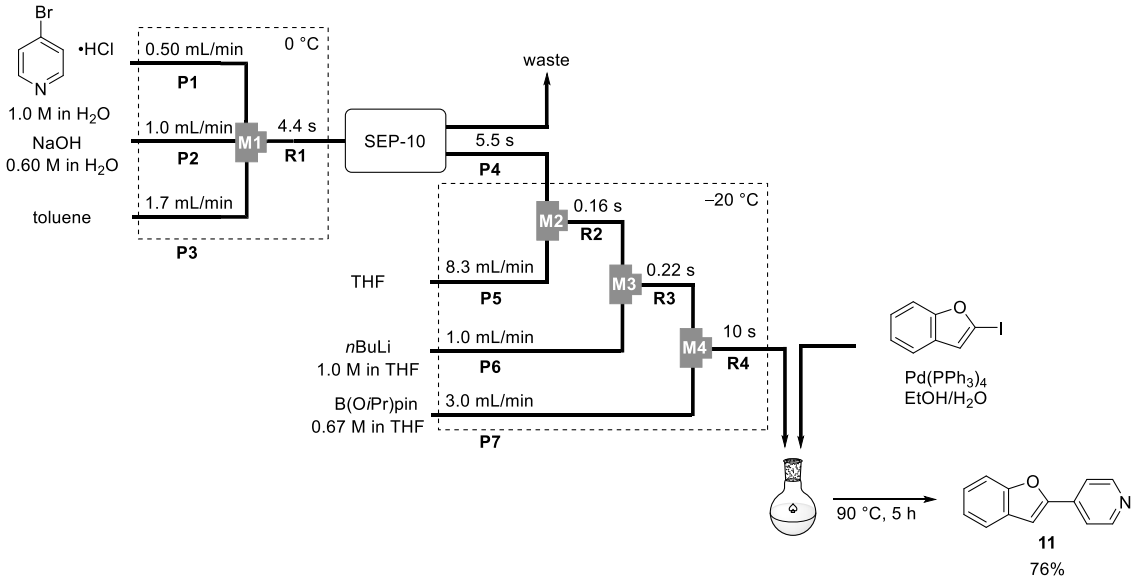

A flow microreactor system consisting of a three-way micromixer (**M1**, φ = 500 μm), three T-shaped micromixers (**M2**–**M4**), four microtube reactors (**R1**–**R4**), seven pre-cooling units (**P1**–**P7**), SEP-10 flow liquid-liquid separator (with a hydrophobic PTFE membrane OB-900) was used. The flow microreactor system before SEP-10 was dipped in a cooling bath (T = 0 °C) and the flow microreactor system after SEP-10 was dipped in a cooling bath (T = −20 °C). An aqueous solution of **1** (1.0 M, flow rate: 0.50 mL/min), an aqueous solution of NaOH (0.60 M, flow rate: 1.0 mL/min), and toluene (flow rate: 1.7 mL/min) were introduced into **M1** using syringe pumps. The mixed solution was passed through **R1** (30 cm, 4.4 s), and the organic and water layer were separated with SEP-10. The organic layer was passed through **P4** and mixed with THF (flow rate: 8.3 mL/min) in **M2**. The mixed solution was passed through **R2** (20 cm, 5.5 s), and mixed with a solution of *n*BuLi (1.0 M in hexane, flow rate: 1.0 mL/min) in **M3**. The mixed solution was passed through **R3** (3.5 cm, 0.22 s), and mixed with a solution of isopropoxyboronic acid pinacol ester (0.67 M in hexane, flow rate: 3.0 mL/min) in **M4**. After a steady state was reached, an aliquot of the reacting solution was collected. To a solution of 2-iodobenzofuran (45.5 mg) and $Pd(PPh_3)_4$ (25.5 mg) in $EtOH/H_2O$ (5 mL, 1/1=v/v) was added the aliquot (5 mL) of the reaction solution containing 4-borylpyridine. The mixture was stirred at 90 °C under argon atmosphere for 5 hours, then was allowed to be cooled to room temperature. After addition of EtOAc and a saturated aqueous solution of NH_4Cl, the organic phase was analyzed by GC to determine the yield of **11** (76%). The spectral data were identical to those of reported in the literature.[8]

2.9 References

1. Z. Tong, O. L. Garry, P. J. Smith, Y. Jiang, S. J. Mansfield, E. A. Anderson, *Org. Lett.* **23**, 4888–4892 (2021).
2. Q. Jiang, L.-Q. Fang, Y.-H. Li, J. Wang, J.-H. Li, *ChemistrySelect.* **8** (2023). doi:10.1002/slct.202300780.
3. H.-J. Zhou, J.-M. Huang, *J. Org. Chem.* **87**, 5328–5338 (2022).
4. A. M. DeBerardinis, M. Turlington, J. Ko, L. Sole, L. Pu, *J. Org. Chem.* **75**, 2836–2850 (2010).
5. X. Zhang, C. Yang, H. Gao, L. Wang, L. Guo, W. Xia, *Org. Lett.* **23**, 3472–3476 (2021).
6. V. Fargeas, F. Favresse, D. Mathieu, I. Beaudet, P. Charrue, B. Lebret, M. Piteau, J.-P. Quintard, *Eur. J. Org. Chem.* **2003**, 1711–1721 (2003).
7. L. Yang, K. Semba, Y. Nakao, *Angew. Chem. Int. Ed.* **56**, 4853–4857 (2017).
8. A. I. Lansakara, D. P. Farrell, F. C. Pigge, *Org. Biomol. Chem.* **12**, 1090–1099 (2014).

Chapter 4
Convergent approach of double intermediates in flow microreactor: flash irreversible generation of carbocations enables direct cross–coupling

Abstract

In biosynthesis, multiple kinds of reactive intermediates are generated, transported, and reacted across different parts of organisms, enabling highly sophisticated synthetic reactions. Herein I report a convergent synthetic approach, which utilizes dual intermediates of cationic and carbanionic species in a single step, hinted at by the ideal reaction conditions. By reactions of unsaturated precursors, such as enamines, with a superacid in a flow microreactor, cationic species, such as iminium ions, are generated rapidly and irreversibly, and before decomposition, they are transported to react with rapidly and independently generated carbanions, enabling direct C-C bond formation. Taking advantage of the reactivity of these double reactive intermediates, the reaction takes place within a few seconds, enabling synthetic reactions which are not applicable in conventional reactions.

Introduction

Proteins are organic molecules with unique functions. In organisms, proteins such as enzymes are intertwined to perform organic reactions and synthesize biogenic molecules, which are essential for maintaining life.[1] Such biosynthesis, which take full advantage of organic molecules, is one of the ideal goals in organic chemistry. During biosynthesis, multiple kinds of "reactive intermediates" are generated, transported, and reacted across different parts of living organisms.[2] The mobility of these intermediates enables high selectivity, even though the reactions occur at rates close to diffusion-limited reactions. In such reactions, the selectivity depends on the rate of transport of the reactants instead of their reaction kinetics. Thus, biological reactions are often considered to occur under ideal reaction conditions, and it is expected that excellent reaction selectivity using active intermediates can be achieved by approaching such conditions in organic synthetic reactions.[3]

I studied the organic synthesis mediated by highly reactive intermediates. In particular, I utilized flow microreactors to develop methods for the fast generation and reactions of short-lived anionic species, which ordinal batch reactors cannot handle.[4] In these methods, unstable anionic species, particularly carbanions, are rapidly and irreversibly generated and immediately react with electrophiles. This leads to the complete conversion of starting materials into highly reactive intermediates, which enable subsequent fast reactions. "Flash" chemistry,[5] which utilizes the anionic reactive intermediates in rapid reactions, has enabled various chemical transformations that traditional methods cannot achieve.

Cations, which are unstable species as well as anions, are also important reactive intermediates, with organic cations being the most significant for organic synthesis.[6] Among a wide range of the conventional methods to generate organic cations, such as acid-promoted methods,[7] diazotization,[8] and chemical oxidation,[9] those involving Lewis acids are the most

frequently utilized. Since this method generates cations in reversible manner, the concentration of the cations is low, making the reaction slow. To overcome this drawback, organic electrosynthesis,[10,11,12] which generates relatively stable organic cations irreversibly, has been developed. Owing to their high reactivity, electrochemically generated cations can react rapidly with nucleophiles. However, in most electrochemical reactions, anodic oxidation requires several hours to generate cationic species,[13] resulting in a slower reaction. I envisaged that if highly unstable and reactive cationic species were generated rapidly, this would lead to a new synthetic approach, where multiple reactive intermediates are utilized in different locations, mimicking an idealized reaction system.

This article reports a proof-of-concept study that uses flowmicro methods to demonstrate irreversible and rapid generation of cationic species, followed by their reactions with rapidly generated carbanions and a direct cross-coupling reaction to generate carbon-carbon bonds within seconds. These achievements showcase a simultaneous use of multiple highly-reactive intermediates, which transform the "flash chemistry" into "flash synthesis," leading to a new synthetic chemistry (Fig. 1).

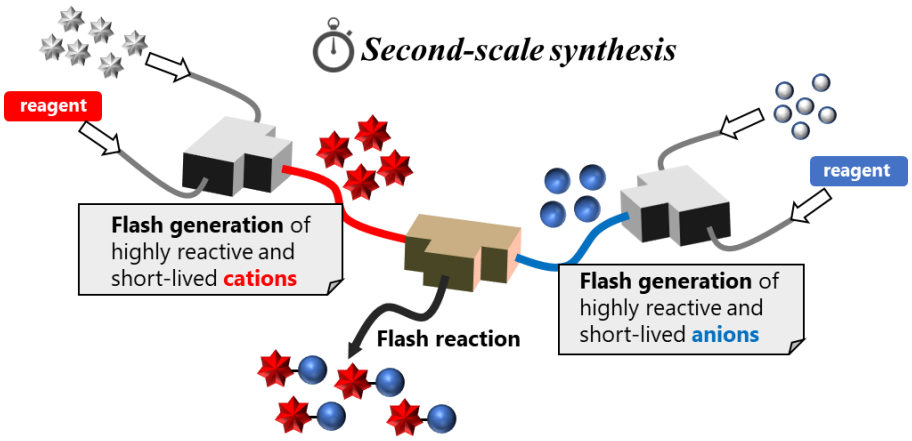

Figure 1. Second-scale synthesis via flash generation of reactive intermediates

Results and discussion

Cationic species generation in batch and flow reactor

To achieve the rapid and irreversible generation of cationic species, I focused on the reactions of vinyl compounds with a strong Brønsted acid as a strong proton donor (Fig. 2).[14] Among a variety of methods for generating cationic species, the use of strong acid may provide a rapid generation of those unstable species without the specific equipment such as flow electrolysis devices. I selected enamines as precursors for iminium ions, and trifluoromethanesulfonic acid (TfOH, pKa 2.6 in acetonitrile[15]) as the proton source because of its high acidity and ease of handling.[16] The reaction of enamines with strong acids generates iminium ions; however, since the enamines may work as nucleophiles, the generated cations easily react with the enamines, resulting in dimerization. Actually, the reaction of enamine **1a** with TfOH in a batch reactor followed by the addition of allyltrimethylsilane afforded a small amount of **3** ,which is amine bearing an allyl group (Fig. 2, Method A), and the major product was dimer **4** (see supporting information Table S4 for detail). While the reaction temperature had no significant effect on the reaction yield, the dropping order of the reagents had an influence on the yield: the yield of the target product was higher in method A and C, in which the enamine solution was dropped over 30 s to the TfOH solution, than in the reverse-drop method. The batch reactions with 1.0 equivalent of TfOH also resulted in low yields (see supporting information). The above

investigations, where dimer **4** was obtained more abundantly than the desired product **3**, indicate that the generated iminium ion **2a** rapidly reacted with the surrounding enamine **1a**. Thus, to achieve the selective generation of **2a** for its reactions with nucleophiles, **1a** must be converted to **2a** before the dimerization.

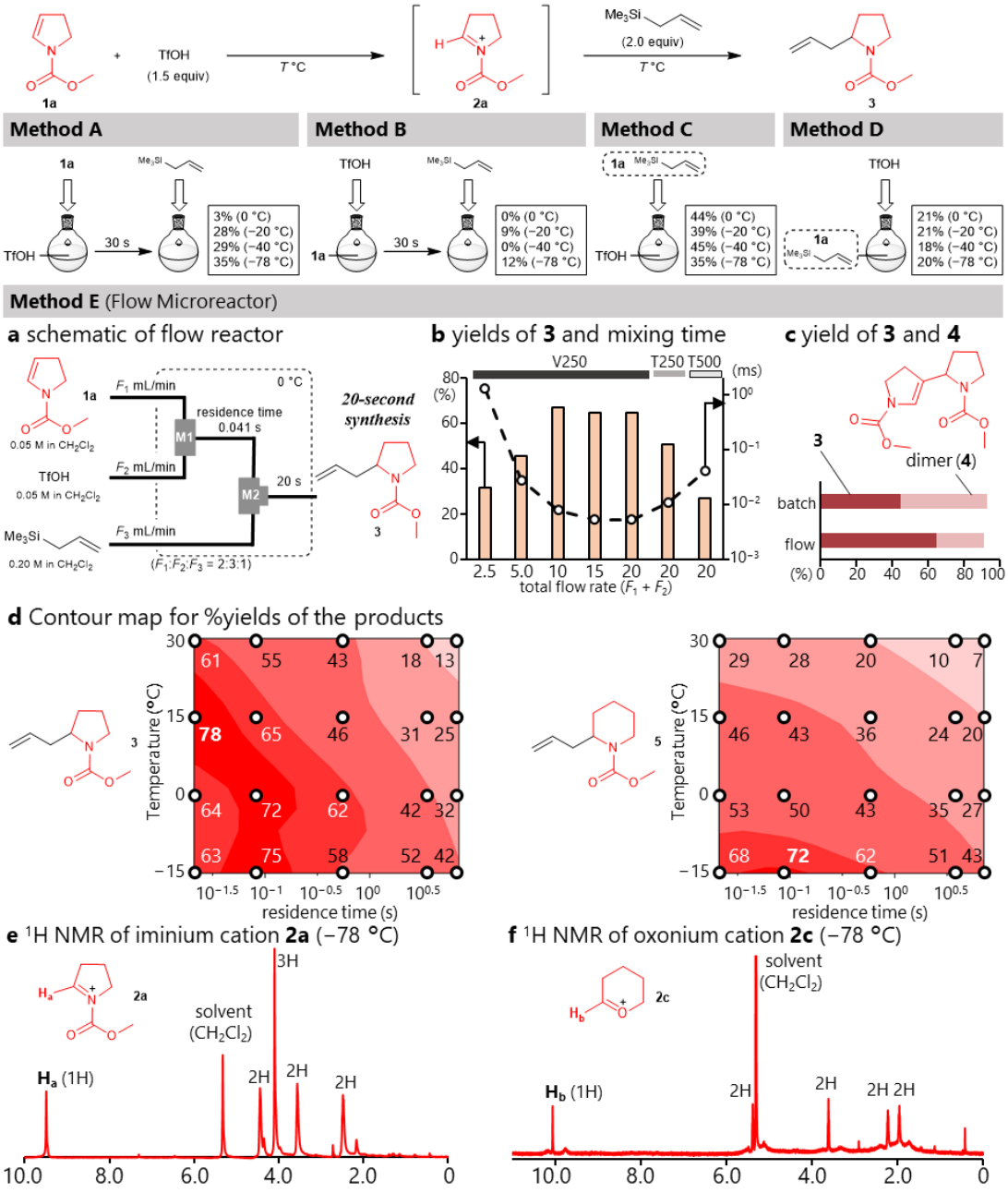

Figure 2. Generation and reaction of onium cations in a batch and flow system.[a]

[a]Methods A–D were done in a batch system, and Method E was done in a flow system composed of two micromixers. Yields were determined by GC. **a**, Schematic for a flow reactor. **M2** is T-shaped mixer with 250 μm inner diameter. **b**, Dependency of yields of **3** and mixing time on flow rates and mixer **M1**. Reaction time between **1a** with TfOH is 0.041 s. For mixers, the alphabet (V and T) denotes the shape of the mixer, whereas the number denotes its inner diameter (μm). bars: yield (%), dots: mixing time (millisecond) determined by Villermaux–

Dushman method. **c**, Yields of **3** and **4** (dimer) determined by GC. Batch: method C at −40 ° C, flow: V250, 20 mL/min. **d**, Contour maps of yields of **3** (left) and **5** (right) using V-250 mixer. Horizontal axis: residence time (s), vertical axis: temperature (° C), the designated number on the circle dot: yield of **3** and **5** (%). **e**, Low temperature NMR analyses of **2a** (left) and **2c** (right). The cationic species were generated in a flow microreactor using CD_2Cl_2 as a solvent, and was flow into an NMR sample tube cooled at −78 ° C. ^1H NMR analyses were done at −78 ° C.

To improve reaction selectivity, flow microreactors have attracted considerable attention for decades.[17,18] In particular, their fast mixing characteristics remarkably affect fast reactions.[19,20] Actually, we have demonstrated that the fast mixing of flow micromixers enabled selective reactions of a sulfur cation with styrenes before their cationic polymerization.[21] Based on this idea, I envisaged that flow microreactor would achieve the selective generation of iminium ion **2a** before their reaction with **1a**, and thus, investigated the reactions of enamines, TfOH, and allylsilanes in a flow microreactor (Fig. 2a). Surprisingly, the desired product was obtained in high yield, especially at a higher flow rate (Fig. 2b, bars). This indicates that the condition improving the mixing efficiency is beneficial for this transformation,[22] which was supported by the reactions using other micromixers. The reactions with a thinner and sharper-angled micromixer, which has a better mixing efficiency,[23] showed higher yield.

For a deeper understanding of the mixing efficiency, I explored the Villermaux–Dushman method, which assesses mixing efficiency of micromixers and estimates mixing time of aqueous medium.[24] Based on Yin's condition,[25] I estimated the mixing time of the solutions introduced into the V-shaped 250 μm micromixer (Fig. 2b, dots). The results clearly showed the difference; the condition with the smallest flow rate (2.5 mL/min) had longer mixing time (more than 1 millisecond), whereas that of other conditions was less than 0.1 millisecond. Although these values are those of aqueous medium, the tendency and scale of the mixing time must be the same. The T-shaped mixers also showed longer mixing time than that of V-shaped mixer. Although an advanced analysis such as CFD simulation must be necessary to gain the accurate one, I calculated the Damköhler number of these conditions to be below 0.1 (see supporting information). This indicates that the mass transport is enough faster than the reaction, which is supported by the fact that higher flow rate than 10 mL/min did not change the product yields.[26] The generation of dimer **4** supports this idea. The best results under the batch condition (Method C, −40 °C) showed non-negligible amount of **4**[27], which is derived from the reaction of **1a** with **2a**, whereas the flow condition (V250, 20 mL/min) showed less amount of **4** (Fig. 2c). Thus, these investigations proved that the reactions with short mixing time can trigger the desired reaction between TfOH and enamine **1a** before it reacts with **2a**. These results indicate that the flow microreactor plays a crucial role in the rapid generation of the iminium ion by adding superacids.

Accurate controllability of the reaction time[28,29] and temperature is also a significant characteristic of flow microreactors.[30,31] We have previously reported that the controllability of flow microreactors can control various unstable and reactive species.[32] Inspired by this previous success, I screened the reaction time in the range of decamilliseconds to seconds and the reaction temperature. The results are summarized as the contour map in the left part of Figure 2d, revealing that the reaction condition with 21 milliseconds of the reaction time and 15 °C of the reaction temperature affords the highest yield of this transformation. This map also indicates that conditions with a lower temperature and shorter reaction time gave a lower product yield, suggesting that these conditions are insufficient for the generation of the iminium ion. Additionally, the lower yield at higher temperatures and longer reaction times could be derived from the decomposition of the iminium ion, such as the β-elimination of the generated

iminium to afford the starting enamine. Although **1a** was not detected after the reactions, the amount of dimer **4**, which is generated from **1a** with iminium ion **2a** was increased when the reaction time and temperature increased. This indicates that at such conditions, **2a** was decomposed to **1a** (supporting information Table S6 for detail). Thus, this contour map can be regarded as a visualization of the stability and reactivity of the generated cation (**2a**). I then investigated the reaction mediated by a 6-membered ring iminium ion (**2b**) and determined the yield of the corresponding product **5** (Fig. 2d, right). Comparing these two contour maps shows that the pyrrolidine-type product **3** can be obtained in higher yields at higher temperatures and longer reaction times.

The irreversible generation of the cationic species was confirmed using a low-temperature NMR study. The reacting solution emitted from the flow reactor was captured in an NMR test tube cooled at −78 °C, and immediately its ^{1}H NMR was measured at the same temperature. The NMR chart shows a highly deshielded proton H_a (9.49 ppm, shown in Fig. 2e, left), indicating the generation of iminium ion **2a** as well as oxocarbenium ion **2c** (Fig. 2e, right, H_b was appeared at 10.07 ppm). Notably, these NMR charts did not show the precursors (enamine **1a** for **2a** and acetal **1c** for **2c**), significantly supporting the irreversible generation of the iminium and oxonium cations. It is noteworthy that the irreversible generation of the iminium ion is crucial for its reaction. When using weaker acids such as benzoic acid (p*K*a 22), acetic acid (p*K*a 24), and trifluoroacetic acid (p*K*a 12 in acetonitrile),[33] their reactions with **1a** and allyltrimethylsilane in the flow microreactor did not afford **3**.

Reactions of cations with nucleophiles and direct cross–coupling reaction

After establishing the flash generation of the cationic species, I investigated their reactions with various carbon nucleophiles (Table 1). C-C bond formed with neutral nucleophiles resulted in good to high yields of the corresponding products (entries 1–9). These nucleophiles are incompatible with conventional methods for reversible cation generation. Additionally, the cations were generated within 82 ms, much faster than conventional electrochemical methods,[34] resulting in a reaction time of only 20 s.

I attempted to develop reactions between multiple reactive species using the flash generation of cationic species and their reactions with neutral nucleophiles. This flow strategy aimed to enable a reaction between the cationic species and carbanions, providing a direct cross-coupling involving C-C bond formation. As a feasibility study, I investigated the reactions of the iminium cation with alkyl metal species as carbanions (*n*Bu^{-}) and different counter ions (Li^{+}, $MgCl^{+}$, and $ZnCl^{+}$; Table 1, entries 10–12). Direct cation-anion coupling afforded the desired product **13**, where a sp^3-sp^3 C-C bond was formed in high yield by virtue of the fast mixing and precise time control together with the precise temperature control of the flow systems. Surprisingly, these cross-coupling reactions were completed within 0.069 s owing to the high reactivities of both the cationic species and carbanions. The flow microreactors enabled the direct cross-coupling of the reactive species that selectively proceeded without many side reactions, such as the ®-elimination of the cation and protonation of the anions by the solvent (dichloromethane). As the electronegativity of the counter ion increased (Li:0.98, Mg:1.31, and Zn:1.65), the flow reaction yield decreased, suggesting that reactive anions are suitable for direct reactions with the cationic species. Moreover, the reaction of the lithium species required the shortest time to complete (0.36 s). This suggests that because of its high reactivity, *n*-butyllithium could react with the onium cation before decomposition. Additionally, the most effective way to achieve rapid reactions is through the direct reaction of cationic species with carbanions bearing a lithium counter ion.

Convergent approach of double short-lived intermediates

Finally, I attempted to establish a biosynthesis-inspired reaction system in which multiple reactive intermediates were generated and reacted in flow condition. We have reported a linear reaction integration in which several intermediates are generated and reacted individually.[35]

Based on the concept of reaction integration,[36] I designed a convergent-type integration that generated cationic species irreversibly at one location and carbanions at another location (Table 2), enabling the simultaneous utilization of multiple reactive intermediates. As carbanions, aryl lithiums, which were generated from the corresponding aryl bromides with *n*BuLi in the flow microreactor,[29] were utilized for this transformation. The coupling of the iminium and oxonium cations with the aryl anions in a flow microreactor resulted in the formation of sp^3-sp^2 carbon-carbon bonds and synthesis of the coupling products in good to high yields (entries 1–12). Various aryl anions, including ones cannot be utilized in batch reactors due to their short lifetime (entry 3 and 10),[37] were used in the reaction with pyrrolidine-type iminium cations **2a**, **2d**, and **2e** (entries 1–10). Moreover, this convergent reaction demonstrated some examples that were not achieved by conventional methods: the mono-selective coupling of dibromoarenes (entry 4),[38] in which transition-metal-catalyzed cross-coupling is seldomly achieved, and the reaction at the *meta*-position of an electron-donating group (entry 6), whose selectivity is prohibited in Friedel-Crafts-type reactions.[39] Iminium cations bearing other protecting groups, *tert*-butoxycarbonyl (Boc) and allyloxycarbonyl (Alloc), which can be easily deprotected under acidic conditions, were used in this reaction system (entries 8–10). Especially, by virtue of the high reactivity, the coupling reaction within one second was demonstrated (entry 10). The reactions of more unstable cations also afforded the products in good to high yields (entries 11 and 12). These results demonstrate the effectiveness of this rapid generation and reaction concept, resulting in direct cross-coupling of various substrates.

Direct cross-coupling with sp carbon

In addition to the flash formation of sp^3-sp^3 and sp^3-sp^2 C-C bonds, I investigated the cross-coupling involving sp^3-sp C-C bond formation.[40] The sp anions were generated from the terminal alkynes and *n*-butyllithium in a flow reactor, which subsequently reacted with the iminium cations to afford the coupling products in good to high yields (Table 2, entries 13–21). Iminium cations with increased instability (entries 20 and 21) and sp anions bearing electrophilic functionalities (entries 14–16)[41] were also applicable in this convergently integrated reaction. Because traditional reactions are inefficient for such transformations, introducing alkynyl groups to the 〈-position of pyrrolidines bearing electron-withdrawing groups in this rapid convergent reaction demonstrated great synthetic utility. As well as the iminium ions, this integrated flow system allowed generation of thionium ion **2f**, which reacted with sp anion to afford the coupling product in a good yield (entry 22).

Further investigation of sp^3-sp coupling showed that repeated lithiation of the alkyne and sp^3-sp coupling yielded unsymmetrical alkynes (Fig. 3). The first alkynylation reaction proceeded rapidly, and after deprotection and isolation, the next alkynylation completed within 2.8 s after the activation of the precursor. This series of reactions enabled the rapid synthesis of unsymmetrical alkynes bearing *N*-containing cyclic motifs. Four types of reactive intermediates were separately generated in different flow paths, and once mixed, their coupling reaction proceeded instantly. This system controls the flow reaction space, regulating the generation time and reactions of the reactive intermediates. Therefore, convergently integrated rapid reactions demonstrated a swift construction of molecular complexity, including alkynes bearing different pyrrolidines at both carbons.

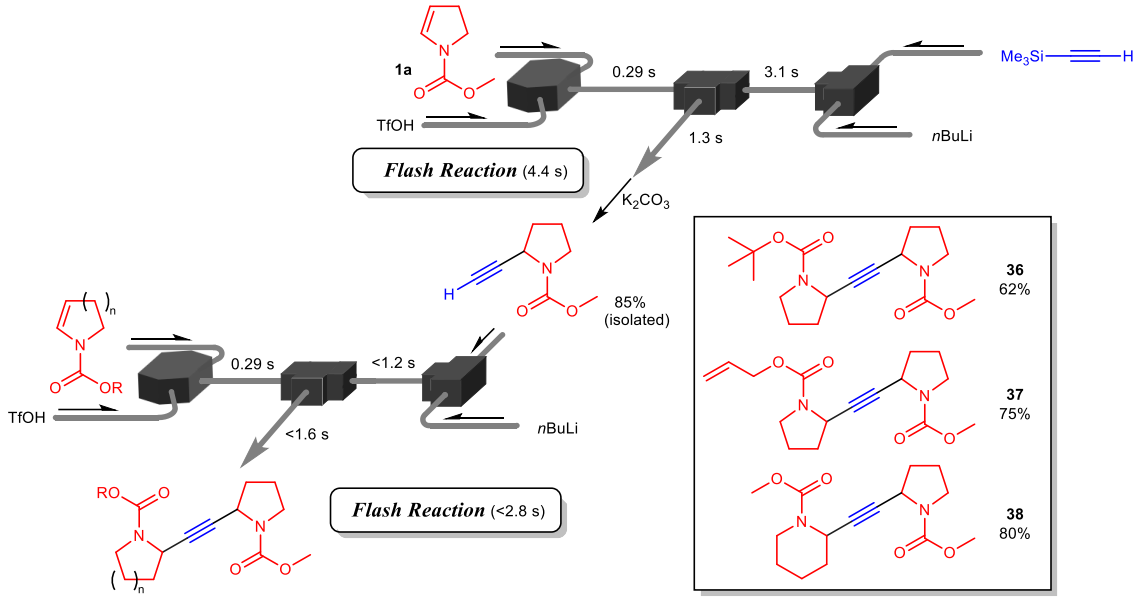

Figure 3. Twice direct cross-coupling reaction using four intermediates.[a]

[a]Flow microreactor system composed of two V-shaped micromixers (inner diameter: 250 μm) and four T-shaped ones (inner diameter: 250 μm) was used. Typical reaction condition for first reaction: cation precursor (0.05 M), TfOH (0.050 M, 2.0 eq.), trimethylsilyl acetylene (0.18 M, 4.3 eq.), and *n*BuLi (0.60 M, 3.6 eq) at −10 °C. Typical reaction condition for second reaction: cation precursor (0.05 M), TfOH (0.050 M, 2.0 eq), terminal alkyne (0.18 M, 8.6 eq.), and *n*BuLi (0.60 M, 7.2 eq.) at −10 °C.

Conclusion

In summary, convergent approach of double intermediates was demonstrated by virtue of flow microreactors. Flow microreactor's capability of rapid and highly-selective reactions enabled unprecedented synthetic method, in which acidic activation of unsaturated precursors irreversibly generates cationic species, preventing undesired dimerization reactions. Cationic species and carbanions were respectively generated in different parts of the flow system, and met together before they decompose, enjoying their high reactivities. It is anticipated that this series of flash reactions could achieve complicated syntheses taking advantage of multiple reactive intermediates, and further investigation is currently underway.

References

1. Cochrane, R. V. K. & Vederas, J. C. Highly Selective but Multifunctional Oxygenases in Secondary Metabolism. *Acc. Chem. Res.* **47**, 3148–3161 (2014).
2. Guo, S.-S., Zhang, T., Garcia-Borràs, M., Hung, Y.-S., Billingsley, J. M., Houk, K. N., Hu, Y. & Tang, Y. Biosynthesis of Heptacyclic Duclauxins Requires Extensive Redox Modifications of the Phenalenone Aromatic Polyketide. *J. Am. Chem. Soc.* **140**, 6991–6997 (2018).
3. Bao, R., Zhang, H. & Tang, Y. Biomimetic Synthesis of Natural Products: A Journey To Learn, To Mimic, and To Be Better. *Acc. Chem. Res.* **54**, 3720–3733 (2021).
4. Colella, M., Tota, A., Takahashi, Y., Higuma, R., Ishikawa, S., Degennaro, L., Luisi, R. & Nagaki, A. Fluoro-Substituted Methyllithium Chemistry: External Quenching Method Using Flow Microreactors. *Angew. Chem. Int. Ed.* **59**, 10924–10928 (2020).
5. Yoshida, J., Takahashi, Y. & Nagaki, A. Flash chemistry: flow chemistry that cannot be done in batch. *Chem. Commun.* **49**, 9896–9904 (2013).
6. Olah, G. A. & Prakash, G. K. S. Carbocation Chemistry (Joen Wiley & Sons, Inc., 2004).
7. Song, Z.-L., Fan, C.-A. & Tu, Y.-Q. Semipinacol Rearrangement in Natural Product Synthesis. *Chem. Rev.* **111**, 7523–7556 (2011).
8. Mo, F., Qiu, D., Zhang, L. & Wang, J. Recent Development of Aryl Diazonium Chemistry for the Derivatization of Aromatic Compounds. *Chem. Rev.* **121**, 5741–5829 (2021).
9. For an example for the chemical-oxidative generation of carbocations, see; Tu, W. & Floreancig, P. E. Oxidative carbocation formation in macrocycles: synthesis of the neopeltolide macrocycle. *Angew. Chem. Int. Ed.* **48**, 4567–4571 (2009).
10. Wiebe, A., Gieshoff, T., Möhle, S., Rodrigo, E., Zirbes, M. & Waldvogel, S. R. Electrifying Organic Synthesis. *Angew. Chem. Int. Ed.* **57**, 5594–5619 (2018).
11. Yan, M., Kawamata, Y. & Baran, P. S. Synthetic Organic Electrochemical Methods Since 2000: On the Verge of a Renaissance. *Chem. Rev.* **117**, 13230–13319 (2017).
12. Other electron-transfer methods such as a photochemical approach can slowly generate cations; see Zhu, Q., Gentry, E. C. & Knowles, R. R. Catalytic Carbocation Generation Enabled by the Mesolytic Cleavage of Alkoxyamine Radical Cations. *Angew. Chem. Int. Ed.* **55**, 9969–9973 (2016).
13. Yoshida, J. & Suga, S. Basic Concepts of "Cation Pool" and "Cation Flow" Methods and Their Applications in Conventional and Combinatorial Organic Synthesis. *Chem. Eur. J.* **8**, 2650–2658 (2002).
14. Lebedel, L., Yamashita, H., Shimizu, Y., Bhuma, N., Abada, Z., Ardá, A., Désiré, J., Michelet, B., Mingot, A., Abou-Hassan, A., Takumi, M., Jiménez-Barbero, J., Nagaki, A., Blériot, Y. & Thibaudeau, S. Insight into the Ferrier rearrangement by combining flash chemistry and superacids. *Angew. Chem., Int. Ed.* **60**, 2036–2041 (2021).

15. Kütt, A., Selberg, S., Kaljurand, I., Tshepelevitsh, S., Heering, A., Darnell, A., Kaupmees, K., Piirsalu, M. & Leito, I. p*K*a values in organic chemistry – Making maximum use of the available data. *Tetrahedron Lett.* **59**, 3738–3748 (2018).
16. Olah, G. A., Prakash, G. K. S., Molnar, A. & Sommer, J. Superacid Chemistry (Wiley, 2009).
17. Gutmann, B., Cantillo, D. & Kappe, C. O. Continuous-Flow Technology—A Tool for the Safe Manufacturing of Active Pharmaceutical Ingredients. *Angew. Chem. Int. Ed.* **54**, 6688–6728 (2015).
18. Capaldo, L., Wen, Z. & Noël, T. A field guide to flow chemistry for synthetic organic chemists. *Chem. Sci.* (2023). DOI: 10.1039/D3SC00992K.
19. Hartman, R. L., McMullen, J. P. & Jensen, K. F. Deciding Whether To Go with the Flow: Evaluating the Merits of Flow Reactors for Synthesis. *Angew. Chem. Int. Ed.* **50**, 7502–7519 (2011).
20. Tonhauser, C., Natalello, A., Löwe, H & Frey, H. Microflow Technology in Polymer Synthesis. *Macromolecules* **45**, 9551–9570 (2012).
21. Ashikari, Y., Saito, K., Nokami, T., Yoshida, J. & Nagaki, A. Oxo-Thiolation of Cationically Polymerizable Alkenes Using Flow Microreactors *Chem. Eur. J.* **25**, 15239–15243 (2019).
22. Morse, P. D., Beingessner, R. L. & Jamison, T. F. Enhanced Reaction Efficiency in Continuous Flow. *Isr. J. Chem.* **57**, 218–227 (2017).
23. Endo, Y., Furusawa, M., Shimazaki, T., Takahashi, Y., Nakahara, Y. & Nagaki, A. Molecular Weight Distribution of Polymers Produced by Anionic Polymerization Enables Mixability Evaluation. *Org. Process Res. Dev.* **23**, 635–640 (2019)
24. Commenge, J.-M. & Falk, L. Villermaux–Dushman protocol for experimental characterization of micromixers. *Chem. Eng. Process.; Process Intensif.* **50**¸ 979–990 (2011).
25. Iv, P., Zhang, L., Srinivasakannan, C., Li, S., He, Y., Chen, K. & Yin, S. Mixing performance in T-shape microchannel at high flow rate for Villermaux–Dushman reaction. *Microchem. J.* **155**, 104662 (2020).
26. Asano, S., Yatabe, S., Maki, T. & Mae, K. Numerical and Experimental Quantification of the Performance of Microreactors for Scaling-up Fast Chemical Reactions. *Org. Process Res. Dev.* **23**, 807–817 (2019).
27. Suga, S., Nagaki, A., Tsutsui, Y. & Yoshida, J. "*N*-Acyliminium Ion Pool" as a Heterodiene in [4+2] Cycloaddition Reaction. *Org. Lett.* **5**, 945–947 (2003).
28. Harenberg, J. H., Weidmann, N. & Knochel. P. Continuous-Flow Reactions Mediated by Main Group Organometallics. *Synlett* **31**, 1880–1887 (2020).
29. Hessel, V., Kralisch, D., Kockmann, N., Noël, T. & Wang, Q. Novel Process Windows for

Enabling, Accelerating, and Uplifting Flow Chemistry. *ChemSusChem* **6**, 746–789 (2013).
30. Fuse, S., Otake, Y. & Nakamura, H. Peptide Synthesis Utilizing Micro-flow Technology. *Chem. Asian J.* **13**, 3818–3832 (2018).
31. Ramanjaneyulu, B. T., Vishwakarma, N. K., Vidyacharan, S., Adiyala, P. R. & Kim, D.-P. Towards Versatile Continuous-Flow Chemistry and Process Technology Via New Conceptual Microreactor Systems. *Bull. Korean Chem. Soc.* **39**, 757–772 (2018).
32. Nagaki, A. Recent topics of functionalized organolithiums using flow microreactor chemistry. *Tetrahedron Lett.* **60**, 150923 (2019).
33. Eckert, F., Leito, I., Kaljurand, I., Kütt, A., Klamt, A. & Diedenhofen, M. Prediction of Acidity in Acetonitrile Solution with COSMO-RS. *J. Comput. Chem.* **30**, 799–810 (2009).
34. Takumi, M., Sakaue, H. & Nagaki, A. Flash Electrochemical Approach to Carbocations. *Angew. Chem. Int. Ed.* **61**, e202116177 (2022).
35. Ashikari, Y., Kawaguchi, T., Mandai, K., Aizawa, Y. & Nagaki, A. A Synthetic Approach to Dimetallated Arenes Using Flow Microreactors and the Switchable Application to Chemoselective Cross-Coupling Reactions *J. Am. Chem. Soc.* **142**, 17039–17047 (2020).
36. Nagaki, A., Ashikari, Y., Takumi, M. & Tamaki, T. Flash Chemistry Makes Impossible Organolithium Chemistry Possible. *Chem. Lett.* **50**, 485–492 (2021).
37. Nagaki, A., Kim, H., Usutani, H., Matsuo, C. & Yoshida, J. Generation and Reaction of Cyano-substituted Aryllithium Compounds Using Microreactors. *Org. Biomol. Chem.* **8**, 1212–1217 (2010).
38. Nagaki, A., Tomida, Y., Usutani, H., Kim, H., Takabayashi, N., Nokami, T., Okamoto, H. & Yoshida, J. Integrated Micro Flow Synthesis Based on Sequential Br-Li Exchange Reactions of p-, m-, and o-Dibromobenzenes. *Chem. Asian J.* **2**, 1513–1523 (2007).
39. Wang, G.-W., Wheatley, M., Simonetti, M., Cannas, D. M. & Larrosa, L. Cyclometalated Ruthenium Catalyst Enables *Ortho*-Selective C–H Alkylation with Secondary Alkyl Bromides. *Chem.* **6**, 1459–1468 (2020).
40. Eckhardt, M. & Fu, G. C. The First Applications of Carbene Ligands in Cross-Couplings of Alkyl Electrophiles: Sonogashira Reactions of Unactivated Alkyl Bromides and Iodides. *J. Am. Chem. Soc.* **125**, 13642–13643 (2003).
41. Nagaki, A., Kim, H. & Yoshida, J. Aryllithium Compounds Bearing Alkoxycarbonyl Groups: Generation and Reactions Using a Microflow System. *Angew. Chem. Int. Ed.* **47**, 7833–7836 (2008).

Supporting Information

9. General Information

Abbreviations. atmospheric pressure chemical ionization (APCI), approximately (approx. or ~), broad (br), butyl (Bu), degrees Celsius (°C), calculated (calcd), deuteritated chloroform ($CDCl_3$), deuteritated dichloromethane (CD_2Cl_2), dichloromethane (CH_2Cl_2), centimeter(s) (cm), doublet (d), Damköhler number (Da), electron ionization (EI), equivalent (equiv or eq), electrospray ionization (ESI), ethyl acetate (EtOAc), gram(s) (g), gas chromatography (GC), gel permeation chromatography (GPC), hour(s) (h), high resolution mass-spectrometry (HRMS), hertz (Hz), coupling constant (*J*), length of tubes (L), liter(s) (L), mol L^{-1} of molar concentration (M), multiplet (m), methyl (Me), metallic functionality (*Met*), milligram(s) (mg), megahertz (MHz), minute(s) (min), milliliter(s) (mL), millimole(s) (mmol), mole(s) (mol), normal (*n*), nuclear magnetic resonance (NMR), parts per million (ppm), polytetrafluoro-ethylene or Teflon (PTFE), quartet (q), Reynold's number (Re), room temperature (25 ± 3 ° C, rt), second(s) (s or sec), singlet (s), triplet (t), tertiary (*t* or *tert*), tri-*n*-butylammonium fluoride (TBAF), trifluoromethanesulfonic acid (TfOH), tetrahydrofuran (THF), tetramethylsilane (TMS), residence time of microtube reactor R_n (t^{Rn}), chemical shift in ppm downfield from TMS (δ), inner diameter of tubes and mixers (φ), micrometer(s) (μm).

General. ^1H, ^{13}C and ^{19}F NMR spectra were recorded in on Varian MERCURY plus-400 (^1H 400 MHz, ^{13}C 100 MHz), JEOL JNM-ECZ400S (^1H 400 MHz, ^{13}C 100 MHz, ^{19}F 376 MHz), or JEOL JNM-ECZ-500R spectrometer (^1H 500 MHz). Chemical shifts are recorded using a solvent ($CHCl_3$: 7.26 ppm, CH_2Cl_2: 5.32 ppm) signal as an internal standard for ^1H NMR, methine signal of $CHCl_3$ for ^{13}C NMR (77.36 ppm) unless otherwise noted. No internal standard for chemical shifts was used for ^{19}F NMR analyses. Because of rotamers, the ^1H and ^{13}C NMR charts of carbamates showed broad peaks. GC analysis was performed on a SHIMADZU GC-2014 gas chromatograph equipped with a flame ionization detector using a fused silica capillary column (column, CBP1; 0.22 mm x 25 m). Temperature of GC oven was 50 °C at first, and after 5min the temperature was increased 10 °C per min. GC yields were calculated by GC analyses with internal standards such as *n*-tetradecane using calibration lines derived from commercial or isolated compounds with the internal standards. UV/Vis measurement was performed on JASCO V730 with a disposable cuvette made of PMMA (manufactured by JASCO Co., optical path length 1.0 cm). Mass spectra were obtained on Thermo Fisher Scientific EXACTIVE plus (ESI and APCI), JEOL JMS-T100CS (ESI), JEOL JMSSX102A (EI), and JEOL JMS-700 (EI). Merck pre-coated silica gel F254 plates (thickness 0.25 mm) were used for TLC analyses. Flash chromatography was carried out on a silica gel

(Kanto Chem. Co., Silica Gel N, spherical, neutral, 40–100 μm). Preparative GPC was carried out on Japan Analytical Industry LC-918 equipped with JAIGEL-1H and 2H using $CHCl_3$ as an eluent. All batch reactions were carried out in a flame-dried glassware under argon atmosphere unless otherwise noted.

Flow Synthesis. Stainless steel (SUS304) T- and V-shaped micromixers with inner diameter of 250 and 500 μm were manufactured by Sanko Seiki Co., Inc. Stainless steel (SUS316) microtube reactors with 1000, 500, and 250 μm inner diameter and PTFE tube with inner diameter of 1000 μm were purchased from GL Sciences. The syringe pumps (Harvard Model PHD ULTRA) equipped with gastight syringes (purchased from SGE) were used for introduction of the solutions into the micromixer systems via stainless steel fittings (GL Sciences, 1/16 OUW). Flow microreactor system is composed with stainless steel pre-cooling units (**P1**, **P2**, etc.), stainless steel microtube reactors (**R1**, **R2**, etc.), T- or V-shaped micromixers (**M1**, **M2**, etc.), and, if necessary, PTFE tube with inner diameter of 1000 μm. Unless otherwise noted, the inner diameter of the stainless and PTFE tubes is 1000 μm, and the length of the pre-cooling units is 100 cm. Unless otherwise noted, the inner diameter of micromixers is 250 μm. The solution of *n*-butyllithium was prepared by dilution of the commercial solution with dehydrated *n*-hexane.

Materials. Dehydrated THF, diethyl ether, dichloromethane and *n*-hexane were purchased from FUJIFILM Wako Pure Chemical Corporation and Kanto Chemical Co., Inc., and were used without further purification. A solution of *n*-butyllithium (in *n*-hexane, 1.6 M) was purchased from Kanto Chemical Co., Inc. and stored at −20 °C. CD_2Cl_2 was purchased from FUJIFILM Wako Pure Chemical Corporation, and dried over molecular sieves 4A before use. 2-Pyrrolidone, 2-piperidone, TfOH, allyltrimethylsilane, 1-trimethylsiloxy-1-cyclohexene, 1-methoxy-1-trimethylsilyloxypropene, 2-trimethylsiloxypropene, 1-phenyl-1-trimethylsiloxyethylene, 3,4-dihydro-2*H*-pyran (**1c**), 4-bromobenzotrifluoride, 1-bromo-4-fluorobenzene, 4-bromobenzonitrile, 1,4-dibromobenzene, 4-bromoanisole, 1-bromo-3-methoxybenzene, 1-bromo-2-methoxybenzene, 1-hexyne, methyl propiolate, glycidyl propargyl ether, 4-ethynylbenzonitrile, 3-ethynylthiophene, trimethylsilylacetylene, phenylacetylene, *n*-butylmagnesium chloride, and TBAF (in THF, 1.0 M) were purchased from commercial suppliers, and were used without further purification. Methyl 2,3-dihydropyrrole-1-carboxylate (**1a**),[1] methyl 3,4-dihydropyridine-2*H*-carboxylate (**1b**),[2] *tert*-butyl 2,3-dihydropyrrole-1-carboxylate (**1d**),[3] and allyl 2,3-dihydropyrrole-1-carboxylate (**1e**)[4] were prepared by protection of 2-pyrrolidone and 2-poperidone,[5] followed by DIBAL reduction and acidic β-elimination.[6] *n*-Butylzinc chloride was synthesized[7] and titrated[8] according to the literature.

10. Synthetic procedures

2.1 Generation and reaction of *N*-acyliminium ion 2a in a batch reactor (Method A–D)

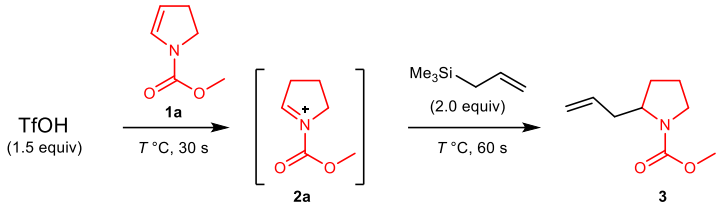

Method A. To a CH_2Cl_2 solution (6.0 mL) of TfOH (0.30 mmol) cooled at *T* °C, a solution of **1a** (0.200 mmol, 4.0 mL) was added for 30 s. After completion of the addition, a CH_2Cl_2 solution of allyltrimethylsilane (0.40 mmol) was added immediately. The reaction mixture was stirred for 60 s, and a solution of TBAF (1.0 M in THF, 0.30 mL) was added for quenching. To the mixture, Et_3N (2.0 mL), brine (2.0 mL) and internal standard were added for GC analyses. The yields are summarized in Supplementary Table S1.

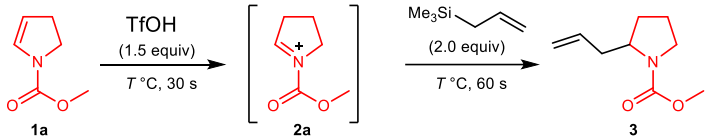

Method B. To a CH_2Cl_2 solution (4.0 mL) of **1a** (0.200 mmol) cooled at *T* °C, a CH_2Cl_2 solution (6.0 mL) of TfOH (0.30 mmol) was added for 30 s. After completion of the addition, a CH_2Cl_2 solution (2.0 mL) of allyltrimethylsilane (0.40 mmol) was added immediately. The reaction mixture was stirred for 60 s, and a solution of TBAF (1.0 M in THF, 0.30 ml) was added for quenching. To the mixture, Et_3N (2.0 mL), brine (2.0 mL) and internal standard were added for GC analyses. The yields are summarized in Supplementary Table S1.

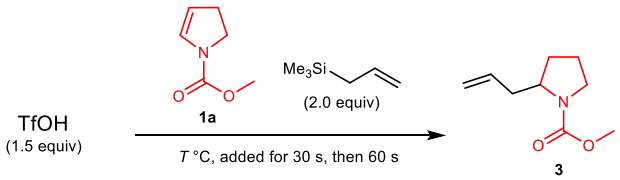

Method C. To a CH_2Cl_2 solution (6.0 mL) of TfOH (0.30 mmol) cooled at *T* °C, a CH_2Cl_2 solution (4 mL) of **1a** (0.200 mmol) and allyltrimethylsilane (0.40 mmol) was added for 30 s. The reaction mixture was stirred for 60 s, and a solution of TBAF (1.0 M in THF, 0.30 mL) was added for quenching. To the mixture, Et_3N (2.0 mL), brine (2.0 mL) and internal standard were added for GC analyses. The yields are summarized in Supplementary Table S1.

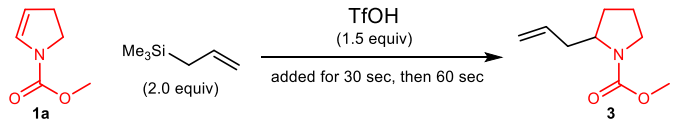

Method D. To a CH_2Cl_2 solution (4.0 mL) of **1a** (0.200 mmol) and allyltrimethylsilane (0.40 mmol), a CH_2Cl_2 solution (6.0 mL) of TfOH (0.30 mmol) was added for 30 s. The reaction mixture was stirred for 60 s, and a solution of TBAF (1.0 M in THF, 0.30 mL) was added for quenching. To the mixture, Et_3N (2.0 mL), brine (2.0 mL) and internal standard were added for GC analyses. The yields are summarized in Supplementary Table S1.

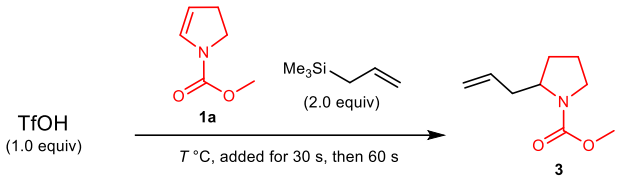

Method C' (TfOH 1 eq). To a CH_2Cl_2 solution (6.0 mL) of TfOH (0.20 mmol) cooled at T°C, a CH_2Cl_2 solution (4 mL) of **1a** (0.200 mmol) and allyltrimethylsilane (0.40 mmol) was added for 30 s. The reaction mixture was stirred for 60 s, and a solution of TBAF (1.0 M in THF, 0.30 mL) was added for quenching. To the mixture, Et_3N (2.0 mL), brine (2.0 mL) and internal standard were added for GC analyses. The yields are summarized in Supplementary Table S1.

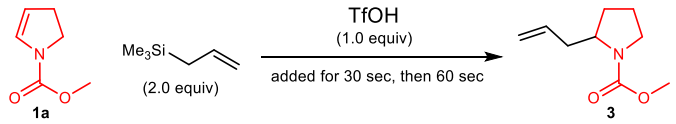

Method D' (TfOH 1 eq). To a CH_2Cl_2 solution (4.0 mL) of **1a** (0.200 mmol) and allyltrimethylsilane (0.40 mmol), a CH_2Cl_2 solution (6.0 mL) of TfOH (0.20 mmol) was added for 30 s. The reaction mixture was stirred for 60 s, and a solution of TBAF (1.0 M in THF, 0.30 mL) was added for quenching. To the mixture, Et_3N (2.0 mL), brine (2.0 mL) and internal standard were added for GC analyses. The yields are summarized in Supplementary Table S1.

Supplementary Table S1. Results of batch reactions[a]

Method	TfOH (eq)	*T* (°C)	conversion (%)	yield of **3** (%)
A	1.5	0	100	3
A	1.5	−20	100	28
A	1.5	−40	100	29
A	1.5	−78	100	35
B	1.5	0	100	0
B	1.5	−20	100	9
B	1.5	−40	100	0
B	1.5	−78	100	12
C	1.5	0	100	44
C	1.5	−20	100	39
C	1.5	−40	100	45
C	1.5	−78	100	35
C’	1.0	0	100	7
C’	1.0	−20	100	7
C’	1.0	−40	100	8
C’	1.0	−78	100	10
D	1.5	0	100	21
D	1.5	−20	100	21
D	1.5	−40	100	18
D	1.5	−78	100	20
D’	1.0	0	100	2
D’	1.0	−20	100	3
D’	1.0	−40	100	2
D’	1.0	−78	100	0

[a]Yields and conversions were determined by GC using an internal standard. Retention time of **3**: 15.7 min

Isolation and quantification of the dimer

After extraction, the crude mixture was purified by flash chromatography (hexane/EtOAc = 4/1) and GPC to afford the dimer (**4**). The yield of is summarized in Supplementary Table S2.

Supplementary Table S2. Yields of dimer **4**[a]

condition	yield (%)	condition	yield (%)
Method A, 0 °C	64	Method B, 0 °C	64
Method A, −20 °C	54	Method B, −20 °C	62
Method A, −40 °C	58	Method B, −40 °C	64
Method A, −78 °C	66	Method B, −78 °C	48
Method C, 0 °C	50	Method D, 0 °C	42
Method C, −20 °C	48	Method D, −20 °C	44
Method C, −40 °C	48	Method D, −40 °C	42
Method C, −78 °C	48	Method D, −78 °C	38
Method C', 0 °C	78	Method D', 0 °C	74
Method C', −20 °C	64	Method D', −20 °C	60
Method C', −40 °C	72	Method D', −40 °C	76
Method C', −78 °C	80	Method D', −78 °C	42
Flow, 2.5 mL/min	40	Flow, 15 mL/min	32
Flow, 5.0 mL/min	30	Flow, 20 mL/min	26
Flow, 10 mL/min	28		

[a]Yields were determined by GC. Flow reactions were carried out using V-250 mixer at 0 °C.

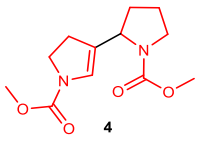

4

Methyl 4-(*N*-methoxycarbonylpyrrolidine-2-yl)-2,3-dihydropyrrole-1-carboxylate (4).
GC retention time: 25.4 min. ^{1}H NMR (400 MHz, $CDCl_3$, rotamer) δ 1.70–1.96 (m, 4 H), 2.40–2.68 (br, 2 H), 3.28–3.48 (br, 2 H), 3.64 (s, 3 H), 3.67 (s, 3 H), 3.69–3.82 (m, 2 H), 4.34-4.50 (br, 1 H), 6.17–6.39 (br, 1 H); ^{13}C NMR (100 MHz, $CDCl_3$, rotamer) δ 23.4 and 24.0, 29.1, 30.3 and 31.1, 45.9 and 46.1, 46.6, 52.6, 52.7, 55.7 and 56.2, 123.91, 124.7 and 125.3, 152.9 and 153.6, 155.9; HRMS (ESI) calcd for $C_{12}H_{18}N_2O_4Na$ $[M+Na]^+$: 277.1159, found: 277.1152.

(1) Effect of flow rate and mixer for generation and reaction of *N*-acyliminium ion 2a in a flow microreactor (Method E)

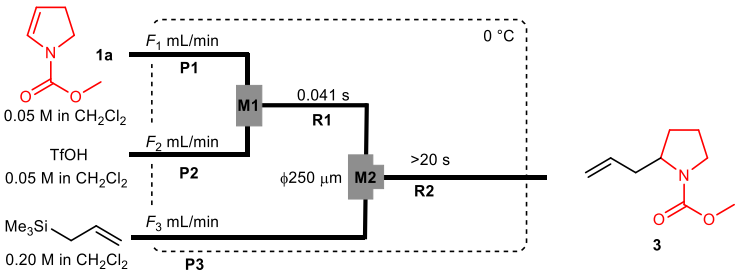

A flow microreactor system consisting of a micromixer (**M1**, V-shaped or T-shaped, φ = 250, or 500 μm) and a T-shaped micromixer (**M2**, φ = 250 μm), two microtube reactors (**R1** and

R2), and three pre-cooling units (**P1**–**P3**) was used. The flow microreactor system was dipped in a cooling bath (0 °C). A solution of **1a** (0.0500 M in CH_2Cl_2, flow rate: F_1 mL/min) and a solution of TfOH (0.050 M in CH_2Cl_2, flow rate: F_2 mL/min) were introduced into **M1** using syringe pumps. The mixed solution was passed through **R1** (φ^{R1} μm, L^{R1} cm, 0.041 s), and was mixed with a solution of allyltrimethylsilane (0.20 M in CH_2Cl_2, flow rate: F_3 mL/min) in **M2.** The resulting solution was passed through **R2** (L^{R2}= 1000 cm). After a steady state was reached, an aliquot of the product solution was collected and was treated with TBAF, Et_3N and brine. The reaction mixture was analyzed by GC. The results are summarized in Supplementary Table S3.

Supplementary Table S3. Flow rate and mixer dependency of the generation and reaction of **2a**[a]

entry	F_1 (mL/min)	F_2 (mL/min)	F_3 (mL/min)	mixer **M1** shape	mixer **M1** φ^{M1} (μm)	tube **R1** φ^{R1} (μm)	tube **R1** L^{R1} (cm)	yield of **3** (%)
1	8	12	4	V	250	500	7.0	65
2	6	9	3	V	250	500	5.25	65
3	4	6	2	V	250	500	3.5	67
4	2	3	1	V	250	250	7.0	46
5	1	1.5	0.5	V	250	250	3.5	32
6	8	12	4	T	250	500	7.0	51
7	8	12	4	T	500	500	7.0	27

[a]Yields were determined by GC using an internal standard. Retention time: 15.7 min

(2) Mass transfer characterization

Villermaux–Dushman protocol for characterization of micromixers (different flow rate)

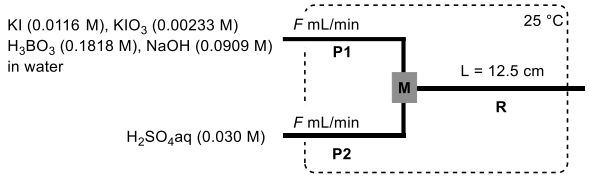

The set of solution concentration was based on the reported condition.[9] A flow microreactor system consisting of micromixer **M** (V- or T-shaped, φ = 250 or 500 μm), microtube reactor **R**, and two pre-cooling units (**P1** and **P2**) was used. The flow microreactor system was dipped in a water bath (25 °C). An aqueous solution containing KI (0.0116 M), KIO_3 (0.00233 M), H_3BO_3 (0.1818 M) and NaOH (0.0909 M) was introduced in **M** using a syringe pump,

whereas an aqueous solution of H_2SO_4 (0.030 M) was also introduced into **M**. The flow rates of those solutions are the same (F mL/min). The solution mixed in **M** was passed through **R** (L = 12.5 cm). After a steady state was reached, an aliquot of the emitting solution was collected and its absorbance at 353 nm was recorded. According to the literature,[10] the mixing time of micromixers can be calculated as below;

$$t_m = 0.33 \times Abs \times [H^+]^{-4.55} \times [KI]^{-1.5} \times [KIO_3]^{5.8} \times [NaOH]^{-2} \times [H_3BO_3]^{-2}$$

where, t_m is mixing time (second), Abs is the absorbance at 353 nm of the mixture, and [*chemical*] is the concentration of the chemical before being mixed. The results of the Villermaux–Dushman protocol is summarized in Supplementary Table S4. The small differences observed in the results without that of 2.5 mL/min are attributed to having reached the limit of detection. Since dichloromethane (the reaction solvent) has lower viscosity and higher density than water, the net mixing time should be shorter than this table.

Supplementary Table S4. Villermaux–Dushman protocol for micromixers[a]

total flow rate (mL/min)	micromixer[b]	absorbance at 353 nm	t_m (ms)	average of t_m (ms)
20	V-250	0.008	0.0035	
		0.012	0.0053	0.0054
		0.017	0.0075	
15	V-250	0.012	0.0053	
		0011	0.0049	0.0054
		0.014	0.0062	
10	V-250	0.016	0.0071	
		0.022	0.0097	0.0080
		0.016	0.0071	
5.0	V-250	0.096	0.042	
		0.060	0.027	0.028
		0.037	0.016	
2.5	V-250	2.90	1.28	
		2.96	1.31	1.29
		2.89	1.27	
20	T-250	0.031	0.014	
		0.023	0.010	0.011
		0.020	0.0088	
20	T-500	0.097	0.043	
		0.088	0.039	0.041
		0.092	0.041	

[a]Total flow rate means sum of the velocity of the solutions introducing micromixer M. Thus, it can be described as $2 \times F$. [b]Alphabet means its shape (V-shape or T-shape), and the number means the inner diameter (μm).

The relation of the mixing time with the yields for the generation and reaction of iminium ion **2a** with allyltrimethylsilane is summarized in Supplementary Figure S1.

Supplementary Figure S1. Yields and mixing time of micromixers[a]

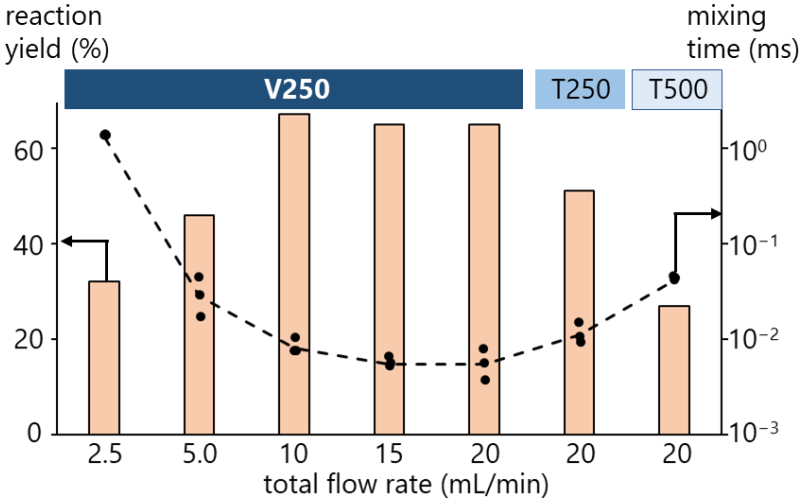

[a]Bars indicate yield of **3** (Supplementary Table S2). Dots indicate mixing time (Supplementary Table S3). Total flow rate means the flow rate introducing to the mixer. Thus, the sum of F_1 and F_2 for reaction yield.

Reynold's Number

The Reynold's number can be calculated according to the following equation;

$$Re = \frac{d \times v \times D_H}{\mu}$$

where, d is density (g/mL, dichloromethane at 0 °C: 1.363),[11] v is velocity (m/s), D_H is hydraulic diameter (m), and μ is viscosity (Pa·s, dichloromethane at 0 °C: 0.5328).[11] Thus, with the best condition (total flow rate: 20 mL/min, temperature: 0 °C, and tube diameter: 500 μm, *vide infra*) can be calculated as 2200, which indicates the condition is in a transition to a turbulent flow regime.

Damköhler Number

The Damköhler number can be defined as follows;[12]

$$Da = \frac{reaction\ rate}{mixing\ rate} \sim \frac{mixing\ time\ scale}{reaction\ time\ scale}$$

Although the value should have a margin of error, the scale of both the reaction time and the mixing time of the cation generation reaction can be estimated. Since Supplementary Table S4 (*vide infra*) indicates the reaction at 0 °C reached the highest yield with 82 ms of the residence time, reaction time is in 10 ms scale. Whereas, above-mentioned Villermaux–Dushman protocol indicates the mixing time for high-yielding condition (total flow rate is higher than 2.5 mL/min) must be smaller than 1 ms. Thus, Da can be determined as smaller than 0.1, which is much smaller than 1.

(3) Reactions of enamines with TfOH followed by reaction with allyltrimethylsilane with varying residence time and temperature

Reactions of 1a (General procedure for making the contour map)

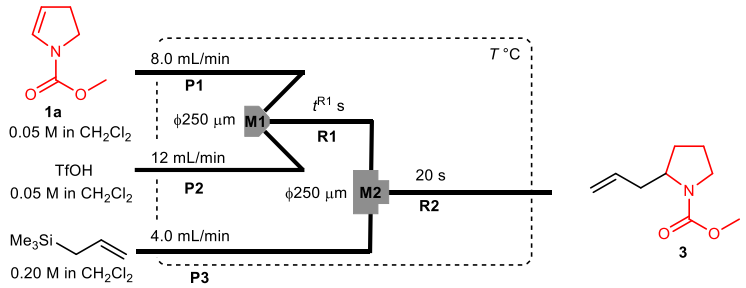

A flow microreactor system consisting of a V-shaped micromixer (**M1**, φ = 250 μm) and a T-shaped micromixer (**M2**, φ = 250 μm), two microtube reactors (**R1** and **R2**), and three pre-cooling units (**P1**–**P3**) was used. The flow microreactor system was dipped in a cooling bath (T°C). A solution of **1a** (0.0500 M in CH_2Cl_2, flow rate: 8.0 mL/min) and a solution of TfOH (0.050 M in CH_2Cl_2, flow rate: 12.0 mL/min) were introduced into **M1** using syringe pumps. The mixed solution was passed through **R1** (φ^{R1} μm, L^{R1} cm, t^{R1} s), and was mixed with a solution of allyltrimethylsilane (0.20 M in CH_2Cl_2, flow rate: 4.0 mL/min) in **M2.** The resulting solution was passed through **R2** (L^{R2}= 1000 cm, t^{R2} = 20 s). After a steady state was reached, an aliquot of the reacting solution was collected and was treated with TBAF, Et_3N and brine. The yield of **3** was analyzed by GC, and was summarized in Supplementary Table S5.

Supplementary Table S5. Yields of **3** with varying temperature (T) and residence time in **R1** (t^{R1})[a]

T (°C)	φ^{R1} (μm)	L^{R1} (cm)	t^{R1} (s)	yield of **3** (%)
30	500	3.5	0.021	61
	1000	3.5	0.082	55
	1000	25	0.59	43
	1000	150	3.5	18
	1000	300	7.1	13
15	500	3.5	0.021	78
	1000	3.5	0.082	65
	1000	25	0.59	46
	1000	150	3.5	31
	1000	300	7.1	25
0	500	3.5	0.021	64
	1000	3.5	0.082	72
	1000	25	0.59	62
	1000	150	3.5	42
	1000	300	7.1	32
-15	500	3.5	0.021	63
	1000	3.5	0.082	75
	1000	25	0.59	58
	1000	150	3.5	52
	1000	300	7.1	42

[a]Yields were determined by GC using an internal standard. Retention time: 15.7 min

Supplementary Table S6. Recovery of **1a** and yield of dimer **4** with varying temperature (T) and residence time in **R1** (t^{R1})[a]

T (°C)	φ^{R1} (μm)	L^{R1} (cm)	t^{R1} (s)	recovery of **1a** (%)	yield of dimer **4** (%)
45	500	3.5	0.021	0	27
30	500	3.5	0.021	0	24
15	500	3.5	0.021	0	23
	1000	25	0.59	0	24
	1000	150	3.5	0	42
	1000	300	7.1	0	44

[a]Yields were determined by GC using an internal standard. Retention time of **1a**: 15.7 min. Retention time of **4**: 25.4 min.

Reactions of 1b

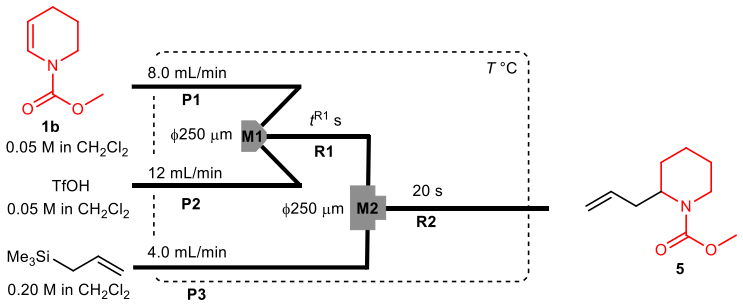

The similar flow microreactor system for **1a** using a solution of **1b** (0.0500 M in CH_2Cl_2, flow rate: 8.0 mL/min), TfOH (0.050 M in CH_2Cl_2, flow rate: 12.0 mL/min), and allyltrimethylsilane (0.20 M in CH_2Cl_2, flow rate: F_3 mL/min) was used. The yield of desired product **5** (methyl 2-allylpiperidine-1-carboxylate) was analyzed by GC. The results are summarized in Supplementary Table S7.

Supplementary Table S7. Yields of **5** with varying temperature (T) and residence time in **R1** (t^{R1})[a]

T (°C)	φ^{R1} (μm)	L^{R1} (cm)	t^{R1} (s)	yield of **5** (%)
30	500	3.5	0.021	29
	1000	3.5	0.082	28
	1000	25	0.59	20
	1000	150	3.5	10
	1000	300	7.1	7
15	500	3.5	0.021	46
	1000	3.5	0.082	43
	1000	25	0.59	36
	1000	150	3.5	24
	1000	300	7.1	20
0	500	3.5	0.021	53
	1000	3.5	0.082	50
	1000	25	0.59	43
	1000	150	3.5	35
	1000	300	7.1	27
-15	500	3.5	0.021	68
	1000	3.5	0.082	72
	1000	25	0.59	62
	1000	150	3.5	51
	1000	300	7.1	43

[a]Yields were determined by GC using an internal standard. Retention time: 15.7 min

(4) Reactions of enamines with other acids

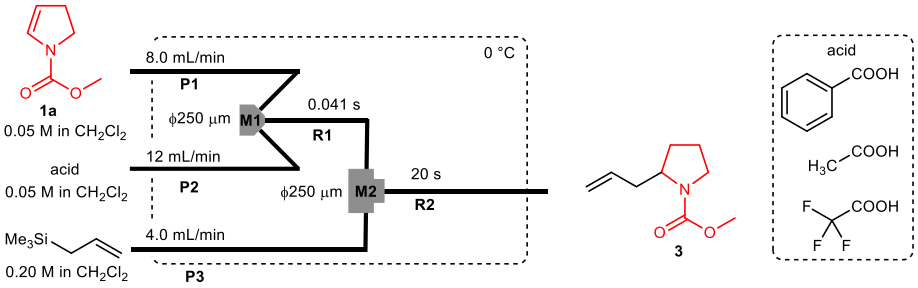

A flow microreactor system consisting of a V-shaped micromixer (**M1**, φ = 250 μm) and a T-shaped micromixer (**M2**, φ = 250 μm), two microtube reactors (**R1** and **R2**), and three pre-cooling units (**P1**–**P3**) was used. The flow microreactor system was dipped in a cooling bath (0 °C). A solution of **1a** (0.0500 M in CH_2Cl_2, flow rate: 8.0 mL/min) and a solution of acid (0.050 M in CH_2Cl_2, flow rate: 12.0 mL/min) were introduced into **M1** using syringe pumps. The mixed solution was passed through **R1** (φ = 500 μm, L^{R1} cm, t^{R1} s), and was mixed with a solution of allyltrimethylsilane (0.20 M in CH_2Cl_2, flow rate: 4.0 mL/min) in **M2.** The resulting solution was passed through **R2** (L^{R2}= 1000 cm, t^{R2} = 20 s). After a steady state was reached, an aliquot of the reacting solution was collected and was treated with TBAF, Et_3N and brine. The reaction was analyzed by GC, revealing that the reactions using benzoic acid, acetic acid, and trifluoroacetic acid did not afford desired product **3**.

(5) Generation of carbocationic species and reactions with nucleophiles

Generation and reactions of *N*-acyliminium ions with neutral nucleophiles

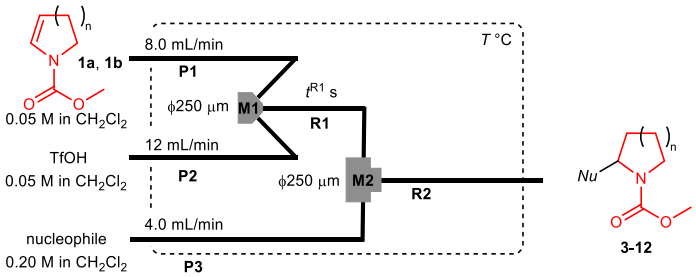

A flow microreactor system consisting of a V-shaped micromixer (**M1**, φ = 250 μm) and a T-shaped micromixer (**M2**, φ = 250 μm), two microtube reactors (**R1** and **R2**), and three pre-cooling units (**P1**–**P3**) was used. The flow microreactor system was dipped in a cooling bath (T = 15 °C). A solution of the cation precursor (0.0500 M in CH_2Cl_2, flow rate: 8.0 mL/min) and a solution of TfOH (0.050 M in CH_2Cl_2, flow rate: 12.0 mL/min) were introduced into **M1** using syringe pumps. The mixed solution was passed through **R1** (φ^{R1} = 500 μm, L^{R1} = 3.5 cm, t^{R1} = 0.021 s), and was mixed with a solution of neutral nucleophile (0.20 M in CH_2Cl_2, flow rate: 4.0 mL/min) in **M2.** The resulting solution was passed through **R2** (L^{R2} = 1000 cm, t^{R2} = 20 s). After a steady state was reached, an aliquot of the product solution was collected, and was treated with TBAF, Et_3N and brine.

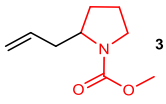

Methyl 2-allylpyrrolidine-1-carboxylate (3).
Obtained from **1a** with allyltrimethylsilane in 78% yield determined by GC yield (retention time 15.7 min). After extraction, the crude product was purified by flash chromatography (hexane/EtOAc = 5/2) to afford **3**. The spectral data were identical to those of reported in the literature.[1]

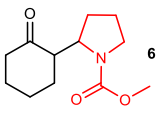

Methyl 2-(2-oxocyclohexyl)pyrrolidine-1-carboxylate (6).
Obtained from **1a** with 1-trimethylsiloxy-1-cyclohexene in 60% yield determined by GC (retention time 22.7 min). After extraction, the crude mixture was purified by flash chromatography (hexane/EtOAc = 5/2) to afford **6**. The spectral data were identical to those of reported in the literature.[13]

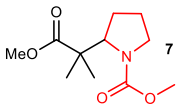

Methyl 2-(1-methoxy-2-methyl-1-oxopropan-2-yl)pyrrolidine-1-carboxylate (7)
Obtained from **1a** with 1-methoxy-1-trimethylsilyloxypropene in 70% yield determined by GC (retention time 22.7 min). After extraction, the crude mixture was purified by flash chromatography (hexane/EtOAc = 5/2) to afford **7**. ^{1}H NMR (400 MHz, $CDCl_3$, rotamer) δ 1.13 (d, *J* = 10.8 Hz, 6 H) , 1.69–1.83 (m, 4 H) , 1.93–1.98 (m, 1 H) , 3.16–3.22 (m, 1 H), 3.63 (s, 3 H) , 3.66 (s, 3 H), 4.26–4.28 (m, 1 H); ^{13}C NMR (100MHz, $CDCl_3$, rotamers) δ 21.8, 22.3, 24.2, 27.3, 47.2, 47.9, 51.8, 52.4, 63.5, 157.6, 177.2; HRMS (EI) calcd for $C_{12}H_{19}NO_3$ $[M]^+$: 225.1365, found 225.1364.

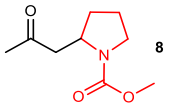

Methyl 2-(2-oxopropyl)pyrrolidine-1-carboxylate (8)
Obtained from **1a** with 2-trimethylsiloxypropene in 83% yield determined by GC (retention time: 18.9 min). After extraction, the crude mixture was purified by flash chromatography (hexane/EtOAc = 5/2) to afford **8**. The spectral data were identical to those of reported in the literature.[13]

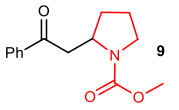

Methyl 2-(2-oxo-2-phenylethyl)pyrrolidine-1-carboxylate (9)

Obtained from **1a** with 1-phenyl-1-trimethylsiloxyethylene (*T* = 0 °C) in 82% yield determined by GC (retention time 26.7 min). After extraction, the crude mixture was purified by flash chromatography (hexane/EtOAc = 5/2) to afford **8**. The spectral data were identical to those of reported in the literature.[13]

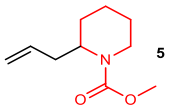

Methyl 2-allylpiperidine-1-carboxylate (5)

Obtained from **1b** with allyltrimethylsilane (*T* = −15 °C, φ^{R1} = 1000 μm, L^{R1} = 3.5 cm, t^{R1} = 0.082 s) in 72% yield determined by GC (retention time 16.1 min). After extraction, the crude mixture was purified by flash chromatography (hexane/EtOAc = 5/1) to afford **5**. The spectral data were identical to those of reported in the literature.[13]

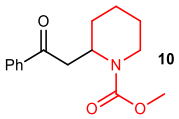

Methyl 2-(2-oxo-2-phenylethyl)piperidine-1-carboxylate (10)

Obtained from **1b** with 1-phenyl-1-trimethylsiloxyethylene (*T* = −15 °C, φ^{R1} = 1000 μm, L^{R1} = 3.5 cm, t^{R1} = 0.082 s, quenched by Et_3N) in 81% yield determined by GC. After extraction, the crude mixture was purified by flash chromatography (hexane/EtOAc = 3/1) to afford **10**. The spectral data were identical to those of reported in the literature.[14]

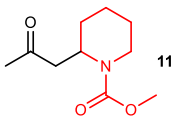

Methyl 2-(2-oxopropyl)piperidine-1-carboxylate (11)

The reaction solution derived from **1b** with 2-trimethylsiloxypropene (*T* = −15 °C, φ^{R1} = 1000 μm, L^{R1} = 3.5 cm, t^{R1} = 0.082 s) was collected for 3.0 min. After working-up, the crude mixture was purified by flash chromatography (hexane/EtOAc = 2/1) to afford **11** in 82% yield (196.8 mg). The spectral data were identical to those of reported in the literature.[14]

Reactions of oxocarbenium ion 2c

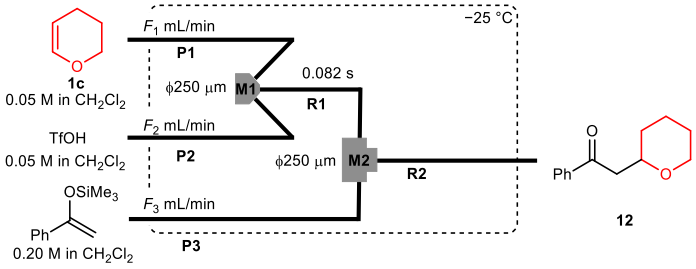

A flow microreactor system consisting of a V-shaped micromixer (**M1**, φ = 250 μm) and a T-shaped micromixer (**M2**, φ = 250 μm), two microtube reactors (**R1** and **R2**), and three pre-cooling units (**P1**–**P3**) was used. The flow microreactor system was dipped in a cooling bath (T = −25 °C). A solution of **1c** (0.0500 M in CH_2Cl_2, flow rate: F_1 mL/min) and a solution of TfOH (0.050 M in CH_2Cl_2, flow rate: F_2 mL/min) were introduced into **M1** using syringe pumps (the sum of F_1 with F_2 is approx. 20 mL/min). The mixed solution was passed through **R1** (L^{R1} = 3.5 cm, t^{R1} = 0.082 s), and was mixed with a solution of 1-phenyl-1-trimethylsiloxyethylene (0.20 M in CH_2Cl_2, flow rate: F_3 mL/min) in **M2.** The resulting solution was passed through **R2** (L^{R2} = 1000 cm, t^{R2} ~ 20 s). After a steady state was reached, an aliquot of the product solution was collected, and was treated with TBAF, Et_3N and brine. The reaction mixture was analyzed by GC with an internal standard (retention time 20.4 min). The results are summarized in Supplementary Table S8. After extraction, the crude mixture was purified by flash chromatography (hexane/EtOAc = 20/1) to afford **2-(2-oxo-2-phenylethyl)tetrahydro-2*H*-pyran** (**12**). The spectral data were identical to those of reported in the literature.[15]

Supplementary Table S8. Yields of **12** with varying equivalent amount of TfOH[a]

F_1 (mL/min)	F_2 (mL/min)	F_3 (mL/min)	equiv. of TfOH	yield of **12** (%)
4	16	4	4.0	54
5	15	3	3.0	48
7	14	2	2.0	34
8	12	1	1.5	10

[a]Yields were determined by GC using an internal standard

Reactions of *N*-acyliminium ion 1a with alkylmetal reagents

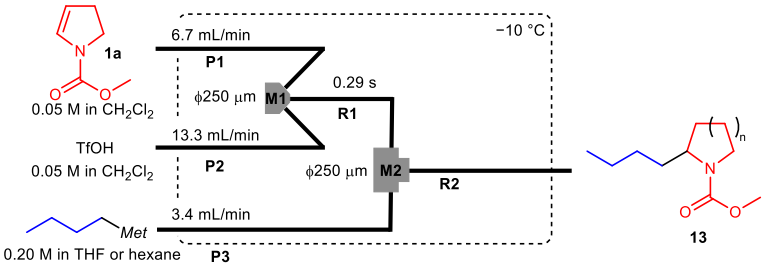

A flow microreactor system consisting of a V-shaped micromixer (**M1**, φ = 250 μm) and a T-shaped micromixer (**M2**, φ = 250 μm), two microtube reactors (**R1** and **R2**), and three pre-cooling units (**P1**–**P3**) was used. The flow microreactor system was dipped in a cooling bath (T = −10 °C). A solution of **1a** (0.0500 M in CH_2Cl_2, flow rate: 6.7 mL/min) and a solution of TfOH (0.050 M in CH_2Cl_2, flow rate: 13.3 mL/min) were introduced into **M1** using syringe pump. The mixed solution was passed through **R1** (L^{R1} = 12.5 cm, t^{R1} = 0.29 s), and was mixed with a solution of alkylmetal reagent (*n*-butyllithium in *n*-hexane, *n*-butylmagnesium chloride in THF, or *n*-butylzinc chloride in THF, flow rate: 3.4 mL/min, concentration: 0.20 M) in **M2.** The resulting solution was passed through **R2** (φ^{R2} μm, L^{R2} cm, t^{R2} s). After a steady state was reached, an aliquot of the reacting solution was collected, and was treated with brine. The reaction mixture was analyzed by GC with an internal standard (retention time 15.6 min). The results are summarized in Supplementary Table S9. After extraction, the crude mixture was purified by flash chromatography (hexane/EtOAc = 20/1) to afford **methyl 2-butylpyrrolidine-1-carboxylate** (**13**). The spectral data were identical to those of reported in the literature.[16]

Supplementary Table S9. Yields of **13** from varying counter ion and reaction time[a]

Met	φ^{R2} (μm)	L^{R2} (cm)	t^{R2} (s)	Yield of **13** (%)
Li	500	3.5	0.017	64
	1000	3.5	0.069	72
	1000	12.5	0.25	73
	1000	50	0.98	72
	1000	200	3.9	69
MgCl	500	3.5	0.017	35
	1000	3.5	0.069	40
	1000	12.5	0.25	60
	1000	50	0.98	65
	1000	200	3.9	62
ZnCl	500	3.5	0.017	0
	1000	3.5	0.069	24
	1000	12.5	0.25	19
	1000	50	0.98	33
	1000	200	3.9	32

[a]Yields were determined by GC using an internal standard

(6) Low-temperature NMR analysis of *N*-acyliminium ion 2a

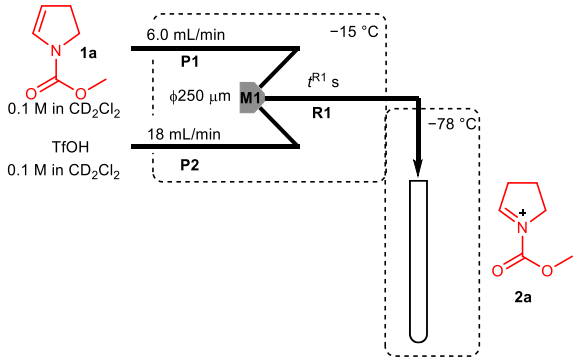

A flow microreactor system consisting of a V-shaped micromixer (**M1**, φ = 250 μm), one microtube reactor (**R1**), and two pre-cooling units (**P1**–**P3**) was used. The flow microreactor system was dipped in two cooling baths (−15 and −78 °C). A solution of **1a** (0.10 M in CD_2Cl_2, flow rate: 6.0 mL/min) and a solution of TfOH (0.10 M in CD_2Cl_2, flow rate: 18 mL/min) were introduced into **M1** using syringe pumps. The mixed solution was passed through **R1** (L^{R1} = 10 cm, t^{R1} = 0.20 s), and was introduced into an NMR test tube cooled at

−78 °C. Immediately the tube was moved to NMR probe cooled at −78 °C, and its ^{1}H NMR was measured at −78 °C. ^{1}H NMR (500 MHz, CD_2Cl_2, −78 °C, rotamers) δ 2.48 (t, J = 7.0 Hz, 2 H) , 3.49–3.61 (br, 2 H) , 4.10 (s, 3 H), 4.38–4.56 (br, 2 H), 9.49 (s, 1 H).

Oxonium ion 2c

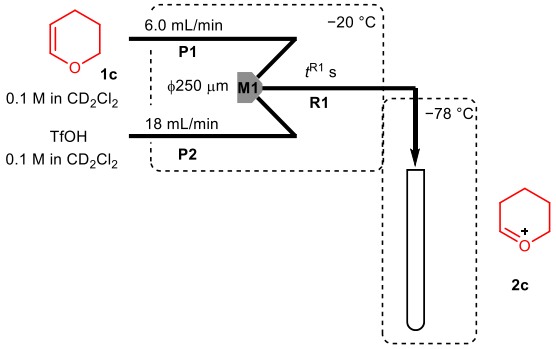

A flow microreactor system consisting of a V-shaped micromixer (**M1**, φ = 250 μm), one microtube reactor (**R1**), and two pre-cooling units (**P1**–**P3**) was used. The flow microreactor system was dipped in two cooling baths (−15 and −78 °C). A solution of **1c** (0.10 M in CD_2Cl_2, flow rate: 6.0 mL/min) and a solution of TfOH (0.10 M in CD_2Cl_2, flow rate: 18 mL/min) were introduced into **M1** using syringe pumps. The mixed solution was passed through **R1** (L^{R1} = 10 cm, t^{R1} = 0.20 s), and was introduced into an NMR test tube cooled at −78 °C. Immediately the tube was moved to NMR probe cooled at −78 °C, and its ^{1}H NMR was measured at −78 °C. ^{1}H NMR (500 MHz, CD_2Cl_2) δ 1.93–1.99 (m, 2 H), 2.20–2.26 (m, 2 H), 3.62 (t, J = 5.0 Hz, 2 H), 5.39 (t, J = 5.0 Hz, 2 H), 10.07 (s, 1 H).

(7) Reaction of carbocationic species with sp2-carbanions

General procedure

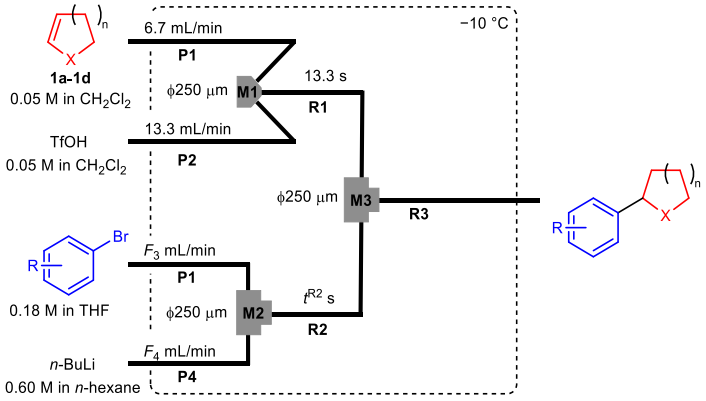

A flow microreactor system consisting of a V-shaped micromixer (**M1**, φ = 250 μm), two T-shaped micromixers (**M2** and **M3**, φ = 250 μm), three microtube reactors (**R1**–**R3**), and four pre-cooling units (**P1**–**P4**) was used. The flow microreactor system was dipped in a cooling bath (T = −10 °C). A solution of the cation precursor (**1a**–**1d**, 0.0500 M in CH_2Cl_2, flow rate: 6.7 mL/min) and a solution of TfOH (0.050 M in CH_2Cl_2, flow rate: 13.3 mL/min) were introduced into **M1** using syringe pumps. The mixed solution was passed through **R1** (L^{R1} = 12.5 cm, t^{R1} = 0.29 s) to **M3**. Whereas, a solution of aryl halides (0.18 M in THF, flow rate: F_3 = 10 mL/min) and a solution of *n*-BuLi (0.60 M in *n*-hexane, flow rate: F_4 = 2.5 mL/min) were introduced into **M2** using syringe pumps, and the mixed solution was passed through **R2** (L^{R2} = 100 cm, t^{R2} = 3.8 s) to **M3**. Those solutions are mixed in **M3**, and the resulting solution was passed through **R3** (L^{R3} = 100 cm, t^{R3} = 1.4 s). After a steady state was reached, an aliquot of the product solution was collected, and was treated with brine. The reaction mixture was analyzed by GC or ^{1}H NMR with an internal standard.

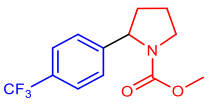

14

Methyl 2-(4-trifluoromethylphenyl)pyrrolidine-1-carboxylate (14)
Obtained from **1a** with 4-bromobenzotrifluoride in 89% yield determined by GC (retention time 20.0 min). After extraction, the crude mixture was purified by flash chromatography (hexane/EtOAc = 4/1) to afford **14**. ^{1}H NMR (400 MHz, $CDCl_3$, rotamers) δ 1.79–1.96 (m, 3 H), 2.28–2.41 (m, 1 H), 3.52–3.73 (m, 5 H), 4.92–5.04 (m, 1 H), 7.24–7.33 (m, 2 H), 7.56 (d, J = 8.0 Hz, 2 H); ^{13}C NMR (100 MHz, $CDCl_3$, rotamers) δ 22.7, 23.7, 34.8, 36.7, 42.3, 47.7, 52.4, 60.6, 61.2, 124.4 (q, J = 271.2 Hz), 125.4, 125.9, 129.0 (q, J = 31.6 Hz), 148.0, 148.4, 155.7; ^{19}F NMR (376 MHz, $CDCl_3$, rotamers) δ −62.3, −62.2; HRMS (ESI) calcd for $C_{13}H_{14}F_3NO_2Na$ $[M+Na]^+$: 296.0857, found: 296.0863.

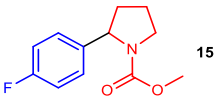

15

Methyl 2-(4-fluorophenyl)pyrrolidine-1-carboxylate (15)
Obtained from **1a** with 1-bromo-4-fluorobenzene (F_3 = 8.0 mL/min, F_4 = 2.0 mL/min, t^{R2} = 4.7 s, t^{R3} = 1.6 s) in 92% yield determined by GC (retention time 19.9 min). After extraction, the crude mixture was purified by flash chromatography (hexane/EtOAc =4/1) to afford **15**. The spectral data were identical to those of reported in the literature.[17]

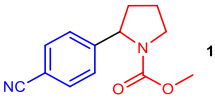

16

Methyl 2-(4-cyanophenyl)pyrrolidine-1-carboxylate (16)
Obtained from **1a** with 4-bromobenzonitrile (F_3 = 8.0 mL/min, F_4 = 2.0 mL/min, L^{R2} = 3.5 cm, t^{R2} = 0.16 s, t^{R3} = 1.6 s) in 66% yield determined by ^{1}H NMR using 1,1,2,2-tetrachloroethane as an internal standard. After extraction, the crude product was purified by flash chromatography (hexane/EtOAc = 3/2) to afford **16**. ^{1}H NMR (400 MHz, $CDCl_3$, rotamers) δ 1.72–1.92 (m, 1 H), 2.26–2.40 (m, 3 H), 3.47–3.69 (m, 5 H), 4.86–4.97 (m, 1 H), 7.20–7.30 (m, 2 H), 7.56 (d, J = 8.0 Hz, 2 H); ^{13}C NMR (100 MHz, $CDCl_3$, rotamers) δ 22.9, 23.9, 34.8, 35.8, 47.4, 47.8, 52.7, 60.8, 61.3, 77.6, 110.7, 119.1, 126.3, 126.5, 132.5, 149.4, 149.9, 155.7; HRMS (ESI) calcd for $C_{13}H_{14}N_2O_2$ Na $[M+Na]^+$: 253.0942, found: 235.0942.

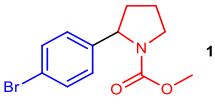

17

Methyl 2-(4-bromophenyl)pyrrolidine-1-carboxylate (17)
Obtained from **1a** with 1,4-dibromobenzene (F_3 = 8.0 mL/min, F_4 = 2.0 mL/min, t^{R2} = 4.7 s, t^{R3} = 1.6 s) in 76% yield determined by GC (retention taime 22.7 min). After extraction, the crude mixture was purified by flash chromatography (hexane/EtOAc = 4/1) to afford **17**. ^{1}H NMR (400 MHz,

$CDCl_3$, rotamers) δ 1.70–1.94 (m, 3 H), 2.23–2.37 (m, 1 H), 3.50–3.74 (m, 5 H), 4.83–4.95 (m, 1 H), 6.99–7.11 (m, 2 H), 7.42 (d, J = 8.0 Hz, 2 H); ^{13}C NMR (100 MHz, $CDCl_3$, rotamers) δ 22.8, 23.9, 34.9, 35.8, 47.2, 47.7, 52.6, 60.5, 61.0, 120.5, 120.6, 127.3, 127.5, 131.6, 142.9, 143.4, 155.7, 155.9; HRMS (ESI) calcd for $C_{12}H_{14}BrNO_2Na$ $[M+Na]^+$: 306.0093, found: 306.0093.

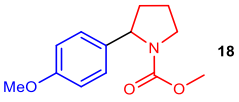

Methyl 2-(4-methoxyphenyl)pyrrolidine-1-carboxylate (18)
Obtained from **1a** with 4-bromoanisole (F_3 = 8.0 mL/min, F_4 = 2.0 mL/min, t^{R2} = 4.7 s, t^{R3} = 1.6 s) in 77% yield determined by GC (retention time 22.3 min). After extraction, the crude mixture was purified by flash chromatography (hexane/EtOAc = 3/2) to afford **18**. ^{1}H NMR (400 MHz, $CDCl_3$, rotamers) δ 1.78–2.02 (m, 3 H), 2.18–2.36 (m, 1 H), 3.49–3.73 (m, 5 H), 3.79 (s, 3 H), 4.83–4.96 (m, 1 H), 6.82–6.89 (m, 2 H), 7.03–7.18 (m, 2 H); ^{13}C NMR (100 MHz, $CDCl_3$, rotamers) δ 22.4, 23.6, 34.6, 35.6, 46.9, 47.3, 52.2, 55.1, 60.1, 60.6, 113.6, 126.3, 126.5, 135.6, 136.0, 155.4, 155.8, 158.3; HRMS (EI) calcd for $C_{13}H_{17}NO_3$ $[M]^+$: 235.1208, found 235.1208.

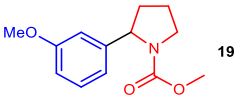

Methyl 2-(3-methoxyphenyl)pyrrolidine-1-carboxylate (19)
Obtained from **1a** with 3-bromoanisole in 83% yield determined by GC (retention time 21.9 min). After extraction, the crude mixture was purified by flash chromatography (hexane/EtOAc = 3/2) to afford **19**. ^{1}H NMR (400 MHz, $CDCl_3$, rotamers) δ 1.80–2.00 (m, 3 H), 2.20–2.37 (m, 1 H), 3.49–3.73 (m, 5 H), 3.79 (s, 3 H), 4.85–4.99 (m, 1 H), 6.66–6.81 (m, 3 H), 7.18–7.25 (m 1 H); ^{13}C NMR (100 MHz, $CDCl_3$, rotamers) δ 22.8, 23.8, 34.9, 35.8, 47.3, 47.7, 52.6, 55.4, 60.9, 61.4, 111.5, 111.8, 117.9, 118.1, 129.6, 145.6, 146.1, 155.8, 156.1, 159.8; HRMS (ESI) calcd for $C_{13}H_{17}NO_3Na$ $[M+Na]^+$: 258.1101, found: 258.1093.

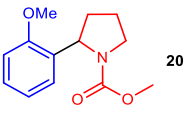

Methyl 2-(2-methoxyphenyl)pyrrolidine-1-carboxylate (20)
Obtained from **1a** with 2-bromoanisole (F_3 = 8.0 mL/min, F_4 = 2.0 mL/min, t^{R2} = 4.7 s, t^{R3} = 1.6 s) in 72% yield determined by GC (retention time 21.3 min). After extraction, the crude mixture was purified by flash chromatography (hexane/EtOAc = 3/2) to afford **20**. ^{1}H NMR (400 MHz, $CDCl_3$, rotamers) δ 1.72–1.95 (m, 3 H), 2.16–2.33 (m, 1 H), 3.46–3.78 (m, 5 H), 3.82–3.98 (m, 3H), 5.14–5.34 (m, 1 H), 6.82–7.13 (m, 3 H), 7.18–7.28 (m, 1 H); ^{13}C NMR (100 MHz, $CDCl_3$, rotamers) δ 22.5, 23.5, 32.9, 33.7, 47.1, 47.6, 52.5, 55.3, 56.4, 56.8, 110.3, 110.5, 120.3, 125.5, 125.6, 127.8, 131.4, 131.9, 155.4, 156.0, 156.2; HRMS (ESI) calcd for $C_{13}H_{17}NO_3Na$ $[M+Na]^+$: 258.1101, found: 258.1093.

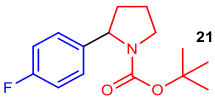

***tert*-Butyl 2-(4-fluorophenyl)pyrrolidine-1-carboxylate (21)**
Obtained from **1d** with 1-bromo-4-fluorobenzene (F_3 = 20 mL/min, F_4 = 5.0 mL/min, t^{R2} = 1.9 s, t^{R3} = 1.0 s) in 80% yield determined by GC (retention time 20.1 min). After extraction, the crude mixture was purified by flash chromatography (hexane/EtOAc = 4/1) to afford **21**. The spectral data were identical to those of reported in the literature.[18]

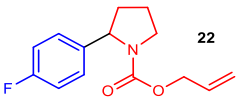

Allyl 2-(4-fluorophenyl)pyrrolidine-1-carboxylate (22)
Obtained from **1e** with 1-bromo-4-fluorobenzene (F_3 = 8.0 mL/min, F_4 = 2.0 mL/min, t^{R2} = 4.7 s, t^{R3} = 1.6 s) in 85% yield determined by GC (retention time 21.0 min). After extraction, the crude mixture was purified by flash chromatography (hexane/EtOAc = 4/1) to afford **22**. ^{1}H NMR (400 MHz, $CDCl_3$) (mixture of rotamers) δ 1.78–1.98 (m, 3 H), 2.23–2.38 (m, 1 H), 3.56–3.71 (m, 2 H), 4.39–4.64 (m, 2 H), 4.88–5.03 (m, 2 H), 5.18–5.36 (m, 1 H), 5.61–6.01 (m, 1 H), 7.00 (t, J = 8.4 Hz, 2 H), 7.10–7.20 (m, 2 H); ^{13}C NMR (100 MHz, $CDCl_3$, rotamers) δ 23.0, 23.9, 35.1, 36.1, 47.3, 47.8, 60.6, 60.9,

65.7, 66.0, 115.2, 115.3, 115.5, 115.5, 116.7, 117.5, 127.2, 133.2 (d, J = 37.4 Hz), 139.8 (d, J = 60.3 Hz), 155.0, 161.9 (d, J = 243.4 Hz); ^{19}F NMR (376 MHz, $CDCl_3$) δ −116.4; HRMS (ESI) calcd for $C_{14}H_{16}FNO_2Na$ $[M+Na]^+$: 272.1067, found: 272.1053.

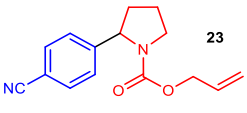

Allyl 2-(4-cyanophenyl)pyrrolidine-1-carboxylate (23)
Obtained from **1e** with 4-bromobenzonitrile (F_3 = 16 mL/min, F_4 = 4.0 mL/min, L^{R2} = 3.5 cm, t^{R2} = 0.082 s, L^{R3} = 30 cm, t^{R3} = 0.35 s) in 70% yield determined by GC (retention time 25.7 min). After extraction, the crude mixture was purified by flash chromatography (hexane/EtOAc = 4/1) to afford **23**. ^{1}H NMR (400 MHz, $CDCl_3$, rotamers) δ 1.78–1.99 (m, 3 H), 2.30–2.45 (m, 1 H), 3.60–3.74 (m, 2 H), 4.38–4.64 (m, 2 H), 4.87–5.06 (m, 2 H), 5.17–5.37 (m, 1 H), 5.58–6.00 (m, 1 H), 7.23–7.34 (m, 2 H), 7.61 (d, J = 8.0 Hz, 2 H); ^{13}C NMR (100 MHz, $CDCl_3$, rotamers) δ 23.1, 24.0, 34.9, 35.9, 47.4, 47.9, 61.0, 61.4, 65.8, 66.1, 110.8, 117.0, 117.7, 119.1, 126.4, 126.5, 132.5, 132.7, 133.1, 149.4, 150.0, 154.9; HRMS (ESI) calcd for $C_{15}H_{16}N_2O_2Na$ $[M+Na]^+$: 279.1104, found: 279.1102.

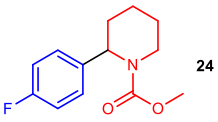

Methyl 2-(4-fluorophenyl)piperidine-1-carboxylate (24)
Obtained from **1b** with 1-bromo-4-fluorobenzene (F_3 = 8.0 mL/min, F_4 = 2.0 mL/min, φ^{R1} = 500 μm, L^{R1} = 3.5 cm, t^{R1} = 0.021 s, t^{R2} = 4.7 s, t^{R3} = 1.6 s) in 73% yield determined by GC (retention time 21.0 min). After extraction, the crude mixture was purified by flash chromatography (hexane/EtOAc = 4/1) to afford **24**. ^{1}H NMR (400 MHz, $CDCl_3$, rotamers) δ 1.35–1.67 (m, 4 H), 1.84–1.95 (m, 1 H), 2.25–2.32 (m, 1 H), 2.73–2.82 (m, 1 H), 3.74 (s, 3 H), 4.03–4.12 (m, 1 H), 5.40–5.48 (m, 1 H), 7.03 (t, J = 8.2 Hz, 2 H), 7.16–7.21 (m, 2 H); ^{13}C NMR (100 MHz, $CDCl_3$, rotamers) δ 19.4, 25.6, 28.3, 40.5, 53.0, 53.1, 115.5, 115.7, 128.3, 128.4, 135.6, 156.9, 161.8 (d, J = 243.4 Hz); ^{19}F NMR (376 MHz, $CDCl_3$, rotamers) δ −116.7; HRMS (ESI) calcd for $C_{13}H_{16}FNO_2Na$ $[M+Na]^+$: 260.1057, found: 260.1054.

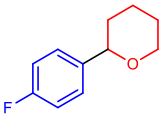

2-(4-Fluorophenyl)tetrahydro-2*H*-pyran (25)
Obtained from **1c** and 1-bromo-4-fluorobenzene (F_3 = 16 mL/min, F_4 = 4.0 mL/min, L^{R1} = 25 cm, t^{R1} = 0.59 s, t^{R2} = 2.4 s, t^{R3} = 1.2 s) in 48% yield determined by GC (retention time 14.8 min). After extraction, the crude mixture was purified by flash chromatography (hexane/EtOAc = 4/1) to afford **23**. The spectral data were identical to those of reported in the literature.[19]

(8) Reaction of carbocationic species with sp-carbanions

General procedure

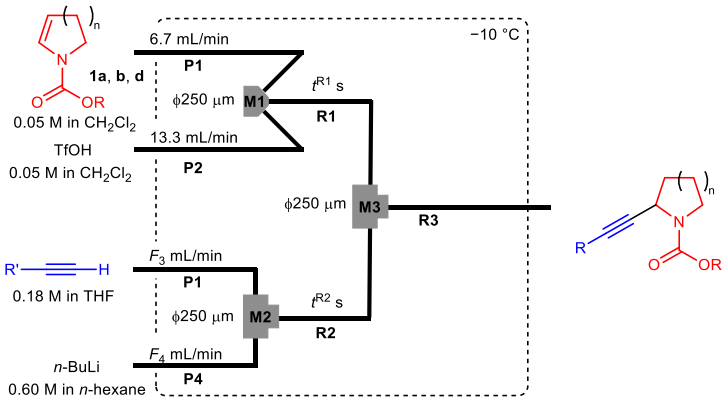

A flow microreactor system consisting of a V-shaped micromixer (**M1**, φ = 250 μm), two T-shaped micromixers (**M2** and **M3**, φ = 250 μm), three microtube reactors (**R1**–**R3**), and four pre-cooling units (**P1**–**P4**) was used. The flow microreactor system was dipped in a cooling bath (T = −10 °C). A solution of the cation precursor (**1a**, **b**, and **d**, 0.0500 M in CH_2Cl_2, flow rate: 6.7 mL/min) and a solution of TfOH (0.050 M in CH_2Cl_2, flow rate: 13.3 mL/min) were introduced into **M1** using syringe pumps. The mixed solution was passed through **R1** (φ^{R1} = 1000 μm, L^{R1} = 12.5 cm, t^{R1} = 0.29) to **M3**. Whereas, a solution of aryl halides (0.18 M in THF, flow rate: 8.0 mL/min) and a solution of *n*-BuLi (0.60 M in *n*-hexane, flow rate: 2.0 mL/min) were introduced into **M2** using syringe pumps, and the mixed solution was passed through **R2** (L^{R2} = 12.5 cm, t^{R2} = 0.59 s) to **M3**. Those solutions are mixed in **M3**, and the resulting solution was passed through **R3** (L^{R3} = 300 cm, t^{R3} = 4.7 s). After a steady state was reached, an aliquot of the product solution was collected, and was treated with brine. The reaction mixture was analyzed by GC using an internal standard.

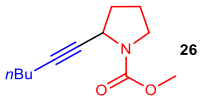

26

Methyl 2-(1-hexyn-1-yl)pyrrolidine-1-carboxylate (26)
Obtained from **1a** with 1-hexyne in 96% yield determined by GC (retention time 18.5 min). After extraction, the crude mixture was purified by flash chromatography (hexane/EtOAc = 4/1) to afford **26**. ^{1}H NMR (400 MHz, $CDCl_3$, rotamers) δ 0.87 (t, J = 6.8 Hz, 3 H), 1.29–1.48 (m, 4 H), 1.83–2.18 (m, 6 H), 3.21–3.39 (m, 1 H), 3.40–3.54 (m, 1 H), 3.70 (s, 3 H), 4.39–4.58 (m, 1 H); ^{13}C NMR (100 MHz, $CDCl_3$, rotamers) δ 13.9, 18.6, 22.1, 23.8, 24.7, 31.1, 33.7, 34.5, 45.9, 46.3, 48.6, 49.0, 52.6, 80.1, 80.4, 82.7, 155.6; HRMS (ESI) calcd for $C_{12}H_{19}NO_2Na$ [M+Na]$^+$: 232.1305, found: 232.1303.

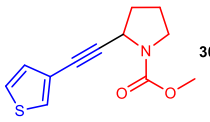

30

Methyl 2-(thiophen-3-ylethynyl)pyrrolidine-1-carboxylate (30)
Obtained from **1a** with 3-ethynylthiophene (F_3 = 16 mL/min, F_4 = 4.0 mL/min, L^{R2} = 100 cm, t^{R2} = 2.4 s, L^{R3} = 200 cm, t^{R3} = 2.4 s) in 84% yield determined by GC (retention time 22.3 min). After extraction, the crude mixture was purified by flash chromatography (hexane/EtOAc = 3/1) to afford **30**. ^{1}H NMR (400 MHz, $CDCl_3$, rotamers) δ 1.90–2.02 (m, 1 H), 2.06–2.24 (m, 3 H), 3.30–3.62 (m, 2 H), 3.70–3.80 (m, 3 H), 4.64–4.83 (m, 1 H), 7.08 (br, 1 H), 7.23 (br, 1 H), 7.40 (br, 1 H); ^{13}C NMR (100 MHz, $CDCl_3$, rotamers) δ 23.8, 24.7, 33.3, 34.1, 45.9, 46.2, 48.8, 49.2, 52.6, 52.7, 77.3, 77.6, 88.9, 89.0, 122.0, 122.1, 125.2, 125.4, 128.7, 128.8, 130.0, 130.2, 155.2, 155.3; HRMS (ESI) calcd for $C_{12}H_{13}NO_2SNa$ [M+Na]$^+$: 258.0559, found: 258.0553.

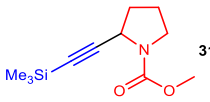

31

Methyl 2-(trimethylsilylethynyl)pyrrolidine-1-carboxylate (31)
Obtained from **1a** with trimethylsilylacetylene (F_3 = 12 mL/min, F_4 = 3.0 mL/min, L^{R2} = 100 cm, t^{R2} = 3.1 s, L^{R3} = 100 cm, t^{R3} = 1.3 s) in 89% yield determined by GC (retention time 16.4 min). After extraction, the crude mixture was purified by flash chromatography (hexane/EtOAc = 9/1) to afford **31**. ^{1}H NMR (400 MHz, $CDCl_3$, rotamers) δ 0.09 (s, 9 H), 1.77–1.92 (m, 1 H) 1.93–2.14 (m, 3 H), 3.20–3.53 (m, 2 H), 3.68 (s, 3 H), 4.37–4.60 (m, 1 H); ^{13}C NMR (100 MHz, $CDCl_3$, rotamers) δ 0.20, 23.8, 24.7, 33.6, 34.2, 45.9, 46.3, 48.9, 49.3, 52.6, 86.4, 86.5, 105.9, 106.0, 155.5; HRMS (ESI) calcd for $C_{11}H_{19}NO_2SiNa$ [M+Na]$^+$: 248.1077, found: 248.1072.

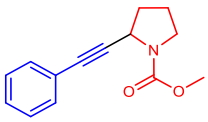

32

Methyl 2-(phenylethynyl)pyrrolidine-1-carboxylate (32)
Obtained from **1a** with phenylacetylene (F_3 = 16 mL/min, F_4 = 4.0 mL/min, L^{R2} = 100 cm, t^{R2} = 2.4 s, L^{R3} = 100 cm, t^{R3} = 1.2 s) in 92% yield determined

by GC (retention time 22.2 min). After extraction, the crude mixture was purified by flash chromatography (hexane/EtOAc = 5/1) to afford **32**. The spectral data were identical to those of reported in the literature.[20]

***tert*-Butyl 2-(trimethylsilylethynyl)pyrrolidine-1-carboxylate (33)**
Obtained from **1d** with trimethylsilylacetylene (F_3 = 16 mL/min, F_4 = 4.0 mL/min, L^{R2} = 100 cm, t^{R2} = 2.4 s, L^{R3} = 100 cm, t^{R3} = 1.2 s) in 92% yield determined by GC (retention time 17.1 min). After extraction, the crude mixture was purified by flash chromatography (hexane/EtOAc = 9/1) to afford **33**. The spectral data were identical to those of reported in the literature.[21]

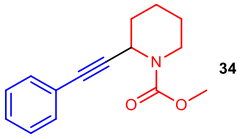

Methyl 2-(phenylethynyl)piperidine-1-carboxylate (34)
Obtained from **1b** and phenylacetylene (F_3 = 12 mL/min, F_4 = 3.0 mL/min, φ^{R1} = 500 μm, L^{R1} = 3.5 cm, t^{R1} = 0.021 s, L^{R2} = 100 cm, t^{R2} = 3.1 s, L^{R3} = 100 cm, t^{R3} = 1.3 s) in 75% yield determined by GC (retention time 22.9 min). After extraction, the crude mixture was purified by flash chromatography (hexane/EtOAc = 9/1) to afford **34**. The spectral data were identical to those of reported in the literature.[20]

Procedure for different reaction temperatures

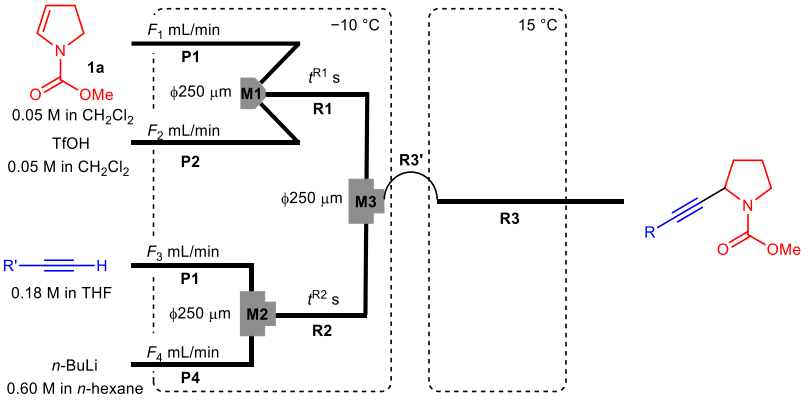

A flow microreactor system consisting of a V-shaped micromixer (**M1**, φ = 250 μm) and two T-shaped micromixers (**M2** and **M3**, φ = 250 μm), three microtube reactors (**R1**–**R3**), a PTFE tube (**R3'**), and four pre-cooling units (**P1**–**P4**) was used. The former part of the flow microreactor system (from the pre-cooling units to **M3**) was dipped in a cooling bath at −10 °C, whereas **R3** is dipped in a water bath at 15 °C. The tubes in different baths were connected by **R3'**. A solution of the cation precursor (**1a**, 0.0500 M in CH_2Cl_2, flow rate: 6.7 mL/min) and a solution of TfOH (0.050 M in CH_2Cl_2, flow rate: 13.3 mL/min) were introduced into **M1** using syringe pumps. The mixed solution was passed through **R1** (L^{R1} = 12.5 cm, t^{R1} = 0.29 s) to **M3**. Whereas, a solution of aryl halides (0.18 M in THF, flow rate: F_3 =8.0 mL/min) and a solution of *n*-BuLi (0.60 M in *n*-hexane, flow rate: F_4 = 2.0 mL/min) were introduced into **M2** using syringe pumps, and the mixed solution was passed through **R2**

(L^{R2} = 12.5 cm, t^{R2} = 0.59 s) to **M3**. Those solutions are mixed in **M2**, and the resulting solution was passed through **R3'** ($L^{R3'}$ = 10 cm, $t^{R3'}$ = 0.16 s) and **R3** (L^{R3} = 200 cm, t^{R3} = 3.1 s). After a steady state was reached, an aliquot of the product solution was collected, and was treated with brine. The reaction mixture was analyzed by GC using an internal standard.

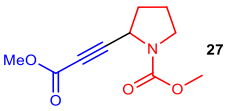

27

Methyl 2-(3-methoxy-3-oxopropynyl)pyrrolidine-1-carboxylate (27)
Obtained from **1a** with methyl propionate in 80% yield determined by GC (retention time 20.4 min). After extraction, the crude mixture was purified by flash chromatography (hexane/EtOAc = 3/1) to afford **27**. ^{1}H NMR (400 MHz, $CDCl_3$, rotamers) δ 1.91–2.02 (m, 1 H), 2.03–2.21 (m, 3 H), 3.29–3.59 (m, 2 H), 3.70–3.79 (m, 6 H), 4.56–4.71 (m, 1 H); ^{13}C NMR (100 MHz, $CDCl_3$, rotamers) δ 23.8, 24.8, 32.4, 33.3, 45.9, 46.3, 48.0, 52.8, 52.8, 73.8, 87.4, 153.9, 155.0, 155.1; HRMS (ESI) calcd for $C_{10}H_{13}NO_4Na$ $[M+Na]^+$: 234.0737, found: 234.0732.

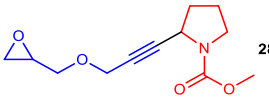

28

Methyl 2-(3-glycidyloxy-1-propynyl)pyrrolidine-1-carboxylate (28)
Obtained in from **1a** with glycidyl propargyl ether (F_3 = 16 mL/min, F_4 = 8.0 mL/min, t^{R2} = 0.29 s, $t^{R3'}$ = 0.12 s t^{R3} = 2.4 s) in 70% yield determined by GC (retention time 22.7 min). After extraction, the crude mixture was purified by flash chromatography (hexane/EtOAc = 3/2) to afford **28**. ^{1}H NMR (400 MHz, $CDCl_3$, rotamers) δ 1.87–1.97 (m, 1 H), 1.98–2.16 (m, 3 H), 2.63 (dd, J = 5.2 Hz, 2.4 Hz, 1 H), 2.81 (t, J = 4.8 Hz, 1 H), 3.14–3.19 (m, 1 H), 3.42–3.56 (m, 3 H), 3.67–3.81 (m, 4 H), 4.15–4.27 (m, 2 H), 4.49–4.65 (m, 1 H); ^{13}C NMR (100 MHz, $CDCl_3$, rotamers) δ 23.7, 24.6, 33.1, 33.9, 44.4, 45.8, 46.1, 50.5, 52.5, 58.9, 70.3, 77.5, 86.7, 86.9, 155.2; HRMS (ESI) calcd for $C_{12}H_{17}NO_4Na$ $[M+Na]^+$: 262.1050, found: 262.1046.

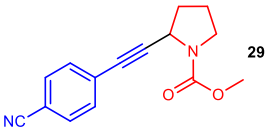

29

Methyl 2-(4-cyanophenylethynyl)pyrrolidine-1-carboxylate (29)
Obtained from **1a** with 4-ethynylbenzonitrile in 90% yield determined by GC (retention time 26.6 min). After extraction, the crude mixture was purified by flash chromatography (hexane/EtOAc = 3/1) to afford **29**. ^{1}H NMR (400 MHz, $CDCl_3$, rotamers) δ 1.94–2.04 (m, 1 H), 2.09–2.23 (m, 3 H), 3.32–3.62 (m, 2 H), 3.72–3.78 (m, 3 H), 4.68–4.85 (m, 1 H), 7.45–7.51 (m, 2 H), 7.55–7.61 (m, 2 H); ^{13}C NMR (100 MHz, $CDCl_3$, rotamers) δ 23.8, 24.7, 33.1, 33.9, 45.9, 46.2, 48.6, 49.1, 52.6, 52.7, 77.6, 80.6, 94.0, 111.4, 118.5, 128.0, 132.0, 132.4, 155.1; HRMS (ESI) calcd for $C_{15}H_{14}N_2O_2Na$ $[M+Na]^+$: 277.0945, found: 277.0942.

Procedure for thionium ion

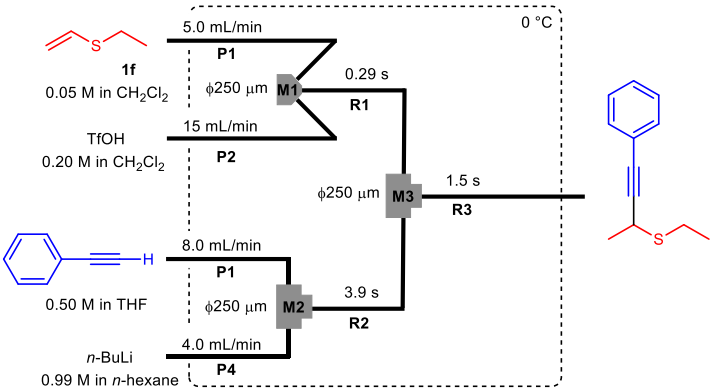

A flow microreactor system consisting of a V-shaped micromixer (**M1**, φ = 250 μm) and two T-shaped micromixers (**M2** and **M3**, φ = 250 μm), three microtube reactors (**R1**–**R3**), and four pre-cooling units (**P1**–**P4**) was used. The flow microreactor system was dipped in a cooling bath (T = 0 °C). A solution of the cation precursor (**1f**, 0.0500 M in CH_2Cl_2, flow rate: 5.0 mL/min) and a solution of TfOH (0.20 M in CH_2Cl_2, flow rate: 15 mL/min) were introduced into **M1** using syringe pumps. The mixed solution was passed through **R1** (φ^{R1} = 1000 μm, L^{R1} = 12.5 cm, t^{R1} = 0.29) to **M3**. Whereas, a solution of phenylacetylene (0.50 M in THF, flow rate: 8.0 mL/min) and a solution of *n*-BuLi (0.99 M in *n*-hexane, flow rate: 4.0 mL/min) were introduced into **M2** using syringe pumps, and the mixed solution was passed through **R2** (L^{R2} = 100 cm, t^{R2} = 3.9 s) to **M3**. Those solutions are mixed in **M3**, and the resulting solution was passed through **R3** (L^{R3} = 100 cm, t^{R3} = 1.5 s). After a steady state was reached, an aliquot of the product solution was collected, and was treated with brine. The reaction mixture was analyzed by GC using an internal standard.

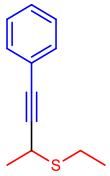

35

Ethyl 4-phenyl-3-butyn-2-yl sulfide (35)
Obtained from ethyl vinyl sulfide (**1f**) with phenylacetylene in 61% yield determined by GC (retention time 16.6 min). After extraction, the crude mixture was purified by flash chromatography and GPC to afford **35**. ^{1}H NMR (400 MHz, $CDCl_3$, rotamers) δ 1.33 (t, J = 7.6 Hz, 3 H), 1.58 (d, J = 7.2 Hz, 3 H), 2.67–2.89 (m, 2 H), 3.88 (q, J = 7.2 Hz, 1 H), 7.28–7.31 (m, 3 H), 7.41–7.43 (m, 2 H); ^{13}C NMR (100 MHz, $CDCl_3$) δ 15.0, 22.1, 25.8, 29.8, 83.2, 90.5, 123.6, 128.4, 128.6, 132.0; HRMS (APCI) calcd for $C_{12}H_{15}S$ $[M]^+$: 191.0889, found: 191.0888.

(9) Twice direct cross-coupling reaction

General procedure

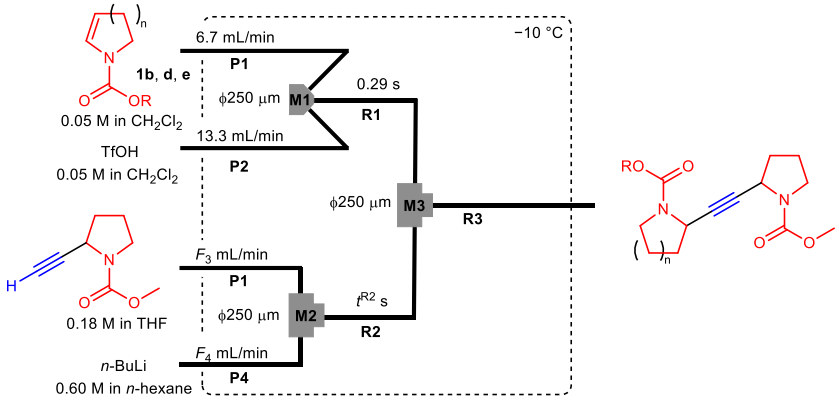

A flow microreactor system consisting of a V-shaped micromixer (**M1**, φ = 250 μm) and two T-shaped micromixers (**M2** and **M3**, φ = 250 μm), three microtube reactors (**R1**–**R3**), and four pre-cooling units (**P1**–**P4**) was used. The flow microreactor system was dipped in a cooling bath (T = −10 °C). A solution of the cation precursor (**1b**, **d**, and **e**, 0.0500 M in CH_2Cl_2, flow rate: 6.7 mL/min) and a solution of TfOH (0.050 M in CH_2Cl_2, flow rate: 13.3 mL/min) were introduced into **M1** using syringe pumps. The mixed solution was passed through **R1** (L^{R1} = 12.5 cm, t^{R1} = 0.29 s) to **M3**. Whereas, a solution of alkynyl pyrrolidine (0.18 M in THF, flow rate: F_3 = 16 mL/min) and a solution of *n*-BuLi (0.60 M in *n*-hexane, flow rate: F_4 = 4.0 mL/min) were introduced into **M2** using syringe pumps, and the mixed solution was passed through **R2** (L^{R2} = 25 cm, t^{R2} = 0.59 s) to **M3**. Those solutions are mixed in **M2**, and the resulting solution was passed through **R3** (L^{R3} = 100 cm, t^{R3} = 1.2 s). After a steady state was reached, an aliquot of the product solution was collected, and was treated with brine. The reaction mixture was analyzed by GC using an internal standard.

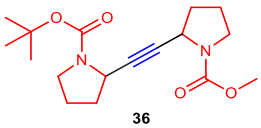

36

***tert*-Butyl 2-((1-(methoxycarbonyl)pyrrolidin-2-yl)ethynyl)pyrrolidine-1-carboxylate (36)**

Obtained from **1d** (F_3 = 8.0 mL/min, F_4 = 2.0 mL/min, t^{R2} 1.2 s, t^{R3} 1.6 s) in 62% yield determined by GC (retention time 25.1 and 25.3 min), indicating diastereomixture (1:1 ratio). After extraction, the crude mixture was purified by flash chromatography (hexane/EtOAc = 1/1) to afford **36**. ^{1}H NMR (400 MHz, $CDCl_3$, rotamer, diasteromixture) δ 1.46 (s, 9 H), 1.79–2.16 (m, 8 H), 3.19–3.54 (m, 4 H), 3.71 (s, 3 H), 4.35–4.61 (m, 2 H); ^{13}C NMR (100 MHz, $CDCl_3$, rotamer, diastereomixture) δ 23.8, 23.9, 24.7, 28.7, 33.5, 34.1, 34.3, 45.8, 46.5, 48.4, 48.8, 52.6, 77.6, 79.7, 81.4, 82.7, 154.3, 155.4; HRMS (ESI) calcd for $C_{16}H_{22}N_2O_4Na$ [M+Na]$^+$: 329.1472, found: 329.1469.

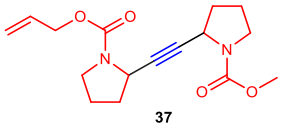

37

Allyl 2-((1-(methoxycarbonyl)pyrrolidin-2-yl)ethynyl)pyrrolidine-1-carboxylate (37)

Obtained from **1e** (t^{R2} 0.59 s, t^{R3} 1.6 s) in 75% yield determined by GC (retention time 25.1 and 25.3 min), indicating diastereomixture (1;1 ratio). After extraction, the crude mixture was purified by flash chromatography (hexane/EtOAc = 1/1) to afford **37**. ^{1}H NMR (400 MHz, $CDCl_3$, rotamer, diasteromixture) δ 1.76–2.15 (m, 8 H), 3.23–3.56 (m, 4 H), 3.71 (s, 3 H),

4.41–4.76 (m, 4 H), 5.14–5.26 (m, 1 H), 5.27–5.35 (m, 1 H), 5.86–6.01 (m, 1 H); ^{13}C NMR (100 MHz, $CDCl_3$, rotamer, diastereomixture) δ 23.8, 24.6, 33.4, 34.2, 45.9, 46.2, 48.3, 48.8, 52.6, 65.8, 65.8, 77.6, 82.0, 116.9, 117.4, 133.3, 154.6, 155.2; HRMS (ESI) calcd for $C_{17}H_{26}N_2O_4Na$ $[M+Na]^+$: 345.1785, found: 345.1781.

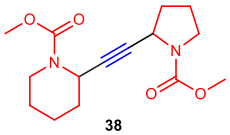

38

Methyl 2-((1-(methoxycarbonyl)pyrrolidin-2-yl)ethynyl)piperidine-1-carboxylate (38)

Obtained from **1b** (t^{R2} 0.59 s, t^{R3} 1.6 s) in 80% yield determined by GC (retention time 25.7 and 25.9 min), indicating diastereomixture (1:1 ratio). After extraction, the crude mixture was purified by flash chromatography (hexane/EtOAc = 1/1) to afford **35**. ^{1}H NMR (400 MHz, $CDCl_3$, rotamers, diastereomixture) δ 1.26–1.46 (m, 1 H), 1.48–1.80 (m, 5 H), 1.83–2.20 (m, 4 H), 2.90–3.13 (m, 1 H), 3.21–3.57 (m, 2 H), 3.65 (s, 3 H), 3.67 (s, 3 H), 3.81–4.08 (m, 1 H), 4.38–4.65 (m, 1 H), 4.88–5.28 (m, 1 H); ^{13}C NMR (100 MHz, $CDCl_3$, rotamer. diastereomixture) δ 20.1, 23.9, 24.8, 25.5, 31.0, 33.5, 34.2, 40.7, 44.6, 45.9, 46.3, 48.4, 48.8, 52.6, 52.9, 80.0, 84.8, 155.7, 155.4; HRMS (ESI) calcd for $C_{15}H_{22}N_2O_4Na$ $[M+Na]^+$: 317.1472, found: 317.1468.

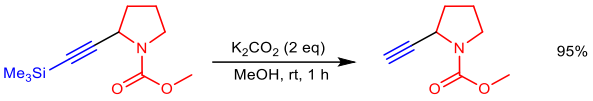

31

To a solution of **31** (1.87 g, 8.30 mmol) in MeOH (40 mL), was added K_2CO_3 (2.30 g, 16.6 mmol). After the mixture was stirred at room temperature for 1 h, it was treated with a saturated aqueous NH_4Cl. The organic layer was separated, and the aqueous layer was extracted with EtOAc three times. After the combined organic extracts were dried over Na_2SO_4, the solid was filtered off and the solvent was evaporated under a reduced pressure. The crude product was purified by flash chromatography using hexane/EtOAc (5/1) as an eluent to afford **methyl 2-ethynylpyrrolidine-1-carboxylate** as a colorless oil (1.21 g, 95%). The spectral data were identical to those of reported in the literature.[22]

(10) References

1. Mikami, R.; Nakamura, Y.; Shida, N.; Atobe, M. *React. Chem. Eng.* **2021**, *6*, 2024.
2. Merx, J.; Houthuijs, K. J.; Elferink, H.; Witlox, E.; Mecinović, J.; Oomens, J.; Martens, J.; Boltje T. J.; Rutjes, F. P. J. T. *Chem. Eur. J.* **2021**, *28*, e202104078.
3. Li, G.; Kates, P. A.; Dilger, A. K.; Cheng, P. T.; Ewing, W. R.; Groves, J. T. *ACS Catal.* **2019**, *9*, 9513.
4. Aguilar, N.; Fernandez, J. C.; Terricabras, E.; Carceller, G. E.; Garcia, F. J.; Salas, S. J. PCT WO2013149996.
5. Yan, J.; Zhang, W.; He, Q.; Hou, J.; Zeng, H.; Wei, H.; Xie, W. *Org. Biomol. Chem.* **2022**, *20*, 2387.
6. Chen, C.; Kattanguru, P.; Tomashenko, O. A.; Karpowicz, R.; Siemiaszko, G.; Bhattacharya, A.; Calasans, V.; Six, Y. *Org. Biomol. Chem.* **2017**, *15*, 5364.
7. Leroux, M.; Vorherr, T.; Lewis, I.; Schaefer, M.; Koch, G.; Karaghiosoff, K.; Knochel, P. *Angew. Chem. Int. Ed.* **2019**, *58*, 8231.
8. Krasovskiy, A.; Knochel, P. *Synthesis* **2006**, 890.
9. lv, P.; Zhang, L.; Srinivasakannan, C.; Li, S.; He, Y.; Chen K.; Yin, S. *Macrochem. J.* **2020**, *155*, 104662.
10. Commenge, J.-M.; Falk, L. *Chem. Eng. Process.; Process Intensif.* **2011**, *50*¸ 979.
11. Phillips, T. W.; Murphy, K. P. *J. Chem. Eng. Data* **1970**, *15*, 304.
12. Asano, S.; Yatabe, S.; Maki, T.; Mae, K. *Org. Process Res. Dev.* **2019**, *23*, 807.
13. Yoshida, J.; Suga, S.; Suzuki, S.; Kinomura, N.; Yamamoto, A.; Fujiwara, K. *J. Am. Chem. Soc.* **1999**, *121*, 9546.
14. Grossmann, O.; Maji, R.; Aukland, M. H.; Lee, S.; List, B. *Angew. Chem. Int. Ed.* **2022**, *61*, e202115036.
15. Sun, Z.; Kumagai, N.; Shibasaki, M. *Org. Lett.* **2017**, *19*, 3727.
16. Okajima, M. *New Developments in "Cation Pool" Method and Their Applications to Microflow Systems*, PhD Dissertation, Kyoto University, Japan, **2005**.
17. Wang, F.; Rafiee, M.; Stahl, S. S. *Angew. Chem. Int. Ed.* **2018**, *130*, 6796.
18. You, T.; Zeng, S.-H. Fan, J.; Wu, L.; Kang, F.; Liu, Y.; Che, C.-M. *Chem. Commun.* **2021**, *57*, 10711.
19. Im, H.; Kang, D.; Choi, S.; Shin, S.; Hong, S. *Org. Lett.* **2018**, *20*, 7437.
20. Wan, M.; Meng, Z.; Lou, H.; Liu, L. *Angew. Chem. Int. Ed.* **2014**, *53*, 13845.
21. Hoshikawa, T.; Kamijo, S.; Inoue, M. *Org. Biomol. Chem.* **2013**, *11*, 164.
22. Ying, W.; Herndon, J. W. *Eur. J. Org. Chem.* **2013**, 3112.

^{1}H, ^{13}C, and ^{19}F NMR spectra

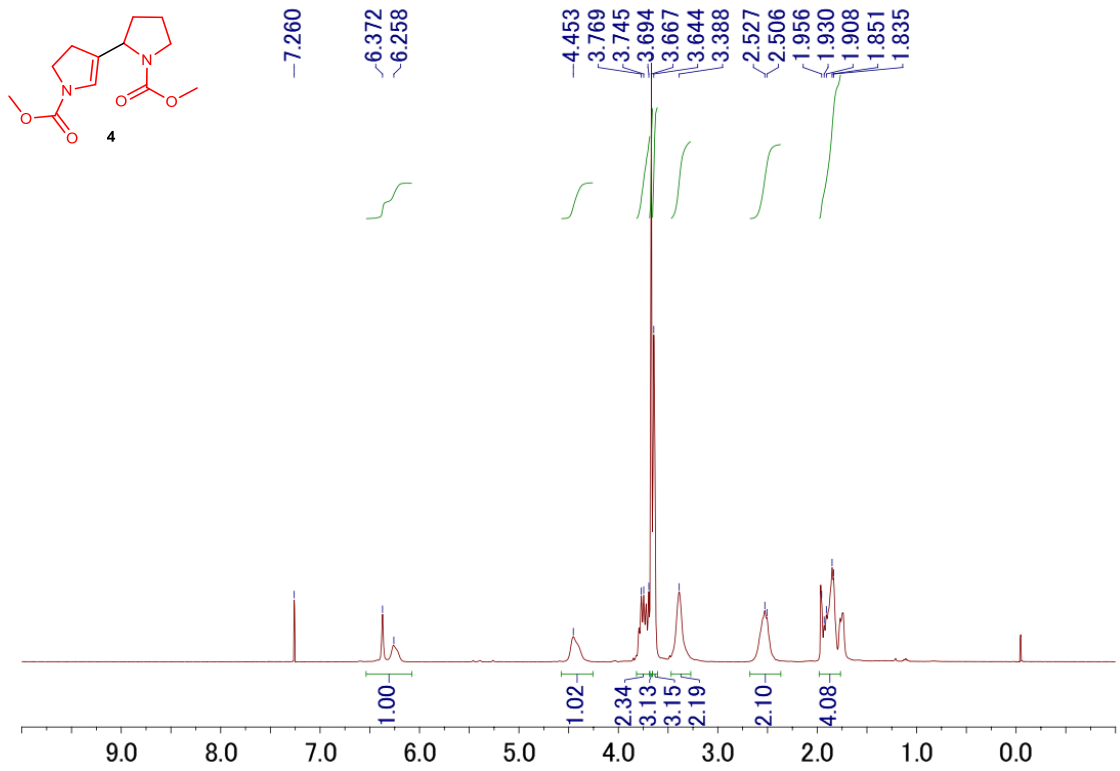

^{1}H NMR spectrum of methyl 4-(*N*-methoxycarbonylpyrrolidine-2-yl)-2,3-dihydropyrrole-1-carboxylate (4) (400 MHz, $CDCl_3$)

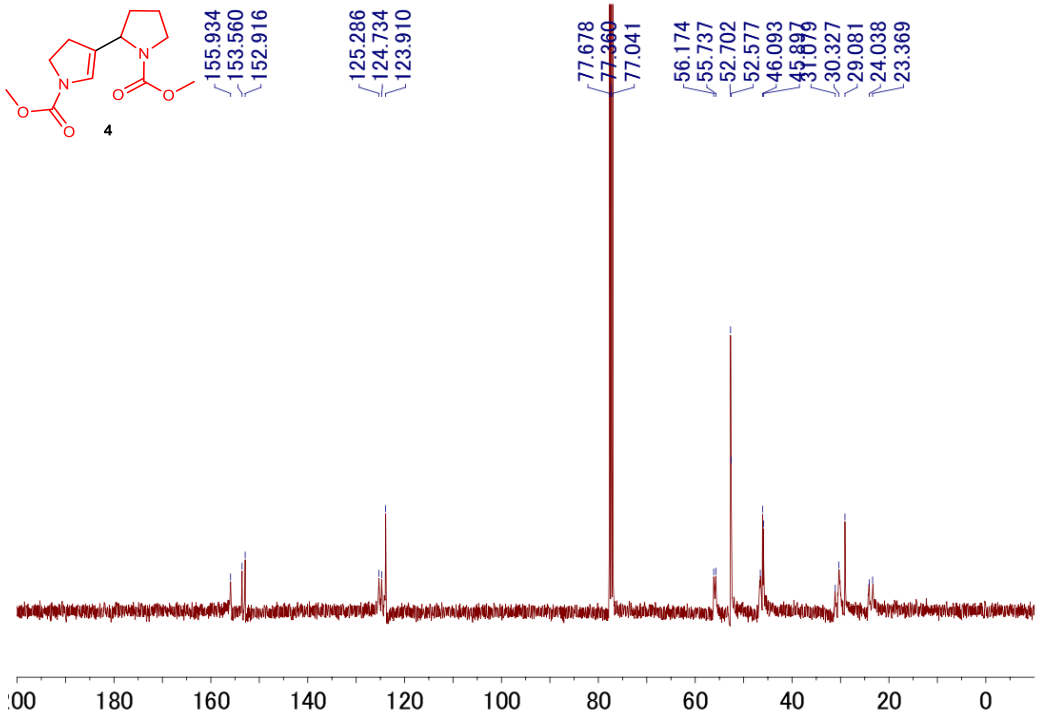

^{13}C NMR spectrum of methyl 4-(*N*-methoxycarbonylpyrrolidine-2-yl)-2,3-dihydropyrrole-1-carboxylate (4) (100 MHz, $CDCl_3$)

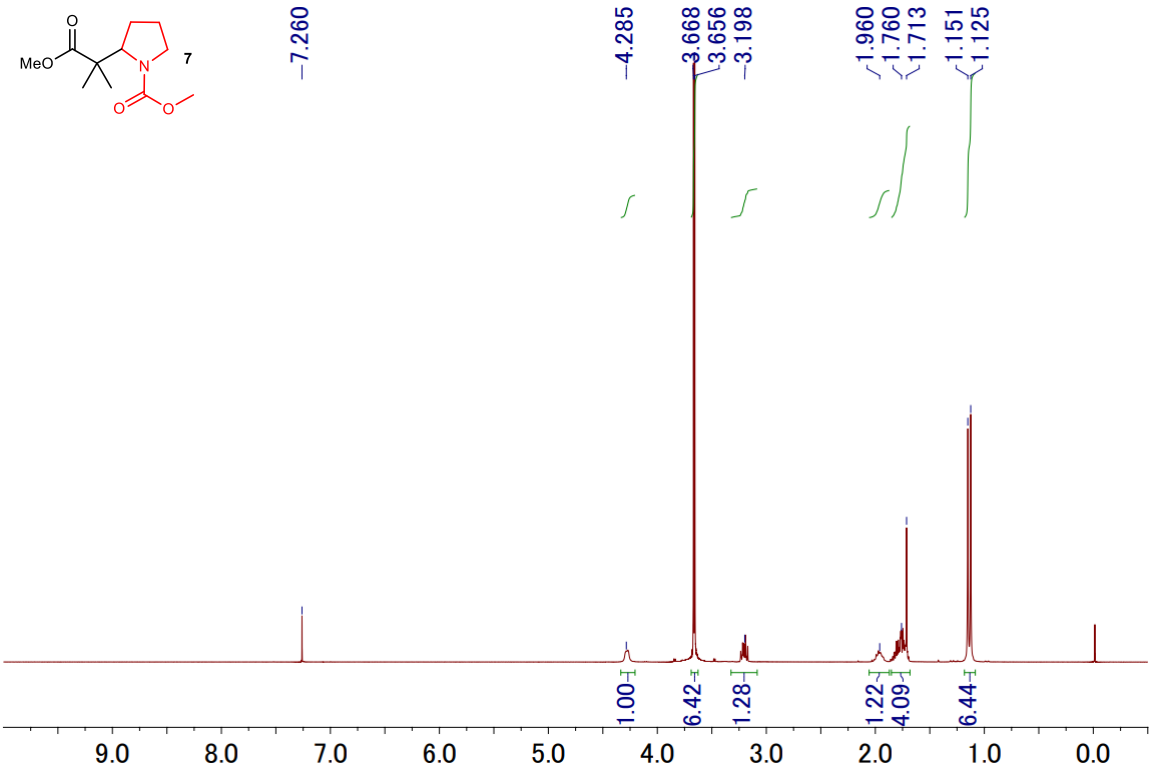

^{1}H NMR spectrum of methyl 2-(1-methoxy-2-methyl-1-oxopropan-2-yl)pyrrolidine-1-carboxylate (7) (400 MHz, $CDCl_3$)

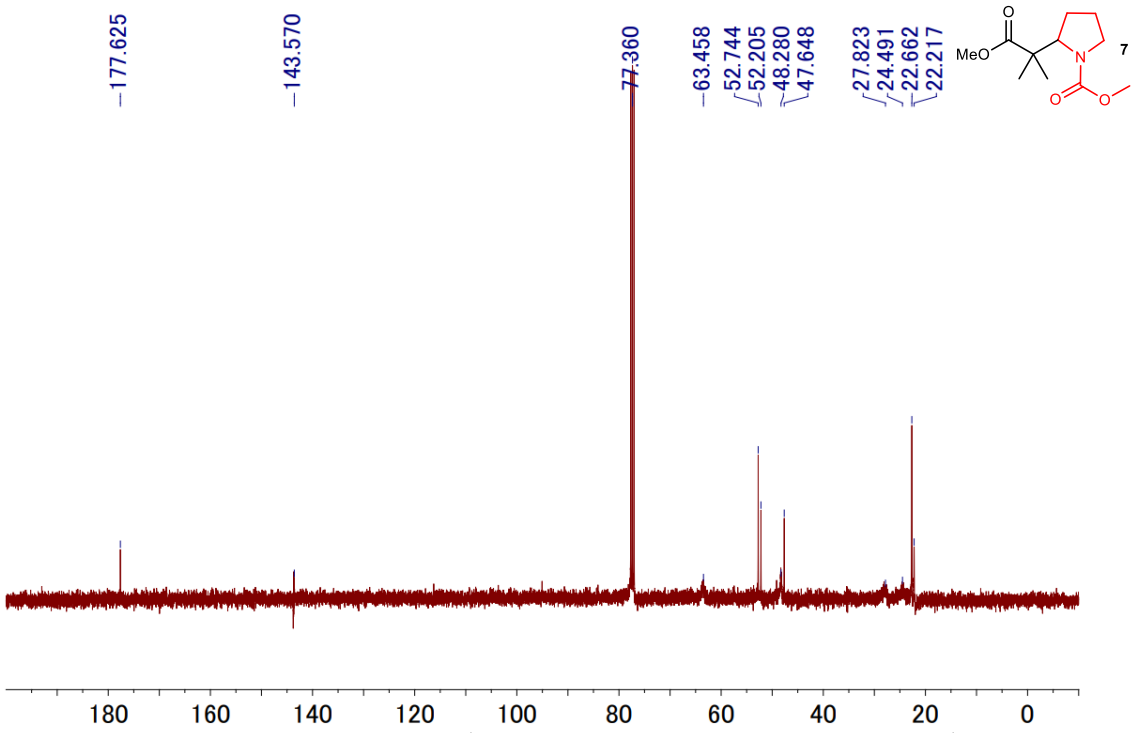

^{13}C NMR spectrum of methyl 2-(1-methoxy-2-methyl-1-oxopropan-2-yl)pyrrolidine-1-carboxylate (7) (100 MHz, $CDCl_3$)

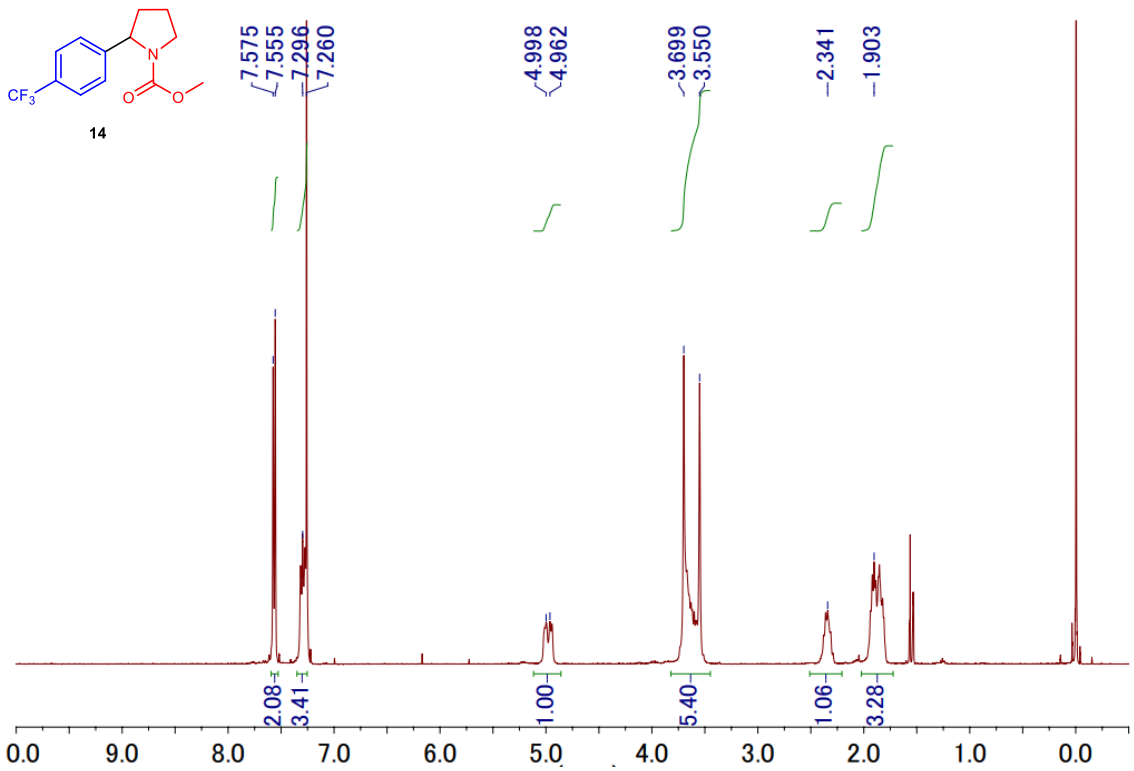

^{1}H NMR of methyl 2-(4-(trifluoromethyl)phenyl)pyrrolidine-1-carboxylate (14) (400 MHz, $CDCl_3$)

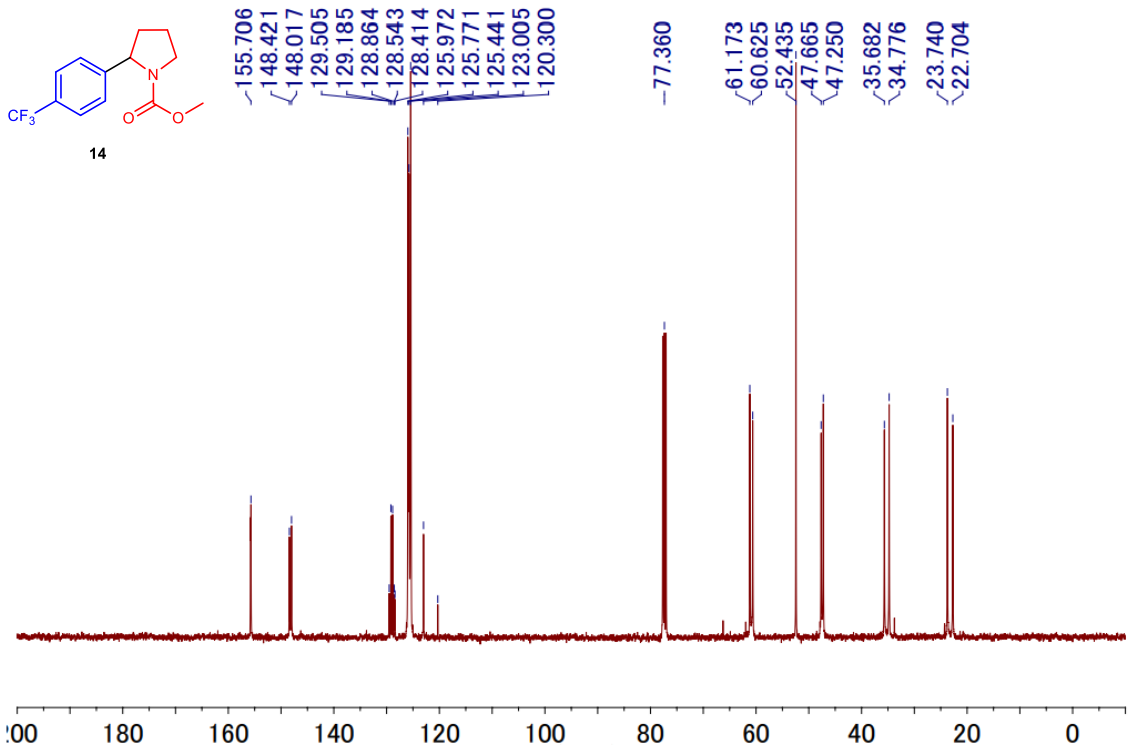

^{13}C NMR spectrum of methyl 2-(4-(trifluoromethyl)phenyl)pyrrolidine-1-carboxylate (14) (100 MHz, $CDCl_3$)

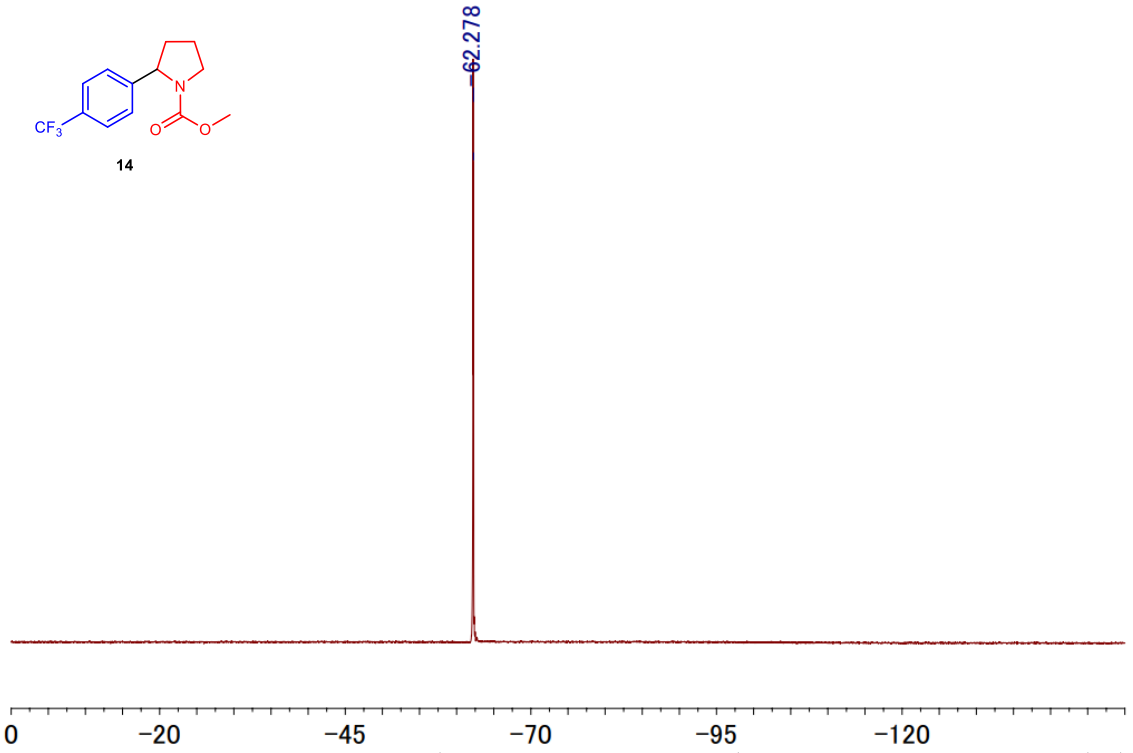

^{19}F NMR spectrum of methyl 2-(4-trifluoromethylphenyl)pyrrolidine-1-carboxylate (14) (376 MHz, $CDCl_3$)

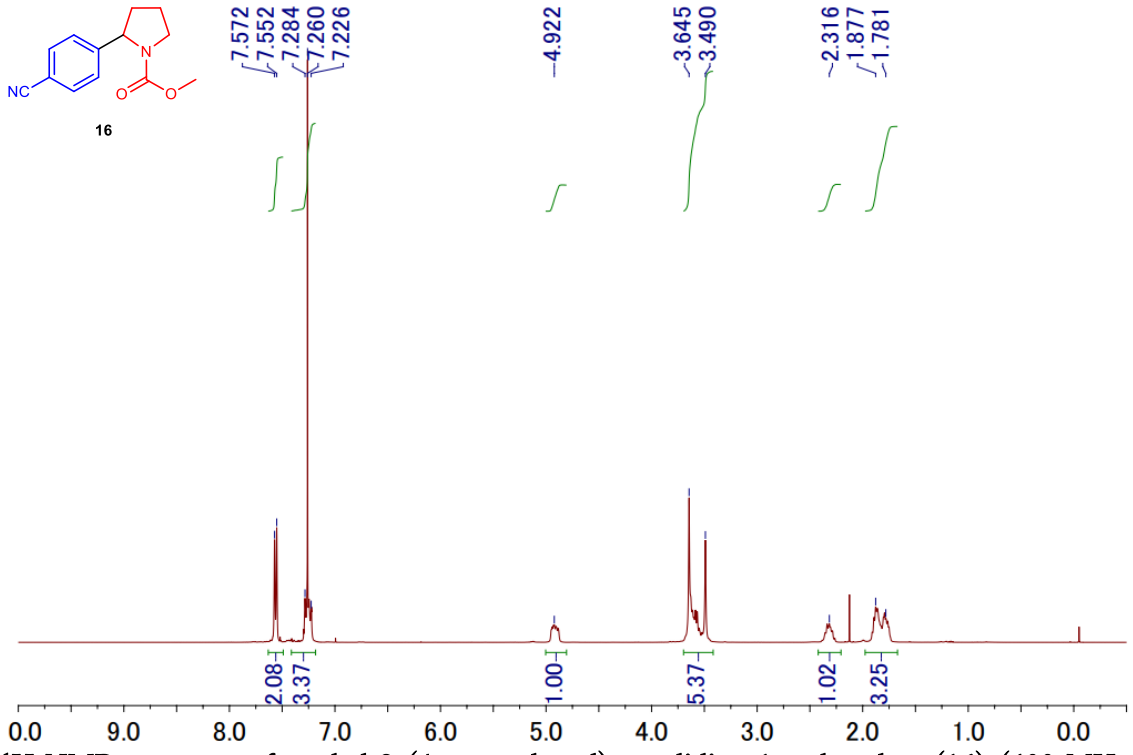

^{1}H NMR spectrum of methyl 2-(4-cyanophenyl)pyrrolidine-1-carboxylate (16) (400 MHz, $CDCl_3$)

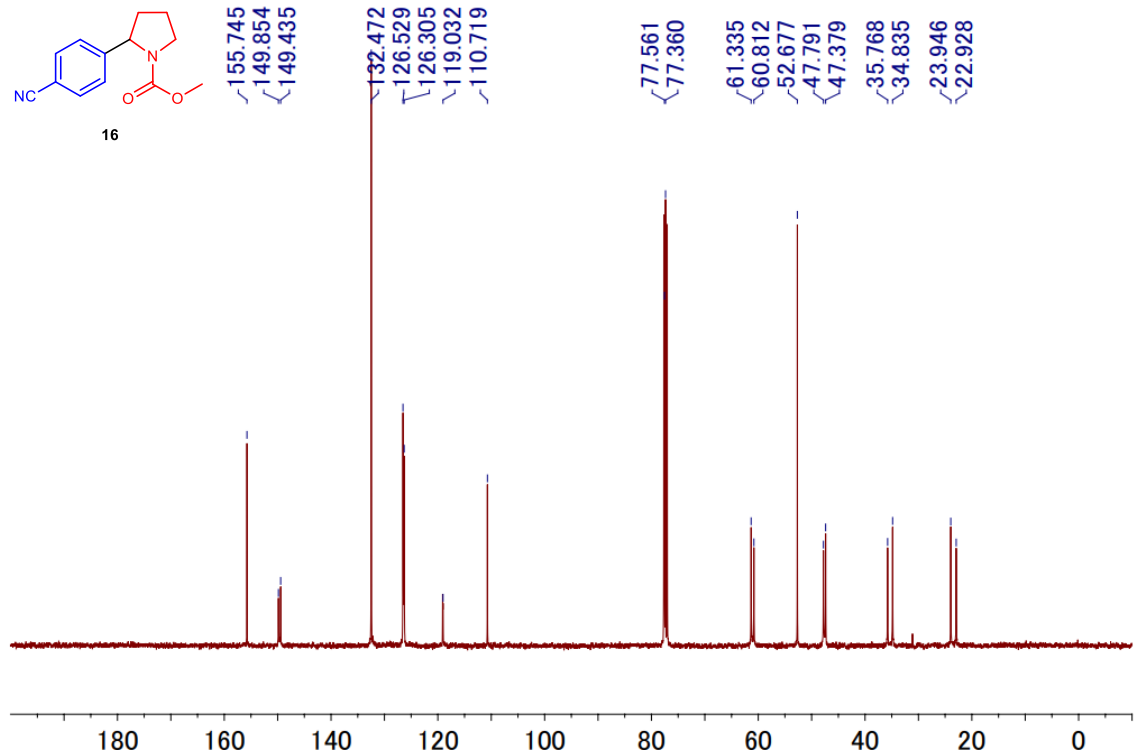

^{13}C NMR spectrum of methyl 2-(4-cyanophenyl)pyrrolidine-1-carboxylate (16) (100 MHz, $CDCl_3$)

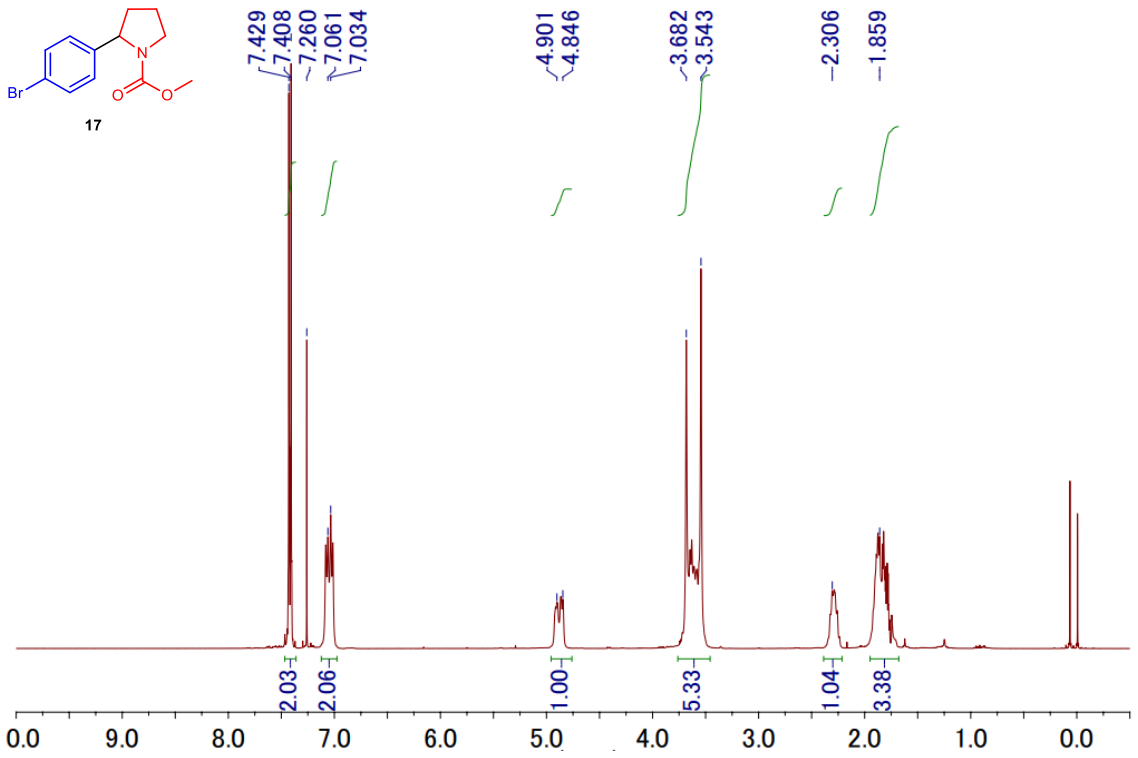

^{1}H NMR spectrum of methyl 2-(4-bromophenyl)pyrrolidine-1-carboxylate (17) (400 MHz, $CDCl_3$)

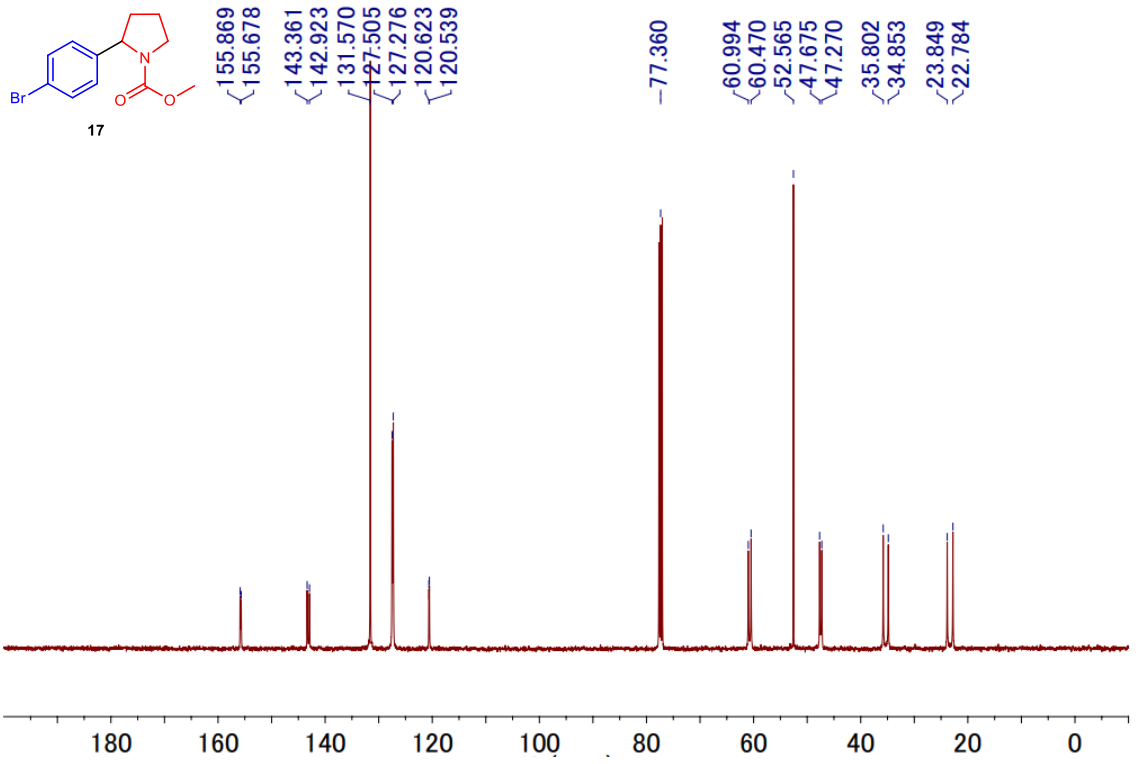

^{13}C NMR spectrum of methyl 2-(4-bromophenyl)pyrrolidine-1-carboxylate (17) (100 MHz, $CDCl_3$)

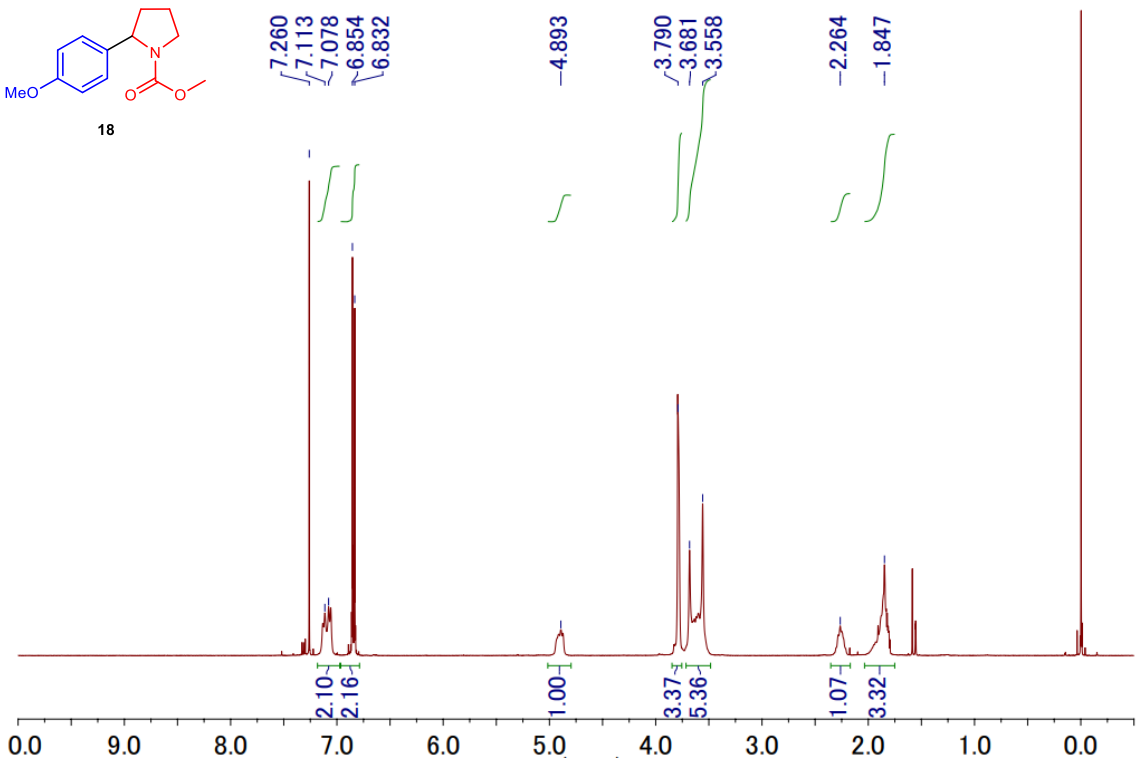

^{1}H NMR spectrum of methyl 2-(4-methoxyphenyl)pyrrolidine-1-carboxylate (18) (400 MHz, $CDCl_3$)

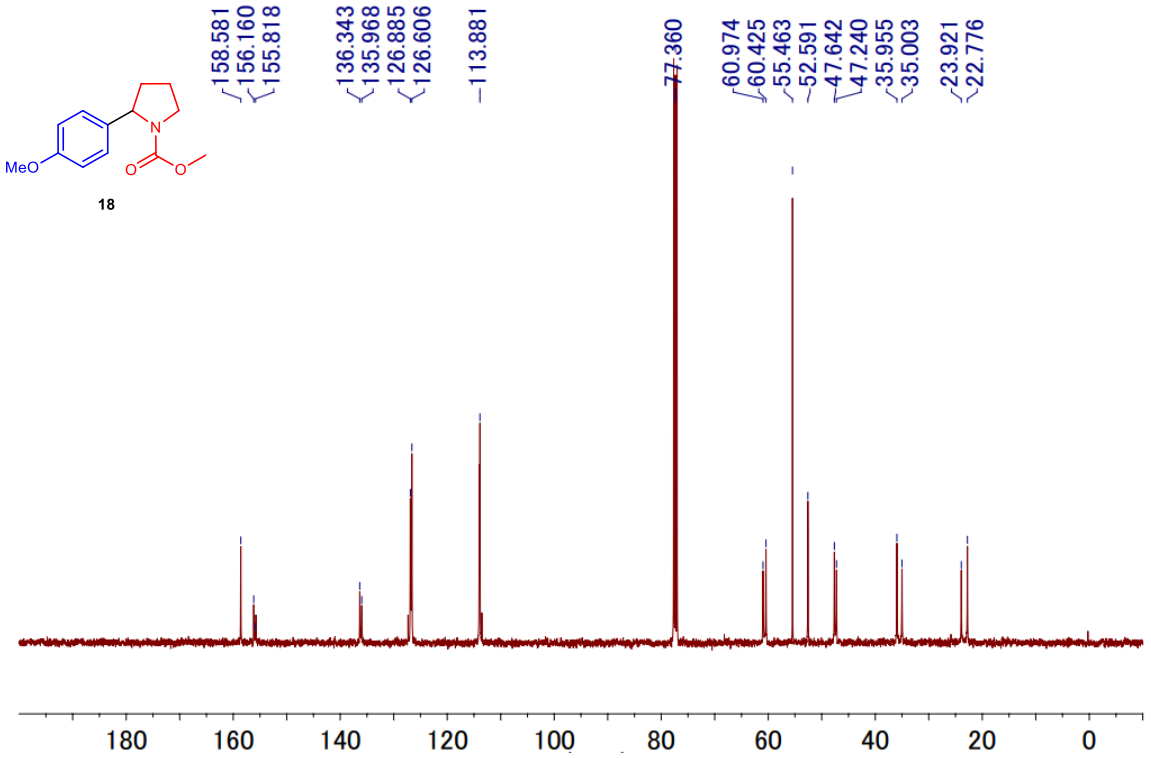

^{13}C NMR spectrum of methyl 2-(4-methoxyphenyl)pyrrolidine-1-carboxylate (18) (100 MHz, $CDCl_3$)

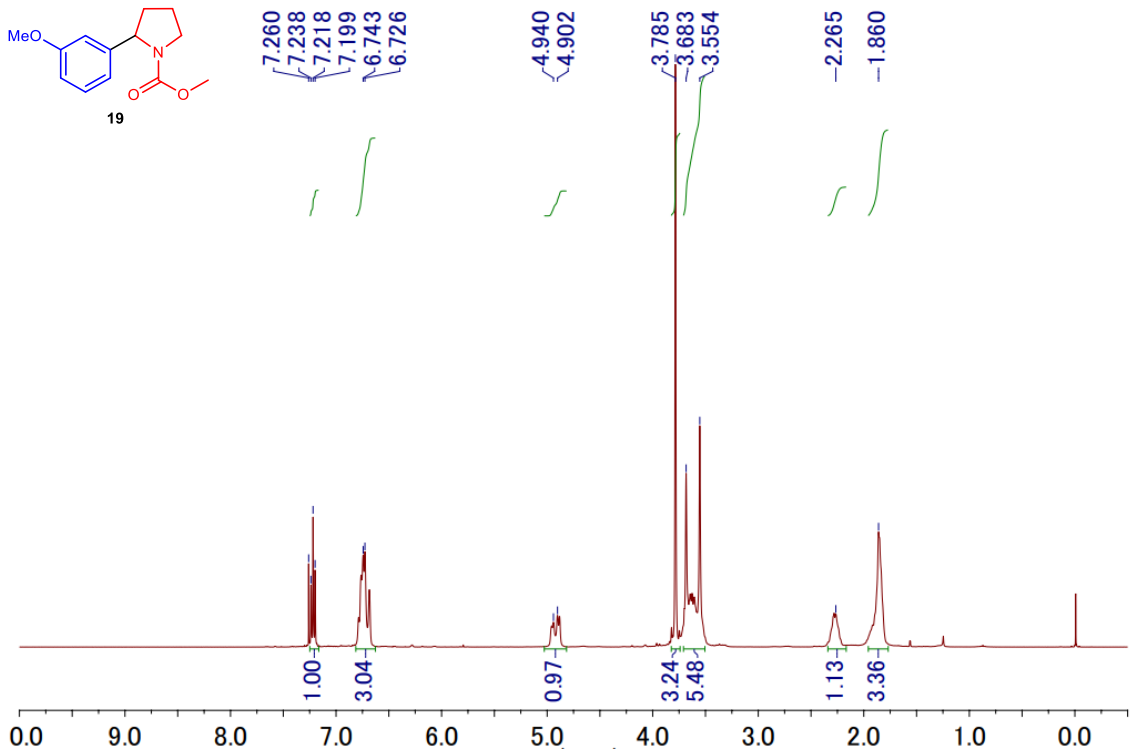

^{1}H NMR spectrum of methyl 2-(3-methoxyphenyl)pyrrolidine-1-carboxylate (19) (400 MHz, $CDCl_3$)

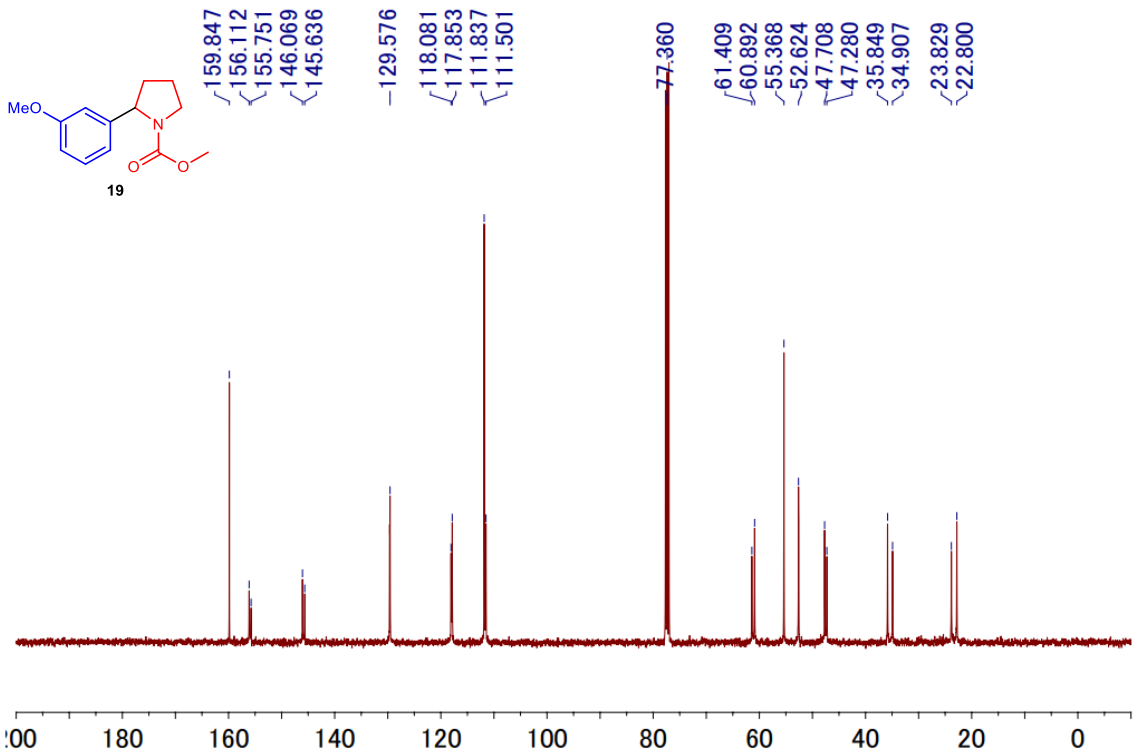

^{13}C NMR spectrum of methyl 2-(3-methoxyphenyl)pyrrolidine-1-carboxylate (19) (100 MHz, $CDCl_3$)

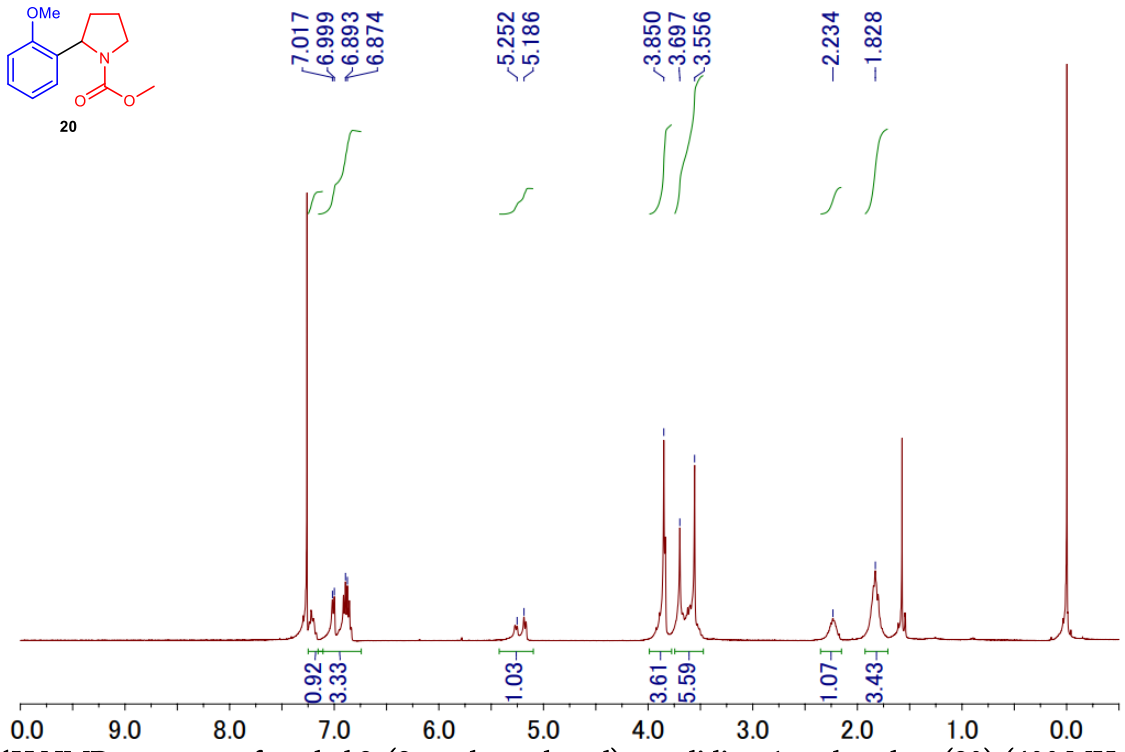

^{1}H NMR spectrum of methyl 2-(2-methoxyphenyl)pyrrolidine-1-carboxylate (20) (400 MHz, $CDCl_3$)

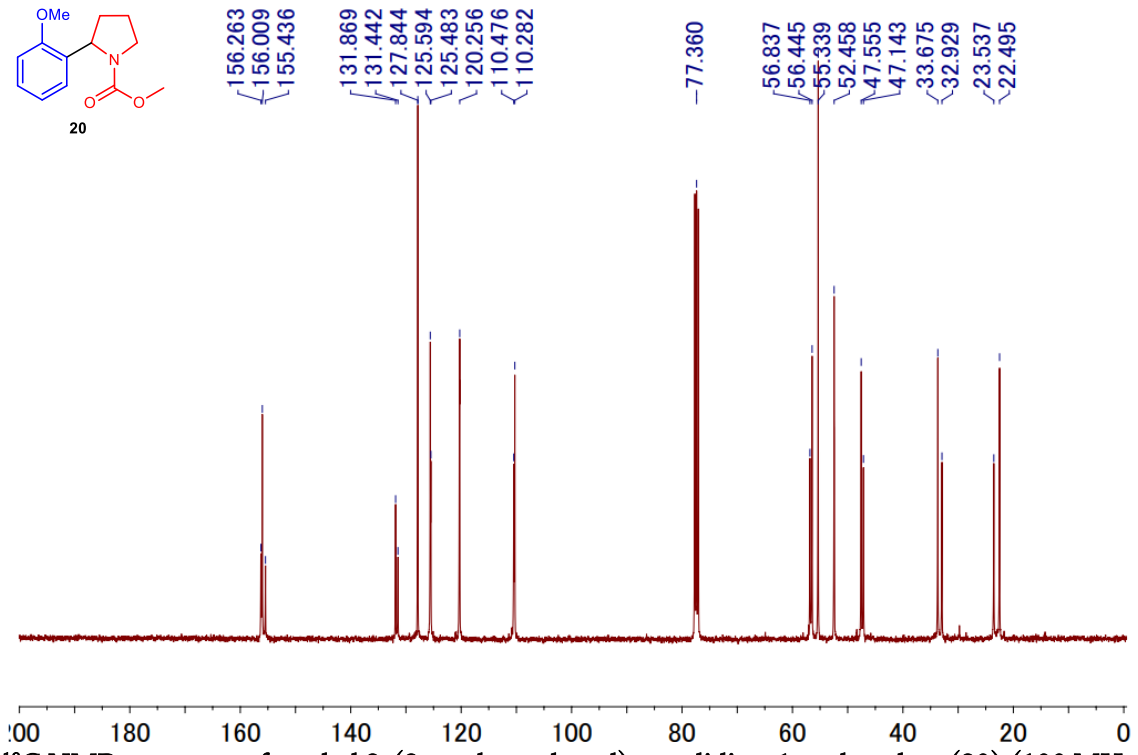

^{13}C NMR spectrum of methyl 2-(2-methoxyphenyl)pyrrolidine-1-carboxylate (20) (100 MHz, $CDCl_3$)

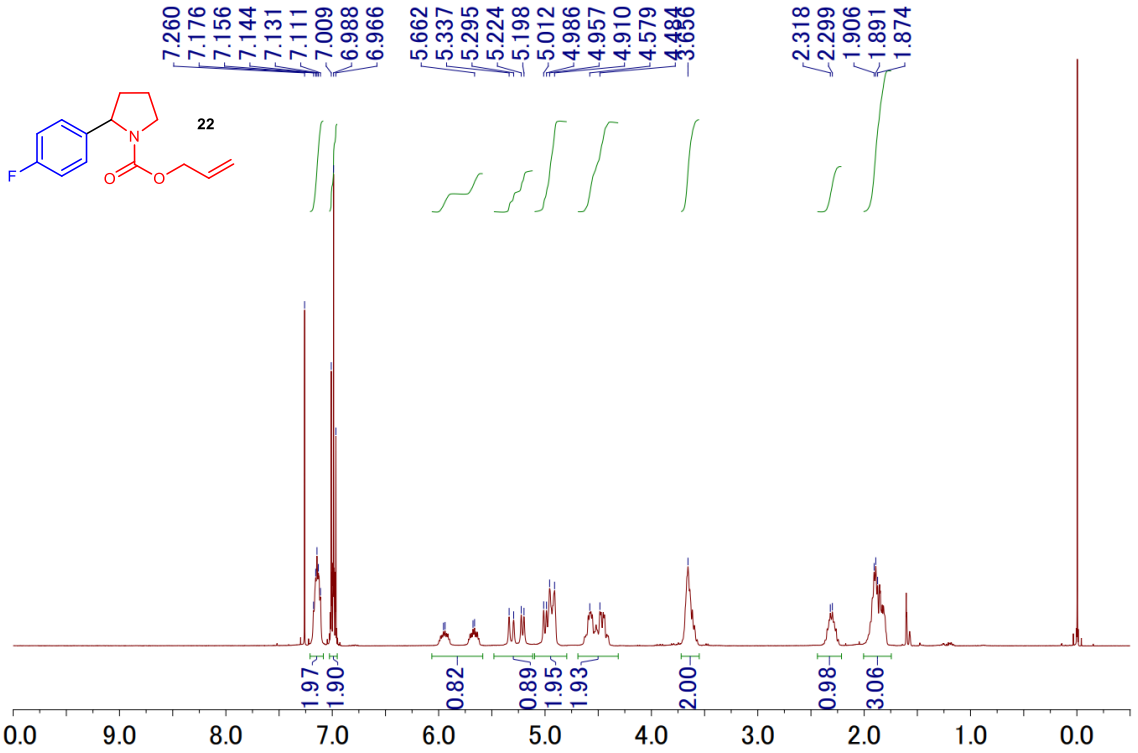

^{1}H NMR spectrum of allyl 2-(4-fluorophenyl)pyrrolidine-1-carboxylate (22) (400 MHz, $CDCl_3$)

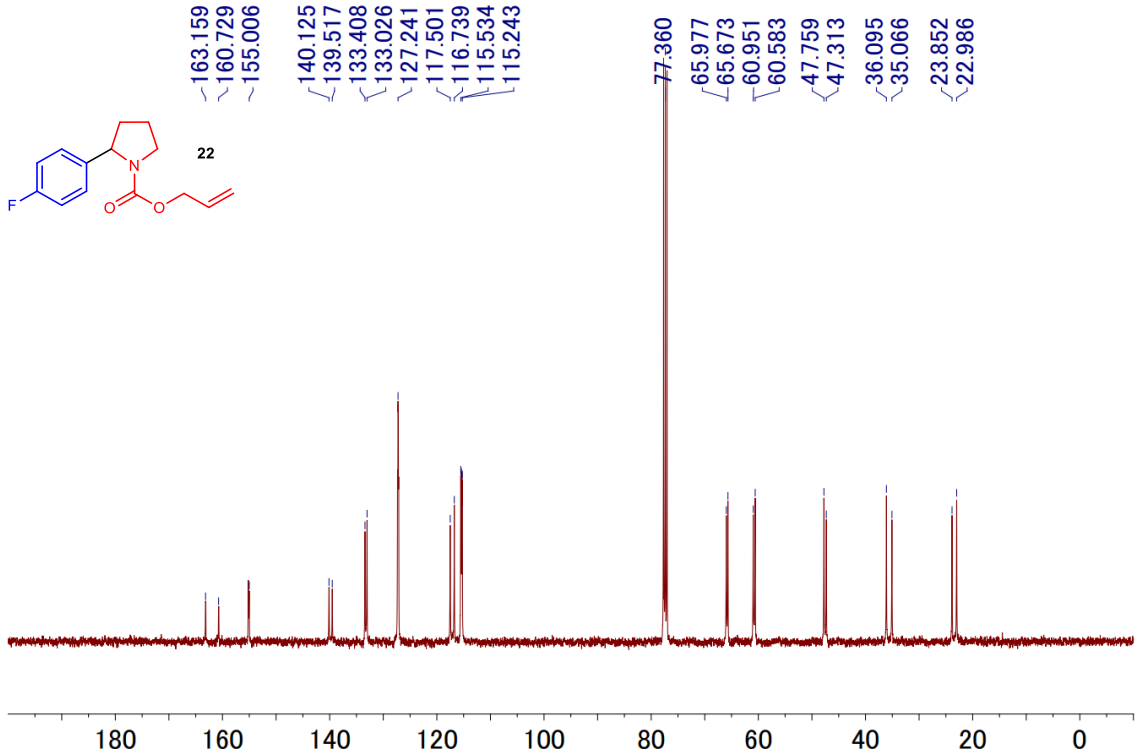

^{13}C NMR spectrum of allyl 2-(4-fluorophenyl)pyrrolidine-1-carboxylate (22) (100 MHz, $CDCl_3$)

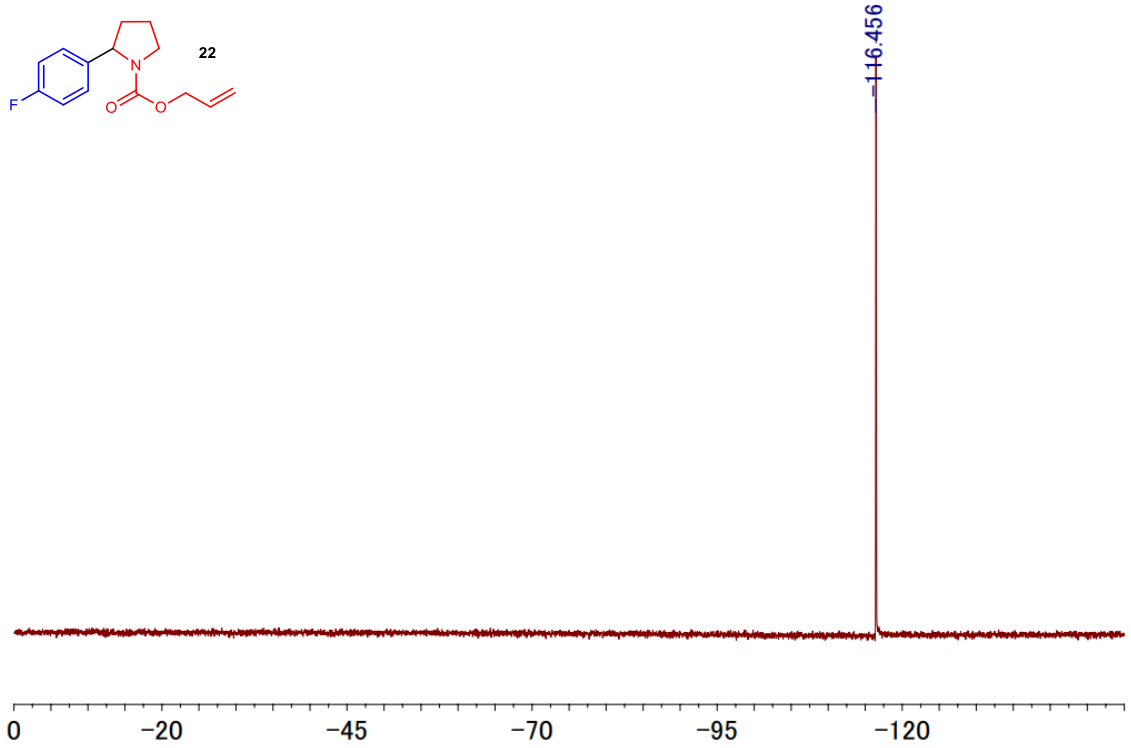

^{19}F NMR spectrum of allyl 2-(4-fluorophenyl)pyrrolidine-1-carboxylate (22) (376 MHz, $CDCl_3$)

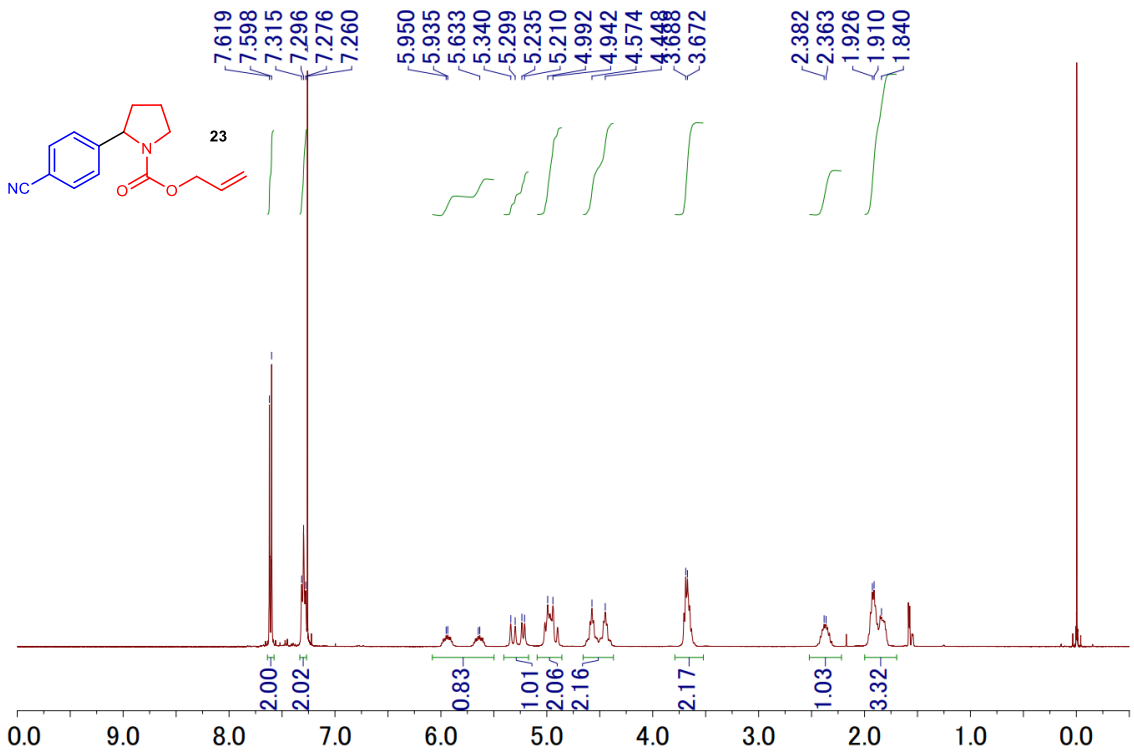

^{1}H NMR spectrum of allyl 2-(4-cyanophenyl)pyrrolidine-1-carboxylate (23) (400 MHz, $CDCl_3$)

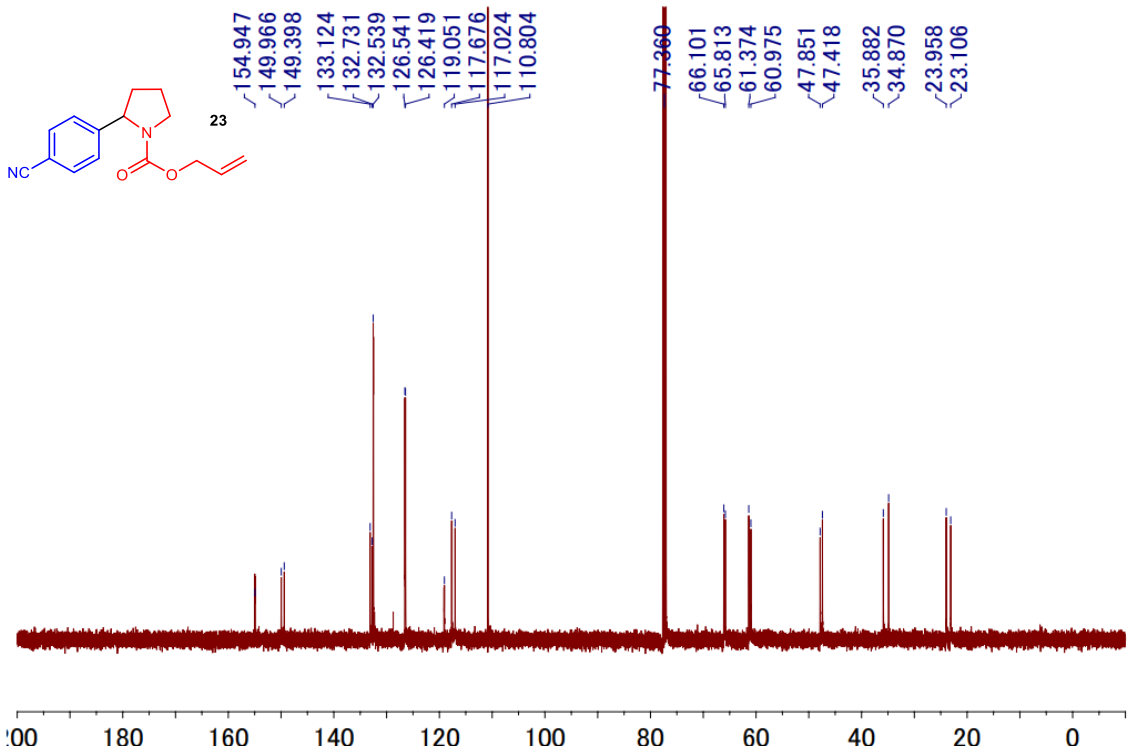

^{13}C NMR spectrum of allyl 2-(4-cyanophenyl)pyrrolidine-1-carboxylate (23) (100 MHz, $CDCl_3$)

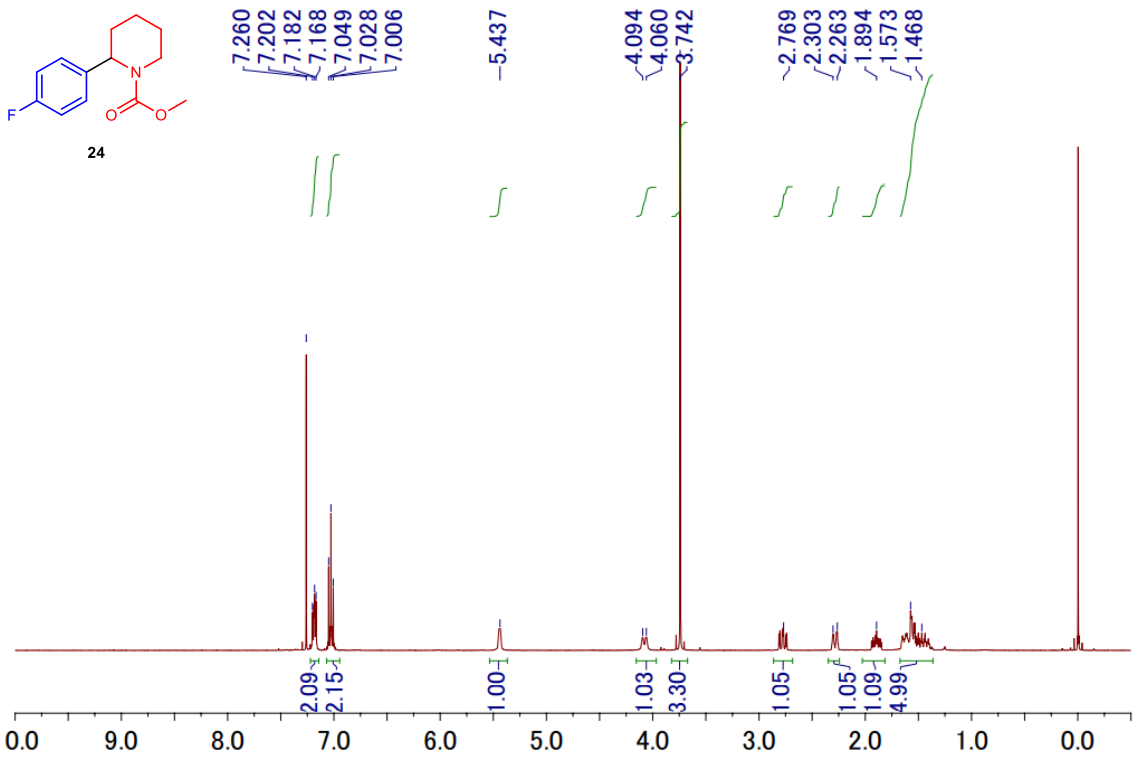

^{1}H NMR spectrum of methyl 2-(4-fluorophenyl)piperidine-1-carboxylate (24) (400 MHz, $CDCl_3$)

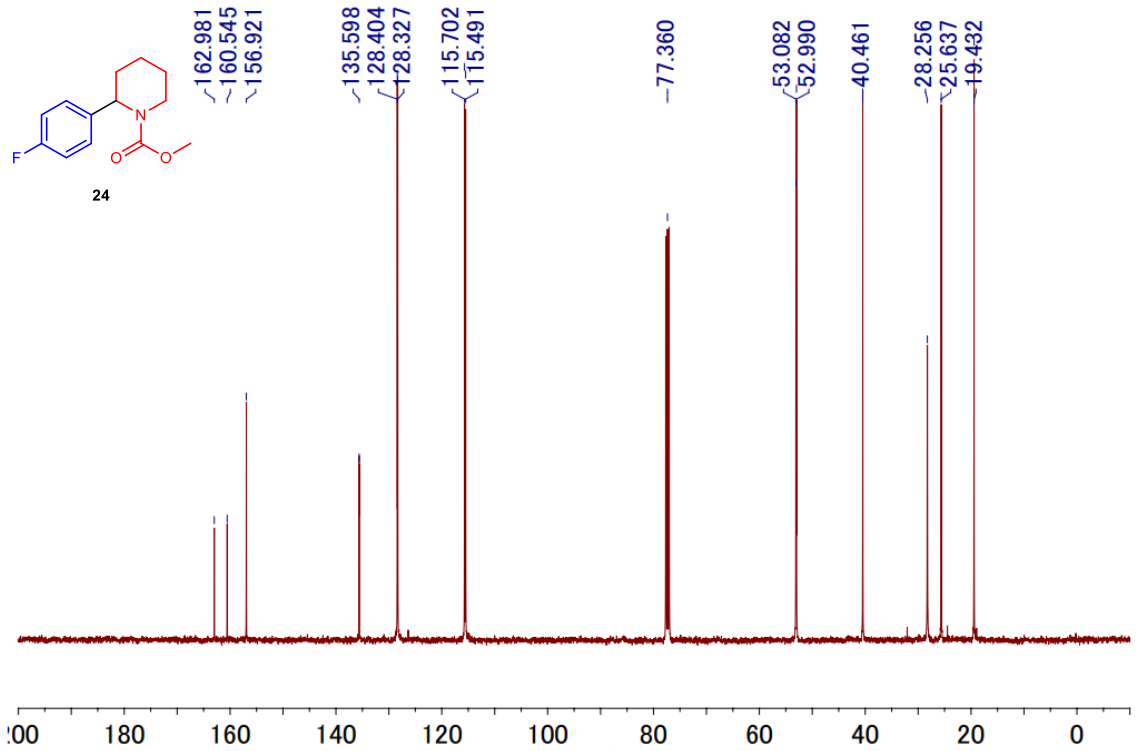

^{13}C NMR spectrum of methyl 2-(4-fluorophenyl)piperidine-1-carboxylate (24) (100 MHz, $CDCl_3$)

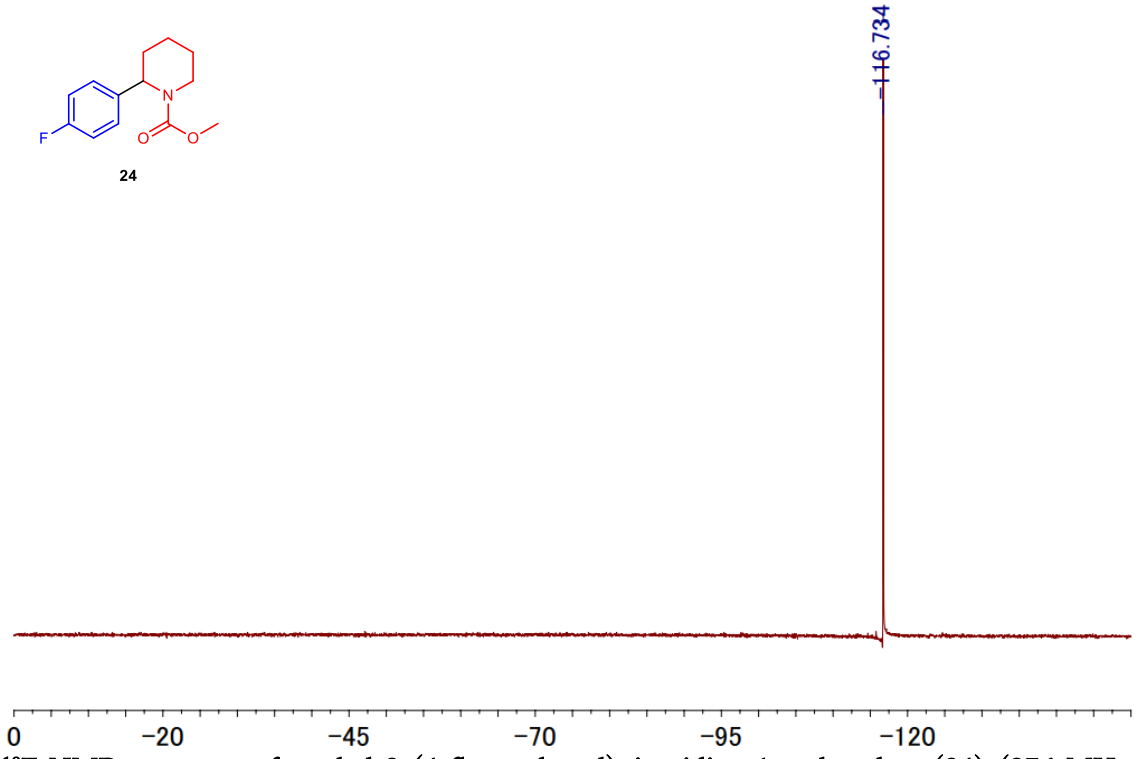

^{19}F NMR spectrum of methyl 2-(4-fluorophenyl)piperidine-1-carboxylate (24) (376 MHz, $CDCl_3$)

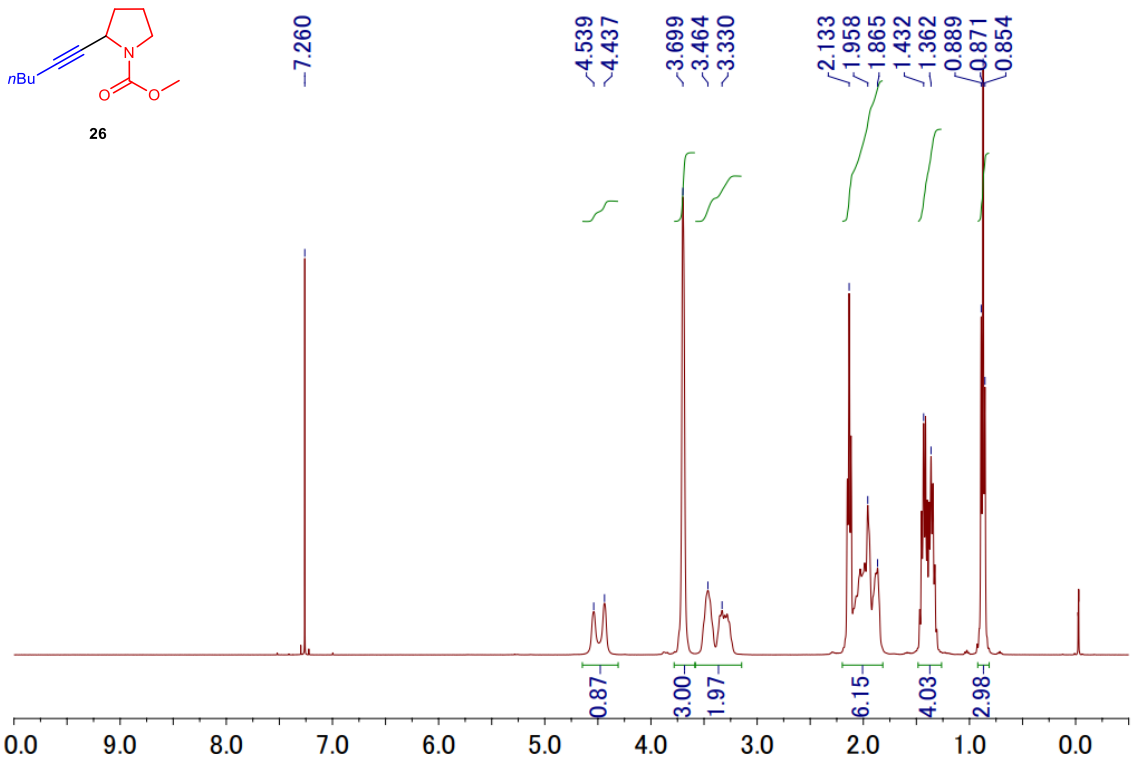

^{1}H NMR spectrum of methyl 2-(1-hexyn-1-yl)pyrrolidine-1-carboxylate (26) (400 MHz, $CDCl_3$)

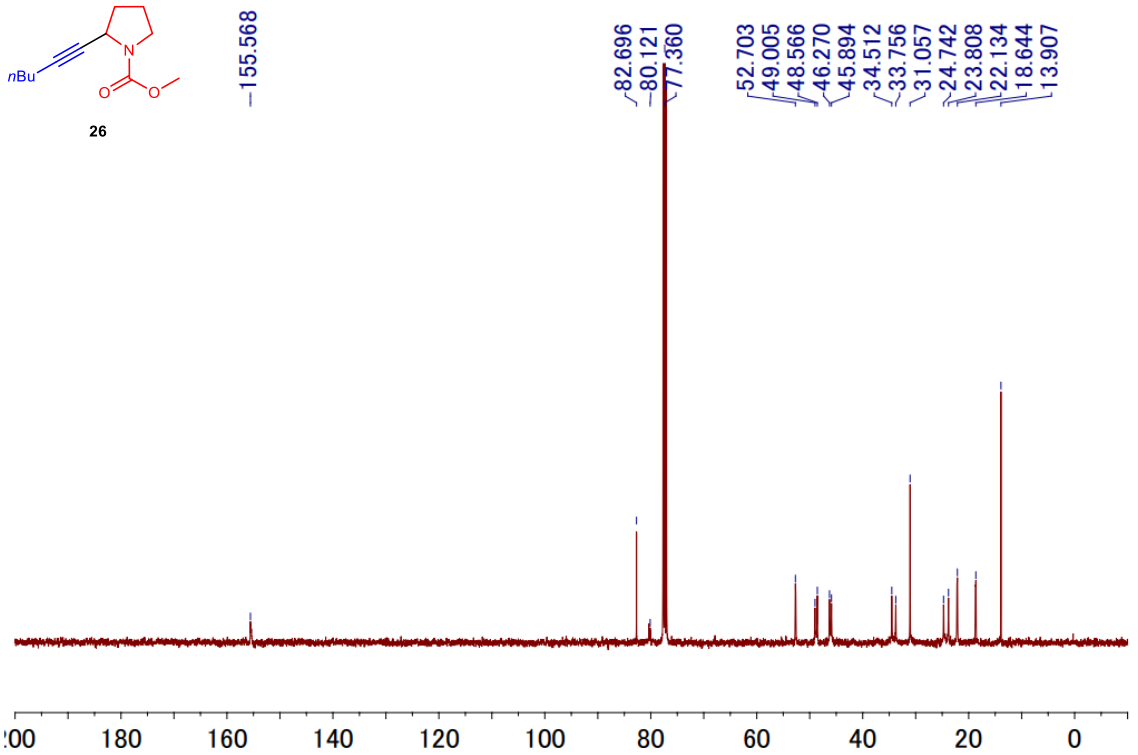

^{13}C NMR spectrum of methyl 2-(1-hexyn-1-yl)pyrrolidine-1-carboxylate (26) (100 MHz, $CDCl_3$)

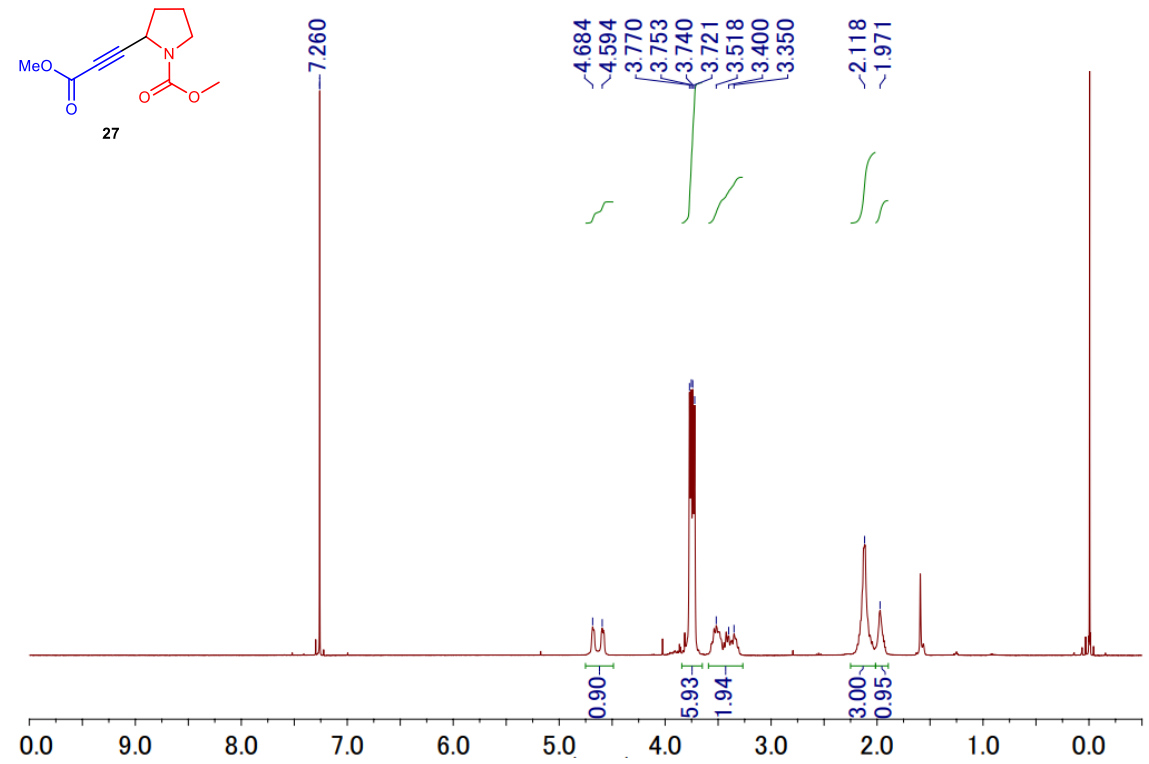

^{1}H NMR spectrum of methyl 2-(3-methoxy-3-oxopropynyl)pyrrolidine-1-carboxylate (27) (400 MHz, $CDCl_3$)

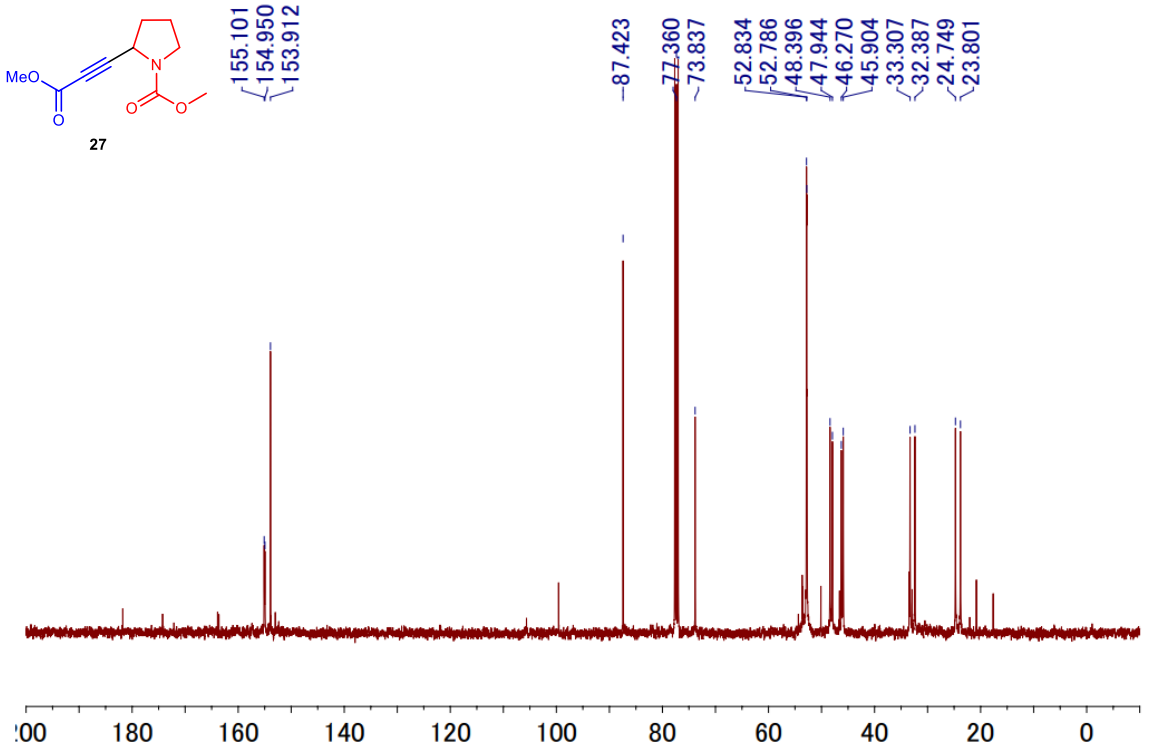

^{13}C NMR spectrum of methyl 2-(3-methoxy-3-oxopropynyl)pyrrolidine-1-carboxylate (27) (100 MHz, $CDCl_3$)

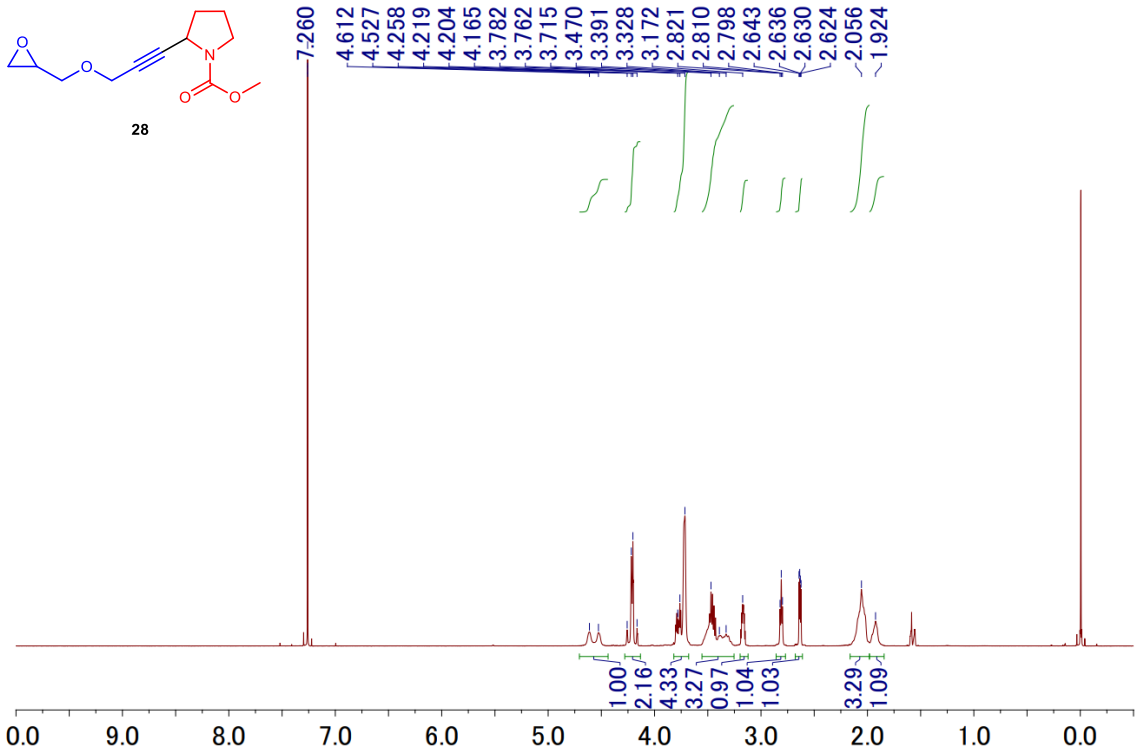

^{1}H NMR spectrum of methyl 2-(3-glycidyloxy-1-propynyl)pyrrolidine-1-carboxylate (28) (400 MHz, $CDCl_3$)

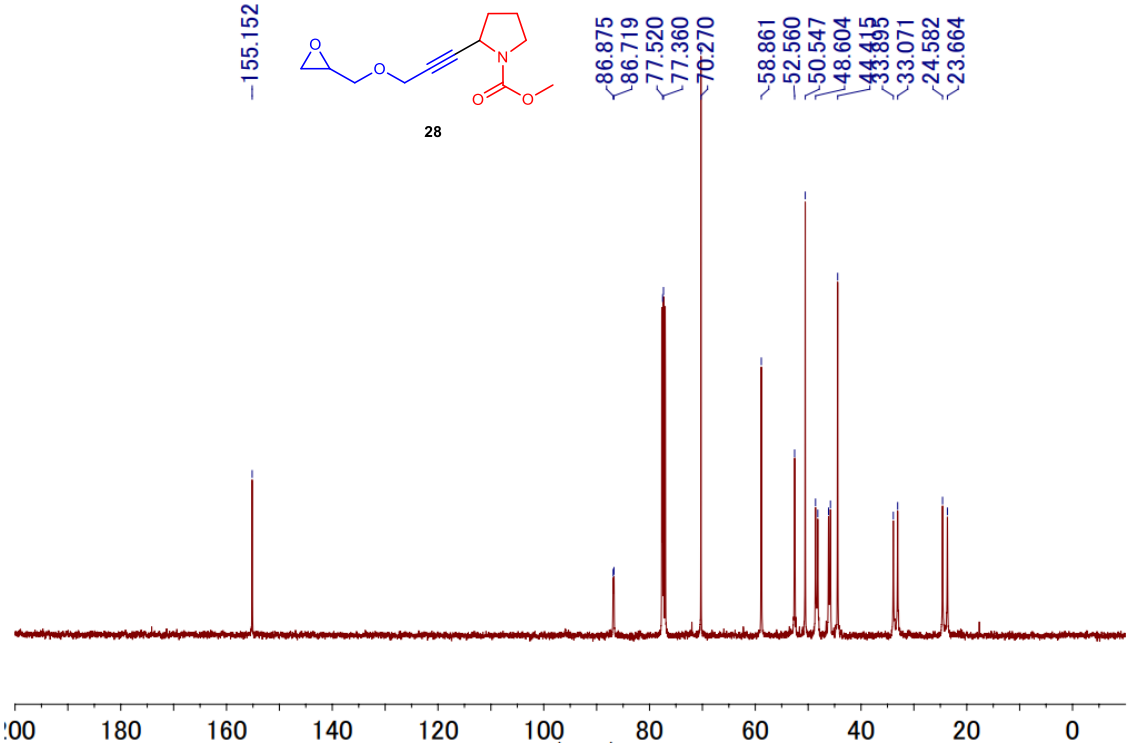

^{13}C NMR spectrum of methyl 2-(3-glycidyloxy-1-propynyl)pyrrolidine-1-carboxylate (28) (100 MHz, $CDCl_3$)

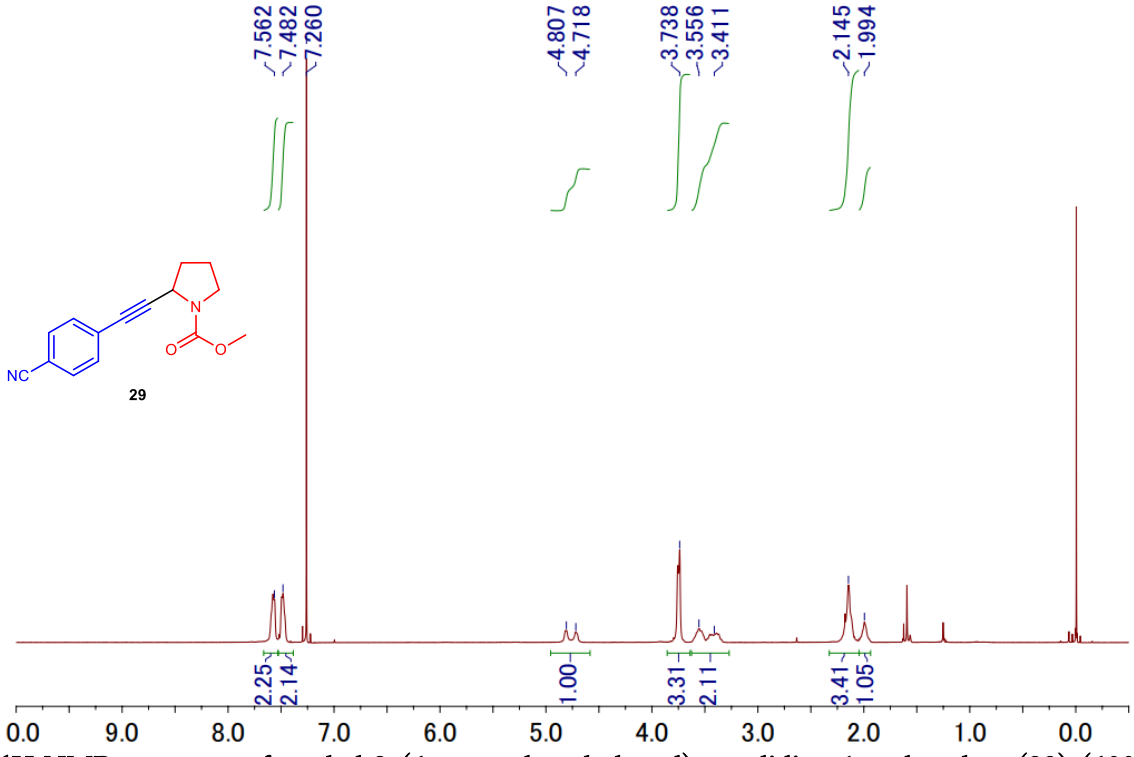

^{1}H NMR spectrum of methyl 2-(4-cyanophenylethynyl)pyrrolidine-1-carboxylate (29) (400 MHz, $CDCl_3$)

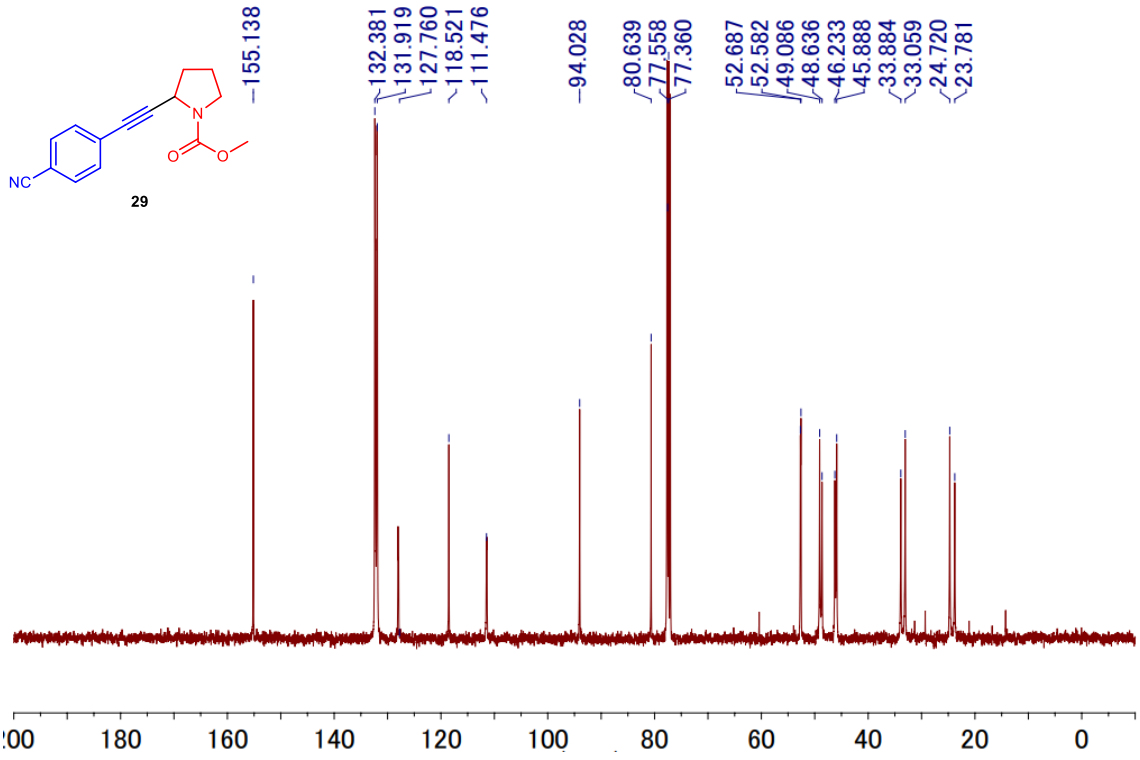

^{13}C NMR spectrum of methyl 2-(4-cyanophenylethynyl)pyrrolidine-1-carboxylate (29) (100 MHz, $CDCl_3$)

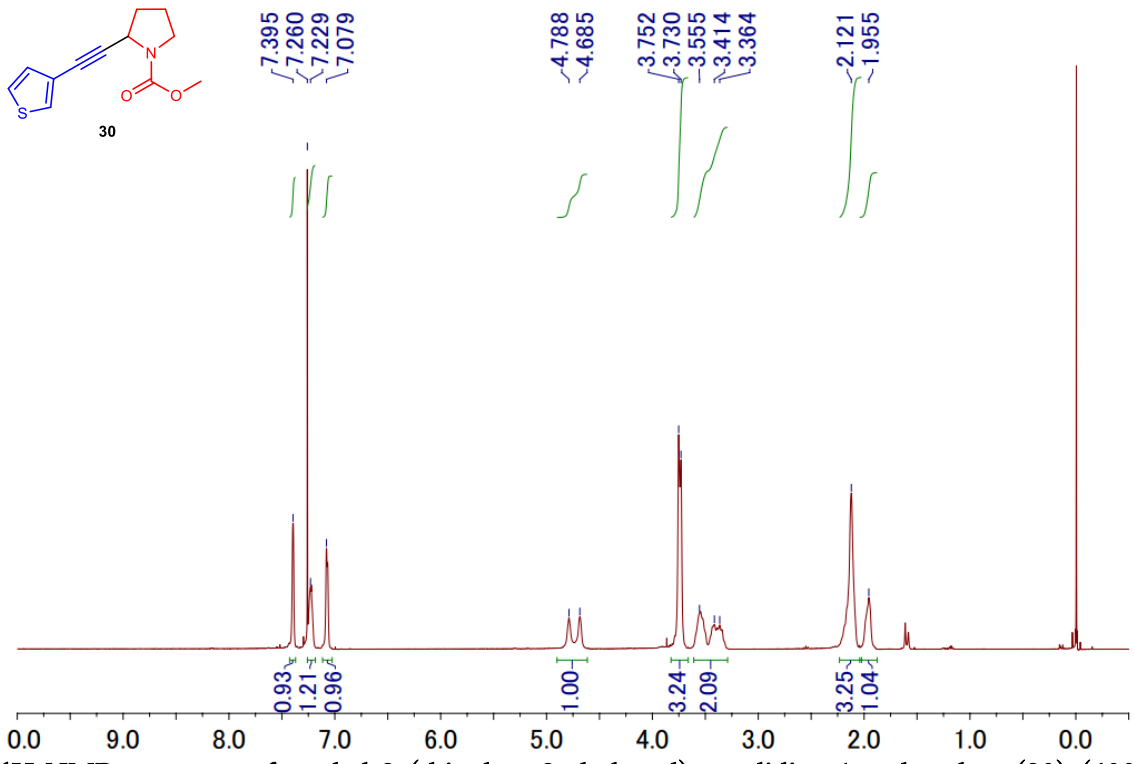

^{1}H NMR spectrum of methyl 2-(thiophen-3-ylethynyl)pyrrolidine-1-carboxylate (30) (400 MHz, $CDCl_3$)

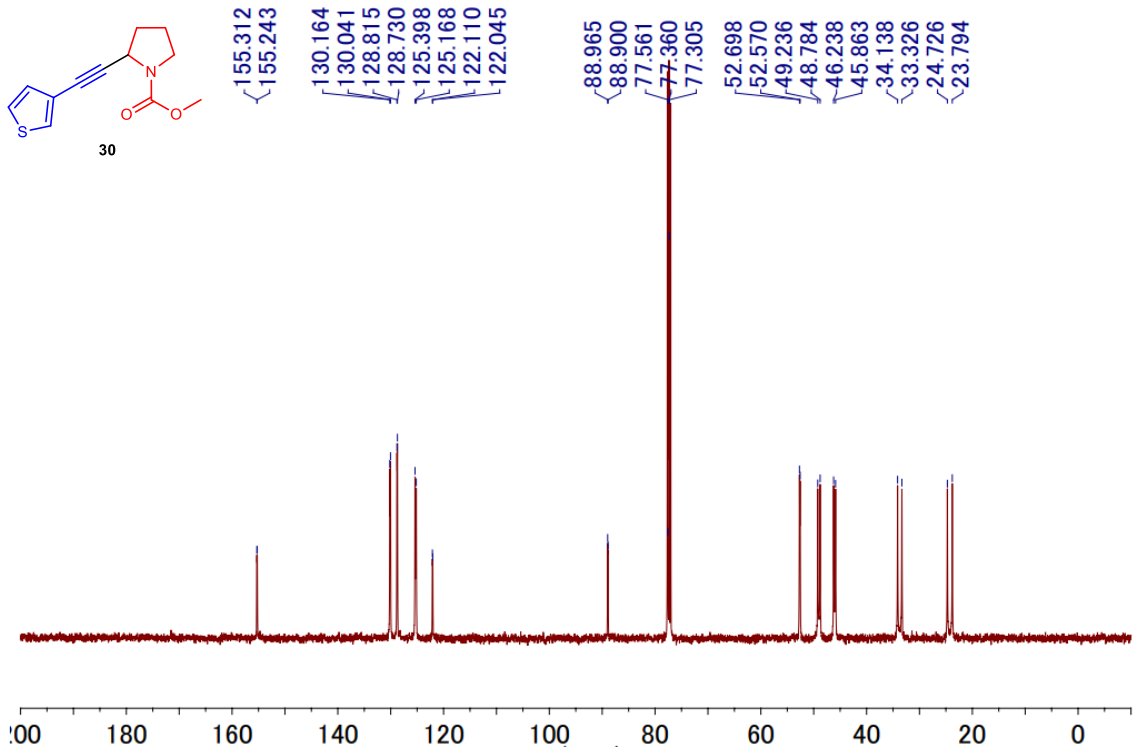

^{13}C NMR spectrum of methyl 2-(thiophen-3-ylethynyl)pyrrolidine-1-carboxylate (30) (100 MHz, $CDCl_3$)

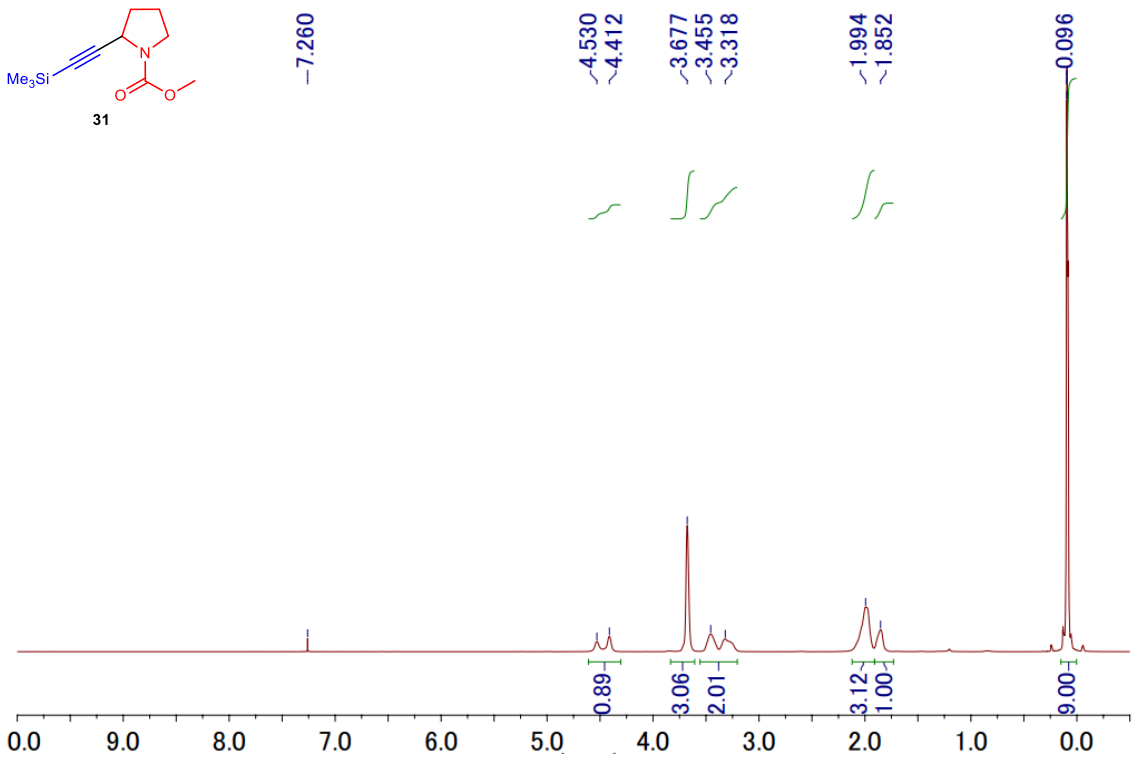

^{1}H NMR spectrum of methyl 2-(trimethylsilylethynyl)pyrrolidine-1-carboxylate (31) (400 MHz, $CDCl_3$)

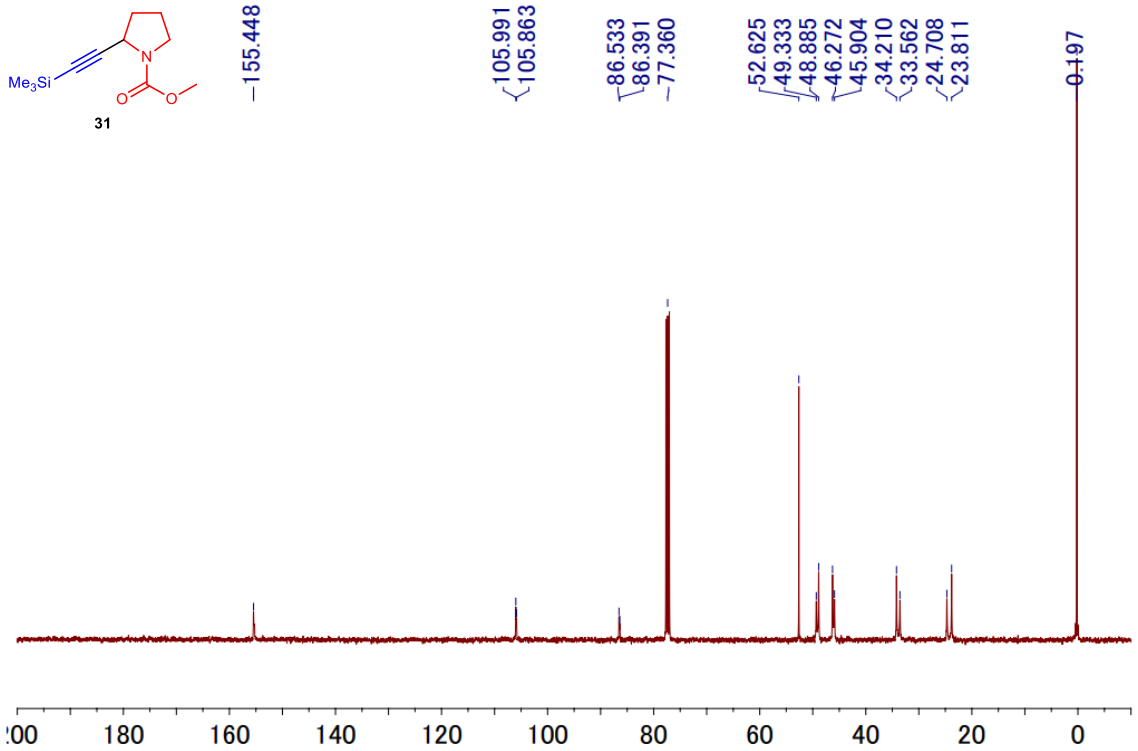

^{13}C NMR spectrum of methyl 2-(trimethylsilylethynyl)pyrrolidine-1-carboxylate (31) (100 MHz, $CDCl_3$)

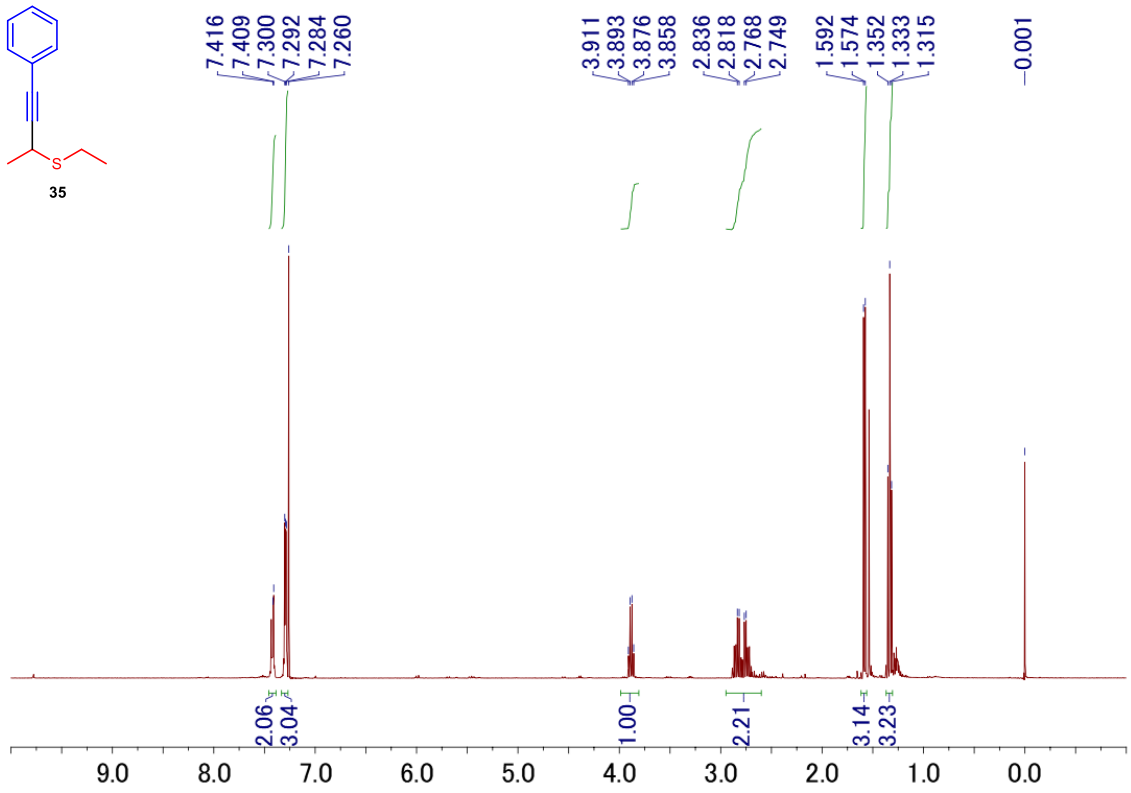

^{1}H NMR spectrum of ethyl 4-phenyl-3-butyn-2-yl sulfide (35) (400 MHz, $CDCl_3$)

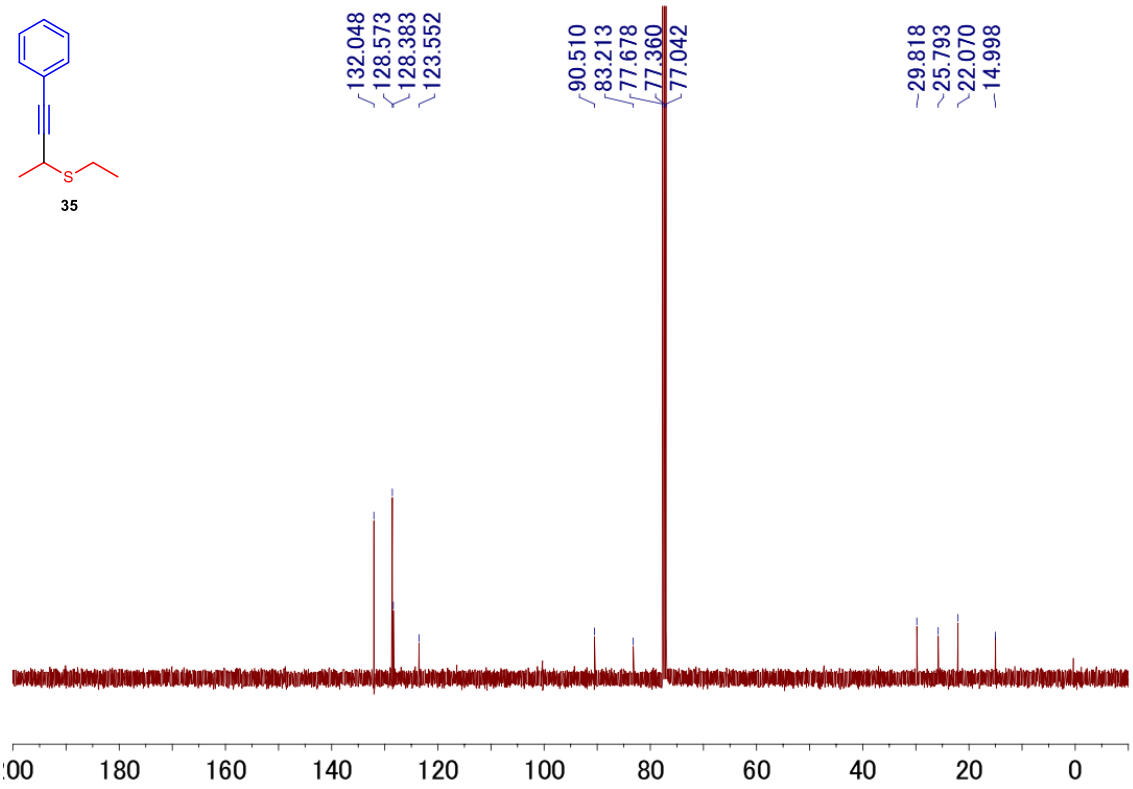

^{13}C NMR spectrum of ethyl 4-phenyl-3-butyn-2-yl sulfide (35) (100 MHz, $CDCl_3$)

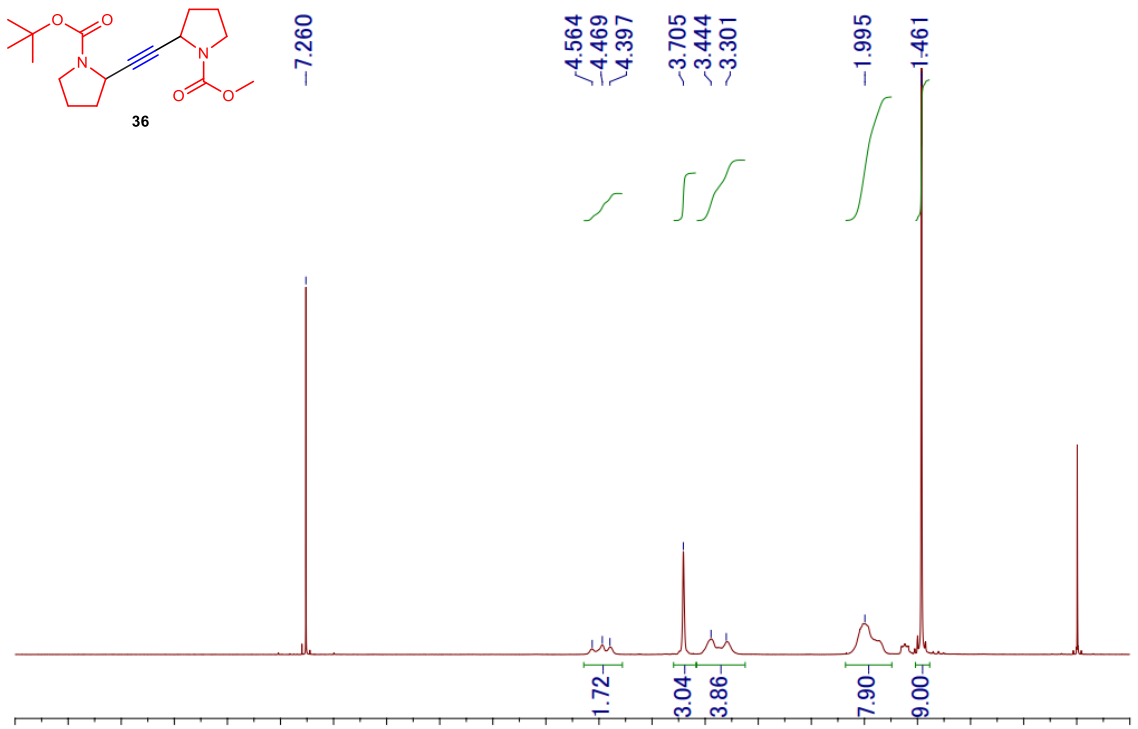

^{1}H NMR spectrum of *tert*-butyl 2-((1-(methoxycarbonyl)pyrrolidin-2-yl)ethynyl)pyrrolidine-1-carboxylate (36) (400 MHz, $CDCl_3$)

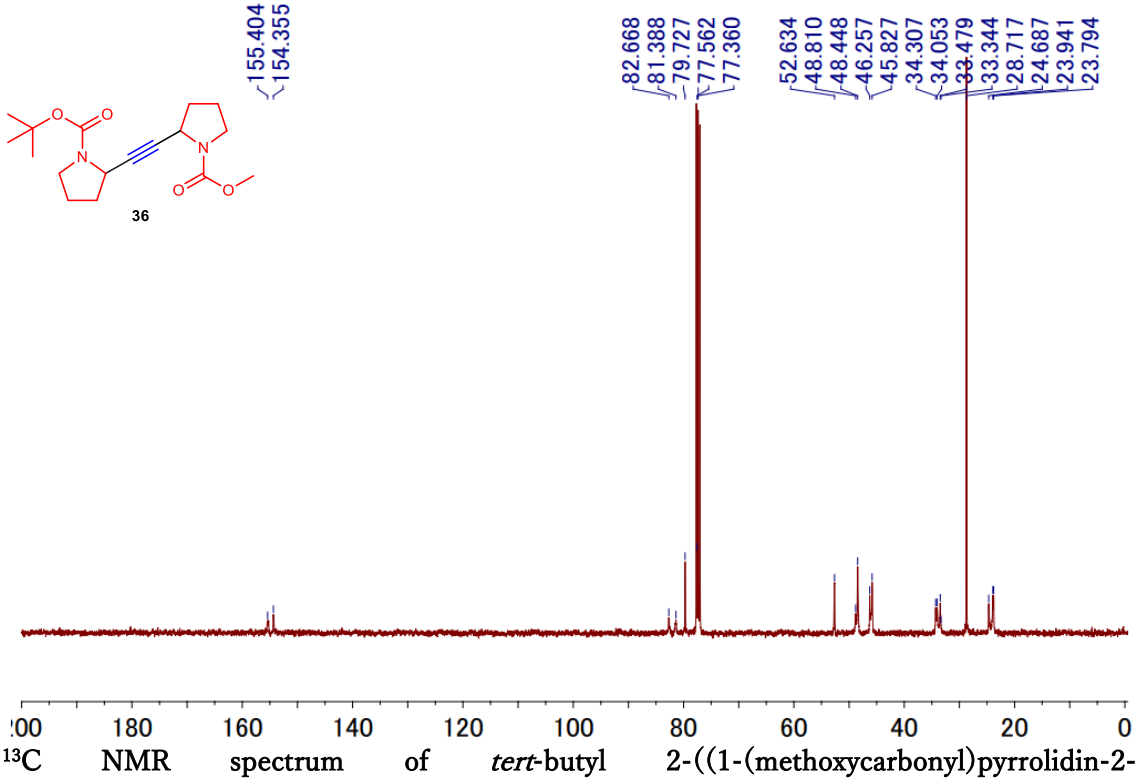

^{13}C NMR spectrum of *tert*-butyl 2-((1-(methoxycarbonyl)pyrrolidin-2-yl)ethynyl)pyrrolidine-1-carboxylate (36) (100 MHz, $CDCl_3$)

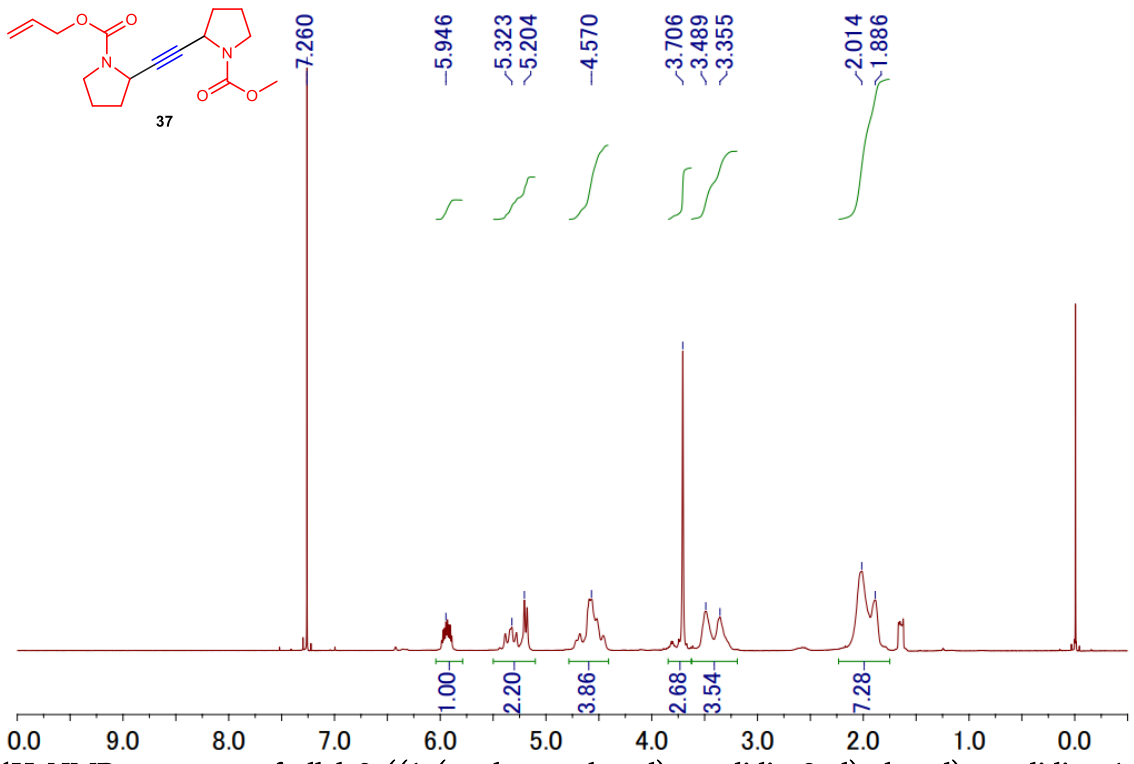

^{1}H NMR spectrum of allyl 2-((1-(methoxycarbonyl)pyrrolidin-2-yl)ethynyl)pyrrolidine-1-carboxylate (37) (400 MHz, $CDCl_3$)

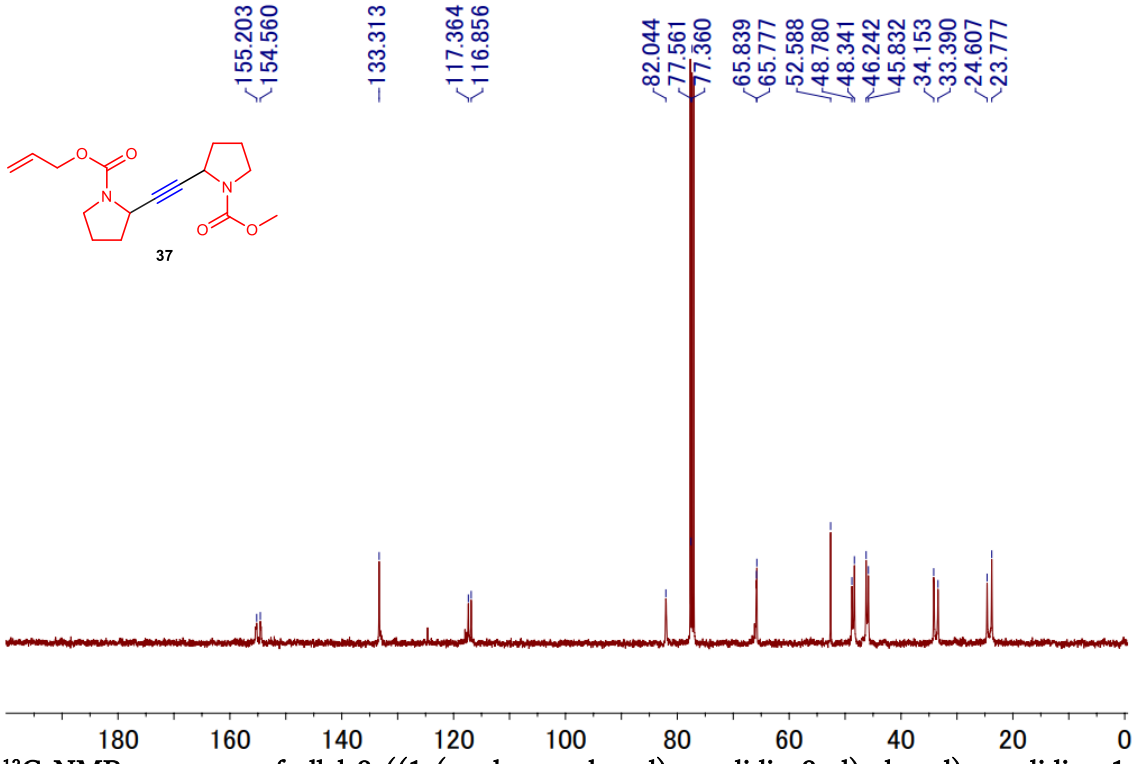

^{13}C NMR spectrum of allyl 2-((1-(methoxycarbonyl)pyrrolidin-2-yl)ethynyl)pyrrolidine-1-carboxylate (37) (100 MHz, $CDCl_3$)

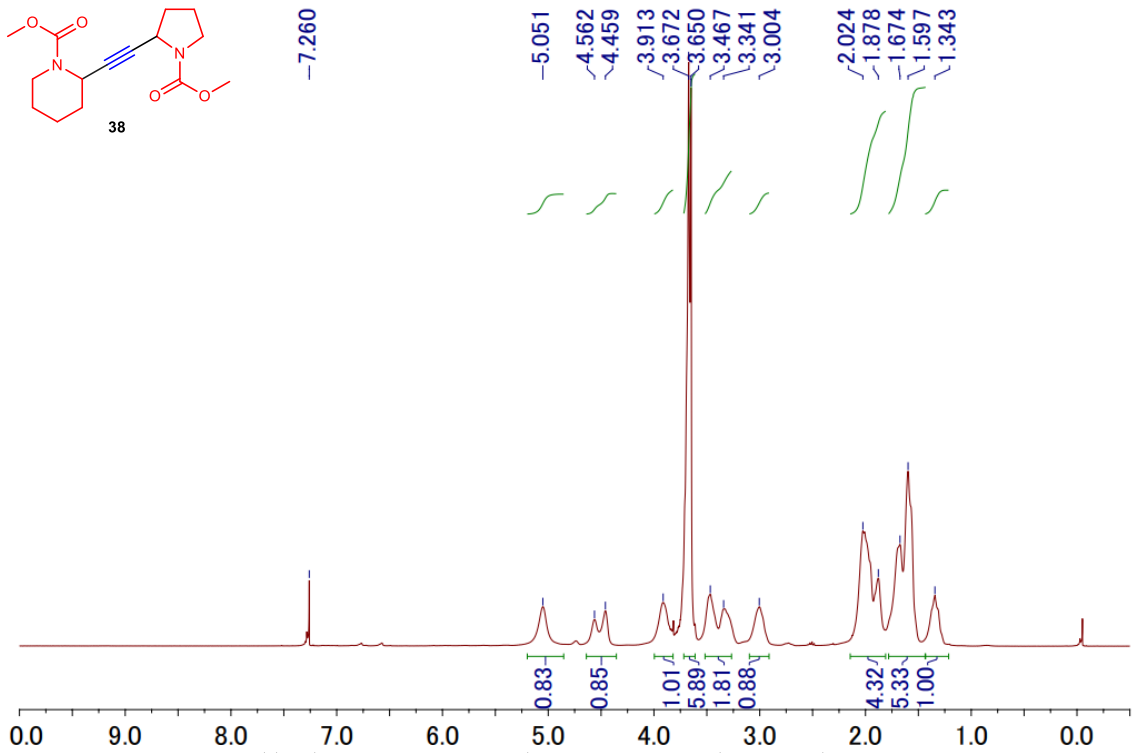

^{1}H NMR methyl 2-((1-(methoxycarbonyl)pyrrolidin-2-yl)ethynyl)piperidine-1-carboxylate (38) (400 MHz, $CDCl_3$)

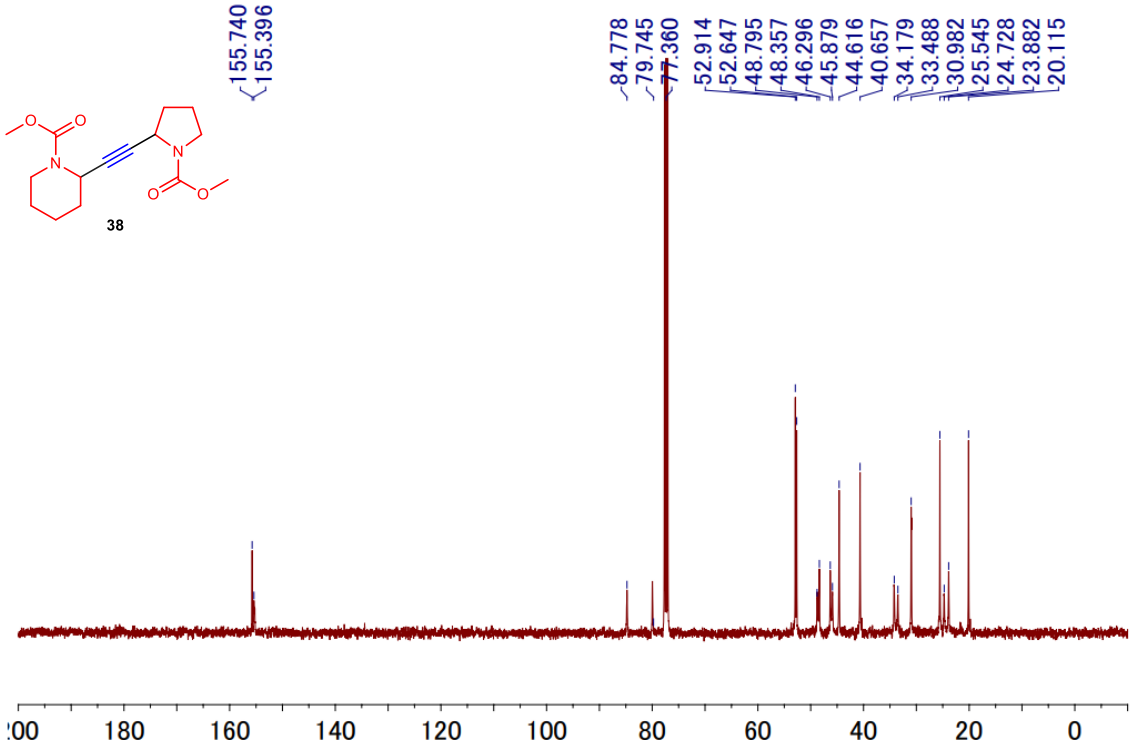

^{13}C NMR methyl 2-((1-(methoxycarbonyl)pyrrolidin-2-yl)ethynyl)piperidine-1-carboxylate (38) (100 MHz, $CDCl_3$)

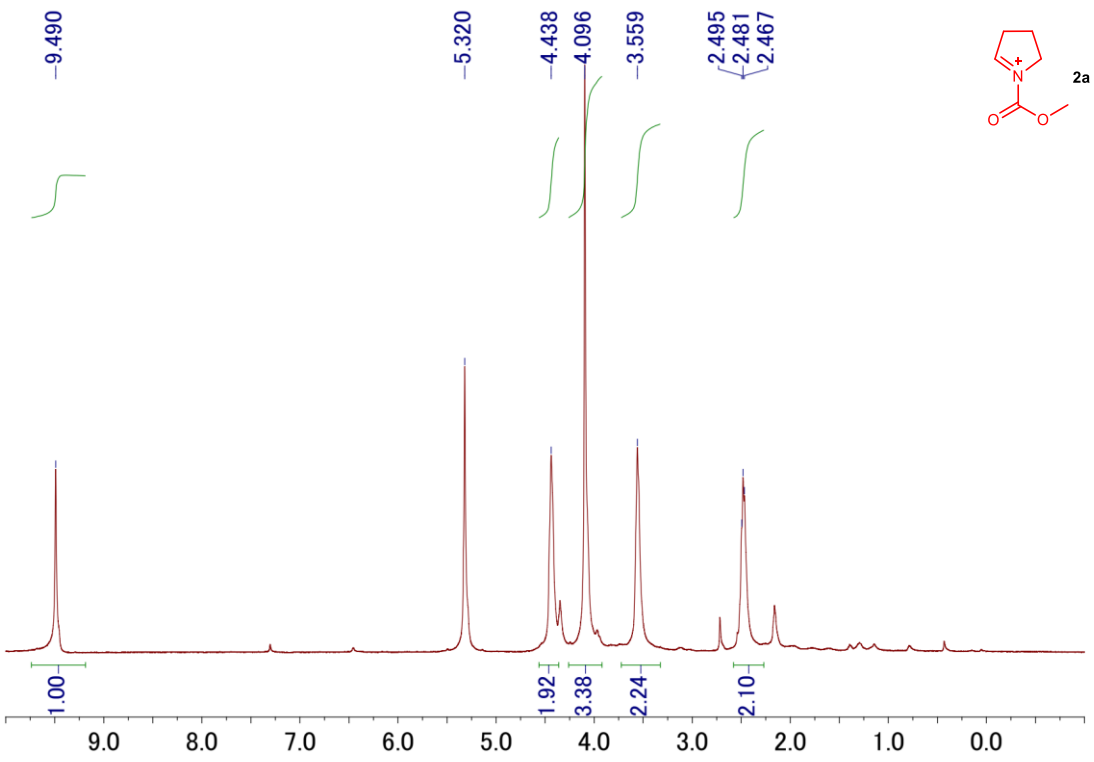

^{1}H NMR spectrum of *N*-acyliminium ion 2a (500 MHz, CD_2Cl_2, −78 °C).

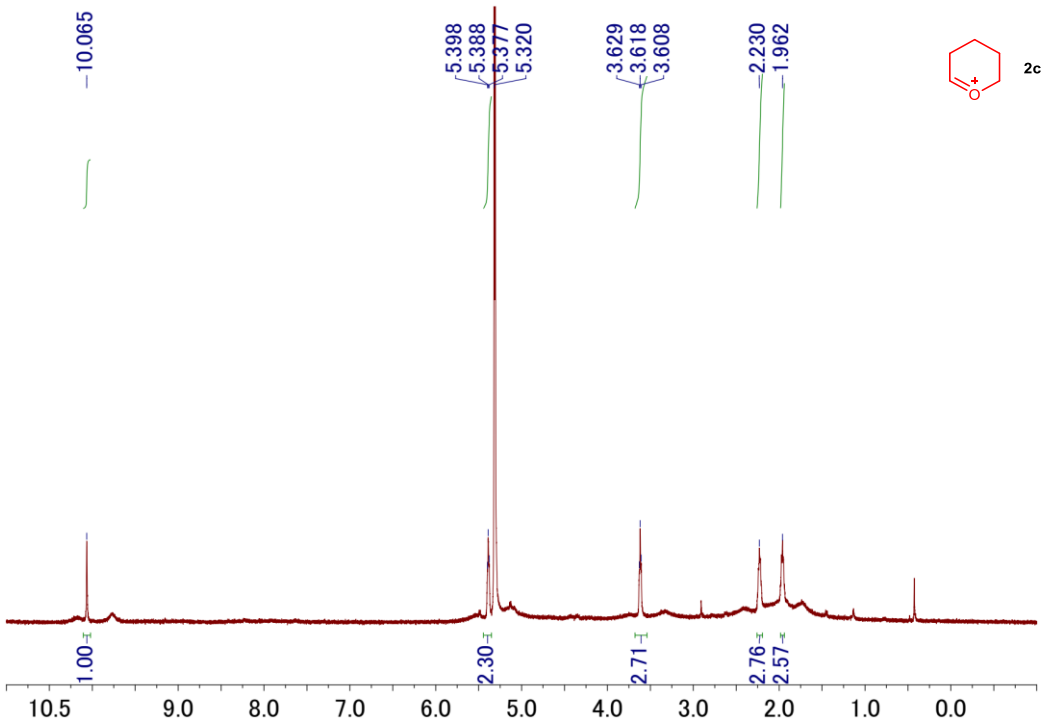

^{1}H NMR spectrum of oxonium ion 2c (500 MHz, CD_2Cl_2, −78 °C).

Conclusion

In this thesis, the author successfully constructed integrated flow systems that enable the efficient synthesis of functional molecules. These systems include methodologies for large-scale production of compounds using integrated flow reactions and a one-flow reaction system that incorporates pretreatment steps, enabling seamless transitions from pretreatment to organic reactions. Furthermore, the author developed a novel method for the rapid and irreversible generation of carbocations, reactive species for integrated reactions, and established a convergent reaction system that allows direct reactions with organolithium compounds.

In Chapter 2, the author focused on the development of large-scale production methods for aromatic boronic acid derivatives using integrated flow systems. This research included applying Suzuki-Miyaura cross-coupling reactions in flow microreactors to achieve a fully integrated, acceraleted coupling reaction within a flow system. By employing precise residence-time control in flow microreactors, the author efficiently synthesized aromatic boronic acid derivatives through lithiation and subsequent borylation of aromatic bromides. Using in-line analytical devices connected to the flow reaction system, the reaction dynamics were monitored, and approximately 200 g of aromatic boronic acid derivatives were continuously synthesized over 60 minutes. Furthermore, a palladium catalyst and a coupling partner were introduced into the borylation reactor to perform the Suzuki-Miyaura cross-coupling reaction. While the reaction initially proceeded slowly, the addition of a controlled amount of water as an additive, combined with improved mixing efficiency, significantly accelerated the reaction, enabling its completion within just 137 seconds.

In Chapter 3, the author developed a flow system that integrates pretreatment processes, including desalting and water separation, into organic reactions using pyridine hydrochlorides as model substrates. By incorporating a water-sensitive organic reaction, the efficacy of this method was verified. Desalting processes yielded 4-bromopyridine, which was then subjected to lithiation and subsequent reactions with electrophiles. Precise residence-time control of the lithiation reaction using a flow microreactor enabled efficient synthesis of the desired products. By integrating a liquid-liquid separation membrane into the system, desalting, water separation, and organic reactions involving 4-bromopyridine hydrochloride were successfully combined in an integrated flow system. Compared to batch processing, this system achieved slightly improved yields, highlighting not only operational efficiency but also the benefit of avoiding the isolation of unstable desalted intermediates.

In Chapter 4, the author investigated the rapid and irreversible generation of carbocations, a key reactive species for reaction integration, and their direct reaction with organolithium compounds through convergent reaction integration. Efficient mixing using flow microreactors enabled the instantaneous activation of olefin derivatives into carbocations by superacids. These carbocations were then reacted convergently with organolithium species in a flow system, where direct reactions between cations and anions resulted in efficient C-C bond formation. It was also revealed that the yield of these reactions depended on the polarity of the anionic species, which was influenced by the choice of countercations (Li > Mg > Zn), with higher polarization resulting in greater reaction efficiency. By varying the precursors for both cationic and anionic species, the system demonstrated broad substrate scope. The developed carbocation generation method and its direct reaction with organolithium species are expected to be applied to a wide range of uses in organic synthesis.

These findings represent significant advancements in the fields of organic and flow chemistry. This thesis lays the groundwork for further advancements in flow chemistry and has the potential to contribute to the development of technologies that may ultimately enhance the quality of life for people worldwide.

References

1) **Soutome, H.**; Maekawa, K.; Ashikari, Y.; Nagaki, A. Highly productive flow synthesis for lithiation, borylation, and/or Suzuki coupling reaction. *Org. Proc. Res. Dev.* **2024**, *28*, 2006.
(*Chapter 2*)

2) **Soutome, H.**; Kimuro, Y.; Kawaguchi, T.; Yoo, D.-E.; Yao, Y.; Oshida, S.; Nakayama, H.; Iwata, M.; Ebisawa, R.; Kikuchi, R.; Tomite, K.; Wada, S.; Ashikari, Y.; Nagaki, A. One-flow operation via 4-bromopyridine enables flash synthesis of AChE inhibitor. *Synthesis* **2024**, *56*, 821.
(*Chapter 3*)

3) **Soutome, H.**; Yamashita, H.; Shimizu, Y.; Takumi, M.; Ashikari, Y.; Nagaki, A. Convergent approach of double intermediates in flow microreactor: flash irreversible generation of carbocations enables direct cross–coupling. *Nat. Commun.* **2024**, *15*, 4873.
(*Chapter 4*)

Acknowledgement

First and foremost, I would like to express my deepest gratitude to Professor Aiichiro Nagaki for offering me the opportunity to join his laboratory as a researcher with professional responsibilities, for his invaluable research guidance, engaging discussions, and profound insights on various aspects of life.

I would also like to extend my sincere thanks to the leadership at AGC Inc.—Dr. Naoki Sugimoto, Mr. Shunsuke Yokotsuka, Dr. Takashi Nakano, Dr. Takashi Okazoe, Dr. Hiroshi Funaki, and Dr. Kyoko Yamamoto—for granting me the opportunity to engage in academic research at the university while maintaining my professional role. Their support and encouragement have been invaluable throughout this journey.

I am deeply grateful to Professor Masaya Sawamura, Professor Takanori Suzuki, Professor Keiji Tanino, and Associate Professor Hisanori Senboku of Hokkaido University for their expert guidance and stimulating discussions related to my doctoral research. My heartfelt thanks also go to Associate Professor Kazuhiro Okamoto, Specially Appointed Assistant Professor Yosuke Ashikari, and Assistant Professor Hiromichi V. Miyagishi for their research guidance, discussions, and support in creating a productive laboratory environment.

I extend my sincere appreciation to my colleagues from various companies who joined the laboratory—Mr. Kensuke Muta (Central Glass Co., Ltd.), Dr. Yusuke Kimuro (Juzen Chemical Co.), Mr. Ryota Yamamoto (Shionogi & Co., Ltd.), Mr. Yuya Yonekura (Toho Chemical Industry Co., Ltd.), and Mr. Yuta Tsuchihashi (Taiyo Nippon Sanso Co.)—for their valuable research discussions and moral support. Special thanks to Mr. Kensuke Muta for his mutual encouragement and thoughtful discussions as we navigated our doctoral journeys together.

To all the members of the laboratory, including Dr. Kyoko Mandai, Dr. Xianzhu Zhong, Dr. Junya Takino, Dr. Mitsunori Fukaya, Dr. Yaping Liu, Ms. Tomoko Kawaguchi, Ms. Rikako Yoshioka, Mr. Dong-eun Yoo, Mr. Mohammed Qenawy, Ms. Yiyue Yao, Mr. Allys Aurélien, Mr. Shuto Oshida, Mr. Hiroki Nakayama, Mr. Masatomo Iwata, Mr. Ruka Ebisawa, Mr. Ryuhei Kikuchi, Mr. Kyohei Tomite, Mr. Shuto Wada, Ms. Moe Adachi, Mr. Takuma Kudo, Mr. Daito Takahashi, Mr. Shingo Taniguchi, and Mr. Kazuki Miyamoto: thank you for your collaboration, support, and encouragement, which greatly enriched my research experience.

I would also like to express my sincere appreciation to my supervisors and colleagues at AGC Inc.—Dr. Shoji Furuta, Mr. Norihide Sugiyama, Dr. Yuichiro Ishibashi, Dr. Yu Ota, Mr. Yoshitaka Nomura, Dr. Asuka Matsunami, Mr. Taihei Taniguchi, Mr. Satoshi Okada, Mr. Hajime Eguchi, Mr. Tomoaki Sakurada, Dr. Hiroki Hayashi, Mr. Yuki Saibe, and Ms. Naomi Inayama —for their guidance, collaboration, and unwavering support throughout my research journey and professional development.

I would like to express my heartfelt gratitude to Professor Shigehiro Yamaguchi (Department of Chemistry, Graduate School of Science, Nagoya University and Institute of Transformative Bio-Molecules), who guided me at the beginning of my research career. He instilled in me an appreciation for the excitement and challenges of organic chemistry, along with the value of critical thinking and meticulous attention to detail in research.

Finally, I extend my deepest gratitude to my wife, Dr. Yuko Soutome, whose steadfast support, companionship, and love enabled me to pursue this doctoral thesis, balance professional responsibilities, and cherish our family life together. Her strength and encouragement sustained me through every challenge. I also wish to thank my daughter, Ms. Ray Michelle Soutome, whose birth during this busy period brought immeasurable joy and a constant reminder of the importance of family amidst the demands of research and work.

Hiroki Soutome